ATTACHMENT 2 TO NL-14-083

NETCO Report NET-300067-01 (non-proprietary)

Entergy Nuclear Operations, Inc.
Indian Point Unit 2
Docket No. 50-247

NET- 300067-01, Rev. 0

Criticality Safety Analysis of the Indian Point Unit 2 Spent Fuel Pool with Credit for Inserted Neutron Absorber Panels

Prepared by:

NETCO, a business unit of Curtiss-Wright Flow Control Corp.

731 Grant Ave

Lake Katrine, New York 12449

Prepared for:

Entergy Nuclear Operations

under

Contract No. 10351857

Rev:	Date:	Prepared By:	Reviewed By:	Approved By:
0	11/6/14	[signature]	Matthew C. Harris	L.P. Maiani

This Page Intentionally Left Blank

Table of Contents

List of Tables

List of Figures

Criticality Safety Analysis of the Indian Point Unit 2 Spent Fuel Pool with Credit for Inserted Neutron Absorber Panels

1 Introduction

This criticality safety analysis documents the technical basis and justification for proposed loading criteria for current and future fuel at the Indian Point Unit 2 spent fuel pool. The proposed loading criteria supports placement of the various types of fuel that are used in Unit 2 and Unit 3 reactors into the Unit 2 spent fuel pool. The analysis bounds the fuel from both units.

1.1 Background

Indian Point Nuclear Power Generating Plant Unit 2 spent fuel pool racks currently use Boraflex™ as the neutron absorber, which is known to degrade over time. Due to this fact, Entergy, the operator of the Indian Point Plant, will no longer take credit for the Boraflex™ but rather install new neutron absorber panels into every cell in the spent fuel pool. These absorber panels will cover two adjacent walls of each cell, and are thin enough to allow for fuel to be inserted and removed from the cells. Once placed in the cells, the absorber panels are not intended to be removed except for repair, replacement, or inspection. The analysis supports two designs of absorber panels. Design constraints are clearly identified and it is possible for alternate absorber panel designs to be used.

Unit 2 and Unit 3 are both 4 loop Westinghouse power plants that utilize the 15x15 fuel assembly design. The physical dimension requirements of the fuel from both units are the same. To date both units have had all their fuel assemblies manufactured by Westinghouse.

1.2 Description of the Analysis

This criticality analysis determines the loading criteria for fuel assemblies in the Unit 2 spent fuel pool by taking credit for inserted absorber panels. The loading criteria will allow for full core off load,

while storing all the current and projected fuel for Units 2 and 3. In addition, nearly all fuel at its final discharged burnup will be able to be stored in Region 2 (see Figure 8.4 for region definitions). The analysis does not credit any Boraflex neutron absorber that might remain in the racks.

Further, the analysis supports a simple framework of operation by establishing one loading curve for all fuel. This operating framework is possible by using conservative assumptions which bound all the fuel. Although there is only one loading curve, flexibility is added by two simple burnup corrections (an 8 GWd/T reduction in the burnup requirement for assemblies on the Region 2 periphery and a 2 GWd/T burnup adder for assemblies with Hf inserts). Finally, the analysis allows for future fuel designs by using bounding fuel parameters rather than the traditional nominal plus tolerance approach.

This new criticality safety analysis for the Indian Point Unit 2 pool follows the most recent methods. This effort has been concurrent with the Nuclear Energy Institute (NEI) working with the NRC to produce guidance for spent fuel pool analysis [27]. The NEI guidance started with the NRC draft Interim Staff Guidance (ISG) DSS-ISG-2010-1 [1].

1.3 Acceptance Criteria

The acceptance criteria of the analysis are to ensure compliance with 10CFR50.68 [2]. Specifically, the analysis demonstrates that:

- the $k_{95/95}$ of the pool is less than 1.0 after accounting for all biases and uncertainties when not taking credit for soluble boron (with a 95% probability at a 95% confidence level) [2],
- the $k_{95/95}$ of the pool is less than 0.95 after accounting for all biases and uncertainties when taking credit for soluble boron (with a 95% probability at a 95% confidence level) [2].

In addition, an engineering safety margin is provided to cover unanticipated issues. The safety margin used is 1%, so that the $k_{95/95}$ target value is 0.99 for no soluble boron and 0.94 with soluble boron.

2 Methodology

The criticality safety analysis performed in this report used a method that is comprised of the following steps. Each step refers to a section in this report where further information is provided.

1. Review the historical and projected fuel designs and inserts for use in Units 2 and 3. Assure that the analysis covers all the designs. (See Sections 3.2 and 3.3)
2. Review the historical and projected operating history of Units 2 and 3. (See Section 5)
3. Review the current Unit 2 racks and projected new absorber panels. (See Sections 3.1 and 3.4)
4. Validate the computer codes for the application. (See Section 4)
5. Deplete the fuel using a 2D lattice representation of the core using bounding depletion assumptions. (See Section 5)
6. Develop an infinite 3D Monte Carlo model of the Region 1 and Region 2 racks using periodic boundary conditions (radially infinite). The axial modeling is finite, including conservative modeling of the axial burnup distribution. (See Section 6)
7. Use the rack and fuel manufacturing tolerances and 3D Monte Carlo model to determine the reactivity associated with the manufacturing uncertainties. (See Section 7)
8. Use the infinite 3D Monte Carlo model with the validation and manufacturing biases and uncertainties to determine the minimum burnup as a function of enrichment and cooling time (loading curve). This analysis is performed with no soluble boron. (See Section 8)
9. Test the Region 1/Region 2 interface and the relaxed periphery requirements using a full pool 3D Monte Carlo model. (See Section 8)
10. Perform accident analyses (dropped assembly, misplaced assembly, over temperature, boron dilution, seismic, and multiple assembly misloads) with the appropriate models. (See Section 9)
11. Summarize the resulting loading requirements and the assumptions made in the analysis. (See Section 10)

2.1 Computer Codes

This analysis uses the t5-depl TRITON module of SCALE 6.1.2 [3] (the most recent version) for the depletion analysis and the CSAS5 module for the criticality analysis. All the analyses are performed using the 238 group ENDF/B-VII library (v7-238) (the most recent library). The CSAS5 module utilizes CENTRM and BONAMI for the resonance self-shielding calculations and KENO V.a for the Monte Carlo calculation of k*. All of the CSAS5 computer runs use a Monte Carlo sampling of at least 1500 generations and 6000 neutrons per generation to achieve a statistical uncertainty in k of less than 0.0002.

The t5-depl sequence of TRITON utilizes CENTRM and BONAMI for the resonance treatment and then uses KENO V.a for the collapsing of the cross-sections from 238 groups to one group for use in ORIGEN. parm=(addnux=4) is used in the analysis which tracks the maximum number of problem specific collapsed isotopes (388). For more details regarding the depletion model, please see Section A.4. At the end of the depletion analysis, the OPUS module is used to output atom densities for use in the criticality model. The input for OPUS specifies 185 isotopes that are carried forward to the criticality analysis (see Appendix A.2 for a list of the 185 isotopes). Immediately after shutdown, there is an increase in reactivity in the first few days due to the decay of Xe-135 and Np-239 (poison is being removed and fissile Pu-239 is being added). Rather than follow this change in reactivity and to assure that the peak reactivity occurs at 72 hours, all of the Xe-135 is converted to Cs-135 and all of the Np-239 is converted to Pu-239.

In addition to using SCALE, a FORTRAN Code was used to interpolate between burnups from the OPUS output and also to decay the isotopic content to the desired cooling time. The FORTRAN code, which has been verified and validated, reads an axial burnup profile to get the shape of the burnup axially, so multiple atom density sets can be made quickly. The code was validated by comparing the k calculated with the code-interpolated number densities to the k calculated with number densities directly

* Throughout this document, k is used as a short hand notation for k-effective or k_{eff}

from SCALE/ORIGEN-S, in which no interpolation was used. Furthermore, SCALE/ORIGEN-S was used to decay to a given cooling time and similar comparisons were made. All the differences were within the statistical uncertainty of the k calculations (see Section 6.4).

Unless otherwise specified, all of the k values reported in this document are raw calculated k values with no adjustment for bias and uncertainty. The final values to be compared to the criticality criteria are the calculated values plus the total bias and uncertainty (notated as "$k_{95/95}$").

3 Input Data

For the criticality analysis, input data is needed for the storage racks (Section 3.1), the fuel assemblies (Section 3.2), the fuel assembly inserts (Section 3.3), and the absorber panels (Section 3.4). In addition to this data, plant operating data was used to assure conservative depletion parameters were selected. The plant operating data is found in Section 5.

3.1 Storage Rack Specifications

Region 1 uses a flux trap for criticality control. Figure 3.1 shows the general arrangement of the cells in Region 1 [4]. Table 3.1 gives the dimensions and tolerances from the manufacturer's drawing [4] for Region 1.

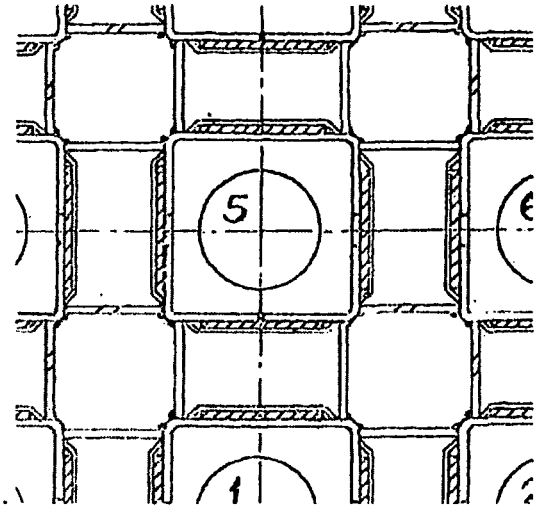

Figure 3.1: Small Section of the Region 1 Rack [4]

Region 2 is a non-flux trap design where receptacle cans with Boraflex sheaths are spaced out creating "resultant" cells between the cans. Figure 3.2 shows two complete cells in the Region 2 type rack [5]. The cell on the left would be called the "resultant" cell. Notice the fuel in the resultant cell is not bounded by four flat walls but rather by the Boraflex sheaths. The dimensions for the Region 2 rack are also shown in Table 3.1 [5].

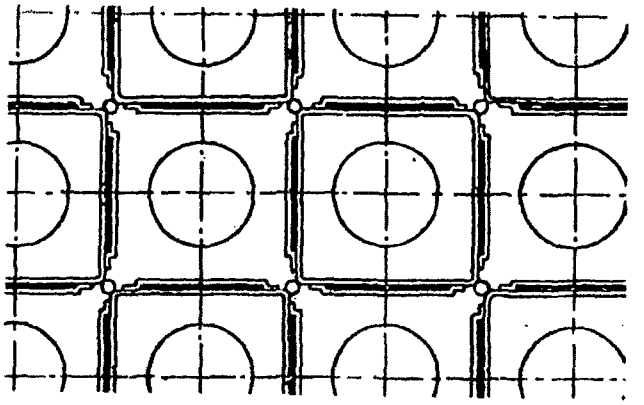

Figure 3.2: Region 2 Rack Showing Cell Boxes and Resultant Cells [5]

Table 3.1: Region 1 and 2 Storage Rack Dimensions [4, 5]

Attribute	Value (inches)	Tolerance
Region 1 Rack [4]		
Vertical cell pitch	10.545	———
Horizontal cell pitch	10.765	———
Cell ID	8.75	———
Cell wall thickness	0.075	± 0.007
Boraflex sheathing width	7.70	Minimum
Boraflex sheathing thickness	0.035*	± 0.003
Boraflex sheathing distance from cell wall	0.112	———
Region 2 Rack [5]		
Cell pitch	9.04	———
Cell ID	8.80	———
Cell wall thickness	0.075	± 0.007
Boraflex sheathing width	8.00	Maximum
Boraflex sheathing thickness	0.035	± 0.003
Boraflex sheathing distance from cell wall	0.092	———

*0.0235" and 0.035" wrappers allowed per drawing

The material of the rack is SS304 [4, 5]. The Boraflex is modeled as water. If any Boraflex remained, it would contain B-10, which would decrease reactivity compared to water. EPRI Technical

Report 103300 [25] concludes the rate of boron carbide loss is proportional to the rate of the silica loss. Therefore, a water displacing material without boron is not credible.

3.2 Fuel Assembly Designs

The Indian Point Units 2 and 3 have used a number of fuel designs, but in all cases the fuel design changes had little impact on criticality. All fuel for both units was purchased from Westinghouse. Westinghouse has used the same fuel clad and pellet dimensions for all its 15X15 designs. The guide tube dimensions have changed as Indian Point changed from the standard Westinghouse 15x15 to Westinghouse OFA 15x15 fuel. The only difference between Standard (LOPAR) and OFA fuel is that the guide tube outer diameter for OFA fuel is slightly smaller but the thickness of the guide tube is unchanged. The effect on reactivity between the two designs is insignificant (see Table 7.2).

The following nomenclature has been used for Indian Point fuel:

1. HIPAR: This was the initial fuel design and used stainless steel guide tubes and Inconel grids.
2. Standard Fuel (LOPAR): Changed from stainless steel to Zircaloy guide tubes.
3. OFA Fuel: Changed to Zircaloy grids and small change to guide tubes.
4. Vantage + Fuel: Added intermediate flow mixing grids, changed the zirconium alloy to ZIRLO™, and added axial blankets
5. Performance + Fuel: Added a protective bottom grid and longer bottom end plugs.
6. 15X15 Upgrade Fuel: Changed the grid design and modified the guide tube dashpot by using a tube-in-tube (more water displacement – less reactive).

Most of the fuel design changes have been related to the grids. The grids are ignored in the criticality modeling, since they displace water in fuel assemblies. PWR fuel designs are under moderated so that there is a negative moderator coefficient of reactivity. Even at cold temperatures the fuel assembly designs are under moderated. With high soluble boron concentrations, it can be non-conservative to

ignore grids, but for borated cases, there is a large margin to the criticality limits (See Section 8.2.6), so ignoring the grids is still acceptable.

Westinghouse has also changed the pellet theoretical density, chamfering and dishing. This is not identified as a fuel design change. For this analysis, a high stack density is used to cover all the previous changes and to allow for future design changes. The stack density is the smeared density of the UO_2 inside the pellet OD. The chamfering and dishing are not modeled. The stack density is always less than the pellet density.

Finally, the initial fuel for Indian Point did not have axial blankets. Several axial blanket designs have been used at the Indian Point Units. This analysis conservatively does not take credit for the lower enriched axial blankets (see Tables 5.1 and 5.2 for axial blanket types used).

The fuel dimensions and tolerances are taken from References 7 and 24. In general, the dimensions used in the analysis are the nominal dimensions plus or minus the tolerance to maximize the reactivity (see Table 3.2). However, this was not done for all the dimensions. The fuel pellet OD and clad ID are increased by more than the typical tolerance from Reference 7 to allow margin for possible future fuel designs. The guide tube tolerance has been shown to be insignificant to the reactivity [27]. However, a small conservative increase in the guide tube thickness was made in the model.

Having more fuel and more water inside the fuel assembly maximizes the reactivity (see Table 7.2). Therefore, maximum stack density, maximum pellet OD, minimum clad OD, smaller guide tube OD and larger guide tube ID were used in the analysis. The assembly pitch in the core for Westinghouse 15x15 plants is 8.466 inches [7]. The most the uniform pin pitch could increase is (8.466 – 15 x 0.563)/15 = 0.0014 inches before assemblies would touch each other in the reactor core. This pin pitch tolerance is analyzed (see Table 7.1) and combined with other manufacturing tolerances. An assumed stack density of 97.5% of the UO_2 theoretical density allows some margin to cover future designs. Dishing and chamfering of the pellets are included in the stack density. A 97.5% stack density means the actual

chamfered and dished sintered pellet density is nearly 99% of the theoretical density of UO_2. If the fuel design changes, the criticality analysis will be valid as long as the maximum stack density, maximum pellet OD, minimum clad OD and minimum guide tube cross-sectional area are maintained (see Table 10.4).

Table 3.2: Fuel Assembly Dimensions [24,7]

Attribute	Value (inches)	Typical Tolerance	Value Used in Analysis
Fuel pellet UO_2 stack density	97.5 %TD	Maximum expected stack density	97.5
Fuel pellet OD	0.3659	[ ]^{a,c}	[ ]^{a,c}
Fuel clad OD	0.4220	[ ]^{a,c}	[ ]^{a,c}
Fuel clad ID	0.3734	[ ]^{a,c}	[ ]^{a,c}
Fuel pin pitch	0.5630	± 0.0014 (using assembly pitch)	0.5630
Active fuel length	144	None (has no effect)	144
Standard Fuel			
Fuel guide tube OD	0.546	Insignificant effect on k [27]	[ ]^{a,c}
Fuel guide tube ID	0.512	Insignificant effect on k [27]	[ ]^{a,c}
OFA Fuel			
Fuel guide tube OD	0.533	Insignificant effect on k [27]	[ ]^{a,c}
Fuel guide tube ID	0.499	Insignificant effect on k [27]	[ ]^{a,c}

The fuel clad and guide tube material is Zirc-4 or Zirlo. For fuel pellets that are coated with ZrB_2 (IFBA), the B-10 loading is assumed to be [mg B^{10}/inch]^{a,c} [24] (1X) for IFBA rods assumed in fresh fuel and [mg B^{10} /inch]^{a,c} (1.5X) for depletion calculations.

3.3 Fuel Assembly Insert Designs

The fuel assemblies used in Indian Point Units 2 and 3 have contained a number of different types of inserts in the guide tubes during operation. They are:

1. Pyrex burnable absorbers
2. Wet Annular Burnable Absorbers (WABA)
3. Unclad Hafnium flux suppression assemblies
4. Primary source assemblies
5. Secondary source assemblies

6. Full Length Control Rods
7. Part Length Control Rods

The final criticality calculations assume no inserts in the guide tubes except for the special case of a control rod in the assembly to reduce the reactivity of assemblies that fail to meet the loading requirements. However, depletion calculations are performed with inserts in order to harden the spectrum and maximize the reactivity of burned fuel. The effect of the inserts is maximized by using the highest boron content and the most water displacement. The boron loading for the burnable absorbers has varied, so the maximum boron loading has been used in the analysis. A Pyrex burnable absorber displaces more water and has a higher B-10 loading than a WABA, so for enrichments where both burnable absorbers are used, the Pyrex burnable absorber is conservatively selected. Pyrex burnable absorbers displace more water than the primary source assemblies. The analysis assumes for fuel ≤ 3.5 wt% (old fuel) that Pyrex burnable absorbers remain in the assembly throughout depletion (see Section 5), so primary sources (which were only in the old fuel) are covered.

Secondary sources displace some water and could have a small effect on the burned fuel reactivity. A WABA rodlet displaces about the same amount of water as a secondary source rodlet but a secondary source assembly contains less rodlets (generally 6 rodlets). Since more water is displaced with the assumed WABA assembly (20 rodlet assembly) than the secondary source assembly, analysis with WABAs would be conservative. Since the WABA is never removed during the depletion, a secondary source that is inserted after the WABA depletion is automatically covered.

Indian Point Units 2 and 3 had 8 part length control rods in Cycle 1. In Cycle 1, for both units, the part length rods were in assemblies that were nominally 2.2 wt% U-235 enriched. These assemblies exceed the Region 2 loading curve minimum burnup for their enrichment by over 10 GWd/T. The reactivity effect due to the use of the part length control rods in Cycle 1 for both units is significantly less than the reactivity effect of the 10 GWd/T excess burnup for these fuel assemblies.

Thimble plugs have also been used at the Indian Point Units, but since these do not extend into the active fuel region they can be ignored.

Tables 3.3 and 3.4 provide the input data used in the analysis. Note that the Pyrex burnable absorber used at Indian Point had a range of B-10 loadings. The highest B-10 loading is conservative for the depletion analysis and that value is in Table 3.4. Further, the largest borosilicate glass dimensions were utilized which is also conservative.

Table 3.3: Control Rod and Hafnium Rod Descriptions [7]

Parameter	Control Rod	Hafnium
Number of Rodlets per assembly	20	20 or less*
Absorber OD (in)	0.3975	0.3810
Absorber Material	Ag-In-Cd (80-15-5 wt%)	Hf
Absorber density (g/cc)	10.17	13.31†
Clad OD (in)	0.4390	0.3810‡
Clad ID (in)	0.4006	none
Clad Material	SS 304	none

Table 3.4: Pyrex and Wet Annular Burnable Absorber Descriptions [6, 7, 24]

Parameter	Pyrex	WABA
Material Inside inner clad	Void	Water
Clad material	SS304	Zr
Inner Clad ID (in)	0.2235	0.225
Inner Clad OD (in)	0.2365	0.267
Absorber ID (in)	0.2430	0.278
Absorber OD (in)	0.3960	0.318
Outer Clad ID (in)	0.4005	0.329
Outer Clad OD (in)	0.4390	0.381
Absorber Material	B_2O_3-SiO_2 (18.1 wt% B_2O_3) Density = 2.23 g/cc†	Al_2O_3-B_4C (0.00603 gm ^{10}B/cm)

* 20 rodlets were used in the analysis. To date the maximum rodlets used is 16.
† From the SCALE manual, Ref. [3].
‡ This is the OD of the unclad Hafnium.

For the special case of crediting a control rod in a fresh assembly in the pool, the Ag-In-Cd content (density) is reduced by 20% to bound manufacturing tolerances and any absorber material loss during operation.

3.4 Absorber Panel Design

The spent fuel pool racks are assumed to have L-shaped borated Al/B_4C absorber panels in every cell. For Region 1, the panels are oriented bottom-right, while for Region 2, they are oriented top-left. This resolves any interface issues between Region 1 and Region 2, since there is a double panel at the interface. There are two analyzed absorber panel designs, which are assumed to have the characteristics shown in Table 3.5. Figures 3.3 and 3.4 illustrate the two designs.

Table 3.5: Absorber Panel Dimensions

Attribute	Value (inches)	Notes
Absorber Panel (primary)		
Areal Density (g B-10/cm^2)	0.015	Minimum
Panel width	Cell ID - 0.03	Minimum
Panel thickness	0.086	Minimum in Region 1
	0.096	Maximum in Region 2
Length		Covers active fuel length
Absorber Panel (alternate)*		
Areal Density (g B-10/cm^2)	0.022 (Region 1) 0.020 (Region 2)	Minimum
Panel width	7.6	Minimum
Panel thickness	0.075	Minimum in Region 1
	0.094†	Maximum in Region 2
Offset from corner	0.64	
Length		Covers active fuel length

* Minor adjustments to these specific dimensions and areal densities are acceptable provided that the panel is shown to be as effective in absorbing neutrons as the primary design.

† For Region 2, in which maximum water displacement is more reactive, the maximum thickness is increased in the model to 0.101 to account for the water displacement of the stainless steel connector that is attached to the absorber panel.

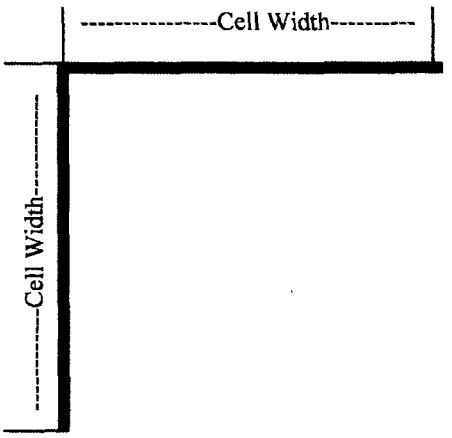

Figure 3.3: L-Shaped Absorber Panel

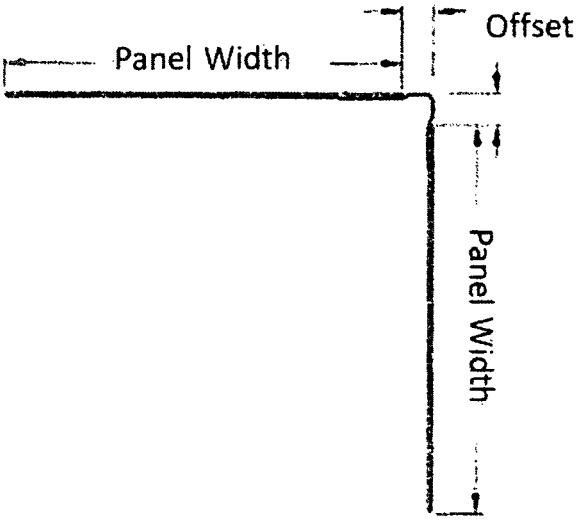

Figure 3.4: Example Alternate Panel Design* [26]

For the primary absorber panel design, the Al/B_4C is L-shaped and continuous and fits snugly inside the rack cell. Therefore, the minimum width of the panel is the cell ID minus the tolerance. Calculations showed that having a minimum panel thickness maximizes the reactivity in Region 1, while a maximum panel thickness maximizes the reactivity in Region 2 (see Table 7.2). For the alternate design, two sheets

* Minor adjustments to these specific dimensions and areal densities are acceptable provided that the panel is shown to be as effective in absorbing neutrons as the primary design.

of Al/B_4C are connected at the corner by an L-shaped stainless steel connector (see Figure 3.4). The minimum panel width is 7.6 inches. All of the loading curve calculations were performed with the primary design. For the alternate design, since the panel width is over an inch shorter than the primary design and there is no Al/B_4C in the corner, the minimum areal density had to be increased from 0.015 to 0.020* in Region 2 and to 0.022* in Region 1, so that the loading requirements would remain the same. Calculations show that any metal (or no metal) used by the alternate design in the corner to connect the panels is acceptable, so long as the connecting metal is no thicker than 0.1 inches (see Figure 6.3).

No references are given for the absorber panel dimensions, since the dimensions in Table 3.5 are design constraints for the absorber panel to be ordered.

4 Validation

The validation of the SCALE 6.1.2, TRITON (t5-depl) and CSAS5 models requires a number of steps. First, since fresh fuel is allowed to be stored in the spent fuel pool, validation for fresh fuel is performed by use of UO_2 critical benchmarks from the OECD/NEA handbook [8]. For the burned fuel, two approaches for validation are used: EPRI Benchmarks [9, 10] and an extension of ISG-8, Rev. 3 [11]. The more limiting of the two approaches is used for the validation of the burned fuel. The extension of ISG-8, Rev. 3 (referred to in this report as Extended ISG-8) is the use of all significant isotopes (185 isotopes) rather than 28 isotopes.

The details of the validation are found in Appendix A. This section describes the method and summarizes the results.

4.1 Fresh Fuel Validation

The validation for fresh fuel follows NUREG/CR-6698 [12]. Two hundred thirty six (236) critical experiments were selected from the OECD/NEA handbook that match the conditions of most spent fuel pools but specifically the Indian Point Unit 2 spent fuel pool. These experiments were analyzed with SCALE 6.1.2 using the 238-group ENDF/B-VII cross-section library. The resulting predicted k's were then tested for trends on the key parameters influencing k. Using these trends, the most limiting bias and uncertainty in the area of applicability was determined. Although some of the trends may not be statistically significant, it is conservative to use all of the trends in determining the limiting bias and uncertainty. Table A.4.1.7 is the area of applicability for the validation. The Indian Point spent fuel pool is covered by the area of applicability of the validation. Specifically,

1. Enrichment: The benchmarks selected range from 2.35 to 4.74 wt% U-235. The fuel in the spent fuel pool ranges from 2.21 to 5 wt% U-235. The bias decreases with enrichment and the slope is small allowing for a small extrapolation (see Table A.4.1.7).

2. Spectrum: The benchmarks cover a wide range of spectrum by varying the pin pitch. The Energy of the Average Lethargy causing Fission (EALF) of the benchmarks ranges from 0.0605 to 0.8485 eV. The calculated EALF in the pool ranges from 0.1 to 0.6 eV.
3. Fuel Pin Pitch: The fuel pin pitch of the benchmarks ranges from 1.075 to 2.54 cm. The Indian Point fuel pin pitch is 1.43 cm.
4. Flux Trap: The benchmarks include spacing between assemblies of 0 to 15.4 cm. The flux trap design for Region 1 is 3.4 to 4.0 cm.
5. Boron Areal Density: The benchmarks range from 0 to 0.067 g B^{10}/cm^2. The spent fuel pool will credit absorber panels with areal densities of 0.015 to 0.022 g B^{10}/cm^2.
6. Soluble Boron: The benchmarks have soluble boron concentrations up to 5030 ppm. The maximum ppm used in the analysis is 2000 ppm.

Details on the area of applicability can be found in Appendix A.

The most limiting bias and uncertainty from the validation was due to a trend in the spectrum, EALF. From this trend, a bias of 0.0029 for EALF up to 0.4 eV and 0.0037 for EALFs from 0.4 to 0.6 eV has been determined. Cases without soluble boron are in the first range of EALF and will use 0.0029 for the bias. Heavily borated cases can have an EALF greater than 0.4 eV and then would use the 0.0037 bias. The 95/95 uncertainty is 0.0050 for all the analyses.

4.2 Burned Fuel Validation – EPRI Approach

EPRI determined the change in k with burnup using measured power distributions from 680 flux maps taken over 44 cycles from 4 different PWRs [9]. With this measured data, EPRI created a set of benchmarks that can be used to validate the change in k with burnup found in other code systems. Since the measured parameter is inferred reactivity, the change in k captures the change in the macroscopic cross-section, which is a function of the isotopic concentrations and cross-sections. The data does not provide any information on individual components of the macroscopic cross-section. The measured

reactivity effect comes from the change in concentration (and cross-section) of all isotopes. This would include any movement of isotopes during power operations, such as gaseous fission products. The measured reactivity also includes any dimensional changes at power, such as crud buildup or creep down of the clad (but not any change in these conditions between hot full power and cold conditions). The SCALE TSUNAMI module was used by EPRI to account for hot to cold variations by a conservative uncertainty [9].

The EPRI benchmarks were analyzed with SCALE 6.1.2 and the 238 ENDF/B-VII cross-section library. The depletion analysis for the spent fuel pool analysis followed exactly the same method as used for the EPRI benchmark analysis (same time steps, same method of interpolating the isotopic content, and the same method of accounting for decay). Appendix A shows the results of the analysis. A conservative bias is determined to be 0.003 in k. The uncertainty about the bias is conservatively 0.0064 in k.

The complete validation for burned fuel using this technique is the fresh fuel bias from Section 4.1 (0.0029 or 0.0037 depending on EALF) plus the delta-k of depletion bias (0.003) with two uncertainties, 0.0050 from the fresh fuel critical experiments and the EPRI benchmark uncertainty (0.0064).

Refer to Appendix A and References 9 and 10 for more details.

4.3 Burned Fuel Validation – Extended ISG-8 Approach

Spent Fuel Project Office Interim Staff Guidance – 8, Rev. 3 – Burnup Credit in the Criticality Safety Analyses of PWR Spent Fuel in Transport and Storage Casks (ISG-8 Rev. 3), follows the traditional approach for transport and storage casks of limiting the number of isotopes that can be considered in the analysis. Spent fuel pool analysis historically utilizes all isotopes. The Extended ISG-8 approach uses the same techniques as developed for ISG-8 but extends the approach to all isotopes.

The ISG-8 approach uses critical experiments to cover the worth of actinide isotopes, a TSUNAMI based estimate of a bias to cover the worth of isotopes not in the critical experiments, and chemical assays to cover the isotopic content.

The critical experiments that most closely match spent nuclear fuel are the HTC critical experiments [13]. These experiments are Mixed Uranium/Plutonium Oxide (MOX) experiments that were designed to match the Uranium and Plutonium isotopic content of 4.5 wt % U-235 fuel burned to 37.5 GWd/T. These experiments were analyzed for this validation. Since there are fuel assemblies in the spent fuel pool that have less burnup, as well as fuel assemblies that have more burnup, additional critical experiments are needed. MOX experiments from the OECD/NEA handbook were added to cover the higher burned conditions and the fresh UO_2 critical experiments from Section 4.1 were added to cover the lower burned conditions.

The most limiting bias and uncertainty from the three sets of experiments: a) fresh UO_2, b) HTC, and c) MOX is used for the bias and uncertainty for the major actinides (U, Pu, Am-241). The most limiting bias and uncertainty comes from the fresh UO_2 experiments, since ENDF/B-VII predicts higher k's for MOX critical experiments than U-235 based systems. Refer to Section A.4.1.10 of Appendix A to see the support for this position. This means that the first component of the bias and uncertainty, the component for the worth of the major actinides, has a bias of 0.0029 or 0.0037 depending on EALF and an uncertainty of 0.0050.

The second component of the validation is to cover the worth of the fission products and minor actinides. ORNL studied the uncertainty in the cross-sections and used TSUNAMI to propagate this uncertainty to a cask system [14]. ORNL then concluded that a bias of 1.5% of the worth of the fission products and minor actinides was conservative. This conclusion was then inserted into ISG-8, Rev. 3. For the Extended ISG-8 approach, the same 1.5% of the worth of the fission products is used, but for all isotopes. This too is supported by the same ORNL report. On page 106 of the ORNL report, the last

sentence states, "An upper value of 1.5% of the worth is also applicable for SNF isotopic compositions consisting of all nuclides in the SFP configuration, as well as the cask configuration as depicted in Table 7.11 and Table 7.12."

The final component of the ISG-8 approach is a bias and uncertainty to cover the isotopic content. ISG-8 endorses the direct difference approach to calculate a bias and uncertainty due to the depletion analysis. The Extended ISG-8 approach utilizes the same direct difference approach and produces the same bias and uncertainty. The only difference with the Extended ISG-8 approach is that it allows the calculated bias and uncertainty to apply to all isotopes. The isotopic content bias and uncertainty is dominated by the highest worth isotopes (U-235, Pu-239, Pu-240, Pu-241). The addition of more small worth isotopes would have a small effect on this bias and uncertainty. Without measured data on these isotopes it is impossible to prove the effect is small but due to use of the EPRI benchmarks we can be certain that the effect is not large. Therefore, it is concluded that in order to allow this extension to the ISG-8 approach, the analysis of the EPRI benchmarks should be performed to exercise all the isotopes against some experimental data.

Appendix A provides the details of the analysis of the chemical assays followed by the direct difference calculations. From this analysis, the bias of isotopic content is 0 and the uncertainty is 0.0002 times the burnup in GWd/T.

4.4 Burned Fuel Validation – Most Limiting Approach

The validation for this criticality safety analysis uses the most limiting of the EPRI or Extended ISG-8 approach. In both approaches, the bias and uncertainty from the fresh UO_2 validation is used. In the ISG-8 approach this is because the UO_2 critical benchmarks are more limiting than the HTC or MOX critical benchmarks. With the EPRI approach there is a remaining uncertainty of 0.0064 and a bias of 0.003 in k. The Extended ISG-8 approach has a bias of 1.5% of the worth of the minor actinides and fission products. The worth of the minor actinides is about 10% in k at normal discharge burnups. This

would create a bias of 0.0015 (0.1*1.5%). The 0.003 bias from the EPRI approach would be equaled if the worth of the minor actinides and fission products were 20% in k. This is never met, so the EPRI bias is more limiting. Finally, uncertainty from the chemical assays is 0.0002 times the GWd/T. In order to reach the EPRI uncertainty of 0.0064 a burnup of 32 GWd/T is required. The actual rack up of biases and uncertainty for the Indian Point Unit 2 spent fuel pool (See Appendix A, Section A.5) has shown that for the maximum credited burnup (42.67 GWd/T), the EPRI approach is more limiting than the Extended ISG-8 approach.

5 Depletion Calculations

Prior to performing the depletion analysis, a thorough review of the historical operation of Indian Point Units 2 and 3 was performed. Specifically, the following items were reviewed:

1. What inserts were in assemblies and what were the designs of these inserts.
2. How much burnup was achieved while the inserts were in the assemblies.
3. How were control rods used during the cycles.
4. What was the soluble boron level during the cycles.
5. What was the maximum average power peaking (used for fuel and moderator temperatures).
6. When were axial blankets introduced and what were the designs.

Tables 5.1 and 5.2 summarize the key depletion parameters by cycle for Indian Point Units 2 and 3 respectively [30]. Control rod operating history is discussed in Section 5.5. T_{in} is the core inlet temperature and T_{ave} is the average moderator temperature in the active fuel (not the vessel average temperature).

Axial blankets (reduced enrichment at the ends of the fuel) reduce the reactivity compared to assuming the highest enrichment over the entire length of the fuel. Several axial blanket designs have been used in Units 2 and 3: 6 inch or 8 inch long blankets, annular and solid pellets, natural or reduced enriched uranium, same or differing enrichments in the top and bottom blankets. Although it would be possible to credit the reduced reactivity caused by the axial blankets, it was decided not to take the credit. This approach yields the simplicity of only one loading curve and flexibility for possible future design modifications for the axial blankets such as enrichment or annular hole size changes. Such changes would have no effect on the criticality safety analysis since the full length uniform enrichment assumption would still be bounding.

The Indian Point fuel management and operating approach changed from annual refueling cycles to two year refueling cycles resulting in higher feed enrichments and heavier use of burnable absorbers. In

order to not penalize the loading curve for older fuel, the depletion analysis was subdivided into fuel assemblies less than or greater than 3.5 wt% U-235. Fuel assemblies over 3.5 wt% U-235 have never been loaded into the core with Pyrex burnable absorbers. Furthermore, historical fuel assemblies under 3.5 wt% U-235 never had IFBA rods.

With a thorough knowledge of the Indian Point Units 2 and 3 operating history, it was possible to select limiting depletion parameters that bound all fuel.

Table 5.1: Key Operating Features by Cycle Used in Indian Point Unit 2

Cycle	Feed Batch ID	Power (MWt)	T_{ave} (°F)	T_{in} (°F)	Cycle Burnup (GWd/T)	Feed Enrich. (wt%)	Blanket	Blanket Enrich. (wt%)	BA* Type	Max BA Loading	Max BA Burnup (GWd/T)	Max Assem. Peaking Factor	Peak Soluble Boron (ppm)
1	A,B,C	2758	[	]	a,c 16.4	2.2/2.8/3.3	none	-	Pyrex	20 Rodlets	18.5	1.23	890
2	D	2758			10.7	3.1	none	-	Pyrex	20 Rodlets	13.0	1.22	993
3	E	2758			10.8	3.2	none	-	Pyrex	7 Rodlets	12.0	1.24	948
4	F	2758			9.8	3.35	none	-	Pyrex	12 Rodlets	12.2	1.25	881
5	G	2758			12.2	3.3	none	-	Pyrex	12 Rodlets	15.0	1.22	908
6	H	2758			13.2	3.2	none	-	Pyrex	20 Rodlets	16.7	1.27	880
7	J	2758			12.4	3.44	none	-	Pyrex	16 Rodlets	15.5	1.25	883
8	K	2758			13.8	3.2/3.44	none	-	WABA	12 Rodlets	17.4	1.27	933
9	L	2758			11.4	3.4/3.7	none	-	WABA	16 Rodlets	14.6	1.28	881
10	M	2758 3071.4			13.3	3.6/4.2	none	-	WABA	20 Rodlets	17.3	1.30	1050
11	N	3071.4			18.1	3.75/4.05	none	-	IFBA WABA	116(1X) 16 Rodlets	24.5	1.35	997
12	P	3071.4			20.7	3.6/4.2/4.6	none	-	IFBA WABA	116(1X) 20 Rodlets	28.1	1.36	1121
13	Q	3071.4			20.9	4.4/4.8	6" annular	2.6	IFBA WABA	148(1.5X) 12 Rodlets	28.8	1.38	1146
14	R	3071.4			19.0	4.6/4.95	6" annular	2.6	IFBA WABA	148(1.5X) 20 Rodlets	26.7	1.40	1069
15	S	3071.4			22.1	4.8	6" annular	2.6	IFBA WABA	148(1.25X) 16 Rodlets	29.9	1.40	1172
16	T	3114.4			23.9	4.6/4.95	8" annular	3.2	IFBA WABA	148(1.5X) 20 Rodlets	32.4	1.35	1164
17	U	3216			18.7	4.0/4.4	8" annular	3.2	IFBA WABA	148(1.25X) 16 Rodlets	24.9	1.33	1065
18	V	3216			24.5	4.6/4.95	8" solid except IFBA	3.2	IFBA WABA	148(1.25X) 20 Rodlets	33.1	1.35	1191
19	W	3216			24.8	4.6/4.95	8" solid except IFBA	3.2 Bot 3.4 Top	IFBA WABA	148(1.25X) 20 Rodlets	32.6	1.31	1244
20	X	3216			23.7	4.8/4.95	8" solid except IFBA	3.2 Bot 3.6 Top	IFBA WABA	148(1.25X) 20 Rodlets	32.3	1.36	1230
21	2A	3216	[	]	25.6	4.6/4.95	8" solid except IFBA	3.6 Bot 4.0 Top	IFBA WABA	148(1.25X) 20 Rodlets	33.8	1.32	1254

* BA is burnable absorber

Table 5.2: Key Operating Features by Cycle Used in Indian Point Unit 3

Cycle	Feed Batch ID	Power (MWt)	T_{ave} (°F)	T_{in} (°F)	Cycle Burnup (GWd/T)	Feed Enrich. (wt%)	Blanket	Blanket Enrich. (wt%)	BA* Type	Max BA Loading	Max BA Burnup (GWd/T)	Max Assem. Peaking Factor	Peak Soluble Boron (ppm)
1	A,B,C	3025	[	]	a,c 17.3	2.25/2.8/3.3	none	-	Pyrex	20 Rodlets	19.4	1.12	899
2	P	3025			11.3	3.1	none	-	Pyrex	12 Rodlets	10.6	1.26	954
3	R	3025			12.8	3.3	none	-	Pyrex	12 Rodlets	16.2	1.27	912
4	S	3025			14.1	3.2/3.4	none	-	Pyrex	20 Rodlets	17.3	1.23	968
5	T	3025			14.3	3.2/3.4	none	-	WABA	16 Rodlets	17.9	1.26	989
6	U	3025			14.8	3.2/3.6	none	-	WABA	12 Rodlets	19.5	1.31	1017
7	V	3025			13.4	3.4/3.8	6" solid	0.72	IFBA WABA	60(1X) 20 Rodlets	18.2	1.35	974
8	W	3025			14.1	3.8/4.2	6" solid	0.74	WABA	12 Rodlets	18.9	1.35	1220
9	X	3025			19.2	4.0/4.4	6" solid	0.74	IFBA WABA	116(1.5X) 20 Rodlets	25.9	1.35	1169
10	Y	3025			22.4	4.4/4.6	6" annular	2.6	IFBA WABA	80(1.5X) 20 Rodlets	31.1	1.38	1163
11	AA	3025			18.7	4.3/4.6	6" annular	2.6	IFBA WABA	80(1.25X) 20 Rodlets	25.9	1.38	1095
12	BB	3025/ 3067			23.0	4.5/4.95	8" annular	3.2	IFBA WABA	100(1.5X) 20 Rodlets	30.3	1.31	1224
13	CC	3067.4			23.7	4.95	8" annular	3.2	IFBA WABA	100(1.5X) 20 Rodlets	32.1	1.36	1246
14	DD	3180/ 3188			25.2	4.6/4.95	8" annular	3.2	IFBA WABA	148(1.25X) 20 Rodlets	33.1	1.31	1240
15	EE	3188.4			24.9	4.6/4.95	8" annular	3.2	IFBA WABA	148(1.25X) 20 Rodlets	32.0	1.28	1228
16	FF	3188.4			24.1	4.6/4.95	8" annular	3.2 Bot 3.6 Top	IFBA WABA	148(1.25X) 20 Rodlets	31.6	1.32	1179
17	GG	3188.4			25.0	4.95	8" solid except IFBA	3.6 Bot 3.8 Top	IFBA WABA	148(1.25X) 20 Rodlets	33.2	1.33	1232
18	3D	3188.4			24.6	4.6/4.95	8" solid except IFBA	3.6 Bot 4.0 Top	IFBA WABA	148(1.25X) 20 Rodlets	32.0	1.30	1258

* BA is burnable absorber

5.1 Limiting Depletion Parameters – Burnable Absorbers

Burnable absorbers harden the spectrum during depletion, which result in more plutonium production and less U-235 consumption for a given burnup [15]. The spectrum hardening comes from the absorption of thermal neutrons by the boron and displacement of the water in the guide tubes. The effect on reactivity also depends on how long (in terms of GWd/T) the burnable absorber remains in the fuel before being removed.

Indian Point Units 2 and 3 have used three types of burnable absorbers: Pyrex, Wet Annular Burnable Absorbers (WABA) and Integral Fuel Burnable Absorbers (IFBA). The Pyrex and WABA designs consist of rodlets mounted to a base plate which sits on the top of the fuel assembly. The number of rodlets varies by position in the core to help control power peaking. The most limiting design has 20 rodlets. The depletion analysis assumes the full 20 rodlets. There have been variations in the boron loading in the burnable absorbers. The highest boron level is most limiting and is assumed in the depletion analysis (see Table 3.4 for the assumed boron level). Pyrex burnable absorbers are more limiting than WABAs since they displace more water. IFBA rods and removable burnable absorbers can be in the assembly at the same time. The number of IFBA rods is varied to aid in power distribution control. The maximum number of IFBA rods (i.e., 148) is assumed. The boron content of the IFBA rods can vary. The maximum boron loading of [mg B^{10} per inch]^{a,c} (1.5X) is assumed in the depletion analysis. Most of the IFBA rods have been at a 1.25X loading (see Tables 5.1 and 5.2).

For fuel enriched to 3.5 wt% U-235 or less, Pyrex burnable absorbers are assumed to be in the assembly throughout the entire burnup. For fuel over 3.5 wt% U-235, WABAs are assumed to be in the fuel and never removed. However, control rods are assumed to be in the fuel for 2 GWd/T before the WABAs are inserted to cover future extended part power operation. Since control rods are more limiting than WABAs and since control rods and WABAs cannot be in the assembly at the same time, the analysis is valid for any amount of WABA burnup as long as the control rod exposure is less than 2 GWd/T. This 2 GWd/T is for the assembly burnup but due to the axial burnup distribution, it is only 1 GWd/T in the

top node. Therefore, operation for a full cycle with the control rods at the "bite" position is prohibited for fuel enriched to greater than 3.5 wt% U-235. The limitation of 2 GWd/T of assembly burnup under control rods will be checked as part of the reload safety checks.

Finally, gadolinium and erbium have not yet been used as burnable absorbers at Indian Point. These burnable absorbers have a negative impact on reactivity due to incomplete burnout of the absorber [16]. If gadolinium or erbium is used in the future, then this criticality analysis is valid.

5.2 Limiting Depletion Parameters – Soluble Boron

Soluble boron hardens the spectrum, making the fuel more reactive for a given burnup. It has been shown that taking the burnup average soluble boron level is acceptable (rather than a time dependent soluble boron) [17]. Tables 5.1 and 5.2 show the peak soluble boron concentration. The average cycle soluble boron concentration is less than 70% of the peak values (confirmed for limiting cases) reported on Tables 5.1 and 5.2. Review of the operating history with fuel less than 3.5 wt% U-235 shows that 800 ppm is higher than any cycle averaged ppm, so 800 ppm was selected for the depletion of this fuel. For fuel enriched to more than 3.5 wt% U-235, a multi-cycle assembly average bounding value of 1000 ppm soluble boron is selected. Since the reload core designer must limit the soluble boron level in order to maintain a negative moderator temperature coefficient, it is unlikely that 1000 ppm burnup averaged soluble boron will ever be a limiting design feature. However, this parameter will be included in the reload design checks. Early shutdown could cause this average soluble boron to be exceeded. To handle this possibility, a special depletion at 1300 ppm was performed. Fuel with a burnup > 12 GWd/T can be placed anywhere in Region 1 and fuel with a burnup < 12 GWd/T can be placed on the periphery of Region 1 or with a control rod inserted and placed anywhere in Region 1.

5.3 Limiting Depletion Parameters – Temperatures

The higher the fuel and moderator temperatures during depletion, the higher the reactivity. As with most parameters assumed during depletion, the time ordering of the effect has a very minor impact on the final reactivity. Therefore, burnup averaging of the fuel and moderator temperature is appropriate. A limiting fuel and moderator temperature can be found by determining the maximum burnup averaged peaking factor. Since criticality requires a volume of low enriched fuel that is much greater than a fuel pin, the average peaking factor of interest is the assembly averaged value. This is easy to determine, since it is simply the assembly burnup divided by the sum of the core average burnup for the cycles that the fuel assembly was in the core. Tables 5.1 and 5.2 show the maximum assembly/burnup averaged peaking for any assembly in the core for that cycle. The discharge average peaking factor will be lower since the peaking factor for an assembly is lower in the second and following cycles.

The Indian Point Units 2 and 3 fuel, which was enriched to less than 3.5 wt% U-235 has been reviewed and the burnup averaged assembly peaking factor was always less than 1.35.

The moderator temperature increases as the water rises through the core. This depletion analysis uses a conservative outlet temperature for the entire length of the fuel. The moderator temperature is determined by multiplying the peaking factor times the enthalpy rise across the core. This delta enthalpy is added to the inlet enthalpy to determine an outlet enthalpy that is then converted to a temperature using the system pressure. The core inlet temperature and outlet temperature at Indian Point Units 2 and 3 have varied over the cycles, so the highest core enthalpy rise is used with the highest core inlet enthalpy. The calculation accounts for the effects of bypass flow. The resulting moderator temperature with a multi-cycle burnup averaged peaking factor of 1.35 is 628 °F (604.4 °K) and the moderator density is 0.64765 g/cc.

The moderator temperature for fuel where the enrichment is greater than 3.5 wt% U-235 requires projection of future peaking and operating conditions. Currently, the reload safety analysis utilizes a

limiting assembly average peaking factor of 1.40 at all times during the cycle. Using a multi-cycle assembly burnup average peaking factor of 1.40 and the highest core delta enthalpies from the past cycles, a moderator temperature of 631 °F (605.9 °K) and a moderator density of 0.64264 gm/cc was determined. This determination accounted for the effects of bypass flow. This approach is conservative, since an assembly cannot operate at the limiting peaking factor throughout its life.

The fuel temperature also needs to be maximized. The same assembly averaged peaking factors were used to burnup average the kw/ft. Figure 5.1 shows the fuel temperature as a function of peaking factor and burnup. These temperatures were generated with INTERPIN-3 [18] and provided in Ref. [32]. The depletion analysis model used a constant fuel temperature for the duration of the burnup. The fuel temperature used in the analysis was conservatively larger than the fuel temperature at any credited time of life (less than 45 GWd/T). The fuel temperature used for fuel under 3.5 wt% U-235 (i.e. fuel with a peaking factor of 1.35 or less) is 1075 °K (1475 °F) and for fuel over 3.5 wt% U-235 (i.e. fuel with a peaking factor of 1.40 or less), it is 1100 °K (1520 °F).

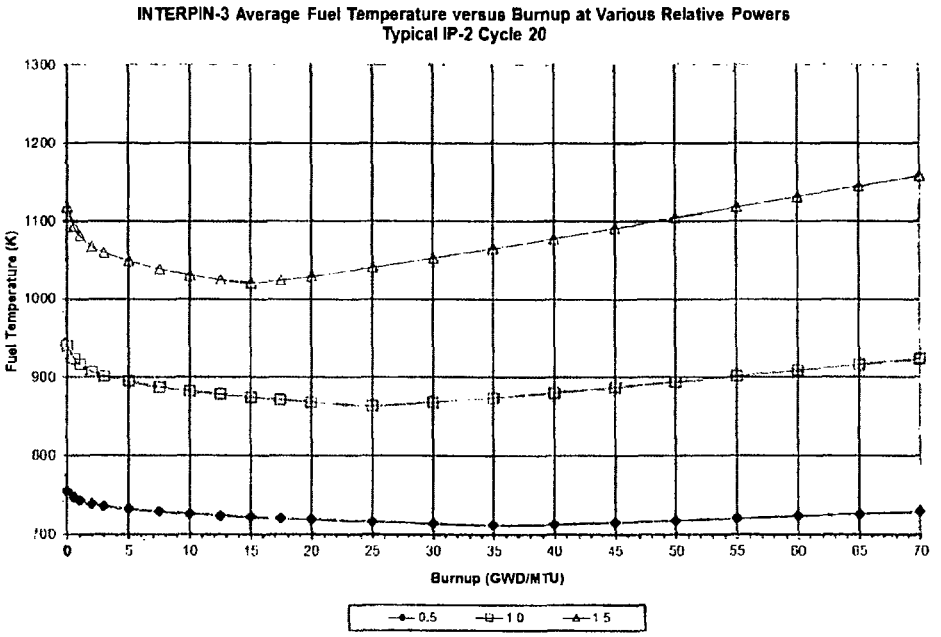

Figure 5.1: Fuel Temperature Change with Burnup and Relative Power

5.4 Limiting Depletion Parameters – Specific Power

ORNL has performed a study of the sensitivity of burnup credit to specific power and determined it is a small effect [17]. For burnup credit using all isotopes, a lower specific power is slightly more reactive. However, the reactivity effect of moderator temperature and fuel temperature increases with higher specific power. The reactivity effect of higher temperatures is larger than the reactivity effect of a lower specific power. Since the fuel can operate at only one specific power, a nominal specific power was selected in conjunction with conservatively selected higher temperatures. This approach is consistent with the ISG for spent fuel pool analysis [1].

As with specific power, the power history also has a small effect [17,19]. References 17 and 19 recommend ignoring any down time and assuming that the reactor is operated at full power over the entire depletion. Reference 19 saw a small positive reactivity increase when the last part of the depletion was performed at lower power. Lower specific power at end of cycle is more reactive because less Pm-149,

the precursor to Sm-149, is produced. This effect has been specifically accounted for in this analysis by reducing the Pm-149 that could be the result of a power coast down (see Section 5.9).

5.5 Limiting Depletion Parameters – Control Rod Operation

The Indian Point Units 2 and 3 have 193 fuel assemblies in the core. Nine of these assemblies are under the Control Bank D (less than 5% of the number of assemblies). Control Bank D is the only control bank allowed in the core at all if the power is greater than 70% of the rated power. Indian Point Units 2 and 3 have not operated with Control Bank D in the core for any significant burnup except at the "bite" position. The bite position is set as the location where the worth of the lead control bank is 2 pcm per step. The bite position changes from cycle to cycle and during cycle operation but is typically between 207 to 217 steps withdrawn, which corresponds to the rod being inserted 8.7 or less inches into the core. The top node in the axial model used for the criticality analysis is 8 inches.

For fuel that is less than or equal to 3.5 wt% U-235, the depletion assumption for the top node is that the control bank is in for the entire burnup. Since this fuel has already been discharged, no control rod insertion below the top node is needed in the analysis.

For fuel enriched above 3.5 wt% U-235, the assembly is depleted with a control rod inserted for 2 GWd/T. Due to the low relative power in the top node (about 0.5) (see Table 6.1), the depletion of the top node with a control rod is 1 GWd/T (all other nodes are burned for 2 GWd/T with the control rod).

Unit 3 never used control rods at the bite position, but Unit 2 positioned its D bank control rods at the bite position through cycle 17. All assemblies that were above 3.5 wt% U-235 enriched that were under Control Bank D for cycles 1 through 17 were evaluated as a special case in the depletion analysis. The reactivity penalty of the bite position versus no bite position was determined to be approximately 1 GWd/T additional required burnup. Each of these assemblies exceeded the burnup requirements by more than 4 GWd/T. Thus these assemblies are acceptable to be loaded in Region 2.

5.6 Summary of Depletion Assumptions for Fuel ≤ 3.5 wt% U-235

Since Pyrex burnable absorbers were not used in fresh fuel for enrichments greater than 3.5 wt% U-235 and IFBA rods were not used for enrichments less than 3.5 wt% U-235, separate depletion assumptions are used. The last fuel of 3.5 wt% U-235 enrichment or less was loaded in Unit 2 in cycle 9 and Unit 3 in cycle 7. Since it is not anticipated that future cycles will use fuel with enrichments less than 3.5 wt% U-235, it was possible to credit the actual operation of this fuel for the selection of limiting depletion parameters, such as the burnup averaged soluble boron concentration and the maximum assembly and burnup averaged moderator outlet temperature.

For fuel enriched to less than or equal to 3.5 wt% U-235 (old fuel), the following depletion assumptions are made:

a. Nominal fuel dimensions at 97.5% theoretical density
b. 800 ppm maximum average boron concentration during depletion (a multi-cycle average)
c. The specific power used during depletion is 39.8 w/g. This is about 8% higher than the nominal specific power (specific power has a very small effect on the final reactivity).
d. Moderator temperature during depletion calculated from a burnup average assembly peaking factor of 1.35 is 628. °F (604.4 °K) and the moderator density is 0.64765 g/cc.
e. Maximum average fuel temperature (or maximum average resonance temperature) during depletion is assumed to be 1075 °K (1475 °F).
f. Assembly is depleted with a 20 rodlet standard BP (Pyrex) and never removed. A Pyrex loading of 18.1 wt% (maximum) is assumed. This depletion will also cover any WABA depletion since WABAs are less limiting than Pyrex. No IFBA is assumed because IFBA was not introduced until later when the utility was ordering fuel greater than 3.5 wt% U-235.
g. A second depletion is performed with a 20 rodlet standard control rod and never removed. The isotopics from this depletion are used for the top node (top eight inches) in the criticality calculation. This assures that the criticality analysis is conservative even if a control rod were in the bite position for the entire life of the assembly.
h. For Pyrex, WABA and control rod depletion, Table 5.3 provides the dimensions and material used.

Table 5.3: Characteristics of Fuel Inserts

Parameter	Pyrex	Control Rod	WABA
Absorber ID (inches)	0.243	0	0.278
Absorber OD (inches)	0.396	0.3975	0.318
B_2O_3 wt%	18.1	-	-
B-10 mg/cm	-	-	6.03
Ag wt%	-	80	-
In wt%	-	15	-
Cd wt%	-	5	-
Absorber density (g/cc)	2.23	10.17	-

5.7 Summary of Depletion Assumptions for Fuel > 3.5 wt% U-235

For fuel enriched to more than 3.5 wt% U-235 (modern fuel), the following depletion assumptions are made (hereinafter referred to as modern depletion assumptions). These assumptions are based on a review of the operation history [30] and are selected to cover anticipated future fuel designs and operation.

a. Nominal fuel dimensions at 97.5% theoretical density
b. 1000 ppm maximum average boron concentration during depletion (a multi-cycle average).
c. The specific power used during depletion is 39.8 w/g (specific power has a very small effect on the final reactivity).
d. Moderator temperature during depletion calculated from a burnup average assembly peaking factor of 1.40 is 631 °F (605.9 °K) and the moderator density is 0.64264 g/cc.
e. Maximum average fuel temperature (or maximum average resonance temperature) during depletion is assumed to be 1100 °K (1520 °F). Maximum average fuel temperature in the top node is assumed to be 930 °K (1214 °F), corresponding to a relative power of 1.0.
f. The fuel assembly is depleted with a control rod inserted for 2 GWd/T. Then the assembly is depleted with a 20 rodlet WABA and never removed. The initial control rod depletion is to cover future extended part power operation with control rods inserted. Although generous, the 2 GWd/T burnup with control rods inserted still needs to be checked. This would be violated only if a fuel cycle is operated at less than full power with control rods for a significant amount of time (greater than 1.4 full power months during a 2 year fuel cycle).
g. In addition to the WABA, the fuel is assumed to have 148 IFBA pins in all but the top node. The IFBA B-10 loading is 1.5X [(mg B-10/inch)][a,c] to cover future designs (residual poison from IFBA is not credited in the criticality model).
h. Similar calculations are performed to confirm that an assembly with an initial WABA depletion that is subsequently placed on the core periphery with a Hafnium flux suppression insert is covered by an adder to the normal loading curve (see Section 8.4).
i. Since IFBA and WABA do not cover the full length of the active fuel, a special depletion for the top node is performed. For fuel enrichments greater than 3.5%, the top node is depleted with a control rod for 1 GWd/T nodal burnup (the axial burnup profile for the top node is always less than 0.5) and then a WABA (no IFBA) at ¼ of the boron and never removed.

j. Justification for this is that the practice of positioning the control rod in the bite position has been discontinued. The boron in a WABA never extends more than 6 inches from the top and the IFBA never extends more than 8 inches from the top of the active fuel region [24].

k. A special depletion was performed for 5.0 wt% fuel under a condition of 1300 ppm. This was done to allow burned fuel to be stored in Region 1 (see Section 8.1).

5.8 Depletion Analysis Details (Time Steps, etc.)

Using the above assumptions, UO_2 fuel was depleted at fuel enrichments of 2.0, 2.5, 3.0, 3.5, 4.0, 4.5, and 5.0 wt% U-235. The burnup points at which the isotopic data is collected are 150, 500, 1000, 1500, 2000, and then every 2000 MWD/MTU after that. Although the depletion is carried out with a full set of 388 nuclides, the isotopics used in the pool model is a reduced set (185 nuclides).

5.9 Reduced Power Operation at End of Life

At end of cycle, the reactor power may be reduced (for example, a planned coastdown). One of the key absorbing fission products, Sm-149, reaches an equilibrium concentration during power operation that is independent of power. However, its precursor, Pm-149, is directly proportional to power. At a reduced power, there is less Pm-149. Pm-149 decays into Sm-149 with a 2.2 day half-life. Thus, if a reactor reduces power at end of cycle, there would be less Sm-149 in the cooled fuel, which is a positive reactivity effect. Therefore, ignoring low power operation during the last month is non-conservative. To account for this effect, the amount of Pm-149 is reduced to one half of the full power content for all criticality calculations (which results in a penalty of about 100 pcm). This covers coastdowns to 50% power. This approach covers all past operating experience and anticipated future operation at the Indian Point plants.

6 Rack Model

This Section describes the infinite models used in most of the analysis. A full pool model was also created to test the reduced burnup requirements for peripheral assemblies, the Region 1/Region 2 interface and to perform analyses of the Dropped Assembly and Misplaced Assembly accidents. The full pool model is described in Section 8.10.

All the infinite models discussed in this Section are finite axially. Section 6.3 describes the axial modeling of the fuel. Above and below the fuel, the models have 50 cm of water followed by a zero flux boundary condition.

Water at the maximum possible density (1.00 g/cc at 4 °C) is assumed, which results in the largest reactivity for both Regions (see Table 8.9).

The Boraflex sheathing width ranges from 7.70 to 8.00 inches (see Table 3.1). The minimum value is used in Region 1, while the maximum value is used in Region 2, because calculations demonstrated that this results in the highest reactivity in each respective region (see Table 7.2). The stainless steel plate that covers the Boraflex is 0.112 ±_____ and 0.092 ±_____ inches off the cell walls for Regions 1 and 2 respectively (from Table 3.1). Since using a smaller separation from the cell wall means that less water is on the inside that is balanced by more water on the outside (and vice versa for a larger distance), this tolerance has no effect on the total mass of water. Therefore, the reactivity effect of this tolerance is insignificant, so the nominal separation is used for all the analyses.

6.1 Region 1 Infinite 2x2 Model

Figure 6.1 is a picture from the KENO model for Region 1.

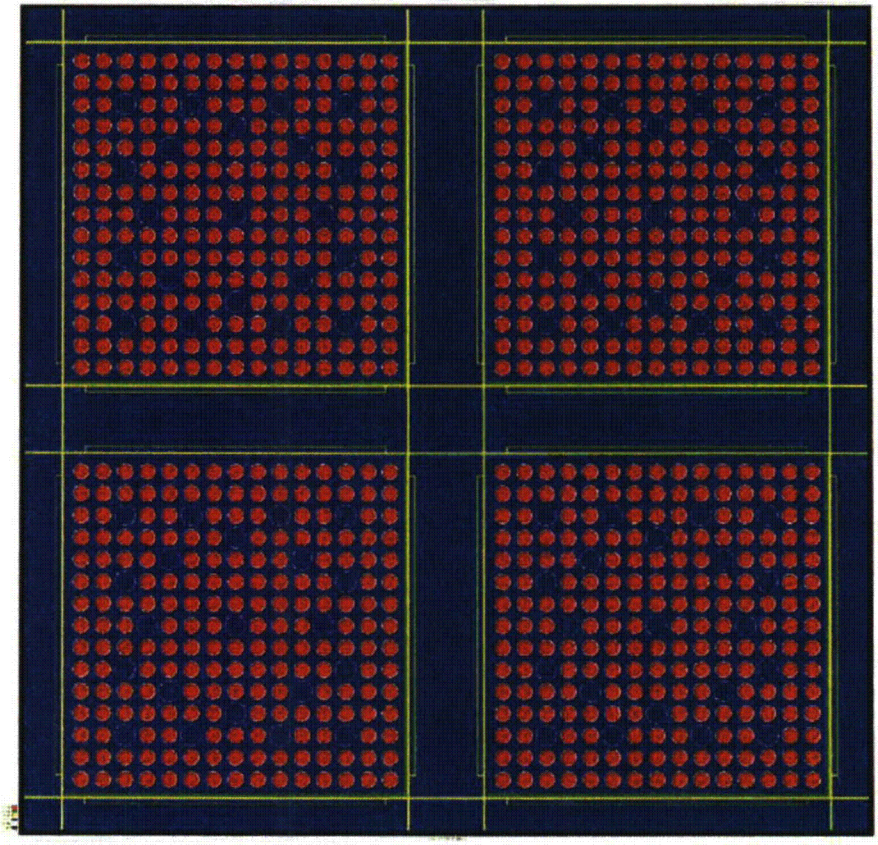

Figure 6.1: Region 1 KENO Model

The absorber panel is shown in green. Inside the Boraflex sheathing is water. No Boraflex is in the model. If any Boraflex material remains, the remaining boron in the material makes the reactivity more negative than water.

The only simplification made is that the connecting steel between cells is modeled as an extension of the cell wall rather than a separate piece of steel. The connecting steel is slightly thicker than the cell wall thickness and modeling it as equal to the cell wall thickness has no effect (as illustrated by the results in Table 7.2).

6.2 Region 2 Infinite 2x2 Model

Figure 6.2 is a picture from the KENO model for Region 2.

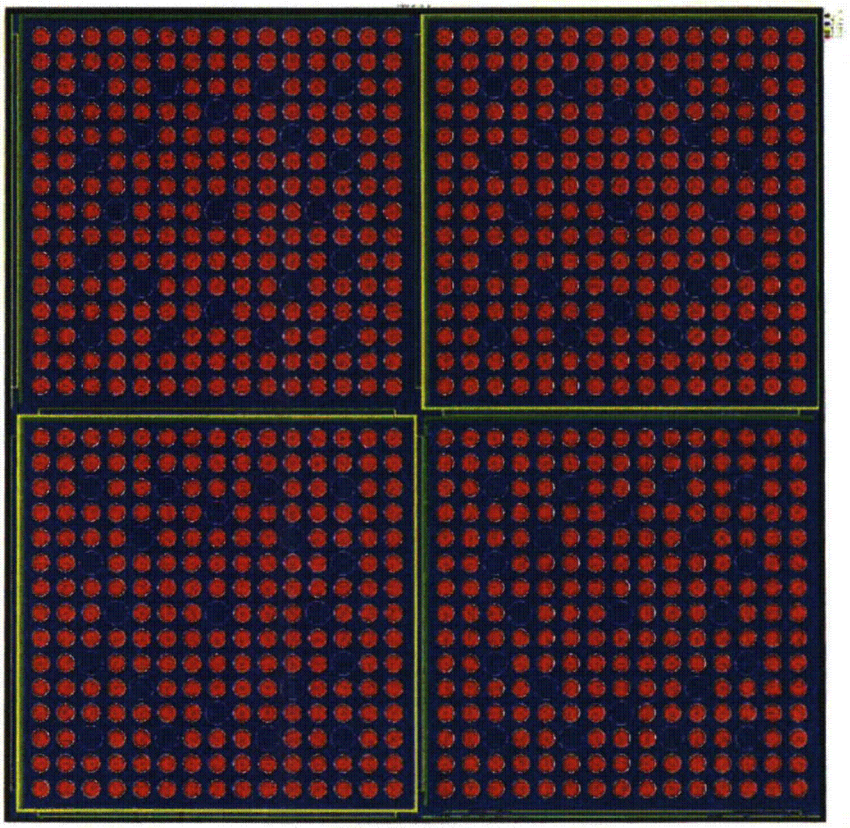

Figure 6.2: Region 2 KENO Model

All of the features of the rack are modeled explicitly. The bottom left of the model is a complete cell box with its Boraflex sheathing. The model is two cell pitches. This requires cutting the cell wall into two pieces. When the periodic boundary condition is applied, the two cell wall pieces fit together to precisely match the actual rack dimensions.

For the alternate panel design, the panel consists of two absorber panels connected with a stainless steel connector. This is modeled as the two panels connected with a zirconium connector that is 0.10 inch thick (shown in Figure 6.3 below). This conservatively accounts for the water displacement of the connector without adding any significant absorbing material.

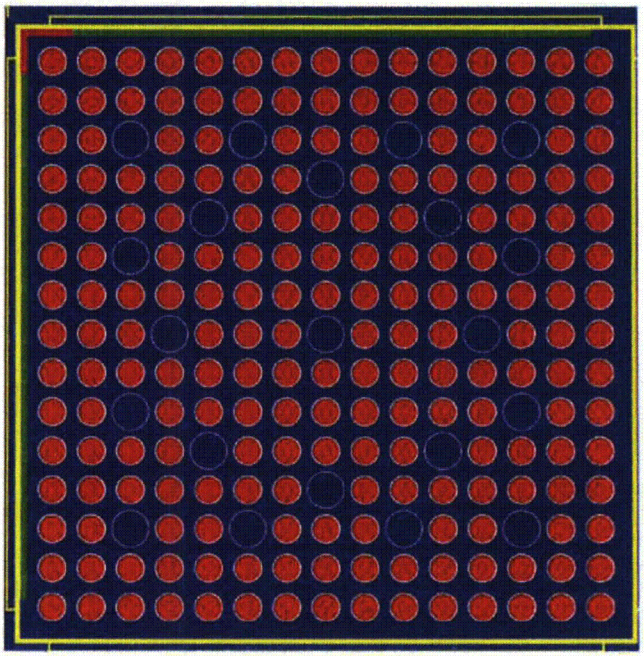

Figure 6.3: KENO Model of the Alternate Panel Design

6.3 Axial Burnup Distribution

To model the fuel assembly isotopic content in three dimensions, an axial burnup profile is needed. For this analysis, the limiting profiles from NUREG/CR-6801 [20] are used. Table 6.1 is taken from NUREG/CR-6801.

Table 6.1: Axial Burnup Profile vs. Burnup Bin [20]

Burnup group	1	2	3	4	5	6	7	8	9	10	11	12
Axial height (%)	Burnup ranges (GWd/MTU)											
	>46	42-46	38-42	34-38	30-34	26-30	22-26	18-22	14-18	10-14	6-10	<6
2.78	0.582	0.666	0.660	0.648	0.652	0.619	0.630	0.668	0.649	0.633	0.658	0.631
8.33	0.920	0.944	0.936	0.955	0.967	0.924	0.936	1.034	1.044	0.989	1.007	1.007
13.89	1.065	1.048	1.045	1.070	1.074	1.056	1.066	1.150	1.208	1.019	1.091	1.135
19.44	1.105	1.081	1.080	1.104	1.103	1.097	1.103	1.094	1.215	0.857	1.070	1.133
25.00	1.113	1.089	1.091	1.112	1.108	1.103	1.108	1.053	1.214	0.776	1.022	1.098
30.56	1.110	1.090	1.093	1.112	1.106	1.101	1.109	1.048	1.208	0.754	0.989	1.069
36.11	1.105	1.086	1.092	1.108	1.102	1.103	1.112	1.064	1.197	0.785	0.978	1.053
41.69	1.100	1.085	1.090	1.105	1.097	1.112	1.119	1.095	1.189	1.013	0.989	1.047
47.22	1.095	1.084	1.089	1.102	1.094	1.125	1.126	1.121	1.188	1.185	1.031	1.050
57.80	1.091	1.084	1.088	1.099	1.094	1.136	1.132	1.135	1.192	1.253	1.082	1.060
58.33	1.088	1.085	1.088	1.097	1.095	1.143	1.135	1.140	1.195	1.278	1.110	1.070
63.89	1.084	1.086	1.086	1.095	1.096	1.143	1.135	1.138	1.190	1.283	1.121	1.077
69.44	1.080	1.086	1.084	1.091	1.095	1.136	1.129	1.130	1.156	1.276	1.124	1.079
75.00	1.072	1.083	1.077	1.081	1.086	1.115	1.109	1.106	1.022	1.251	1.120	1.073
80.56	1.050	1.069	1.057	1.056	1.059	1.047	1.041	1.049	0.756	1.193	1.101	1.052
86.11	0.992	1.010	0.996	0.974	0.971	0.882	0.871	0.933	0.614	1.075	1.045	0.996
91.67	0.833	0.811	0.823	0.743	0.738	0.701	0.689	0.669	0.481	0.863	0.894	0.845
97.22	0.515	0.512	0.525	0.447	0.462	0.456	0.448	0.373	0.284	0.515	0.569	0.525

In general, the profile becomes less limiting as the burnup increases. However, there are some burnup bins in which the profile becomes more severe as the burnup increases. For example, an assembly having a burnup of 15 GWd/T would have to use a very reactive shape (14-18), but if the burnup were only 13 GWd/T, the shape is much less reactive. To ensure that all burnup bins are conservative, a burnup bin that has this characteristic (the shape is less severe at a lower burnup) is assumed to have the more limiting shape from the higher burnup. So the burnup profile used in the entire range 0-18 GWd/T is the one in the 14-18 GWd/T burnup bin. Furthermore, there are discontinuities at the burnup bin boundaries. To eliminate these discontinuities in a conservative manner, the shape in any bin is assumed to occur at the maximum burnup in the bin and for any burnup in between these burnup points, the shape is linearly interpolated (the shapes are not changing rapidly between burnup bins). For example, suppose an assembly has a burnup of 39 GWd/T. Using NUREG/CR-6801 directly, the top node would have a

relative burnup of 0.525. In this analysis, however, the top node would have a relative burnup of only 0.467 (linearly interpolating between 0.447 at 38 GWd/T and 0.525 at 42 GWd/T). This ensures no discontinuities and all burnup shapes are conservative.

According to Reference [23], the assembly having the most reactive axial burnup profile of all Indian Point fuel is R-08. This profile was modeled in a 4.5 wt% assembly burned to 39 GWd/T and cooled for 72 hours (the approximate loading curve burnup). The k using the R-08 profile was 0.9547. The k using the DOE shape was 0.9632, which shows that the DOE shape is bounding even for R-08. Furthermore, R-08 is actually axially blanketed (top blanket enriched to 2.6 wt%) *and* the top node was under a control rod for its entire depletion. So the R-08 profile is very unrealistic and not physical for non-blanketed fuel. In order to determine a more realistic reactivity, the axial blanket and control rod depletion were modeled explicitly and the k decreased to 0.9388. So the DOE shapes in conjunction with non-blanketed fuel are bounding for all the non-blanketed fuel at Indian Point and conservative for axial blanket fuel.

For the analysis, the lower 10 nodes were averaged into one node. This does not affect the calculation of k, since the top half of the assembly dominates the reactivity. In fact, averaging the lower 10 nodes effectively brings the bottom lower burned fuel toward the more reactive top so the approach is conservative (but a negligible effect).

6.4 Interpolation of Isotopics and Cooling Time Verification

With isotopics from the depletion calculations recorded every 2 GWd/T (see Section 5.8), the isotopics at any particular burnup can be interpolated. Since the burnup delta is small between burnup points, linear interpolation can be used. To validate this approach, the isotopics at 40 GWd/T were interpolated from the OPUS plot files (OPUS plot files are an output option in the TRITON module of SCALE) at 38 GWd/T and 42 GWd/T at 5.0 wt% U-235 enrichment. The isotopics were input into the Region 2 KENO model and the calculated k was 0.96653 ± 0.00015. Another case used isotopics directly from the OPUS plot files at 40 GWd/T. The calculated k was 0.96651 ± 0.00015. The difference is well within the Monte Carlo statistics. A similar verification was performed at 11 GWd/T, where an

interpolation between 9 and 13 was compared to the direct calculation at 11 GWd/T. The calculated k using the direct isotopics was 1.1366 ± 0.0002, while the interpolated case was 1.1362 ± 0.0002, a difference of only 0.0004, which is within the expected Monte Carlo variation.

To check the cooling time model used in the interpolation program, a special depletion was performed at 5.0 wt% U-235 to a burnup of 40 GWd/T. Then SCALE was used to decay the isotopes for 72 hours, 1 year, 5 years, and 25 years. The interpolation program was also used to decay the isotopes to the same cooling times. Table 6.2 shows the results of the verification of the cooling time. The differences are within the Monte Carlo statistics (2 sigma of ± 0.0004) except for the case at 25 years. The calculated k from the interpolation program at 25 years is conservative.

Table 6.2: Verification of Cooling Time Model in the Interpolation Program

Cooling Time	SCALE/ORIGEN k	Interpolation Program k	Difference
72 hours	1.0023	1.0023	-
1 year	0.9993	0.9996	0.0003
5 years	0.9847	0.9848	0.0001
25 years	0.9449	0.9457	0.0008

6.5 Convergence of Calculations

The convergence of the 2x2 (or 1x1) reflected model k calculation was generally achieved after only a few hundred generations. However, all of the CSAS5 computer runs use a Monte Carlo sampling of at least 1500 generations and 6000 neutrons per generation. Convergence could have been a problem in the past, when very few neutron histories were run (300,000 total neutron histories vs. 9 million today).

The full pool model convergence required knowledge of the most reactive location to be used for a starting source. When the most reactive location was not known, several starting sources were used.

6.6 *Summary of Modeling Assumptions*

The following is a summary of the modeling assumptions:

1. Bounding fuel stack density and bounding dimensions for pellet OD, clad OD/ID, and guide tube OD/ID are used.

2. Axial blankets are ignored.

3. Grids are ignored (grids displace water which causes k to decrease).

4. No Boraflex in the Boraflex sheathing and the Boraflex is replaced with water (if any Boraflex remained, it would be less reactive than water).

5. NUREG/CR-6801 bounding axial burnup profiles are used for all fuel (bounding for non-blanketed fuel and is conservative for axial blanket fuel).

6. Top and bottom of fuel assembly is 50 cm of water (conservative compared to 50/50 steel/water and other minor end fitting components – see Section 8.5).

7. Isotopics can be linearly interpolated between burnup steps that are 2 GWD/T apart (verified by comparison to non-interpolated isotopics).

8. Periodic boundary conditions are used to represent an infinite array.

7 Sensitivity Analysis

This Section presents analysis of the sensitivity of the models to the manufacturing tolerances. After the sensitivity is determined, the rack up of the uncertainties and biases is presented.

7.1 Tolerances

Calculations were performed to quantify the reactivity effect of changes due to manufacturing tolerances. For Region 2 the tolerance calculations were performed at the highest credited burnup conditions (5 wt% U-235 and 42.67 GWd/T) and a low burned condition (2.5 wt% U-235 and 12.31 GWd/T). Table 7.1 presents the tolerance reactivity effects for Region 1 (fresh 5 wt% U-235 fuel) and Region 2. The tolerance effects were not very sensitive to the enrichment/burnup conditions and the largest values from Table 7.1 are used in the rack up of uncertainties.

Table 7.1: Tolerance Reactivity Effects

Tolerance	Value (in)	Δk Region 1	Δk Region 2
High Burnup Case			Base k = 0.9639
Fuel pin pitch	+0.0014		0.0021
Rack cell pitch - horizontal	___		0.0035*
Rack cell pitch - vertical	___		
Rack cell ID	___		0.0002
Rack cell wall thickness	±0.007		0.0002
Boraflex sheathing thickness	±0.003		0.0001
Eccentricity	-		0.0001
Fuel Enrichment	+0.05%		0.0030 @ 5.0
Low Burnup Case		Base k = 0.9717	Base k = 0.9696
Fuel pin pitch	+0.0014	0.0022	0.0016
Rack cell pitch - horizontal	___	0.0039	0.0035*
Rack cell pitch - vertical	___	0.0041	
Rack cell ID	___	0.0020	0.0001
Rack cell wall thickness	±0.007	0.0008	0.0002
Boraflex sheathing thickness	±0.003	0.0004	0.0001
Eccentricity	-	0.0001	0.0001
Fuel enrichment	+0.05%	0.0022 @ 5.0 wt%	0.0050 @ 2.0 wt%

* Both horizontal and vertical pitch were changed at the same time in Region 2

PWR fuel assemblies are designed to be under moderated at power, so the moderator temperature coefficient is negative to prevent large power excursions. Therefore, increasing water between the fuel rods (and ignoring grids) increases k. This is demonstrated by calculations of the reactivity from varying the pin pitch (shown in Table 7.1), guide tube diameter (Table 7.2), and the fuel clad outer diameter (Table 7.2). For this analysis, the fuel pin clad outer diameter is set to its minimum value. Also, the water displacement of the guide tubes is at the minimum. These parameters have sufficiently small tolerances that bounding values were used. The grids are conservatively ignored since they displace water around the fuel pins. The fuel pin pitch tolerance (0.0014 inch) used in this analysis is the maximum pin separation possible before assemblies would touch in the reactor. The impact of increasing the pin pitch is one of the larger reactivity effects from the manufacturing tolerances. Since it causes a change in the spectrum in the assembly, the reactivity effect is about the same in Region 1 and Region 2.

The fuel enrichment uncertainty used here is the uncertainty associated with ordering fuel. The as-built uncertainty is much smaller. Once the as-built enrichment is known, the as-built enrichment should be used to compare against the loading curve. If the as-built enrichment is not known, then it is acceptable to use the ordered enrichment. The fuel enrichment uncertainty in Region 2 is a function of enrichment and is linearly interpolated using the two points shown in Table 7.1 (the uncertainty changes monotonically between enrichments).

A tighter rack cell pitch increases k of the pool for both regions because the fuel assemblies are closer together. Also, a tighter pitch reduces the moderation prior to the neutrons hitting the absorber panels. The Region 1 change in k for reducing the cell pitch is much larger due to the decrease in the flux trap. However, since the vertical and horizontal tolerances are independent of each other, the net effect for Region 1 is only mildly larger than Region 2.

In calculating the reactivity of increasing the cell ID, the cell pitch is maintained. This means the reactivity effect in Region 1 is mainly due to decreasing the flux trap. Region 2 is not a flux trap design, so the effect on k is small.

Calculations demonstrated that having maximum water at the edge of the cell maximizes the reactivity in Region 1, while having minimum water at the edge maximizes the reactivity in Region 2 (see Table 7.2). Since bounding values are used for the absorber panel thickness and the Boraflex sheathing width, a minimum panel thickness and minimum Boraflex sheathing width are used in Region 1, while a maximum panel thickness and maximum sheathing width are used in Region 2.

Eccentric positioning of the assemblies in the cell (moving four assemblies together in a repeating infinite array) has very little effect on k. In fact, the effect was smaller than the expected Monte Carlo variation, even after increasing the number of neutrons being followed by a factor of 4. This result is common for racks with absorber panels. This negligible eccentricity is included as an uncertainty.

Calculations confirmed that the highest reactivity occurs with maximum water density (see Section 8.7). Therefore, all analyses were performed at a water density of 1.00 g/cc (4 °C).

Table 7.2: Miscellaneous Reactivity Effects

Case (base k =0.9639)	Δk from base	Notes
Max panel thickness in Region 1	-0.0003	Min thickness is limiting
Max sheathing width in Region 1	0.0000	Within statistics
Min panel thickness in Region 2	-0.0003	Max thickness is limiting
Min sheathing width in Region 2	-0.0002	Max width is limiting
Guide and Instrumentation Tube Diameter reduced to OFA dimensions	0.0000	Within statistics
Decrease clad ID by [ ]^{a,c} inch	-0.0001	All of these results show that the correct bounding fuel dimensions are being used
Increase clad OD by [ ]^{a,c} inch	-0.0024	
Decrease pellet density by 1%	-0.0001	
Decrease pellet OD by [ ]^{a,c} inch	-0.0002	
Decrease GT ID by [ ]^{a,c} inch	-0.0002	
Increase GT OD by [ ]^{a,c} inch	-0.0002	

No calculations of sensitivities were made with borated water. The borated conditions have excess margin, which cover any differences in sensitivity with borated water.

7.2 Calculation of Biases and Uncertainties

The total bias and uncertainty that needs to be applied to the raw calculated k consists of the following components:

- Bias and uncertainty from the critical experiment validation
- Bias and uncertainty from the depletion reactivity validation
- Fuel tolerance uncertainties for pin pitch and enrichment
- Rack tolerance uncertainties for cell pitch, cell ID, cell wall thickness, and sheathing thickness
- Uncertainty for eccentric positioning
- Uncertainty in the reactor record burnup
- Monte Carlo statistical uncertainty in the k calculations

The biases are added together and the uncertainties are statistically combined. From the validation section, the critical experiment bias is 0.0029 for unborated conditions and 0.0037 for borated conditions. The critical experiment uncertainty is 0.0050 for both unborated and borated conditions. The depletion reactivity bias is 0.003 using the EPRI benchmarks (see Section A.4.2). Alternatively, using the Extended ISG-8 approach (see Section A.4.3.4) the depletion reactivity bias is 1.5% of the minor actinide and fission product worth. At 5.0 wt%, 43 GWd/T, 72 hour cooling in Region 2, a calculation determined that the minor actinide and fission product worth is 0.1168 (1.0677 – 0.9509). So the bias using the extended ISG-8 approach at 43 GWd/T is 0.1168*0.015 = 0.0018. The depletion reactivity uncertainty using the EPRI benchmarks is 0.0064 for all burnups. The depletion reactivity uncertainty using ISG-8 (chemical assays) is 0.0002 x BU from Section 4. So at 43 GWd/T, the chemical assay uncertainty is 0.0086. It turns out that the combination of a smaller bias and a larger uncertainty for the ISG-8 approach

is less limiting than using the EPRI benchmarks at 43 GWd/T. Since the maximum burnup in the loading curves is only 42.67 GWd/T (5 wt%, 0 years cooling time), the EPRI benchmarks are used for the depletion reactivity bias (0.003) and uncertainty (0.0064).

The uncertainty in the reactor record burnup is assumed to be 5% of the burnup. The effect on reactivity can be calculated by comparing the k calculated for the same enrichment at two different burnups. For example, at 5.0 wt% U-235, the k at 38 GWd/T was 0.9948 while the k at 42 GWd/T was 0.9658. So the Δk due to a 5% burnup uncertainty at 42 GWd/T is

$$(0.9948 - 0.9658)*0.05*42 / (42 - 38) = 0.0152\ \Delta k$$

The same calculation at 3.0 wt%, 18 GWd/T (using calculated k's at 18 and 21 GWd/T) is

$$(0.9943 - 0.9592)*0.05*18 / (21 - 18) = 0.0105\ \Delta k$$

To simplify the burnup uncertainty calculation for all burnups greater than 18 GWd/T, the following linear relationship is derived from these two points.

$$\text{Burnup Uncertainty } (\Delta k) = 0.0072 + 0.00019 \times BU$$

This relationship was found to be conservative for all burnups greater than 18 GWd/T and overly conservative for burnups less than 18 GWd/T. For burnups less than 18 GWd/T, the maximum slope was found to be 0.005 Δk per GWd/T and so the burnup uncertainty is:

$$0.005 \times .05 \times BU = 0.00025 \times BU$$

As an example of the total rack up, Table 7.3 summarizes all of the biases and uncertainties for 5.0 wt% U-235 fuel burned to 43 GWd/T in Region 2 under unborated conditions.

Table 7.3: Rack Up of Biases & Uncertainties in Region 2 for 5 wt% Fuel at 43 GWd/T

Uncertainty	Bias	Δk
Validation (critical experiments)	0.0029	0.0050
Depletion reactivity uncertainty	0.0030	0.0064
Burnup uncertainty	-	0.0154
Fuel pin pitch	-	0.0021
Fuel enrichment	-	0.0030
Rack cell pitch	-	0.0035
Rack cell ID	-	0.0002
Rack cell wall thickness	-	0.0002
Boraflex sheathing thickness	-	0.0001
Eccentricity	-	0.0001
Monte Carlo statistics	-	0.0005
Total Rack Up (Δk = RSS)	0.0059	0.0182
Total Bias and Uncertainty		**0.0241**

In this example, the bias plus uncertainty is 0.0241. To provide an engineering margin of 0.01, the target k would be 0.99 – 0.0241 = 0.9659. Note that the uncertainty is dominated by the validation, depletion and burnup uncertainty. Small changes in the manufacturing tolerances will have no effect on the statistically combined uncertainties.

Table 7.4 presents the rack up of biases and uncertainties for Region 1 with fresh fuel. For Region 1, the target k would be 0.99 – 0.0111 = 0.9789. For burned fuel in Region 1, we would also have to add burnup and depletion reactivity biases and uncertainties, which would increase the total bias and uncertainty to 0.0167 at 12 GWd/T. So the target k for burned fuel in Region 1 would be 0.9733.

For the borated condition, the uncertainties will be slightly different [27] but these differences are insignificant when compared to the large margin for the borated condition shown in Section 8.

* Using the Extended ISG-8 approach, the depletion bias is 0.0018 and the depletion uncertainty is 0.0086. Using these values in the total rack up, the total bias is 0.0047 and the total uncertainty is 0.0191 for a total bias and uncertainty of 0.0238, which shows that using the EPRI depletion bias and uncertainty is more limiting (0.0241) than using the Extended ISG-8 approach.

Table 7.4: Rack Up of Biases and Uncertainties for Region 1

Uncertainty	Bias	Δk
Validation (critical experiments)	0.0029	0.0050
Depletion reactivity uncertainty	-	-
Burnup uncertainty	-	-
Fuel pin pitch	-	0.0022
Fuel enrichment*	-	-
Rack cell pitch - horizontal		0.0039
Rack cell pitch - vertical	-	0.0041
Rack cell ID	-	0.0020
Rack cell wall thickness	-	0.0008
Boraflex sheathing thickness	-	0.0004
Eccentricity	-	0.0001
Monte Carlo statistics	-	0.0005
Total Rack Up	0.0029	0.0082
Total Bias and Uncertainty		**0.0111**

* If 5.0 wt% is assumed in the criticality model, the enrichment uncertainty is zero because the maximum nominal enrichment of the fuel is 4.95 wt%.

8 Results

With the biases and uncertainties determined, the minimum loading requirements can be calculated. These minimum loading requirements meet the 10CFR50 requirements. Specifically, $k_{95/95}$ must be less than 1.0 with no soluble boron credit and less than 0.95 with credit for soluble boron. For this analysis, these limits are met while maintaining a 1% margin in k. Therefore, for this analysis, it has been demonstrated that for all unborated cases $k_{95/95}$ is less than 0.99 and for the borated cases $k_{95/95}$ is less than 0.94 after adding biases and uncertainties.

8.1 Region 1

Table 8.1 below summarizes the Region 1 results.

Calculations show that fresh 5.0 wt% U-235 fuel with 48 IFBA rods can be stored in Region 1 to meet the criticality requirements ($k_{95/95} < 0.99$ after accounting for all biases and uncertainties). The calculated k for this case is 0.9717. After adding Region 1 biases and uncertainties of 0.0111 from Table 7.4, the $k_{95/95}$ is 0.9828. For fresh 5.0 wt% U-235 fuel with no IFBA rods, the assemblies can be stored on the periphery of Region 1 (see Section 8.10) or they can be stored anywhere if they have a control rod inserted.

For burned fuel, no credit is taken for IFBA or any insert in the guide tubes. Calculations show that 5.0 wt% U-235 fuel burned to 12 GWd/T meet the criticality requirements for Region 1. Note that for this particular depletion, a soluble boron concentration of 1300 ppm was used so that once burned fuel that was in a very short cycle can still be stored anywhere in Region 1 as long as the minimum burnup of 12 GWd/T is met. Burned fuel with less than 12 GWd/T burnup can be stored on the periphery of Region 1 or stored anywhere in Region 1 if the fuel assembly has a control rod inserted.

Table 8.1: Calculated k's in Region 1

Case	k	Bias & Uncertainty	$k_{95/95}$
Base Case (5.0 wt% U-235 fuel with 48 IFBA)	0.9717	0.0111	0.9828
Burned Fuel (5.0 wt% U-235 burned to 12 GWd/T at 1300 ppm)	0.9650	0.0167	0.9817
1 out of 4 cells filled with water (no absorber panel in cell)	0.9144	0.0111	0.9255
Empty cell filled with air	0.9245	0.0111	0.9356
Empty cell filled with aluminum	0.9255	0.0111	0.9366
Empty cell filled with concrete	0.9222	0.0111	0.9333
Empty cell filled with steel	0.9233	0.0111	0.9344
Empty cell filled with Zircaloy	0.9255	0.0111	0.9366
Missing panel, control rod in fuel assembly (base case fuel)	0.9729	0.0111	0.9840
5.0 wt% U-235, no IFBA, control rod in fuel assemblies	0. 7964	0.0111	0.8075
Base Case with alternate panel design 0.022 areal density	0.9716	0.0111	< 0.99*
Burned Fuel Case with alternate panel design 0.022 areal density	0.9645	0.0167	0.9812

8.1.1 Missing Panel in Region 1

A case was also run in which there is an empty cell that has no absorber panel (one empty cell out of four cells in the 2x2 array). The lack of fuel in the cell more than offsets the reactivity due to the lack of an absorber panel in the cell. The cell does not have to be empty, only that there is no fuel. Concrete, steel, air, Zircaloy, aluminum and water were modeled and all of these materials meet the criticality requirements (see Table 8.1). Alternatively, a fuel assembly can be placed in the cell having the missing absorber panel as long as it contains a control rod (a control rod is worth more than an absorber panel, see Table 8.1). Placing a fuel assembly into a cell that has a missing panel is considered an accident (see Section 9).

* To allow for small changes in k due to minor variations in the final design of the alternate panel

8.1.2 Alternate Panel Design in Region 1

The fresh fuel, 48 IFBA case was run for the alternate panel design at an areal density of 0.022 g $^{10}B/cm^2$ and the calculated k was 0.9716 compared to the base case of 0.9717. Even if there was a slight difference in tolerance effects due to the alternate panel design, there is 0.007 margin to the design goal of 0.99. Since the most reactive fuel was analyzed, the alternate design will result in a $k_{95/95}$ less than 0.99.

8.2 Region 2

The minimum burnup requirements (loading curve) for Region 2 are presented in Table 8.2.

Table 8.2: Minimum Burnup Requirements (GWd/T) in Region 2

Enrichment* (wt% U-235)	Cooling Time (years)						
	0†	1	2	5	10	15	25‡
2.0	3.20	3.10	3.08	3.00	3.00	3.00	3.00
2.5	15.17	14.85	14.66	13.97	13.20	12.84	12.31
3.0	21.28	21.17	20.98	20.66	20.26	19.98	19.65
3.5	27.53	27.10	26.63	25.56	24.29	23.50	22.45
4.0	33.82	33.43	33.05	32.04	30.72	29.70	28.44
4.5	38.98	38.65	37.99	36.49	34.67	33.69	32.60
5.0	42.67	42.14	41.78	40.78	39.72	38.96	37.68

Table 8.2 gives the burnup requirement in GWd/T as a function of initial U-235 enrichment and cooling time. As discussed later, the burnup requirements are adjusted if the assembly had a hafnium insert, has fuel pins removed, or is placed on the periphery. The table can be linearly interpolated to find the required burnup at any enrichment/cooling time combination. No extrapolation is allowed, so fuel at enrichments less than 2.0 wt% U-235 must use the 2.0 wt% U-235 minimum burnup requirements and fuel cooled more than 25 years must use the 25 year cooling value. For illustrative purposes only, the

* For axially blanketed fuel, the enrichment to be used is the enrichment of the center section between the blanket material
† No cooling is actually 72 hours. This is the cooling time that maximizes k
‡ Fuel cooled to more than 25 years must use the 25 year burnup requirements

loading curve is compared to the 2013 inventory in the Indian Point Unit 2 spent fuel pool as shown in Figure 8.1. This figure shows that only a few assemblies violate the loading curve and would have to be stored in Region 1 or contain a control rod if in Region 2.

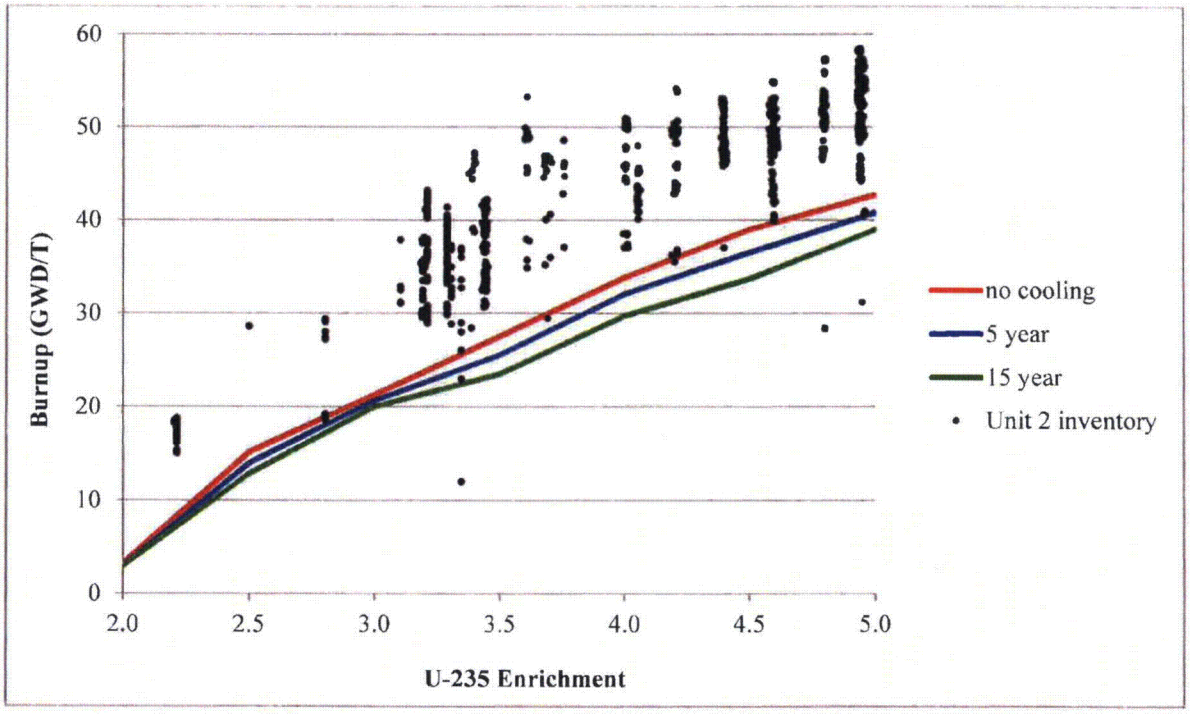

Figure 8.1: Loading Curve vs. Unit 2 Inventory (2013)

8.2.1 Curve Fit

The burnup values in Table 8.2 can be fit to a curve having the following functional form where *enr* is the initial U-235 enrichment in wt% and *CT* is the cooling time in years:

$$(A1 + A2enr + A3enr^2 + A4enr^3)\ \exp[-(A5 + A6enr + A7enr^2 + A8enr^3)\ CT\ ] + A9 + A10enr + A11enr^2 + A12enr^3$$

Two curves were generated – one curve for enrichments from 2.0 to 3.5 and another one for enrichments greater than 3.5 to 5.0. The resulting coefficients are shown in Table 8.3. The coefficients contain an adjustment to ensure that all burnups calculated by the equation are greater than the burnups

from the table. Using the curve fit results in a maximum penalty of 0.2 GWd/T for low enrichments and 0.4 GWd/T for high enrichments when compared to the tabulated values shown in Table 8.2.

Table 8.3: Coefficients for Curve Fit of Minimum Burnup Requirements

Coefficient	Enrichment 2.0 – 3.5 wt% U-235	Enrichment >3.5 – 5.0 wt% U-235
A1	-226.183	448.616
A2	257.56	-327.34
A3	-95.573	79.9045
A4	11.6921	-6.43034
A5	0.957861	0
A6	-0.57489	0
A7	0.092684	0.013029
A8	0	-0.00203
A9	0.1	-481.261
A10	-29.7478	343.449
A11	22.7422	-78.3549
A12	-3.56276	6.07956

8.2.2 Confirmation Calculations for Region 2

To be sure that all burnup/enrichment/cooling time combinations given in the loading curve meet the criticality requirements, each loading curve burnup/enrichment/cooling time point was run in the 2x2 KENO model to verify that each point meets the criticality requirements. The calculated k's are shown in Table 8.4.

Table 8.4: Calculated k Values at Each Burnup Point

Enrichment (wt% U-235)	Cooling Time (years)						
	0	1	2	5	10	15	25
2.0	0.9718	0.9710	0.9708	0.9707	0.9700	0.9696	0.9689
2.5	0.9699	0.9698	0.9695	0.9698	0.9704	0.9698	0.9697
3.0	0.9660	0.9657	0.9658	0.9654	0.9652	0.9650	0.9646
3.5	0.9672	0.9671	0.9672	0.9669	0.9672	0.9670	0.9676
4.0	0.9661	0.9659	0.9656	0.9654	0.9657	0.9663	0.9668
4.5	0.9642	0.9641	0.9660	0.9660	0.9656	0.9651	0.9650
5.0	0.9651	0.9646	0.9641	0.9642	0.9632	0.9635	0.9652

The total uncertainty is the bias plus a statistical combination of all the uncertainties (see Section 7.2). These total uncertainties are shown in Table 8.5.

Table 8.5: Total Bias and Uncertainty at Each Burnup Point

Enrichment (wt% U-235)	Cooling Time (years)						
	0	1	2	5	10	15	25
2.0	0.0164	0.0164	0.0164	0.0164	0.0164	0.0164	0.0164
2.5	0.0169	0.0168	0.0168	0.0168	0.0167	0.0167	0.0166
3.0	0.0210	0.0210	0.0210	0.0209	0.0209	0.0209	0.0208
3.5	0.0219	0.0218	0.0217	0.0216	0.0214	0.0213	0.0211
4.0	0.0227	0.0227	0.0226	0.0225	0.0222	0.0221	0.0219
4.5	0.0235	0.0234	0.0233	0.0231	0.0228	0.0226	0.0225
5.0	0.0240	0.0239	0.0238	0.0237	0.0235	0.0234	0.0232

After adding the total uncertainty to the calculated k's, all points are less than 0.99 as shown in Table 8.6. The values in Table 8.6 do not always match the sum of Tables 8.4 and 8.5 due to round off, since each table was developed using more significant digits before rounding for the table.

Table 8.6: $k_{95/95}$ at Each Burnup Point For Region 2

Enrichment (wt% U-235)	Cooling Time (years)						
	0	1	2	5	10	15	25
2.0	0.9882	0.9873	0.9872	0.9870	0.9863	0.9859	0.9852
2.5	0.9867	0.9866	0.9863	0.9866	0.9871	0.9864	0.9863
3.0	0.9871	0.9867	0.9868	0.9864	0.9861	0.9859	0.9854
3.5	0.9890	0.9889	0.9889	0.9885	0.9886	0.9883	0.9887
4.0	0.9889	0.9885	0.9882	0.9879	0.9879	0.9884	0.9887
4.5	0.9876	0.9875	0.9893	0.9890	0.9884	0.9877	0.9875
5.0	0.9891	0.9885	0.9880	0.9879	0.9868	0.9869	0.9884

8.2.3 Use of Control Rods in Region 2

A calculation was performed to show that a control rod inserted into a fresh 5.0 wt% U-235 assembly in Region 2 meets the criticality requirements. The calculated k is 0.9292 (a 2x2 array of fresh assemblies with each assembly containing a control rod). The analysis was performed with fresh assemblies

containing no IFBA rods. Since the k of the 2x2 calculation is less than the base case for Region 2 (see Table 8.7), this shows that a fresh assembly with a control rod can be stored anywhere in Region 2. Further, any assembly having any burnup depleted under any condition can be stored anywhere in Region 2 provided it contains a control rod.

8.2.4 Missing Panel in Region 2

As in Region 1, the lack of fuel in a cell more than offsets the reactivity due to the lack of an absorber panel in a cell. A case was run for a 5.0 wt% assembly burned to 42.67 GWd/T with one water hole and no panel in the cell. The cell does not have to be empty, only that there is no fuel assembly. The cell can be filled with a block of concrete, steel, air, Zircaloy, water, or aluminum having the outer dimensions of a fuel assembly. All of these materials meet the criticality requirements (see Table 8.7). Other burnup/enrichment configurations were not run because there is a large margin to the requirements.

Alternatively, a fuel assembly meeting the loading curve can be placed in the cell having the missing panel as long as the fuel assembly contains a control rod. The negative reactivity worth of a control rod is more than that of an absorber panel (see Table 8.7).

Table 8.7: Additional Sensitivity Calculations for Region 2

Case	k	Bias & Uncertainty	$k_{95/95}$
Base Case* (5.0 wt% U-235 fuel at 42.67 GWd/T, 72 hour)	0.9639	0.0240	0.9879
Empty cell filled with water (no absorber panel in cell)	0.8744	0.0240	0.8984
Empty cell with air (no absorber panel in cell)	0.9195	0.0240	0.9435
Empty cell with aluminum (no absorber panel in cell)	0.9310	0.0240	0.9550
Empty cell with concrete (no absorber panel in cell)	0.9163	0.0240	0.9403
Empty cell with steel (no absorber panel in cell)	0.9205	0.0240	0.9445
Empty cell with zirc (no absorber panel in cell)	0.9333	0.0240	0.9573
Missing panel, control rod in fuel assembly (base case fuel)	0.9567	0.0240	0.9807
No missing panels, fresh 5.0 wt% U-235 no IFBA, control rod in fuel assembly	0.9292	0.0102	0.9394
Alternate panel design, 0.020 areal density (base case fuel)	0.9630	0.0240	0.9870
Low burned fuel (2.5 wt%, 12.31 GWd/T, 25 year, no missing panels)	0.9696	0.0166	0.9862
Alternate panel design for the above low-burned fuel case	0.9683	0.0166	0.9849

* The base case identified here was for a depletion in which the WABA was removed after 35 GWd/T.

8.2.5 Alternate Absorber Panel Design in Region 2

The base case (5.0 wt% at 42.67 GWd/T) was run for the alternate absorber design at an areal density of 0.020 g B10/cm^{2}and results in a k of 0.9630 compared to the base case k of 0.9639. A low burnup case (2.5 wt% at 12.31 GWd/T) was also run with the alternate design. The k was 0.9683 compared to the primary design k of 0.9696. This demonstrates that the loading curves are valid for the alternate design.

8.2.6 Expanded Cooling Time Calculations

It is generally accepted that the most reactive time after discharge is immediately after core offload (72 or 100 hours) with no credit for Xe-135 or Np-239 (all of the Np-239 is immediately converted to Pu-239 and all of the Xe-135 is immediately converted to Cs-135). To test this assumption, additional cooling time calculations between 72 hours and 1 year were performed (72 hours, 100 hours, 8 days, 16 days, 30 days, 60 days, 0.3 year, 0.6 year, and 1 year)..

As shown in Figure 8.2, the k generally decreases with time and the k is largest at 72 hours and 100 hours (the k is the same). The statistical uncertainty in these calculations is 0.0002 (2 sigma) so although there appears to be a non-decreasing behavior between 16 and 60 days, it is not significant.

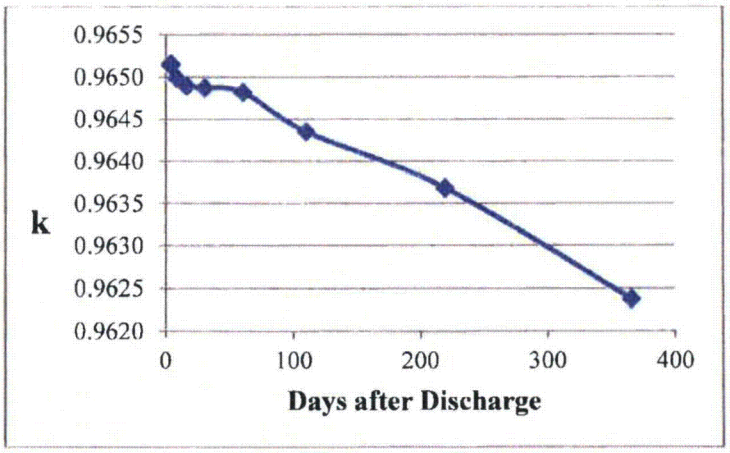

Figure 8.2: k as a Function of Cooling Time

8.3 Borated Conditions

The most limiting acceptance criteria is for the unborated condition so the loading criteria have been set using models that did not contain soluble boron. In order to confirm that the $k_{95/95}$ is less than 0.95 at a boron content that will be maintained even under a boron dilution accident (Section 9.5) a limited number of additional calculations were performed. The soluble boron concentration of 700 ppm was used for these calculations since this concentration can be easily supported by the boron dilution analysis and it yields significant margin in k. For Region 1, the calculated k at 700 ppm with water at 100 °C is 0.8790 (see Table 8.9). With bias and uncertainty this becomes $k_{95/95} = 0.8900$. Due to the difference between 0.89 and the target value of 0.94, no further calculations are warranted. For Region 2, the 5.0 wt% U-235 loading curve points at 72 hour and 25 year cooling were run with 700 ppm boron in the pool water (42.67 GWd/T at 72 hours and 37.68 GWd/T at 25 years). The calculated k at 72 hours was 0.8899, while the k at 25 years was 0.8906. With the bias and uncertainty applied, the $k_{95/95}$ to be compared to the regulatory limit of 0.95 becomes 0.9139 and 0.9138 for the 72 hour and 25 year cooling times respectively.

The bias and uncertainty used here for both Region 1 and 2 was from the unborated analysis. Calculation of borated uncertainties is not needed due to the large margin from the regulatory limit. Even if borated uncertainties were calculated, it would be expected that they would be smaller, since the primary uncertainty is the burnup uncertainty and the reactivity worth of burnup decreases with boron. Furthermore, ignoring the grids is still conservative at 700 ppm.

8.4 Depletion Effect of Hafnium Flux Suppression Inserts

To determine the reactivity effect of having a hafnium rod inserted, a special depletion was performed. For the first 8 GWd/T, the assembly is depleted with a 20 rodlet hafnium insert (full length). The hafnium insert is then replaced by a fresh 20 rodlet WABA plus 148 IFBA rods and never removed. Since the hafnium inserts harden the spectrum more than WABAs (Ref. 7, Table 4.7.7), depleting with

the hafnium first is conservative for the WABA depletion and no estimate of the burnup for changing from WABA to hafnium depletion is required. The burnup requirements for this case were then calculated using the same procedures as were used for the loading curve. Enrichments were 4.0, 4.5, and 5.0 and cooling times were 72 hours and 25 years. Table 8.8 shows the burnup required for this special depletion to meet the 0.99 $k_{95/95}$ target value after accounting for all biases and uncertainties.

Table 8.8: Hafnium Depletion Results

Enrichment (wt% U-235)	Cooling Time	Normal Burnup Requirement (GWd/T)	Hafnium Depletion Burnup Requirement (GWd/T)	Increased Burnup Required For Hafnium Depletion Case (GWd/T)
4.0	72 hr	33.82	34.89	1.07
4.5	72 hr	38.98	39.69	0.71
5.0	72 hr	42.67	43.98	1.31
4.0	25 yr	28.44	29.13	0.69
4.5	25 yr	32.60	33.20	0.60
5.0	25 yr	37.18	37.82	0.64

For simplicity and to provide margin, a 2 GWd/T increase in the loading curve is required for any assembly having any burnup with a hafnium insert. Please note that if an assembly exceeds the loading curve requirements prior to loading a hafnium insert, no burnup adder is required since additional burnup (where IFBAs are ignored) always reduces reactivity regardless of spectrum.

8.5 Axial Reflector

All of the analyses were performed with a water axial reflector (50 cm at top and bottom). Unburned fuel reactivity is dominated by the center and so the results are not sensitive to the axial reflector modeling. Burned fuel is top peaked and so is more sensitive to axial reflector modeling. To test the appropriateness of using 50 cm of water as the axial reflector for burned fuel, several other configurations were analyzed. The bottom reflector has an insignificant effect due to the axial burnup distribution (reactivity is driven by the low burnup in the top nodes), so cases were run to test only the top reflector. Starting with the 5 wt% U-235, 42.67 GWd/T burnup, 72 hour case, which has a calculated k of 0.9639,

some modifications to the top reflector were made. With a 50/50 mix of steel and water at the top, the calculated k was 0.9613, so the water reflector k of 0.9639 is more limiting. With 100% steel at the top, k was 0.9729, which demonstrates that pure steel is more limiting. The fuel pin above the active fuel is actually composed of a spring inside a plenum and the rods extend above the active fuel at least 6 inches. Using the fuel clad OD and the pin pitch, the fuel rod is 44% and water is 56% of the total area. So to simulate the plenum and spring, a mixture of 56% water, 22% steel and 22% void (fission gas) is used for the 6 inches directly above the active fuel. Then 100% steel is used above that. The k for this case was 0.9613, so the current analysis is conservative compared to the realistic case.

8.6 Volatile Fission Gases

There may be some leakage of fission gases from the active fuel. To quantify this effect, the 5.0 wt%, 72 hour case (42.67 GWd/T) was run in which all of the krypton, xenon, and iodine isotope concentrations were set to zero. The k for this case was 0.9699 compared to the unperturbed k of 0.9639 (see Table 8.7), a difference of 0.0060. If 10% of the fission gases were released [29], the Δk would be 0.0060 x 0.10 = 0.0006. This small amount could be included as a bias in the final calculations. Alternatively, the top axial reflector could be modeled more realistically, which gives a Δk benefit of 0.0027, which easily covers the 10% fission gas release. Therefore, no bias for volatile fission gases is needed.

8.7 Temperature Effects

Table 8.9 summarizes the base case calculations at 4 different temperatures (4, 20, 70, and 100 °C). The results demonstrate that the reactivity is largest at 4 °C in both regions under unborated conditions. The reactivity increases slightly under borated conditions in Region 1 with increasing temperature but there is excess margin for the borated condition.

Table 8.9: Calculated k as a Function of Temperature

Temperature (°C)	Density (g/cc)	Region 1 (0 ppm)	Region 1 (700 ppm)	Region 2 (0 ppm)	Region 2 (700 ppm)
4	1.0000	0.9717	0.8777	0.9639	0.8928
20	0.9982	0.9714	0.8778	0.9634	0.8924
70	0.9778	0.9710	0.8789	0.9553	0.8883
100	0.9584	0.9696	0.8790	0.9492	0.8848

8.8 Fuel Geometry Changes during Burnup

There are geometry changes during burnup, such as pellet densification, crud buildup, clad creep down and fuel rod growth. Recent work by the industry has shown that these effects are insignificant [22,27].

8.9 Depletion of Fuel < 3.5 wt% with Modern Depletion Assumptions

Historical low enriched fuel used Pyrex burnable absorbers and was burned with the control rods at the bite position. In order to accommodate this, the loading curves were generated using separate depletion assumptions for enrichments below and above 3.5 wt% U-235. However, although not currently anticipated, there may be a need for loading new fuel enriched below 3.5 wt% U-235. A special depletion was performed to cover this possibility. A depletion at 3.5 wt% was performed using the depletion assumptions selected for modern fuel (see Table 10.5). The k for 3.5 wt% at 27.53 GWd/T, 72 hour cooling was 0.9650. The k for 3.5 wt% at 27.53 GWd/T, 72 hour using the older depletion assumptions (Pyrex burnable absorber, lower temperatures, rodded top node, etc.) was 0.9665. So the loading curve for 3.5 wt% or less is valid for either set of depletion assumptions. The reason for this is that although the older depletion assumption is less limiting for fuel below the top node, the older depletion assumes that the top node is rodded its entire life. Modern depletion assumes the top node can be rodded for only a short time (i.e., the bite position is not allowed). The rodded top node balances the less reactive lower nodes so that the net difference between the two depletion assumptions is very small.

8.10 Reduced Periphery Requirements & Region 1/Region 2 Interface

Since the neutron leakage at the edge of the pool reduces the reactivity worth of the assemblies on the periphery of the pool, it is possible to relax the requirements for these assemblies. In Region 1, the assemblies on the periphery do not need any IFBA rods or burnup. In Region 2, the assemblies on the periphery, which are 4.0 wt% U-235 or greater, are allowed to have 8 GWd/T less burnup than the Region 2 loading curve. In order to prove that these reductions are acceptable, a full pool model was created. This section describes the full pool model and the results of the periphery assembly analysis. This section also confirms the interface between Region 1 and Region 2 does not need any special requirements.

8.10.1 Full Pool Model

The full pool model is used to:

a) Verify reduced requirements for the periphery assemblies,

b) Verify that the Region 1/Region 2 interface has an insignificant effect on k, and

c) Show an acceptable soluble boron concentration for a single dropped assembly or misplaced assembly (see Section 9).

The full pool model was created by taking the 2x2 model for Region 2 and the 1x1 model for Region 1 described in Section 6 and using them as units that were reproduced in arrays. The model has 4 large arrays (see Figure 8.4 for module identification):

1. Region 1 module A (10X8),
2. Region 1 modules B and C (combined as 21X9),
3. Region 2 modules D, E-1, F-1, F-2, G-1, and G-2 (combined as 24X32), and
4. Region 2 modules E-2, E-3, and H.

Modules E-2, E-3, and H are 11 cells across (north to south) but since the modeling is using 2x2 units, these modules were conservatively modeled as 12 cells across. This conservatively makes the pool larger but the impact is negligible. In the east to west direction these modules have an even number of cells so no modification was necessary. However, module H has a cutout for the fuel elevator and failed fuel containers. This cutout was conservatively ignored. The pool has some small extra space between modules. This space is conservatively removed in the full pool model.

The pool dimensions come from Holtec Drawing No. 397 [21]. The drawing shows the smallest separation between any module and the wall is 1.25 inches (Region 1 left wall). This minimum separation is assumed on all sides. The pool has a 0.25 inch stainless steel liner and a concrete wall outside the liner.

Figure 8.3 shows the full pool model. The pink is concrete. The model starts on the left with 19.69 inches (50 cm) of concrete. This is followed by a 0.25 inch stainless steel liner. Next is a 1.25 inch water gap. After this the Region 1 arrays are added. This then sets the left boundary for the smaller Region 2 array. Then there is a 1.25 inch water gap on the right followed by the 0.25 inch liner and then 19.69 inches (50 cm) of concrete. The large Region 2 array is set to be against the left side of the smaller Region 2 array. This arrangement means the left side of the large array of Region 2 is not directly under the larger Region 1 array. This offset is caused by the separation between Region 2 modules that is ignored in this model. A block of concrete is added to the left of the large Region 2 array. This block does not have the stainless steel liner but is separated from Region 2 by the same 1.25 inches of water. When changing the reflector for studies, the same model setup is maintained, so all the 0.25 inch liners change or all the 1.25 inch water gaps change at once. Figure 8.4 is the pool taken from Holtec Drawing No. 397 [21]. As can be seen when comparing Figures 8.3 and 8.4, the full pool model has extra water below Region 1 module A and this is consistent with the real pool. The full pool model has extra water above Region 2 module H and this is consistent with the pool drawing.

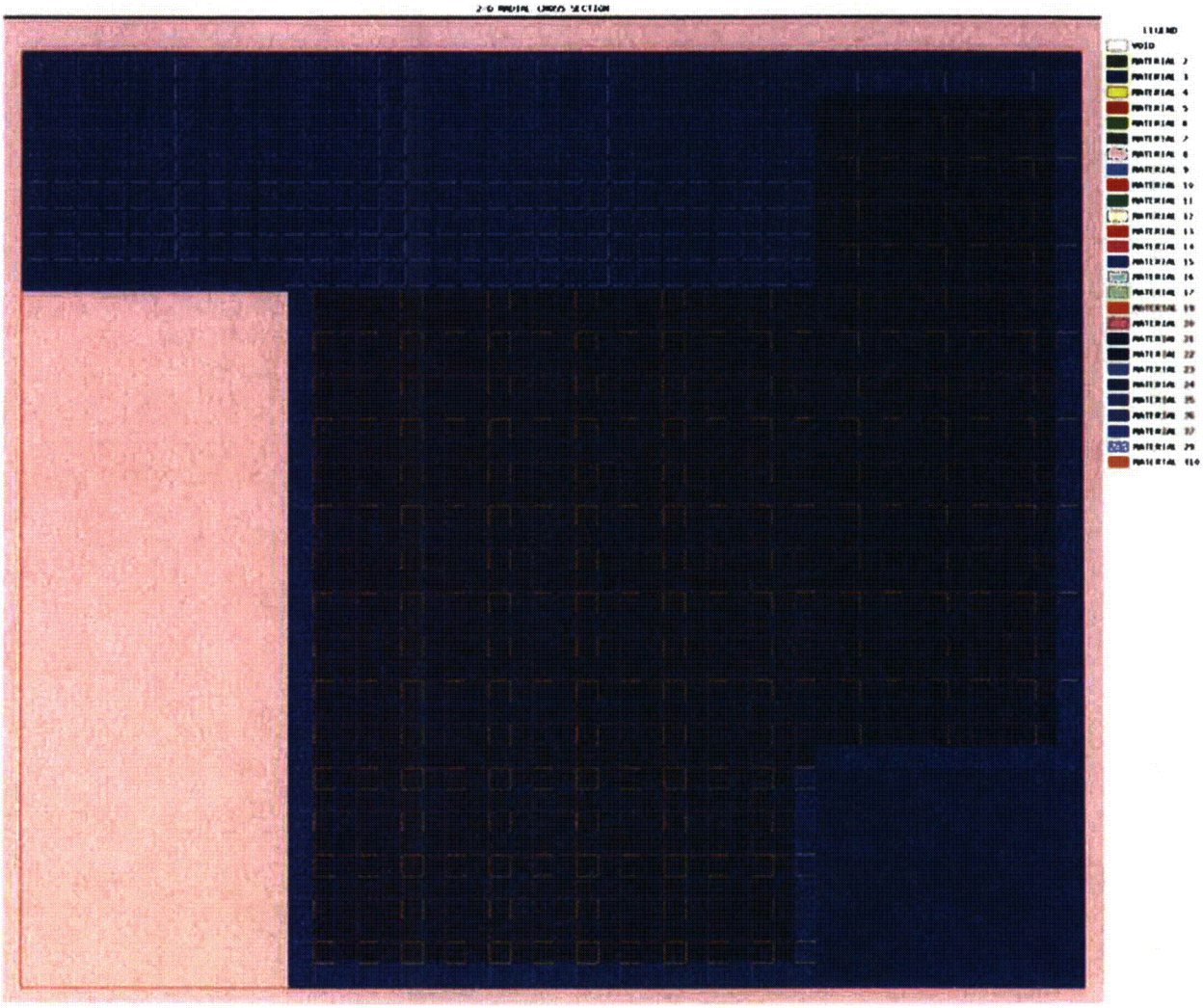

Figure 8.3: Full Pool Model

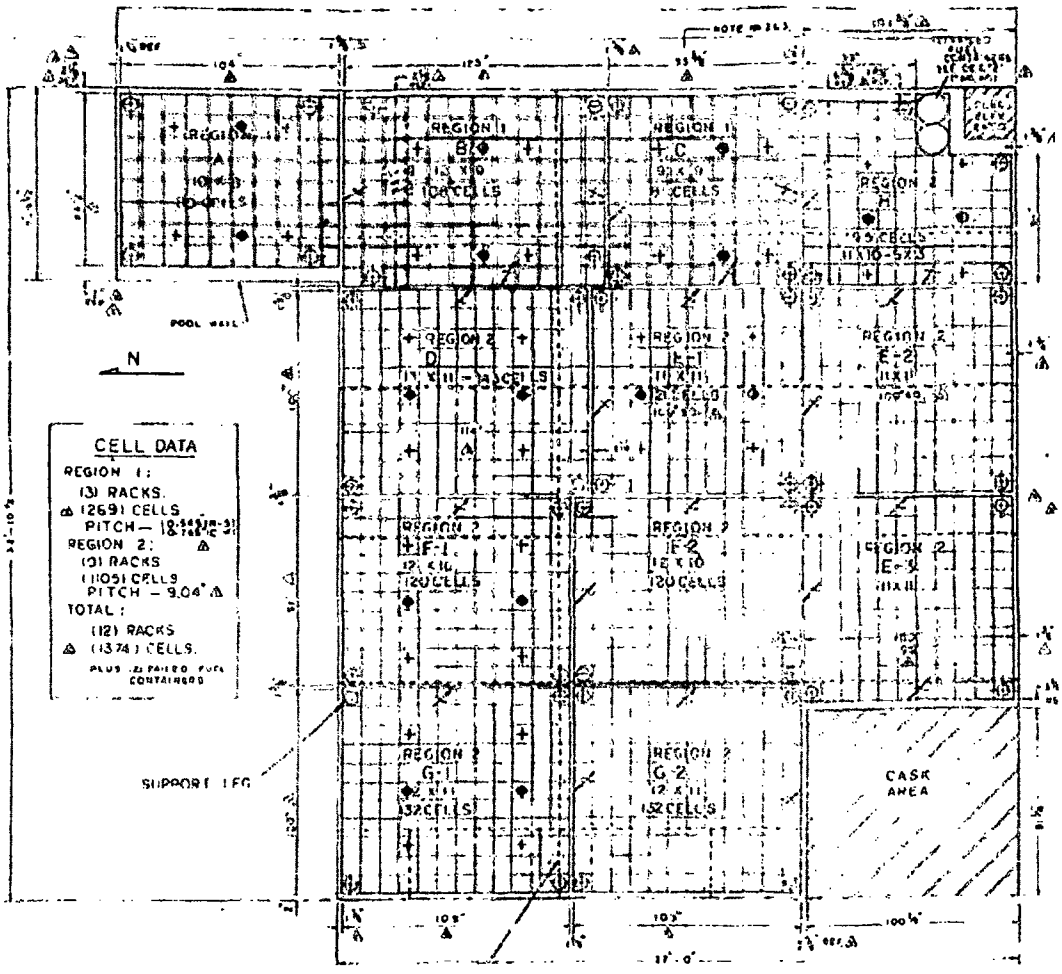

Figure 8.4: Indian Point Unit 2 Spent Fuel Pool Taken From Holtec Drawing #397 [21]

Figure 8.5 shows an enlargement of the top left corner of the pool. Several points should be noticed. First, the model has steel extensions on the outside of the module due to replicating the cell. The real modules do not have these. Second, on the wall side of the module, the model has the sheath for the old absorber panels. These are not on the real module outside walls. Thus, there is some excess steel on the outside. A calculation was performed where a 0.1 inch steel plate was placed on the edge of the repeating Region 1 cells. K_{eff} increased only 0.0025 so there is confidence that the extra steel on the outside of the model is negligible or slightly conservative. Finally, note that the absorber panels (light blue) are in the bottom right. This means the most reactive periphery is at the top and left side for Region 1.

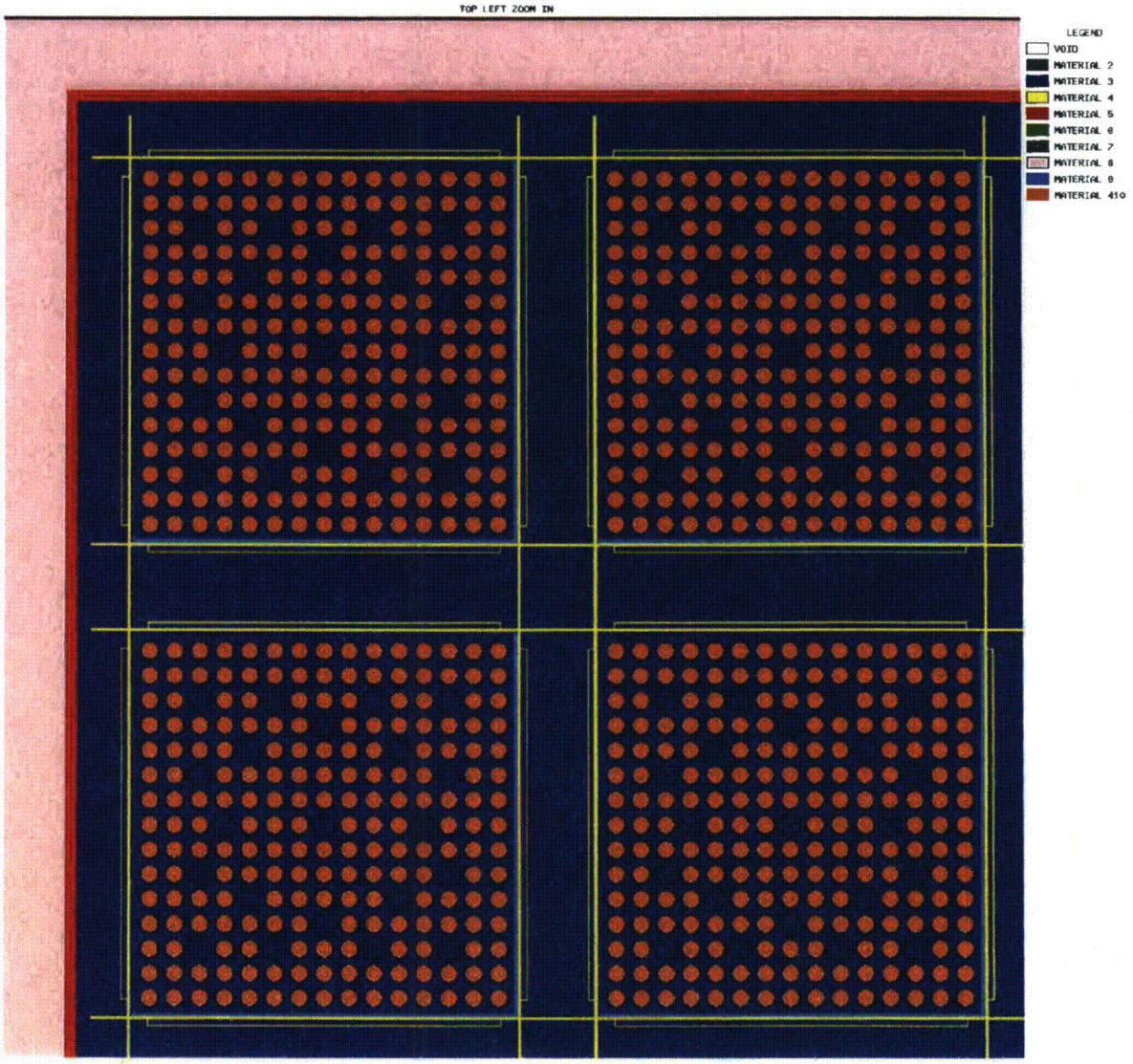

Figure 8.5: Enlargement of the Top Left Corner of the Pool Model

Figure 8.6 shows an enlargement of the bottom left corner of the full pool model. Note that the resultant cell has the absorber sheath and some of a cell wall on the outside. The actual rack has a plate 0.075 inches thick. The total of the sheath and the partial cell wall is 0.075 inches, so by chance the correct amount of steel is on the outside of the resultant cells. The standard cells in the full pool model have an absorber sheath on the outside wall that does not exist in the real rack. The calculation with the 0.1 inch steel plate placed on the outside of the model described in the previous paragraph provides

confidence that this extra sheath in the model is negligible or slightly conservative. Note that the absorber panels (green in this case) for Region 2 are in the top left making the bottom and right sides more sensitive to the periphery.

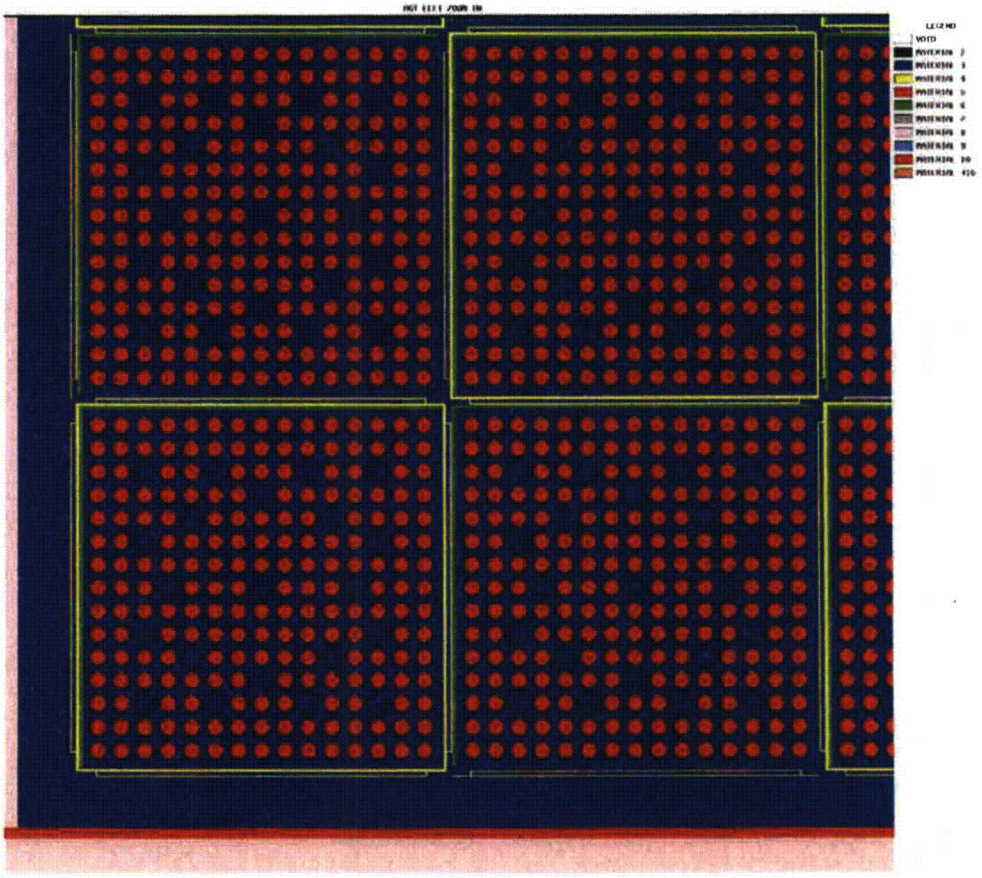

Figure 8.6: Enlargement of the Bottom Left Corner of the Pool Model

Figure 8.7 shows an enlargement of the left side of the bottom of the Region 1/Region 2 interface. Note that the absorber panels for the two regions (light blue for Region 1 and green for Region 2) create an effective flux trap. The distance between the two regions in the full pool model is 0.9 inches. The real separation is 1.375 inches. The smaller separation is conservative as shown by the rack pitch tolerance calculations in Section 7.1. The real pool has absorber sheaths on the outside of both the Region 1 and 2 rack modules at the interface. The full pool model has the Region 1 modules consistent with reality but has less steel on the outside of Region 2. Section 7.1 concluded that more water (less steel) between cells

in Region 1 is conservative. Therefore, the full pool model with less steel between the racks is acceptable.

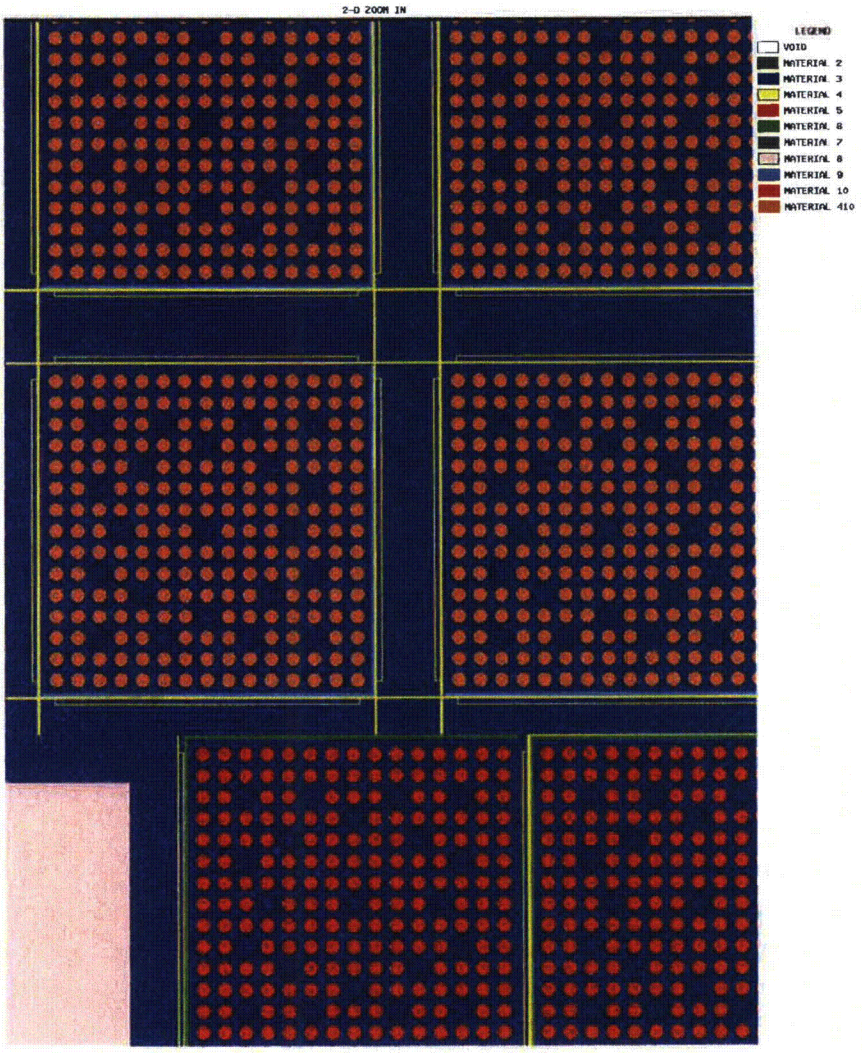

Figure 8.7: Enlargement of the Left Side of the Bottom of the Region 1/Region 2 Interface

Calculations were performed to confirm that the k of the finite model of each region is similar, but lower than the k from the infinite models described in Section 6. Since the reduced periphery burnup criteria (lowered by 8 GWd/T) only applies for enrichments equal to or greater than 4 wt%, the Region 2 analysis of the full pool model is performed at 28.44 GWd/T at 4 wt% U-235 and 25 yr cooling (the lowest burnup) and 42.67 GWd/T at 5 wt% and 72 hours cooling (the highest burnup). The full pool

model was run without fuel assemblies in Region 1 for the Region 2 only models. For the Region 1 only models, no fuel was put in the fuel rods of Region 2 (replaced with void). If fuel was in both regions, the k would correspond to the region with the higher k. Table 8.10 shows the k's of the finite and infinite models.

Table 8.10: Infinite (Section 6) Versus Finite (Full Pool Model)

Region	Enrichment (wt% U^{235})	Burnup (GWd/T)	Cooling	k_{inf}	σ	k_{finite}	σ
1	5*	0	0	0.97182	0.00005	0.9666	0.0001
2	4	28.44	25 yr	0.96677	0.00011	0.9650	0.0001
2	5	42.67	72 hr	0.96395	0.00011	0.9626	0.0001

*The Region 1 fuel contains 48 IFBA rods

As can be seen in Table 8.10, the infinite model is slightly conservative for the pool. The finite model of Region 2 is from 0.13% to 0.17% lower in k. The finite model for Region 1 is less by more than 0.5% in k. This larger decrease is expected since Region 1 is much smaller.

8.10.2 Results of Reduced Periphery and Region 1/Region 2 Interface Analysis

This section presents a set of calculations to confirm that the relaxed periphery requirements are acceptable. Figure 8.8 shows the location of the cells where the peripheral relaxation is permitted. Note that due to model simplifications of Module H, the cells near the failed fuel containers are not considered peripheral cells.

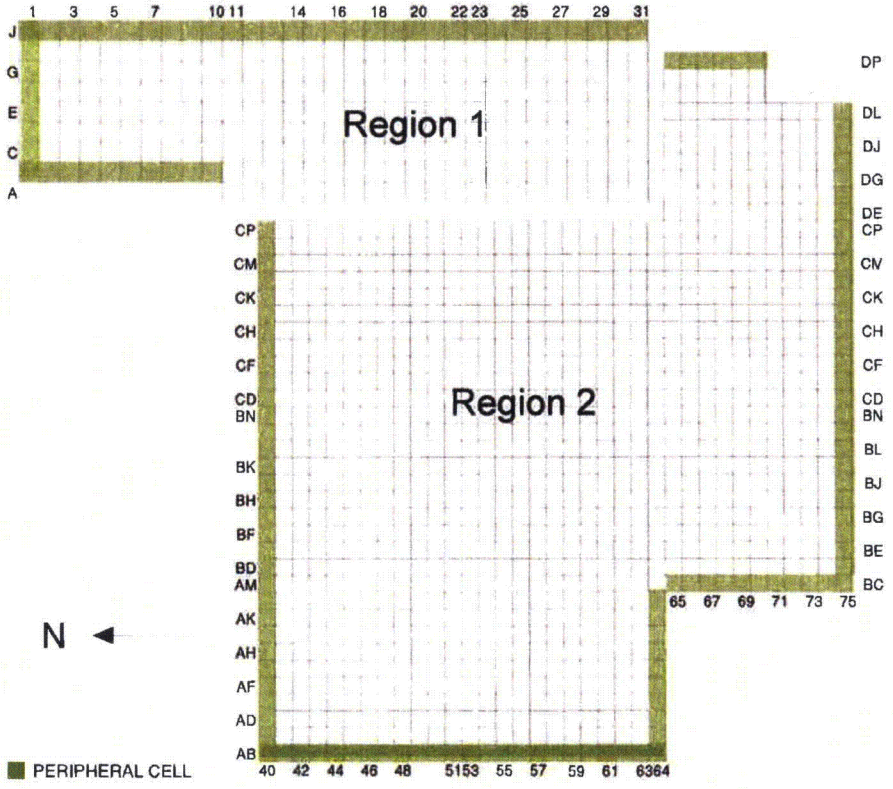

Figure 8.8: Location of the Peripheral Cells with Reduced Requirements

In a large pool model, the calculated k will reflect the k of the most reactive region, yielding little information on less reactive portions of the pool. Since the calculated k for Region 2 is lower than Region 1, the periphery calculations for Region 2 have to be performed without fuel in Region 1. Even though the k is lower in Region 2, Region 2 has less margin, since the uncertainty is higher.

All of the analysis with the full pool model uses at least 3000 generations with 12000 neutrons per generation. Even though this is a very large number of neutrons, care must be taken to assure that the effect of concern is seen, because the model is so large. To do this, the starting source is specified in the region of concern. Sometimes it is not clear where the highest reactivity lies, so several starting source distributions are used in successive runs.

Table 8.11 presents the results of calculations that were performed to confirm the 8 GWd/T lower burnup requirement for Region 2 periphery assemblies.

Table 8.11: Region 2 Periphery Tests (No Fuel in Region 1)

Enrichment* (wt% U^{235})	Burnup** (GWd/T)	Starting Source***	Calculated k_{eff}	σ	Bias + Uncertainty ****	$k_{95/95}$ *****
4	28.44/20.44	Corner	0.9652	0.0001	0.0219	0.9871
4	28.44/20.44	Right	0.9650	0.0001	0.0219	0.9869
4	28.44/20.44	Left	0.9654	0.0001	0.0219	0.9873
5	42.67/34.67	Corner	0.9628	0.0001	0.0240	0.9868
5	42.67/34.67	Right	0.9624	0.0001	0.0240	0.9864
5	42.67/34.67	Left	0.9624	0.0001	0.0240	0.9864

*4 wt% cases are cooled 25 years. 5 wt% cases are cooled 72 hours.
**The first burnup is the burnup in non-periphery cells. The second burnup is the burnup in periphery cells.
***Starting source location: Corner: the cask area corner. Right: right side. Left: Left side.
****Bias and uncertainty for the highest burnup taken from Table 8.5
*****To be compared to licensing limit, less than 1.0. 1% margin to limit is used.

Several observations can be made from the data in Tables 8.10 and 8.11. The periphery cases in Table 8.11 have k's that are nearly equal to the cases without the reduced burnup on the periphery. This means that the local k on the periphery is about equal to the k in the center of the region and therefore, the reduced burnup requirements on the periphery are confirmed. Finally, after adding the bias and uncertainty, the target limiting $k_{95/95}$ (0.99) is met.

Table 8.12 shows the results of calculations performed with fuel in both regions. These calculations demonstrate that the reactivity is driven by Region 1, since the Region 1 k is higher. These full pool models use the most reactive Region 2 fuel, which is the 4 wt% fuel with 25 years cooling and 28.44/20.44 GWd/T burnups. Since a constant 8 GWd/T burnup relaxation for the periphery is utilized rather than a fraction of the burnup requirements, the fuel with the lowest non-periphery burnup requirements (i.e., 4 wt%, 25 years cooled) is the most reactive peripheral fuel.

Table 8.12: Region 1 Periphery Tests (4 wt% 28.44/20.44 GWd/T Fuel in Region 2)

Starting Source*	Calculated k_{eff}	σ	Bias + Uncertainty	$k_{95/95}$**
Interface	0.9759	0.0001	0.0111	0.9870
Left	0.9781	0.0001	0.0111	0.9892

*Starting source location. Interface: bottom of Region 1 at the Region1/2 interface. Left: Left side of Region 1.
**To be compared to licensing limit, less than 1.0. 1% margin to limit is used.

Table 8.12 demonstrates that taking out the IFBAs in the periphery assemblies increases k slightly. The increased k (0.9781) is slightly larger than the infinite model (0.9718 from Table 8.10). However, there was margin in Region 1, so the final $k_{95/95}$ is still less than the target $k_{95/95}$ of 0.99. In order to find the most reactive location in a large model, the starting source location can be varied. The two calculations in Table 8.12 only differed in the starting source location. When the source was started at the Region 1 – 2 interface, the higher reactivity corner was not found.

Table 8.12 also demonstrates that the Region 1/Region 2 interface does not have the limiting k. The calculated k, using the starting source at the interface, is lower than the k using the source placed at the left edge of the model, where there is fuel with no IFBA. Clearly, the fully converged calculated k should not depend on the location of the starting source, but placing the starting source at areas of concern provides confirmation that the k of the location of concern was truly evaluated. The k calculation with the starting source at the interface has a lower k since there were generations included in the final calculation of k before the more reactive peripheral assemblies were found. However, there were plenty of neutrons at the interface to assure that k at the interface is within the limits. This result is expected since the absorber panels face each other at the interface creating a flux trap.

Table 8.13 presents the results of calculations performed to test the sensitivity to the pool reflectors. For some of the runs, no fuel was in the Region 1 cells, so the reflector sensitivities on Region 2 can be seen. The first observation is that the pool reflectors have no effect on the Region 2 results. This is because leakage has a bigger effect on k than the 8 GWd/T reduction in the burnup requirement. For Region 2, the k is controlled by the center of the region. For Region 1, results show that concrete is a

better reflector than water (the concrete used is a conservative mixture created by Oak Ridge – named as *orconcrete*). As the water gap is reduced, k increases. The results are not sensitive to the liner thickness.

Table 8.13: Reflector Tests (4 wt% 28.44/20.44 GWd/T Fuel in Region 2)

Water Gap to Cell Wall (cm)	Steel Liner Thick. (cm)	Region 1 Fuel	Starting Source*	Calculated k_{eff}	σ	Bias + Uncertainty	$k_{95/95}$**
5.6	0.635	Yes	R1 Left	0.9765	0.0001	0.0111	0.9876
12.4	0.635	Yes	R1 Left	0.9753	0.0001	0.0111	0.9864
3.175	0.635	Yes	R1 Left	0.9781	0.0001	0.0111	0.9892
5.6	5.0	Yes	R1 Left	0.9772	0.0001	0.0111	0.9883
5.6	0.001	Yes	R1 Left	0.9773	0.0001	0.0111	0.9884
3.175	0.635	No	Right	0.9650	0.0001	0.0219	0.9869
10.0	0.635	No	Right	0.9650	0.0001	0.0219	0.9869
1.0	0.635	No	Right	0.9647	0.0001	0.0219	0.9866
3.175	5.0	No	Right	0.9649	0.0001	0.0219	0.9868
3.175	0.001	No	Right	0.9650	0.0001	0.0219	0.9869

*Starting source location. R1 Left: Left side of Region 1. Right: Right side of Region 2.
**To be compared to licensing limit, less than 1.0. 1% margin to limit is used.

An additional calculation was performed on the full pool model, where a small layer of steel was added at the outside of the fuel rack. The result was that k increased, which confirms that the extra steel (Boraflex sheathing, and Region 1 cell separator beams) that is at the edge of the full pool model is conservative.

Since all the $k_{95/95}$'s of the analyses are less than the target limiting k (0.99), the reduced requirements for the periphery are confirmed.

8.11 Failed Fuel Containers

The southeast corner (please note that on the drawings in this report North points left) of the spent fuel pool contains two 16" circular pipes and are labeled "failed fuel containers." These containers have been used to store pieces of failed fuel rods, neutron sources, and fission chambers. The neutron sources and fission chambers contain too little fissile material to be a concern. The fission chambers have less than 10 mg U-235 each [30]. The neutron sources also have a very small amount of fissile material. The ANSI/ANS 8.1 standard [33] states that 700 grams of U-235 in any configuration is always subcritical. However, the failed fuel containers are not fully decoupled from the Module H of Region 2. In order to

set a conservative limit on the fuel that can be in the failed fuel containers, the 2x2 Region 2 model was modified by (1) removing the absorber panel from the lower right cell and the upper right cell and (2) in each of these cells, placing a regular array of 36 fresh 5.0 wt% fuel pins (6x6). In the two left cells, illustrated in Figure 8.9, are burned 5.0 wt% fuel assemblies at the loading curve burnup. The k for this configuration was 0.9374, which is less reactive than the loading curve. Based on this result, 36 fuel pins could be loaded into each failed fuel container with no criticality concern.

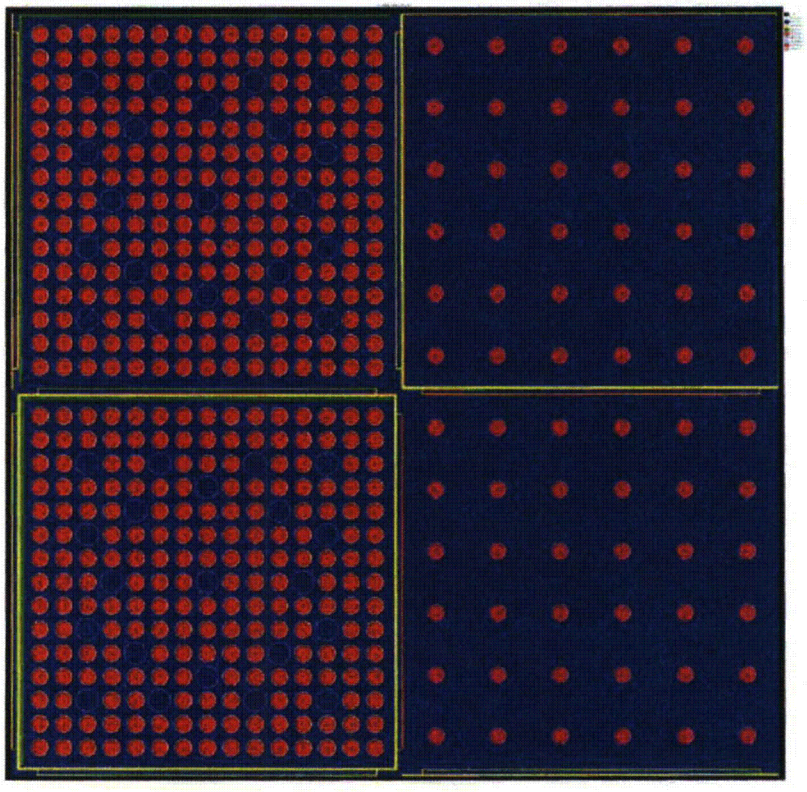

Figure 8.9: Model for Failed Fuel Container Analysis

8.12 Fuel Rod Storage Basket

The Indian Point SFP can have movable fuel rod storage baskets that can be used to store fuel rods. These baskets can fit in a storage cell and they have 52 holes for storing fuel rods. This was modeled as 52 fresh 5.0 wt% fuel rods in Region 2 (see Figure 8.10). The k for this configuration was 0.9195, which is well below the loading curve k. Therefore, the fuel rod storage basket can be stored anywhere in Region 1 or Region 2.

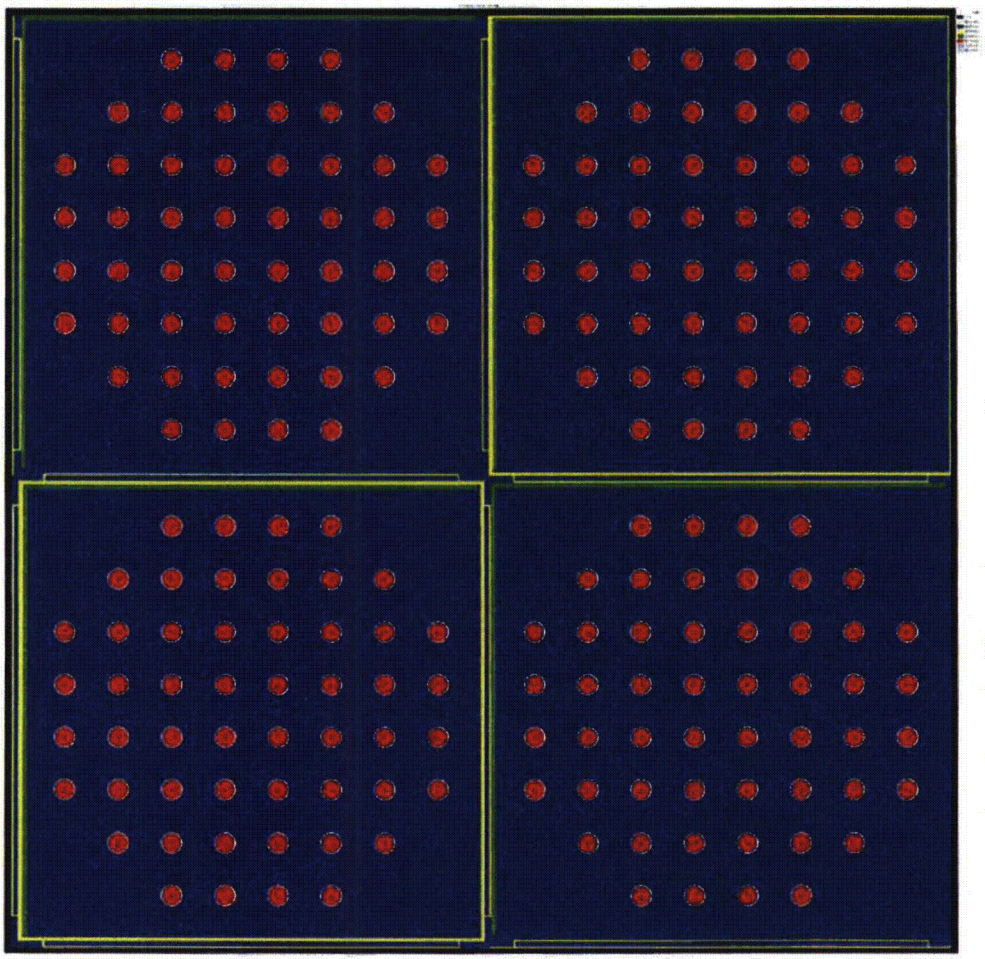

Figure 8.10: Model for the Fuel Rod Storage Basket

8.13 Assemblies with Missing Fuel Rods

Usually, when a fuel assembly has one or more failed fuel rods, the failed fuel rod is removed and replaced with a stainless steel rod having the same outer dimension as a fuel rod. If this is done, there is no criticality concern since the reconstituted assembly would be less reactive than the original assembly. However, if a failed fuel rod is removed but not replaced with a stainless steel rod, the reactivity increases because there is more water available. An analysis was done in which one or more fuel rods are removed from an assembly to estimate the effect on k. It was determined that k gradually increases as more fuel rods are removed up to and including 36 missing fuel rods. If more than 36 fuel rods are removed, k begins to decrease (see Figure 8.11). The delta k with 36 missing fuel rods (see Figure 8.12) was 0.0184 (a 2x2 array with all 4 assemblies having 36 missing rods) compared to the base case k of 0.9639 with no missing rods. For simplicity, a burnup adder of 4 GWd/T would cover this reactivity increase for an assembly with any number of missing rods. There is only one fuel assembly in the pool (assembly ID of T67) that has a missing fuel rod. This assembly has only one missing fuel rod. The initial fuel enrichment for this assembly was 4.952% and so the burnup requirement would be 42.67 GWd/T with no cooling time credit. The actual burnup of T67 is 49.81 GWd/T so it exceeds the requirement by more than the 4 GWd/T adder for missing fuel rods. If any assembly in the future is re-constituted without replacing fuel rods with stainless steel rods, then 4 GWd/T would have to be added to the loading curve requirement before it could be stored in Region 2. This adder covers any number of missing fuel rods and there is no other loading restriction (two or more fuel assemblies with missing rods could be stored next to each other as long as the 4 GWd/T adder is used for both assemblies).

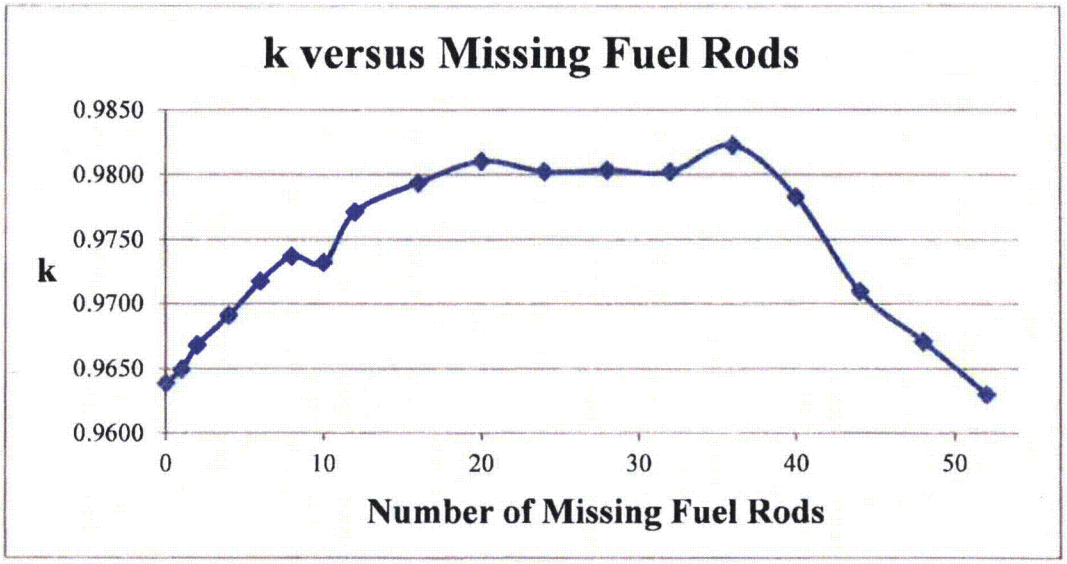

Figure 8.11: k versus Missing Fuel Rods

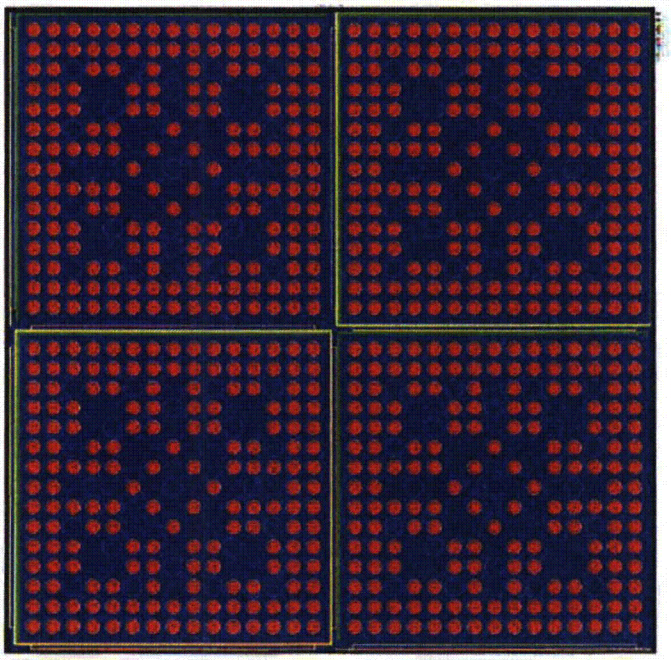

Figure 8.12: Model for Assemblies with 36 Missing Fuel Rods

9 Accident Conditions

The following accidents were analyzed:

- A fresh assembly misplaced outside of the fuel racks but next to the fuel racks,
- A fresh assembly dropped into an empty cell that is missing an absorber panel,
- An over-temperature accident (water boiling in the pool as a result of loss of cooling), and
- A multiple misload event.

Three more accident conditions were considered, but no analysis was necessary. An assembly dropped horizontally on top of other assemblies was not specifically analyzed, because the assemblies are de-coupled as a result of the structure above the active fuel. The horizontal assembly would rest more than 20 inches above the top of the active fuel of the assemblies in the rack. This accident would be covered by the more severe accident of a fresh assembly dropped into an empty cell that is missing an absorber panel. The second accident condition would be a single misloaded assembly. For example, an assembly that is supposed to have a control rod inserted but does not. All violations of the loading requirements (See Tables 10.1 and 10.2) are bounded by a fresh assembly dropped into an empty cell that is missing an absorber panel. The third accident condition is an under-temperature accident (water freezing). This was not considered because the analysis already assumes water at the maximum possible density (near freezing). The last subsection of this Section describes why a seismic event does not cause a criticality concern.

9.1 Misplaced Assembly

For the misplaced fuel assembly accident, it is assumed that a fresh 5.0 wt% U-235 fuel assembly is placed in the pool next to the rack in the most reactive location. There are two locations which could be limiting for a misplaced assembly. One is the corner of the cask loading area. This location is an inside corner so it would interact with the rack on two sides of the misplaced assembly. This corner also allows lower burned peripheral assemblies and the absorber inserts are on the opposite side of the rack cells from

the misplaced assembly. Figure 9.1 shows the misplaced assembly. The most reactive periphery condition is at 4 wt% (lowest enrichment where a reduced peripheral burnup is allowed) and 25 years cooling. The most reactive misplaced fuel is assumed to be 5 wt% with no IFBA and no burnup. Table 9.1 presents the results of this misplaced assembly accident analysis. As can be seen from Table 9.1, 1200 ppm of soluble boron reduces the final $k_{95/95}$ below the target of 0.94. The analysis used a starting source placed near the misplaced assembly.

The second limiting misplaced assembly assumes a fresh fuel assembly is in the fuel elevator and another fresh assembly is wedged in between the rack and the assembly in the fuel elevator. For conservative analysis of this case it is assumed that the misplaced assembly and the assembly in the fuel elevator are both fresh 5 wt% U-235 enriched assemblies with no IFBA rods. Further it is assumed that there is no separation between the two fresh fuel assemblies and no separation from the rack. This misplaced assembly is also shown on Figure 9.1. Figure 9.1 is the model used for the fuel elevator misplaced assembly. The starting source for the fuel elevator case was concentrated around the fuel elevator. Table 9.1 also contains the results for this misplaced assembly analysis. It is more limiting but the 1200 ppm soluble boron still reduces the final $k_{95/95}$ below the target of 0.94.

The minimum soluble boron allowed by the Technical Specifications is much higher than 1200 ppms (currently 2000 ppm), so this accident condition meets the regulatory requirements.

Table 9.1: Misplaced Fuel Assembly Analysis
(Misplaced Assembly is 5 wt% U-235 with no Burnup or IFBA)

Reg. 2 Enrichment* (wt% U^{235})	Reg 2 Burnup** (GWd/T)	Soluble Boron (ppm)	Calculated k_{eff}	σ	Bias + Uncertainty	$k_{95/95}$***
4	28.44/20.44	0	1.04892	0.0002	0.0219	1.0708
4	28.44/20.44	1200	0.89369	0.0001	0.0219	0.9156
4	28.44/20.44	1200	0.90490	0.0001	0.0219	0.9268

* 4 wt% cases are cooled 25 years.
**The first burnup is the burnup in non-peripheral cells. The second burnup is the burnup in periphery cells.
***To be compared to licensing limit, less than 0.95. 1% margin to limit is used.

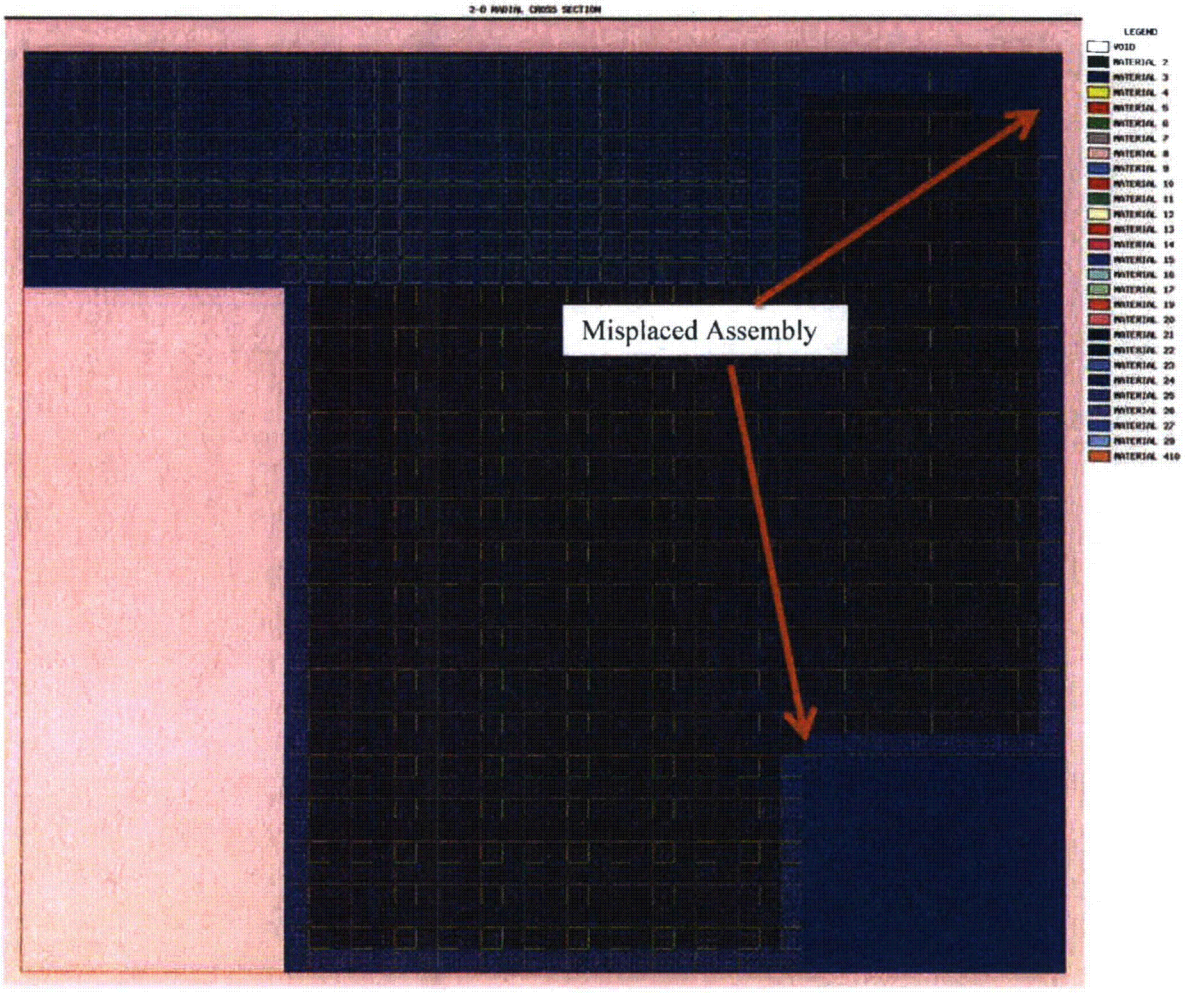

Figure 9.1: Full Pool Model with Misplaced Assembly

9.2 Dropped Assembly

For the dropped assembly accident, it is assumed that a fresh 5 wt% U-235 assembly is dropped into a cell where the absorber panel has been removed (e.g.; for inspection). This accident also covers a situation where the dropped assembly severely damages the absorber panel at the same time. It is then further assumed that when the assembly dropped, the grids failed, which allows for full expansion of the pin pitch (this assumption of expansion of the pin pitch goes beyond traditional assumptions but due to

the available margin, this assumption can be made and removes any concerns about fuel grid failure after the drop). The pin pitch expansion is modeled as the maximum uniform expansion that would fit in the cell. The location of the most limiting position for the dropped assembly is not obvious, so several possible locations were analyzed in the same model.

Figure 9.2 shows the full pool model for the dropped assembly analysis with the 6 dropped assemblies that were analyzed. The different potentially limiting dropped assemblies are tested by changing the starting source. The Region 2 fuel is the 4 wt% U-235 fuel and 28.44/20.44 GWd/T burnup at 25 years cooling (the condition with the least margin to the criticality limits, see Table 8.11). Region 1 contains the most reactive fuel allowed; fresh 5 wt% fuel with 48 IFBA rods, except the periphery Region 1 assemblies have no IFBA rods.

Table 9.2 presents the results of the analysis. The most limiting position for the dropped assembly is the bottom left corner of Region 2. This is most limiting since it puts together 4 low burned assemblies without an absorber panel between two of these assemblies. The right side of Region 2 always has an absorber panel separating the low burned periphery and the interior assemblies. The bottom row of Table 9.2 is highlighted, since it represents a dropped assembly, where the assembly does not come apart and maintains its normal pin pitch. This scenario was considered since at high soluble boron concentration, the larger pitch may not be the most limiting. As seen in Table 9.2, the larger pin pitch is more limiting. As can be seen in Table 9.2, 1200 ppm (rather than the initial guess of 1500 ppm) is sufficient to meet the limiting criteria of 0.95. The minimum soluble boron allowed by the Technical Specifications (currently 2000 ppm) is much higher than 1200 ppm, so this accident condition also meets the regulatory requirements.

Table 9.2: Dropped Fuel Assembly Cases

Starting Source*	Soluble Boron (ppm)	Calculated k_{eff}	σ	Bias + Uncertainty	$k_{95/95}$**
Right	1500	0.8773	0.0001	0.0219	0.8992
Corner	1500	0.8737	0.0001	0.0219	0.8956
Center	1500	0.8735	0.0002	0.0219	0.8954
Bottom Corner	1500	0.8817	0.0001	0.0219	0.9036
Bottom Corner	1200	0.9104	0.0001	0.0219	0.9323
Bottom Corner	1200	0.8959***	0.0002	0.0219	0.9178

*Right: right side of Region 2. Corner: cask loading area corner. Center: center of Region 2. Bottom Corner: bottom left corner of Region 2.
**To be compared to licensing limit, less than 0.95. 1% margin to limit is used.
***Same as the case above except no expanded pin pitch

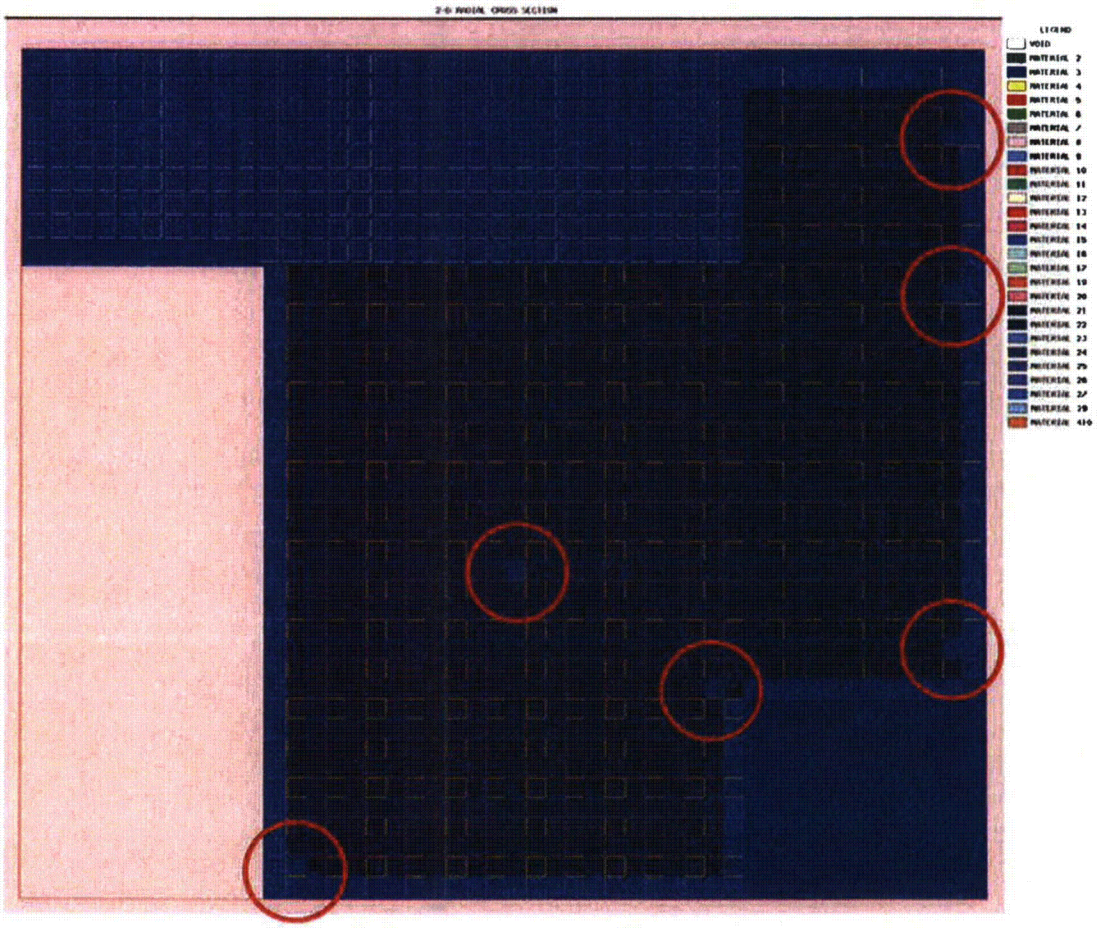

Figure 9.2: Full Pool Model with 6 Dropped Assemblies

9.3 Over Temperature

As shown in Section 8.7, raising the temperature lowers k, even up to 100 °C. Under borated conditions, some of the calculated k's go up with temperature, but not enough to overcome the negative reactivity of the boron. The over temperature accident condition meets the regulatory requirements.

9.4 Multiple Misloads

A case was run assuming that the entire Region 2 rack was filled with fresh 5.0 wt% fuel having 64 IFBA rods at a 1.25X IFBA loading. With 2000 ppm boron in the pool water (the current Technical Specification requirement at Indian Point), the k was 0.9210. The total bias and uncertainty of fresh fuel in Region 2 is 0.0095, so the $k_{95/95}$ is 0.9305 which is less than the borated goal of 0.94. Less than 64 IFBA rod fuel has been ordered in the past for Indian Point, but plans for future assemblies use 64 or more IFBA rods. Many years ago Unit 2 had used 48 IFBA rods in 4.4 wt% U-235 fuel assemblies, but never less than 64 IFBA rods at 1.25X for higher enrichments. Unit 3 used a small number of feed assemblies with only 48 IFBA rods in Cycle 15 (current cycle is Cycle 18). A multiple misload of fresh 5.0 wt% fuel with less than 64 IFBA rods is therefore very unlikely. However, analysis was performed to determine how many 5 wt% U-235 enriched assemblies with **no** IFBA rods would need to be placed together to reach $k_{95/95}$ of 0.95 with 2000 ppm soluble boron. It required 12 of these no IFBA 5 wt% assemblies to be loaded together in a pool where all the rest of the assemblies were at the loading curve limits to reach the calculated k of 0.9307. Adding bias and uncertainty, the final $k_{95/95}$ becomes 0.9402.

Another multiple misload of all once burned fuel in Region 2 (5.0 wt% at 18 GWd/T) gives a k of 0.9219 at 2000 ppm. At 18 GWd/T, the total bias and uncertainty is 0.0178, so the $k_{95/95}$ is 0.9397, which meets the criterion of < 0.94 while the regulatory requirement is < 0.95. Normal first cycle burnup is more than 20 GWd/T, so a multiple misload of assemblies with less than 18 GWd/T is very unlikely. In fact, all feed assemblies for all cycles in Indian Point Units 2 and 3 with greater than 4.5 wt% U-235 enrichment have exceeded this burnup in the first cycle. Lower enrichments would need less burnup for the same reactivity.

For Region 1, if all the fuel was 5 wt% U-235 with no IFBA rods and the pool had 2000 ppm of soluble boron, the calculated k is 0.8022. Since after adding biases and uncertainties this is much less than 0.94, there is no concern about multiple misloads in Region 1.

Two additional features of this criticality analysis make multiple misloads unlikely. First, there is no credit for any checkerboard arrangement. Second, the Region 2 minimum burnup requirements are sufficiently low so that very few burned assemblies would fail to meet the requirements (requiring them to be stored in Region 1). Since there is very little burned fuel that needs to be stored in Region 1, there is no reason to store fresh fuel in Region 2. Therefore, a misload of a fresh fuel assembly without a control rod in Region 2 would be easily noticed by its shiny look (compared to all of the other assemblies in Region 2).

At the minimum SFP boron concentration of 2000 ppm, even multiple misloads will be safely subcritical. It is not credible to assume that a multiple misload and a boron dilution event would take place at the same time. Therefore, the criticality safety requirements are met by use of the double contingency principle.

9.5 Boron Dilution Accident

Crediting 700 ppm of soluble boron reduces the calculated k plus biases and uncertainty below 0.94. The boron dilution analysis of record [28] shows that dilution from the Technical Specification required 2000 ppm to 700 ppm is not credible.

9.6 Seismic Event

The absorber panels will be designed to withstand a design basis seismic event. Therefore, the absorber panels will remain in place and the rack configuration will not change significantly following a design basis seismic event. Since the absorber panels remain in place, no special analysis is needed.

10 Summary

This section summarizes the results of the criticality analysis. The section starts with a review of allowable fuel loading for the Indian Point Unit 2 spent fuel pool. This is followed by a review of the assumptions used to justify the allowable loading conditions. The racks are not expected to change, so the assumptions in the analysis are found in Section 3.4, and not repeated here. However, the absorber panels have not yet been ordered, so Section 10.2 reviews the requirements for the absorber panels. The fuel manufacturer may change in the future, so the fuel design requirements are repeated in Section 10.3. Finally, core operating conditions not precluded by the current Technical Specifications are utilized in this analysis. These core operating condition requirements are listed in Section 10.4.

10.1 Summary of Allowable Fuel Loading

Fresh fuel of 5.0 wt% U-235 or lower can be loaded anywhere in Region 1, as long as it contains at least 48 IFBA rods with a minimum 1X B10 loading. Burned fuel at a burnup of 12 GWd/T or more can be stored anywhere in Region 1. Fresh fuel with less than 48 IFBA rods or burned fuel with less than 12 GWd/T burnup can be stored on the periphery of Region 1. The periphery is defined as all the cell locations of the last row on the three sides of Module A that face away from Module B and all the cells on the last row of the face of Module B and Module C that is adjacent to the pool wall. Cells in the second row or further in Modules A, B, or C cannot take peripheral credit even if the outer row is empty. See Figure 8.8 for a graphical presentation of the location of the peripheral cells. If any fuel assembly contains a control rod, it can be located anywhere in Region 1, regardless of the number of IFBAs or burnup. A Region 1 cell which does not contain an absorber panel does not affect the loading requirements of any other cell in Region 1, so long as the cell that is missing an absorber panel contains a fuel assembly with a control rod or does not contain a fuel assembly.

Region 2 is primarily intended to be for discharged fuel. The only allowable way to load fresh fuel in Region 2 requires a control rod to be inserted in the assembly. The minimum burnup requirements for

Region 2 are presented in Table 10.1 as a function of fuel enrichment and cooling time. Linear interpolation can be used to determine the minimum burnup requirements at any enrichment or cooling time.

Table 10.1: Region 2 Minimum Burnup (GWd/T) Requirements[a-c,f]

	Cooling Time (years)						
Enrichment	**0**	**1**	**2**	**5**	**10**	**15**	**25[e]**
2.0[d]	3.20	3.10	3.08	3.00	3.00	3.00	3.00
2.5	15.17	14.85	14.66	13.97	13.20	12.84	12.31
3.0	21.28	21.17	20.98	20.66	20.26	19.98	19.65
3.5	27.53	27.10	26.63	25.56	24.29	23.50	22.45
4.0	33.82	33.43	33.05	32.04	30.72	29.70	28.44
4.5	38.98	38.65	37.99	36.49	34.67	33.69	32.60
5.0	42.67	42.14	41.78	40.78	39.72	38.96	37.68

Notes:

(a) Fuel assemblies with initial enrichments ≥ 4.0 wt% that do not meet the burnup requirements may be stored in peripheral cells provided the burnup requirements, reduced by 8 GWd/T, are met. If the fuel assembly contained a Hafnium flux suppressor insert then the burnup requirements may be reduced by 6 GWd/T if stored in a peripheral cell. The peripheral locations are shown on Figure 8.8.

(b) Fuel assemblies that contained a Hafnium flux suppressor insert and the burnup prior to the final cycle does not meet the burnup requirements, then 2 GWd/T must be added to the burnup requirements.

(c) Linear interpolation between enrichment levels and cooling times to determine minimum burnup requirements is permitted.

(d) Fuel assemblies with initial enrichments less than 2.0 wt% must meet the 2.0 wt% minimum burnup requirement. For axially blanketed fuel, the enrichment to be used is the enrichment of the center section between the blanket material.

(e) Fuel assemblies with cooling times greater than 25 years must meet the 25 year burnup requirement.

(f) Fuel assemblies with any fuel rods removed and not replaced (normally with stainless steel rods) must add 4 GWd/T to the burnup requirements. As for Region 1, a Region 2 cell which does not contain an absorber panel does not affect the loading requirements of any other cell in Region 2, so long as the cell which is missing an absorber panel does not contain a fuel assembly or contains a fuel assembly with a control rod.

Any fuel, including unburned 5 wt% U-235 fuel with no restriction on the number of IFBA rods, may be stored in Region 2 if the assembly contains a control rod.

The above loading requirements have been summarized below in Table 10.2.

Table 10.2: Summary of Loading Restrictions

	Loading Restriction
Region 1	Fresh fuel assemblies with initial enrichments of 5.0 wt% U-235 or less and 48 or more IFBA rods (@ [mg B-10/inch] [a,c] or greater) may be stored in any location in Region 1.
	Burned fuel assemblies with initial enrichments of 5.0 wt% U-235 or less with a burnup of 12 GWd/T or more may be stored in any location in Region 1.
	Any fuel assembly (fresh or burned) that contains an RCCA may be stored in any location in Region 1 with no restrictions on the number of IFBA rods or burnup.
	Any fuel assembly (fresh or burned) may be stored in locations designated as peripheral cells in Region 1 with no restrictions on the number of IFBA rods or burnup.
Region 2	Burned fuel assemblies that satisfy the requirements of Table 10.1* may be stored in any location in Region 2.
	Any fuel assembly (fresh or burned) that contains an RCCA can be stored anywhere in Region 2 with no restrictions on the number of IFBA rods or burnup.
	Burned fuel assemblies that satisfy the requirements of Table 10.1 *reduced by 8 GWd/T* may be stored in locations designated as peripheral cells in Region 2.**

* For assemblies that had a Hafnium insert and the burnup prior to the final cycle does not meet the burnup requirements of Table 10.1, then 2 GWd/T must be added to the values given in Table 10.1.

** For assemblies on the periphery that had a Hafnium insert and the burnup prior to the final cycle does not meet the burnup requirements of Table 10.1, then 6 GWd/T can be subtracted from the values given in Table 10.1.

10.2 Absorber Panel Requirements

To meet the assumptions of this criticality analysis, the absorber panels must satisfy the requirements specified in Table 10.3 below. If the alternate design is chosen, the minimum areal density must be 0.020 g B-10/cm^2 for panels in Region 2 and 0.022 g B-10/cm^2 for panels in Region 1. For the alternate design, the connector can be any material and can be any thickness up to 0.10 inch.

Table 10.3: Absorber Panel Requirements

Attribute	Value (inches)	Notes
Absorber Panel (primary)		
Areal Density (g B-10/cm^2)	0.015	Minimum
Panel width	Cell ID - .03	Minimum
Panel thickness	0.086	Minimum in Region 1
	0.096	Maximum in Region 2
Length		Covers active fuel length
Absorber Panel (alternate)*		
Areal Density (g B-10/cm^2)	0.020 in Region 2 0.022 in Region 1	Minimum
Panel width	7.6	Minimum
Panel thickness	0.075	Minimum in Region 1
	0.094	Maximum in Region 2
Offset from corner	0.64	
Length		Covers active fuel length

* A vendor is not bound by these specific dimensions and areal densities. As long as the panel is shown to be as effective in absorbing neutrons as the primary design, it would be acceptable.

10.3 Fuel Requirements

To meet the assumptions of this criticality analysis, the fuel design must meet the design assumptions given on Table 10.4. The guide tube dimensions are flexible as long as the cross-sectional area is at least 0.0243 square inches.

Table 10.4: Fuel Design Requirements

Attribute	Value (inches)	Notes
Fuel pellet UO_2 stack density	97.5 %TD	Maximum stack density*
Fuel pellet OD	[ ]^{a,c}	Maximum
Fuel clad OD	[ ]^{a,c}	Minimum
Fuel clad ID	[ ]^{a,c}	Maximum
Fuel pin pitch	0.5630	Nominal
Guide tube cross sectional area	0.0243 in^2	Minimum Nominal

* This density includes the effect of dishing and chamfering.

10.4 Reactor Operation Limits

The depletion parameters were selected to cover anticipated future operation, however, verification is required. Table 10.5 lists the operating assumptions used in the depletion analysis for fuel enriched to greater than 3.5 wt%*. The temperature and soluble boron assumptions are averages over the total burnup (multi-cycle) for a given assembly. These assumptions will be verified as part of the reload design process. The process normally assumes a range of previous cycle burnups. If the plant is shutdown outside of this range or before the reload analysis for the following cycle is completed, the assumptions listed in Table 10.5 must be confirmed for each assembly that is to be placed into Region 2 or a non-peripheral location of Region 1. If an assembly is depleted such that any of the Table 10.5 parameters are not met, then the assembly would have to be stored in Region 1 or with a control rod inserted until an assembly-specific analysis can be performed and approved. Note that if an assembly meets the burnup requirements (GWd/T) and the operating limits, any additional burnup does not need to meet the operating limits.

Table 10.6 is provided for older fuel enriched to 3.5 wt% or less to verify that the existing fuel meets the assumptions of the criticality analysis. Table 10.6 is not to be used for future fuel.

* If fuel less than or equal to 3.5 wt% is ever used in the future, the same requirements shown in Table 10.5 apply. Table 10.5 should be used for all future fuel regardless of enrichment.

Table 10.5: Fuel Assembly Operating Requirements for Fuel Enriched > 3.5 wt%*

Parameter	Value	Notes
Maximum assembly average moderator outlet temperature during depletion†	631 °F (605.9 °K)	This value can be demonstrated by a maximum assembly and burnup averaged peaking factor. This corresponds to a maximum burnup averaged peaking factor of 1.40 with current thermal design flow conditions.
Maximum WABA loading	20 rodlet WABA at 0.00603 g ^{10}B/cm per rodlet	Design changes that increase water displacement are not covered.
Maximum IFBA rods and ^{10}B loading	148 IFBA rods [mg ^{10}B/inch]^{a,c} (1.5X) per rod	Credit for IFBAs used with fresh fuel use a minimum 1X loading.
Maximum Operation with Control Rods	≤ 2 GWd/T	This control rod inserted burnup covers rods inserted to any depth.
Maximum Burnup Averaged Soluble Boron	≤ 1000 ppm	This is an average for all cycles in which the assembly was depleted. For burned assemblies stored in Region 1, this requirement is relaxed to < 1300 ppm.
Average Power During the Last 30 Days of Operation	> 50%	To cover reduced power operation at end of cycle prior to offload

* If fuel less than or equal to 3.5 wt% is ever used in the future, the same requirements shown in Table 10.5 apply. Table 10.5 should be used for all future fuel regardless of enrichment.
† If the peaking factor is less than 1.40, the moderator outlet temperature requirement is met.

Table 10.6: Fuel Assembly Operating Requirements for Fuel Enriched ≤ 3.5 wt%*

Parameter	Value	Notes
Maximum assembly average moderator outlet temperature during depletion†	628 °F (604.4 °K)	This value can be demonstrated by a maximum assembly and burnup averaged peaking factor. This corresponds to a maximum burnup averaged peaking factor of 1.35 with current thermal design flow conditions.
Maximum BA loading	20 rodlet Pyrex at a boron loading of 18.1 wt% B_2O_3	No limit on when the Pyrex is removed.
Maximum Operation with Control Rods	≤ 2 GWd/T	This control rod inserted burnup is the assembly average burnup during which control rods were inserted below the top node. The top node can have the rod inserted throughout life.
Maximum Burnup Averaged Soluble Boron	≤ 800 ppm	This is an average for all cycles in which the assembly was depleted.
Average Power During the Last 30 Days of Operation	> 50%	To cover reduced power operation at end of cycle prior to offload

* This table is provided only to certify that older fuel ≤ 3.5 wt% satisfies the older operating requirements. For future fuel, Table 10.5 should be used regardless of enrichment.

† If the peaking factor is less than 1.35, the moderator outlet temperature requirement is met.

References

[1] K. Wood, DSS-ISG-2010-1, "Draft Staff Guidance Regarding the Nuclear Criticality Safety Analysis for Spent Fuel Pools." Accession Number ML102220567, Nuclear Regulatory Commission, Rockville, MD, August 2010.

[2] Code of Federal Regulations, Title 10, Part 50, Section 68, "Criticality Accident Requirements."

[3] *Scale: A Comprehensive Modeling and Simulation Suite for Nuclear Safety Analysis and Design*, ORNL/TM-2005/39, Version 6.1, June 2011. Available from Radiation Safety Information Computational Center at Oak Ridge National Laboratory as CCC-785. Includes 6.1.2 update dated 2/28/13.

[4] "Rack Construction (SH'T. 2) Region 1 Storage Racks," Drawing Number 398 Rev5, March 19, 1990, Project No. 81000, P. O. No. 8-24470, Holtec International, Mount Laurel, NJ.

[5] "Rack Construction (SH'T. 1) Region 2 Storage Racks," Drawing Number 400 Rev5, March 19, 1990, Project No. 81000, P. O. No. 8-24470, Holtec International, Mount Laurel, NJ.

[6] G. Radulescu, I. C. Gauld, and G. Ilas, *SCALE 5.1 Predictions of PWR Spent Nuclear Fuel Isotopic Compositions*, ORNL/TM-2010/44, Oak Ridge National Laboratory, Oak Ridge, Tennessee, USA, March 2010.

[7] *Licensing Report on the Inter-Unit Transfer of Spent Nuclear Fuel at the Indian Point Energy Center,* Holtec Report No. HI-2094289. Rev. 6, April 17, 2012.

[8] *International Handbook of Evaluated Criticality Safety Benchmark Experiments*, NEA/NSC/DOC(95)3, Volume IV, Nuclear Energy Agency, OECD, Paris, September, 2010.

[9] K. S. Smith, et al., *Benchmarks for Quantifying Fuel Reactivity Depletion Uncertainty*, EPRI, Palo Alto, CA, Technical Report Number 1022909 (2011).

[10] D. B. Lancaster, *Utilization of the EPRI Depletion Benchmarks for Burnup Credit Validation*, EPRI, Palo Alto, CA, 1025203 (2012).

[11] U.S. Nuclear Regulatory Commission, *Spent Fuel Project Office Interim Staff Guidance – 8, Rev. 3 – Burnup Credit in the Criticality Safety Analyses of PWR Spent Fuel in Transport and Storage Casks*, U.S. Nuclear Regulatory Commission, April, 2012.

[12] J.C. Dean and R.W. Tayloe, Jr., *Guide for Validation of Nuclear Criticality Safety Calculational Methodology*, NUREG/CR-6698, Nuclear Regulatory Commission, Washington, DC January 2001.

[13] D. E. Mueller, K. R. Elam, and P. B. Fox, *Evaluation of the French Haut Taux de Combustion (HTC) Critical Experiment Data*, NUREG/CR-6979 (ORNL/TM-2007/083), prepared for the US Nuclear Regulatory Commission by Oak Ridge National Laboratory, Oak Ridge, Tenn., September 2008.

[14] J. M. Scaglione, D. E. Mueller, J.C. Wagner and W. J. Marshall, *An Approach for Validating. Actinide and Fission Product Burnup Credit Criticality Safety Analyses—Criticality (keff) Predictions*, US Nuclear Regulatory Commission, NUREG/CR-7109, Oak Ridge National Laboratory, Oak Ridge, Tenn. (2012).

[15] J.C. Wagner and C. V. Parks, *Parametric Study of the Effect of Burnable Poison Rods for PWR Burnup Credit,* US Nuclear Regulatory Commission, NUREG/CR-6761, Oak Ridge National Laboratory, Oak Ridge, Tenn. (2002).

[16] C. E. Sanders and J.C. Wagner, *Study of the Effect of Integral Burnable Poison Rods for PWR Burnup Credit,* US Nuclear Regulatory Commission, NUREG/CR-6760, Oak Ridge National Laboratory, Oak Ridge, Tenn. (2002).

[17] C. V. Parks, M. D. DeHart, and J.C. Wagner, *Review and Prioritization of Technical Issues Related to Burnup Credit for LWR Fuel,* US Nuclear Regulatory Commission, NUREG/CR-6665, Oak Ridge National Laboratory, Oak Ridge, Tenn. (2000).

[18] D. Hagrman, *INTERPIN-3 User's Manual,* SSP-01/430, Studsvik Scandpower, Inc. (2001).

[19] M. D. DeHart, *Sensitivity and Parametric Evaluations of Significant Aspects of Burnup Credit for PWR Spent Fuel Packages*, ORNL/TM-12973, Lockheed Martin Energy Research Corp., Oak Ridge National Laboratory, May 1996.

[20] J.C. Wagner, M. D. DeHart, and, C. V. Parks, *Recommendations for Addressing Axial Burnup in PWR Burnup Credit Analyses,* US Nuclear Regulatory Commission, NUREG/CR-6801, Oak Ridge National Laboratory, Oak Ridge, Tenn. (2003).

[21] "Pool Layout Spent Fuel Storage Racks," Drawing Number 397 Rev 4, December 8, 1989, Project No. 81000, P. O. No. 8-24470, Holtec International, Mount Laurel, NJ.

[22] "NEI 12-16, Guidance for Performing Criticality Analyses of Fuel Storage at Light-Water Reactor Plants," Slides from NEI/NRC on meeting September 24, 2013, Adams Accession Number, ML13264A008.

[23] NET-300042-01, Rev. 1, "Interim Reactivity Analysis of the Indian Point Unit 2 Spent Fuel Pool," September, 2012.

[24] Indian Point Unit 2 Updated Final Safety Analysis Report (UFSAR), Revision 24, 2013.

[25] K. Lindquist, et al., *Guidelines for Boraflex Use in Spent-Fuel Storage Racks*, EPRI, Palo Alto, CA, Technical Report Number 103300 (1993).

[26] Letter from Tom Duberville of Holtec International to Joe DeFrancesco of Entergy-Indian Point, "Holtec International DREAM Insert; basic specification data," September 19, 2013.

[27] *Guidance for Performing Criticality Analyses of Fuel Storage at Light-Water Reactor Power Plants*, Revision 1, NEI 12-16, Nuclear Energy Institute, Washington, DC, April 2014.

[28] NET-173-02. Rev.1, "Indian Point Unit 2 Spent Fuel Pool (SFP) Boron Dilution Analysis, September 2001.

[29] Regulatory Guide 1.183, "Alternative Radiological Source Terms for Evaluating Design Basis Accidents at Nuclear Power Reactors," July, 2000.

[30] Design Input Record, EN-DC-149R14 140218, Indian Point, February 17, 2014

[31] [NOT USED]

[32] R. E. Griffith to G. Delfini, "Fuel Temperatures vs Burnup Curves for Indian Point Unit 2," Entergy Inter-Office Correspondence, CEO2013-00107, August 15, 2013, supported by Entergy Calculation package NEAD-SR-2013/023, EC 4611.

[33] ANSI/ANS-8.1-1998 (R2007), "Nuclear Criticality Safety in Operations with Fissionable Materials Outside Reactors," American Nuclear Society, La Grange Park, Illinois.

Appendix A: Validation of SCALE 6.1.2 for Criticality Analysis of Fresh and Burned Fuel

A.1. Objective

This appendix determines the computer code and cross-section library bias and uncertainty in the k's calculated for the Indian Point Units 2 and 3 spent fuel pools when using SCALE 6.1.2 [1] and the 238 group ENDF/B-VII cross-section library. The bias and uncertainties determined in this Appendix covers both fresh and burned fuel.

A.2. Method

The bias and uncertainty is determined as a bias and uncertainty in the initial condition of the fuel and then an additional bias and uncertainty due to the change in reactivity with burnup. This Appendix is divided into three sections: 1) Laboratory critical experiments (Fresh UO_2, HTC criticals, and MOX criticals), 2) EPRI benchmarks, and 3) Chemical Assays.

The initial condition bias and uncertainties come from the fresh UO_2 criticals. With the burned fuel, two approaches will be used to determine the bias and uncertainty in the depletion reactivity: 1) Extended ISG-8, and 2) EPRI benchmark based.

In the Extended ISG-8 approach, a bias and uncertainty due to the change in isotopic content is determined and an additional bias and uncertainty due to the cross-sections of isotopes not contained in the initial fresh fuel criticals is included. The HTC and MOX criticals are analyzed to determine if the major actinides introduce a bias and uncertainty not found in the fresh UO_2 experiments. Then a bias of 1.5% of the fission product and minor actinide worth is added. This bias and uncertainty (zero uncertainty is used) is based on the NRC approved method for the transport analysis given in ISG-8, Rev. 3 [9]. ISG-8, Rev. 3, however, is restricted to 28 isotopes and this analysis "extends" this to all significant (185) isotopes (see Table A.3.1). The last sentence of Section 7 of NUREG/CR-7109 [32] states, "An upper value of 1.5% of the worth is also applicable for SNF isotopic compositions consisting of all nuclides in the SFP configuration." The 1.5% bias on the worth of fission products and minor actinides is applied to all of the non-major actinides in the 185 isotopes. The analysis of the EPRI benchmarks [10,11] provide confidence that the isotopes not included in the chemical assays do not have a significant error that would overwhelm the 1.5% bias.

The EPRI benchmarks provide a direct measure of the change in reactivity with burnup. They can be used directly for the desired validation. In order to assure conservatism, the more limiting bias and uncertainty from either the Extended ISG-8 approach or the EPRI benchmark approach will be used. Note that the EPRI benchmarks are also used as part of the Extended ISG-8 approach. Although the EPRI benchmarks do not provide information for individual isotopes, all the isotopes used in the Extended ISG-8 are in the analysis of the EPRI benchmarks. The reactivity of the extension isotopes is

generally based on only cross-section measurement data. The EPRI benchmarks provide some assurance that there is not a gross transcription error in the cross-section data.

A.3. Computer Codes Used

This analysis uses the CSAS5 module of SCALE 6.1.2 [1] for the criticality analysis and the t5-depl module for the depletion analysis. All the analyses are performed using the 238 group ENDF/B-VII library (v7-238). The CSAS5 module executes the CENTRM and BONAMI programs for the resonance self-shielding calculations and KENO V.a for the Monte Carlo calculation of k. All the computer runs use a large Monte Carlo sampling of at least 1500 generations and 6000 neutrons per generation.

The t5-depl implements CENTRM and BONAMI for the resonance treatment and then uses KENO V.a for the collapsing of the cross-sections from 238 groups to one group for use in ORIGEN. parm=(addnux=4) is used in the analysis which utilizes the maximum number of problem specific collapsed isotopes (388). At the end of the depletion analysis, the OPUS module is used to output atom densities (for the EPRI benchmark work) or grams per MTU for the chemical assay work. The input for OPUS could specify any set of isotopes. For this validation, the OPUS input is set for 185 isotopes that are carried forward to the criticality analysis.

Although it may seem that there was a significant reduction in isotopes from the 388 isotopes with the addnux=4 set, many of the isotopes are for structural materials rather than fission products. All of the eliminated isotopes have low atom densities in spent fuel and do not have a large cross section to compensate for the low atom density. Of the 388 isotopes only 185 isotopes have any significant impact on k. The 185 isotopes are listed in Table A.3.1. Since for the short cooling times the peak reactivity is desired, the Xe-135 is directly converted to Cs-135 and the Np-239 is directly converted to Pu-239. I-135 and Ru-105 have sufficiently short half-lives that they decay away to daughters which are followed before 72 hours of cooling. After 72 hours, only 181 isotopes are followed. At low burnups some additional isotopes are eliminated if their atom densities are less than 1E-12.

Since SCALE 6.1 does not output isotopic data for burnups after cooling for less than the maximum specified burnup, a small Fortran program was used to decay the isotopic content to the desired cooling time. The Fortran program was only used in support of the EPRI benchmark analysis by decaying the isotopes for 100 hours, 5 years and 15 years. The computer code was confirmed by comparison to direct decay performed by SCALE. The Fortran program could be avoided for the validation, but was used to match the method used in the pool criticality analysis, where multiple cooling times and burnups make direct calculation with SCALE very time consuming.

Table A.3.1: 185 Isotopes Used in the Analysis

Ag-109	Cm-243	Gd-160	Nd-145	Rb-85	Sm-153	Te-130
Ag-110m	Cm-244	Ge-73	Nd-146	Rb-86	Sm-154	Te-132
Ag-111	Cm-245	Ge-76	Nd-147	Rb-87	Sn-115	U-234
Am-241	Cm-246	Ho-165	Nd-148	Rh-103	Sn-116	U-235
Am-242m	Cs-133	I-127	Nd-150	Rh-105	Sn-117	U-236
Am-243	Cs-134	I-129	Np-237	Ru-100	Sn-118	U-237
As-75	Cs-135	I-131	Np-238	Ru-101	Sn-119	U-238
Ba-134	Cs-136	I-135	Np-239	Ru-102	Sn-120	Xe-128
Ba-135	Cs-137	In-115	O-16	Ru-103	Sn-122	Xe-129
Ba-136	Dy-160	Kr-82	Pd-104	Ru-104	Sn-123	Xe-130
Ba-137	Dy-161	Kr-83	Pd-105	Ru-105	Sn-124	Xe-131
Ba-138	Dy-162	Kr-84	Pd-106	Ru-106	Sn-125	Xe-132
Ba-140	Dy-163	Kr-85	Pd-107	Ru-99	Sn-126	Xe-133
Br-81	Dy-164	Kr-86	Pd-108	Sb-121	Sr-86	Xe-134
Cd-110	Er-166	La-138	Pd-110	Sb-123	Sr-88	Xe-135
Cd-111	Eu-151	La-139	Pm-147	Sb-124	Sr-89	Xe-136
Cd-112	Eu-152	La-140	Pm-148	Sb-125	Sr-90	Y-89
Cd-113	Eu-153	Mo-100	Pm-148m	Se-76	Tb-159	Y-90
Cd-114	Eu-154	Mo-95	Pm-149	Se-77	Tb-160	Y-91
Cd-115m	Eu-155	Mo-96	Pm-151	Se-80	Tc-99	Zr-91
Cd-116	Eu-156	Mo-97	Pr-141	Se-82	Te-122	Zr-93
Ce-140	Gd-152	Mo-98	Pr-143	Sm-147	Te-124	Zr-95
Ce-141	Gd-154	Mo-99	Pu-238	Sm-148	Te-125	Zr-96
Ce-142	Gd-155	Nb-95	Pu-239	Sm-149	Te-126	
Ce-143	Gd-156	Nd-142	Pu-240	Sm-150	Te-127m	
Ce-144	Gd-157	Nd-143	Pu-241	Sm-151	Te-128	
Cm-242	Gd-158	Nd-144	Pu-242	Sm-152	Te-129m	

A.4. Analysis

The analysis is broken into three major sections: Laboratory Critical Experiments, EPRI Benchmarks, and Extended ISG-8 Chemical Assay Analysis.

A.4.1 Laboratory Critical Experiments

A.4.1.1 Introduction

The validation consists of modeling 236 fresh UO_2 critical experiments and the determination of the bias and the uncertainty in the calculation of k for fresh fuel. This validation follows the direction of NUREG/CR-6698, "Guide for Validation of Nuclear Criticality Safety Calculational Methodology" [2]. The guide establishes the following steps for performing the validation:

1. Define operation/process to identify the range of parameters to be validated
2. Select critical experiment data
3. Model the experiments
4. Analyze the data
5. Define the area of applicability of the validation and limitations

It further defines the steps of "Analyze the data" as:

1. Determine the Bias and Bias Uncertainty
2. Identify Trends in Data, Including Discussion of Methods for Establishing Bias Trends
3. Test for Normal or Other Distributions
4. Select the Statistical Method for Treatment of Data
5. Identify and Support Subcritical Margin
6. Calculate the Upper Safety Limit

This approach will be followed for this validation analysis.

A.4.1.2 Definition of the Range of Parameters to Be Validated

The validation guidance document [2] states:

> *"Prior to the initiation of the validation activity, the operating conditions and parameters for which the validation is to apply must be identified. The fissile isotope, enrichment of fissile isotope, fuel density, fuel chemical form, types of neutron moderators and reflectors, range of moderator to fissile isotope, neutron absorbers, and physical configurations are among the parameters to specify. These parameters will come to define the area of applicability for the validation effort."*

Almost all pool applications have common neutronic characteristics and therefore can be validated together. The racks are assumed to be flooded with water at near room temperature and below 100° C. The fuel is low enriched uranium dioxide (less than or equal to 5.0 wt% U-235). The fuel is in pellets with a density of greater than 94% of the theoretical density. The only significant neutron moderators are water and the oxygen in the fuel pellet. The neutron absorbers credited are boron (as plates, perhaps rods,

or in solution) and Ag-In-Cd control rods. The reflectors are water, steel, or concrete. The fuel is in assemblies, but the analysis is also valid for disassembled assemblies. The assembly arrangement can vary by design from totally isolated assemblies to a close packed array of assemblies.

A.4.1.3 Selection of the Fresh UO_2 Critical Benchmark Experiments

The UO2 benchmarks that were selected met the following criteria:

- Low enriched (5 wt% U-235 or less) UO2 to cover the principle isotopes of concern.
- Fuel in rods to assure that the heterogeneous analysis used in SCALE also is applied in the benchmark analysis.
- Square lattices to assure the lattice features of SCALE used in the rack analysis are also modeled in the critical benchmarks selected.
- Presence of soluble boron, borated steel, boron bearing rods, sheets of aluminum with boron, Boraflex, or Ag-In-Cd.
- No emphasis on a feature or material not of importance to the rack analysis.

The OECD/NEA *International Handbook of Evaluated Criticality Safety Benchmarks Experiments* [3] is now considered as the appropriate reference for criticality safety benchmarks. This handbook has reviewed the available benchmarks and evaluated the uncertainties in the experiments. The appropriate modeling is presented. All of the experiments used in this validation were taken from this handbook. Volume IV of the handbook is for low enriched uranium systems. The section of Volume IV of interest to this validation is the "Thermal Compound Systems." All of the experiments selected are numbered LEU-COMP-THERM-0XX. This validation will refer to the experiments LEU-COMP-THERM-0XX as just XX where any leading zero is not included.

There are more critical experiments in the handbook that meet the requirements for this validation than would be necessary to use. However, most of the applicable available benchmarks were used. There are 85 sets of benchmarks in the September 2010 version of the handbook. 22 of these sets were eliminated, since they were for hexagonal arrays. 4 more sets were eliminated due to enrichments of 7 wt% U-235 or higher. 10 experimental sets were not for water moderated fuel rods. 4 experimental sets were eliminated due to high uncertainties. This leaves 45 benchmark sets of which 31 sets were used for this validation. The 14 unused benchmark sets were reviewed to be sure that there was no feature of the experimental set that was missing in the selected 31 sets.

The selected 31 benchmark sets include critical experiments from six different critical experiment facilities. The fuel was mainly clad in aluminum, but experiments with stainless steel and zirconium cladding were also in the set.

The critical benchmark sets generally contained multiple experiments, but not all cases from each critical benchmark set is used. In some sets there are experiments that emphasize features that are out of the scope of this validation, such as lead or copper reflectors. The 31 selected benchmark sets resulted in **236 experiments** that are used for the statistical analysis. Since boron absorption is important to criticality of the spent fuel pool, it is important that of these 236 experiments, 41 experiments used soluble boron and 28 experiments used boron containing absorber plates.

A later section will evaluate the area of applicability provided by this selection of critical benchmarks.

Table A.4.1.1 provides a summary of all the low enriched thermal experiments (non-U metal) from the OECD/NEA handbook [3] and why some experiments were not used.

Table A.4.1.1: Selection Review of OECD/NEA Criticality Benchmarks
(All Experiments Start With LEU-COMP-THERM-)

Benchmark Number	Description	Lab	Selected
1	WATER-MODERATED U(2.35)O_2 FUEL RODS IN 2.032-CM SQUARE-PITCHED ARRAYS	PNL	All 8
2	WATER-MODERATED U(4.31)O_2 FUEL RODS IN 2.54-CM SQUARE-PITCHED ARRAYS	PNL	All 5
3	WATER-MODERATED U(2.35)O_2 FUEL RODS IN 1.684-CM SQUARE-PITCHED ARRAYS (GADOLINIUM WATER IMPURITY)	PNL	None. Gd impurity not well known. Not benchmark quality.
4	WATER-MODERATED U(4.31)O_2 FUEL RODS IN 1.892-CM SQUARE-PITCHED ARRAYS (GADOLINIUM WATER IMPURITY)	PNL	None. Gd impurity not well known. Not benchmark quality.
5	CRITICAL EXPERIMENTS WITH LOW-ENRICHED URANIUM DIOXIDE FUEL RODS IN WATER CONTAINING DISSOLVED GADOLINIUM	PNL	None. No sample SCALE decks. Soluble Gd not used in pools.
6	CRITICAL ARRAYS OF LOW-ENRICHED UO_2 FUEL RODS WITH WATER-TO-FUEL VOLUME RATIOS RANGING FROM 1.5 TO 3.0	JAEA	All 18
7	WATER-REFLECTED 4.738-WT.%-ENRICHED URANIUM DIOXIDE FUEL-ROD ARRAYS	Valduc	Only 4 cases used rest are in hexagonal arrays.
8	CRITICAL LATTICES OF UO_2 FUEL RODS AND PERTURBING RODS IN BORATED WATER	B&W	All 17
9	WATER-MODERATED RECTANGULAR CLUSTERS OF U(4.31)O_2 FUEL RODS (2.54-CM PITCH) SEPARATED BY STEEL, BORAL, COPPER, CADMIUM, ALUMINUM, OR ZIRCALOY-4 PLATES	PNL	21 cases used. Did not include Copper cases since no copper in pools.
10	WATER-MODERATED U(4.31)O_2 FUEL RODS REFLECTED BY TWO LEAD, URANIUM, OR STEEL WALLS	PNL	22 cases used. Did not use lead cases since no lead in pools.

Benchmark Number	Description	Lab	Selected
11	CRITICAL EXPERIMENTS SUPPORTING CLOSE PROXIMITY WATER STORAGE OF POWER REACTOR FUEL (PART I - ABSORBER RODS)	B&W	All 15
12	WATER-MODERATED RECTANGULAR CLUSTERS OF U(2.35)O_2 FUEL RODS(1.684-CM PITCH) SEPARATED BY STEEL, BORAL, BOROFLEX, CADMIUM,OR COPPER PLATES (GADOLINIUM WATER IMPURITY)	PNL	None. Gd impurity not well known. Not benchmark quality.
13	WATER-MODERATED RECTANGULAR CLUSTERS OF U(4.31)O_2 FUEL RODS (1.892-CM PITCH) SEPARATED BY STEEL, BORAL, BOROFLEX, CADMIUM, OR COPPER PLATES, WITH STEEL REFLECTING WALLS	PNL	5 cases used. Did not use the 2 cases with copper.
14	WATER-REFLECTED ARRAYS OF U(4.31)O_2 FUEL RODS (1.890-CM AND 1.715-CM SQUARE PITCH) IN BORATED WATER	PNL	None used. High boron content uncertainty. Not benchmark quality.
15	THE VVER EXPERIMENTS: REGULAR AND PERTURBED HEXAGONAL LATTICES OF LOW-ENRICHED UO_2 FUEL RODS IN LIGHT WATER	KFKI	None used due to hex arrays.
16	WATER-MODERATED RECTANGULAR CLUSTERS OF U(2.35)O_2 FUEL RODS (2.032-CM PITCH) SEPARATED BY STEEL, BORAL, COPPER, CADMIUM, ALUMINUM, OR ZIRCALOY-4 PLATES	PNL	26 cases used. Did not use the 6 copper cases
17	WATER-MODERATED U(2.35)O_2 FUEL RODS REFLECTED BY TWO LEAD, URANIUM, OR STEEL WALLS	PNL	23 cases used. Did not use the 6 cases with a lead reflector.
18	LIGHT WATER MODERATED AND REFLECTED LOW ENRICHED URANIUM DIOXIDE (7 WT.%) ROD LATTICE	Winfrith	None used. Only 1 case with no SCALE sample deck. Complex system.
19	WATER-MODERATED HEXAGONALLY PITCHED LATTICES OF U(5%)O_2 STAINLESS STEEL CLAD FUEL RODS	Kurchatov Institute	None used due to hex arrays.
20	WATER-MODERATED HEXAGONALLY PITCHED PARTIALLY FLOODED LATTICES OF U(5%)O_2 ZIRCONIUM CLAD FUEL RODS, 1.3-CM PITCH	Kurchatov Institute	None used due to hex arrays.

Benchmark Number	Description	Lab	Selected
21	HEXAGONALLY PITCHED PARTIALLY FLOODED LATTICES OF U(5%)O_2 ZIRCONIUM CLAD FUEL RODS MODERATED BY WATER WITH BORIC ACID	Kurchatov Institute	None used due to hex arrays.
22	UNIFORM WATER-MODERATED HEXAGONALLY PITCHED LATTICES OF RODS WITH U(10%)O_2 FUEL	Kurchatov Institute	None used due to hex arrays.
23	PARTIALLY FLOODED UNIFORM LATTICES OF RODS WITH U(10%)O_2 FUEL	Kurchatov Institute	None used due to hex arrays.
24	WATER-MODERATED SQUARE-PITCHED UNIFORM LATTICES OF RODS WITH U(10%)O_2 FUEL	Kurchatov Institute	Did not use either case due to 10 wt% U-235 enrichment
25	WATER-MODERATED HEXAGONALLY PITCHED LATTICES OF U(7.5%)O_2 STAINLESS-STEEL-CLAD FUEL RODS	Kurchatov Institute	None used due to hex arrays.
26	WATER-MODERATED U(4.92)O_2 FUEL RODS IN 1.29, 1.09, AND 1.01 CM PITCH HEXAGONAL LATTICES AT DIFFERENT TEMPERATURES	IPPE	None used due to hex arrays.
27	WATER-MODERATED AND LEAD-REFLECTED 4.738% ENRICHED URANIUM DIOXIDE ROD ARRAYS	Valduc	None used due to lead reflector.
28	WATER-MODERATED U(4.31)O_2 FUEL RODS IN TRIANGULAR LATTICES WITH BORON, CADMIUM AND GADOLINIUM AS SOLUBLE POISONS	PNL	None used due to hex arrays.
29	WATER MODERATED AND WATER REFLECTED 4.74% ENRICHED URANIUM DIOXIDE ROD ARRAYS SURROUNDED BY HAFNIUM PLATES	Valduc	None used. No SCALE sample decks. hf plates cases without hf have the same pitch and pin as benchmark 7 above. No significant additional value
30	VVER PHYSICS EXPERIMENTS: REGULAR HEXAGONAL (1.27-CM PITCH) LATTICES OF LOW-ENRICHED U(3.5 WT.% 235U)O_2 FUEL RODS IN LIGHT WATER AT DIFFERENT CORE CRITICAL DIMENSIONS	Kurchatov Institute	None used due to hex arrays.
31	WATER-MODERATED HEXAGONALLY PITCHED PARTIALLY FLOODED LATTICES OF U(5%)O_2 ZIRCONIUM-CLAD FUEL RODS, 0.8-CM PITCH	Kurchatov Institute	None used due to hex arrays.

Benchmark Number	Description	Lab	Selected
32	UNIFORM WATER-MODERATED LATTICES OF RODS WITH U(10%)O_2 FUEL IN RANGE FROM 20°C TO 274°C	Kurchatov Institute	None used due to hex arrays.
33	REFLECTED AND UNREFLECTED ASSEMBLIES OF 2 AND 3%-ENRICHED URANIUM FLUORIDE IN PARAFFIN	ORNL	None used. Not UO_2
34	FOUR 4.738-WT.%-ENRICHED URANIUM DIOXIDE ROD ASSEMBLIES CONTAINED IN CADMIUM, BORATED STAINLESS STEEL, OR BORAL SQUARE CANISTERS, WATER-MODERATED AND -REFLECTED	Valduc	6 cases used. Did not use cases with gap less than 2.5 cm due to high uncertainty. Did not use Cd plate cases since Cd plates not in pool.
35	CRITICAL ARRAYS OF LOW-ENRICHED UO_2 FUEL RODS IN WATER WITH SOLUBLE GADOLINIUM OR BORON POISON	JAEA	Used 2 cases. Did not use the case with dissolved Gd. (not like pool).
36	THE VVER EXPERIMENTS: REGULAR AND PERTURBED HEXAGONAL LATTICES OF LOW-ENRICHED UO_2 FUEL RODS IN LIGHT WATER - Part 2	KFKI	None used due to hex arrays.
37	WATER-MODERATED AND PARTIALLY CONCRETE-REFLECTED 4.738-WT.%-ENRICHED URANIUM DIOXIDE ROD ARRAYS	Valduc	None used. No SCALE sample decks.
38	WATER-MODERATED 4.738-WT.%-ENRICHED URANIUM DIOXIDE ROD ARRAYS NEXT TO A BORATED CONCRETE SCREEN	Valduc	None used. No SCALE sample decks. Used a borated concrete reflector (not like pool).
39	INCOMPLETE ARRAYS OF WATER-REFLECTED 4.738-WT.%-ENRICHED URANIUM DIOXIDE FUEL-ROD ARRAYS	Valduc	Used all 17 cases.
40	FOUR 4.738-WT.%-ENRICHED URANIUM DIOXIDE ROD ASSEMBLIES CONTAINED IN BORATED STAINLESS STEEL OR BORAL SQUARE CANISTERS, WATER MODERATED AND REFLECTED BY LEAD OR STEEL	Valduc	Used 4 cases. Did not use lead reflector cases.
41	STORAGE ARRAYS OF 3%-ENRICHED LWR ASSEMBLIES: THE CRISTO II EXPERIMENT IN THE EOLE REACTOR	Cadarache	Did not use the 5 cases due to complex geometry and no SCALE sample deck.

Benchmark Number	Description	Lab	Selected
42	WATER-MODERATED RECTANGULAR CLUSTERS OF U(2.35)O_2 FUEL RODS (1.684-CM PITCH) SEPARATED BY STEEL, BORAL, BOROFLEX, CADMIUM, OR COPPER PLATES, WITH STEEL REFLECTING WALLS	PNL	Used 5 cases. Did not use copper cases.
43	CRITICAL LOADING CONFIGURATIONS OF THE IPEN/MB-01 REACTOR WITH A HEAVY SS-304 REFLECTOR	IPEN	Used only one case. Rest of cases were not significantly different.
44	CRITICAL LOADING CONFIGURATIONS OF THE IPEN/MB-01 REACTOR WITH UO_2, STAINLESS STEEL AND COPPER RODS	IPEN	Used only one case. Rest of cases were not significantly different.
45	PLEXIGLAS OR CONCRETE-REFLECTED U(4.46)$_3O_8$ WITH H/U=0.77 AND INTERSTITIAL MODERATION	Rocky Flats	None used since not pin geometry.
46	Not included in 2010 Handbook		
47	FUEL TRANSPORT FLASK CRITICAL BENCHMARK EXPERIMENTS WITH LOW-ENRICHED URANIUM DIOXIDE FUEL	Winfrith	None used. 3 complex cases. No SCALE sample decks.
48	LIGHT WATER MODERATED AND REFLECTED LOW-ENRICHED (3 WT.% 235U) URANIUM DIOXIDE ROD LATTICES	Winfrith	All 5 cases used
49	MARACAS PROGRAMME: POLYTHENE-REFLECTED CRITICAL CONFIGURATIONS WITH LOW-ENRICHED AND LOW-MODERATED URANIUM DIOXIDE POWDER, U(5)O_2	Valduc	None used. Powder rather than pellets. Not similar to pools.
50	149SM SOLUTION TANK IN THE MIDDLE OF WATER-MODERATED 4.738-WT.%-ENRICHED URANIUM DIOXIDE ROD ARRAYS	Valduc	7 cases used. Did not use cases with dissolved Sm. This is not typical of pools.
51	CRITICAL EXPERIMENTS SUPPORTING CLOSE PROXIMITY WATER STORAGE OF POWER REACTOR FUEL (PART II - ISOLATING PLATES)	B&W	9 cases used. Did not use cases with the borated Al plates since primary source listed a high uncertainty in the boron content.
52	URANIUM DIOXIDE (4.738-WT.%-ENRICHED) FUEL ROD ARRAYS MODERATED AND REFLECTED BY GADOLINIUM NITRATE SOLUTION	Valduc	None used due to hex arrays.

Benchmark Number	Description	Lab	Selected
53	VVER PHYSICS EXPERIMENTS: REGULAR HEXAGONAL (1.27 CM PITCH) LATTICES OF LOW-ENRICHED U(4.4 WT.% 235U)O_2 FUEL RODS IN LIGHT WATER AT DIFFERENT CORE CRITICAL DIMENSIONS	Kurchatov Institute	None used due to hex arrays.
54	CRITICAL LOADING CONFIGURATIONS OF THE IPEN/MB-01 REACTOR WITH UO_2, AND UO_2-Gd_2O_3 RODS	IPEN	Used only one case. Rest of cases were not significantly different.
55	LIGHT-WATER MODERATED AND REFLECTED LOW-ENRICHED URANIUM (3 wt.% 235U) DIOXIDE ROD LATTICES	Winfrith	Neither case used. Complex geometry no KENO-V.a sample deck
56	CRITICAL EXPERIMENT WITH BORAX-V BOILING WATER REACTOR TYPE FUEL ASSEMBLIES	INL	None used. No sample SCALE decks. Complex BWR geometry.
57	4.738-WT.%-ENRICHED URANIUM DIOXIDE FUEL ROD ARRAYS REFLECTED BY WATER IN A DRY STORAGE CONFIGURATION	Valduc	None used. No sample SCALE decks.
58	CRITICAL LOADING CONFIGURATIONS OF THE IPEN/MB-01 REACTOR WITH LARGE VOID IN THE REFLECTOR	IPEN	None used. No sample SCALE decks.
59	Not included in 2010 Handbook		
60	RBMK GRAPHITE REACTOR: UNIFORM CONFIGURATIONS OF U(1.8, 2.0, or 2.4% 235U)O_2 FUEL ASSEMBLIES, AND CONFIGURATIONS OF U(2.0% 235U)O_2 ASSEMBLIES WITH EMPTY CHANNELS, WATER COLUMNS, AND BORON OR THORIUM ABSORBERS, WITH OR WITHOUT WATER IN CHANNELS	Kurchatov Institute	None used. RBMK – not typical of LWRs
61	VVER PHYSICS EXPERIMENTS: HEXAGONAL (1.27-CM PITCH) LATTICES OF U(4.4 WT.% 235U)O_2 FUEL RODS IN LIGHT WATER, PERTURBED BY BORON, HAFNIUM, OR DYSPROSIUM ABSORBER RODS, OR BY WATER GAP WITH/WITHOUT EMPTY ALUMINIUM TUBES	Kurchatov Institute	None used due to hex arrays.
62	2.6%-ENRICHED UO_2 RODS IN LIGHT-WATER MODERATOR WITH BORATED STAINLESS STEEL PLATE: SINGLE ARRAYS	JAEA	None used. No SCALE sample decks.

Benchmark Number	Description	Lab	Selected
63	LIGHT-WATER MODERATED AND REFLECTED LOW-ENRICHED URANIUM (3 wt.% 235U) DIOXIDE ROD LATTICES WITH DISCRETE POISON-ROD ARRAYS	Winfrith	None used. No SCALE sample decks.
64	Not included in 2010 Handbook		
65	CRITICAL CONFIGURATIONS OF 2.6%-ENRICHED UO_2 ROD ARRAYS IN LIGHT-WATER MODERATOR WITH BORATED STAINLESS STEEL PLATE: COUPLED ARRAYS	JAEA	None used. No SCALE sample decks.
66	PLEXIGLAS-REFLECTED, CONCRETE-REFLECTED, OR THIN STEEL-REFLECTED $U(4.46)_3O_8$ WITH H/U=0.77 AND HEU DRIVERS	Rocky Flats	None used. Not an array of rods.
67	Not included in 2010 Handbook		
68	PLEXIGLAS-REFLECTED, CONCRETE-REFLECTED, OR THIN STEEL-REFLECTED $U(4.48)_3O_8$ WITH H/U=1.25 OR H/U=2.03 AND HEU DRIVERS	Rocky Flats	None used. Not an array of rods.
69	PLEXIGLAS-REFLECTED $U(4.48)_3O_8$ WITH H/U=1.25 OR H/U=2.03 AND INTERSTITIAL MODERATION	Rocky Flats	None used. Not an array of rods.
70	VVER PHYSICS EXPERIMENTS: REGULAR HEXAGONAL (1.10-CM PITCH) LATTICES OF LOW-ENRICHED U(6.5 WT.% 235U)O_2 FUEL RODS IN LIGHT WATER AT DIFFERENT CORE CRITICAL DIMENSIONS	Kurchatov Institute	None used due to hex arrays.
71	LOW MODERATED 4.738-WT.%-ENRICHED URANIUM DIOXIDE FUEL ROD ARRAYS	Valduc	All 4 cases used.
72	UNDER-MODERATED 4.738-WT.%-ENRICHED URANIUM DIOXIDE FUEL ROD ARRAYS REFLECTED BY WATER OR POLYETHYLENE	Valduc	Used 3 cases. Did not use Polyethylene reflector cases.
73	UNDER-MODERATED 4.738-WT.%-ENRICHED URANIUM DIOXIDE FUEL ROD ARRAYS REFLECTED BY WATER WITH HETEROGENEITIES	Valduc	None used. No SCALE sample decks.
74	Not included in 2010 Handbook		

Benchmark Number	Description	Lab	Selected
75	VVER PHYSICS EXPERIMENTS: HEXAGONAL (1.10 CM PITCH) LATTICES OF LOW-ENRICHED U(6.5 WT.% 235U)O_2 FUEL RODS IN LIGHT WATER, PERTURBED BY BORON ABSORBER RODS AND WATER HOLES	Kurchatov Institute	None used due to hex arrays.
76	LIGHT WATER MODERATED AND REFLECTED LOW ENRICHED URANIUM (3 WT.% 235U) DIOXIDE ROD LATTICES WITH EX-CORE DETECTOR FEATURE	Winfrith	None used. No KENO Va sample decks.
77	CRITICAL LOADING CONFIGURATIONS OF THE IPEN/MB-01 REACTOR	IPEN	Only one case used. Rest of cases same materials with small modification of arrays. Not sufficiently independent.
78	Not included in 2010 Handbook		
79	WATER-MODERATED U(4.31)O_2 FUEL ROD LATTICES CONTAINING RHODIUM FOILS	SNL	None used due to hex arrays..
80	Not included in 2010 Handbook		
81	PWR TYPE UO_2 FUEL RODS WITH ENRICHMENTS OF 3.5 AND 6.6 WT.% WITH BURNABLE ABSORBER ("OTTO HAHN" NUCLEAR SHIP PROGRAM, SECOND CORE)	ANEX	Single case not use. No sample SCALE deck. Unusual case.
82	CRITICAL LOADING CONFIGURATIONS OF THE IPEN/MB-01 REACTOR WITH LOW ENRICHED FUEL AND BURNABLE POISON RODS	IPEN	Used only one case. Rest of cases were not significantly different.
83	CRITICAL LOADING CONFIGURATIONS OF THE IPEN/MB-01 REACTOR WITH A BIG CENTRAL VOID	IPEN	Used only one case. Rest of cases were not significantly different.
84	CRITICAL LOADING CONFIGURATIONS OF THE IPEN/MB-01 REACTOR WITH A CENTRAL CRUCIFORM ROD	IPEN	Used the single case..
85	VVER PHYSICS EXPERIMENTS: REGULAR HEXAGONAL (1.27 CM PITCH) LATTICES OF LOW-ENRICHED U(6.5 WT.% 235U)O_2 FUEL RODS IN LIGHT WATER AT DIFFERENT CORE CRITICAL DIMENSIONS	Kurchatov Institute	None used due to hex arrays..

Benchmark Number	Description	Lab	Selected
86	VVER PHYSICS EXPERIMENTS: HEXAGONAL LATTICES (1.275 CM PITCH) OF LOW ENRICHED U(3.6, 4.4 WT.% 235U)O_2 FUEL ASSEMBLIES IN LIGHT WATER WITH H3BO3	NRI	None used due to hex arrays..
87	VVER PHYSICS EXPERIMENTS: HEXAGONAL LATTICES (1.22-CM PITCH) OF LOW-ENRICHED U(3.6, 4.4 WT.% U235)O_2 FUEL ASSEMBLIES IN LIGHT WATER WITH VARIABLE FUEL-ASSEMBLY PITCH	NRI	None used due to hex arrays..
88	Not included in 2010 Handbook		
89	CRITICAL LOADING CONFIGURATIONS OF THE IPEN/MB-01 REACTOR WITH UO_2 AND BORATED STAINLESS STEEL PLATES	IPEN	Used only one case. Rest of cases were not significantly different.
90	CRITICAL LOADING CONFIGURATIONS OF THE IPEN/MB-01 REACTOR WITH UO_2 AND STAINLESS STEEL RODS	IPEN	Used only one case. Rest of cases were not significantly different.
91	CRITICAL LOADING CONFIGURATIONS OF THE IPEN/MB-01 REACTOR WITH UO_2, STAINLESS STEEL AND GD2O3 RODS	IPEN	Used only one case. Rest of cases were not significantly different.
92	Not included in 2010 Handbook		
93	DEUTERIUM CRITICAL ASSEMBLY WITH 1.2% ENRICHED URANIUM VARYING COOLANT VOID FRACTION AND LATTICE PITCH	PNC	Not used since cases use D_2O rather than H_2O
94	VVER PHYSICS EXPERIMENTS: REGULAR HEXAGONAL (1.10 CM PITCH) TWO-REGION LATTICES OF LOW-ENRICHED U(6.5 AND 4.4 WT.% 235U)O_2 FUEL RODS IN LIGHT WATER AT DIFFERENT CORE CRITICAL DIMENSIONS	Kurchatov Institute	None used due to hex arrays.

A.4.1.4 Computer Analysis of the Fresh UO_2 Benchmark Critical Experiments

SCALE input decks exist on the OECD/NEA handbook [3] disc for many of the critical experiments. In general, these input decks were used with minor modifications. None of the decks were for SCALE 6.1.2 or the ENDF/B-VII library. The number of neutrons per generation and the number of generations were, in general, too low. All the decks were modified to 6000 neutrons per generation and 1500 generations. This was sufficient to make the Monte Carlo uncertainty to be 0.0002 or about one tenth the experimental

uncertainty. The input decks matched the isotopic content given in the handbook but this was confirmed. The geometric modeling in the decks also matched the descriptions in the handbook but this too was confirmed. In short, although there was considerable help by starting with the input files given in the handbook, the ownership of the files was taken, as required by NUREG/CR-6698 [2] and as stated in section 2.3:

> *For specific critical experiments, the facility or site may choose to use input files generated elsewhere to expedite the validation process. The site has the responsibility for ensuring that input files and the options selected are appropriate for use. Regardless of the source of the input file, the site must have reviewed the description of each critical experiment and determined that the representation of the experiment, including simplifying assumptions and options, are consistent with the intended use. In other words, the site must assume ownership of the input file.*

Table A.4.1.2 shows the results of the analysis of the 236 critical experiments, along with parameters that are used to check for trends in the results. The spectral index, the Energy of the Average Lethargy of the neutrons causing Fission (EALF) is a calculated value from the SCALE output.

Table A.4.1.2: Critical Experiment Results with SCALE 6.1.2 and ENDF/B-VII

Benchmark ID	Case No.	Enrichment (wt% U-235)	Fuel Pin Diameter (cm)	Fuel Pin Pitch (cm)	EALF (eV)	Meas. Uncertainty (delta k)	k_{eff}
LCT-1	1	2.350	1.270	2.032	0.0964	0.003	0.9979
	2	2.350	1.270	2.032	0.0957	0.003	0.9975
	3	2.350	1.270	2.032	0.0950	0.003	0.9968
	4	2.350	1.270	2.032	0.0955	0.003	0.9974
	5	2.350	1.270	2.032	0.0942	0.003	0.9954
	6	2.350	1.270	2.032	0.0952	0.0027	0.9976
	7	2.350	1.270	2.032	0.0934	0.0031	0.9972
	8	2.350	1.270	2.032	0.0945	0.003	0.9962
LCT-2	1	4.310	1.415	2.540	0.1132	0.002	0.9971
	2	4.310	1.415	2.540	0.1129	0.002	0.9987
	3	4.310	1.415	2.540	0.1129	0.002	0.9984
	4	4.310	1.415	2.540	0.1119	0.0018	0.9979
	5	4.310	1.415	2.540	0.1103	0.0019	0.9962
LCT-6	1	2.596	1.417	1.849	0.2366	0.002	0.9977
	2	2.596	1.417	1.849	0.2432	0.002	0.9987
	3	2.596	1.417	1.849	0.2495	0.002	0.9987
	4	2.596	1.417	1.956	0.1818	0.002	0.9984
	5	2.596	1.417	1.956	0.1871	0.002	0.9986
	6	2.596	1.417	1.956	0.1927	0.002	0.9983
	7	2.596	1.417	1.956	0.1977	0.002	0.9989
	8	2.596	1.417	1.956	0.2028	0.002	0.9986
	9	2.596	1.417	2.150	0.1359	0.002	0.9988
	10	2.596	1.417	2.150	0.1394	0.002	0.9988
	11	2.596	1.417	2.150	0.1427	0.002	0.9985
	12	2.596	1.417	2.150	0.1462	0.002	0.9982
	13	2.596	1.417	2.150	0.1497	0.002	0.9981
	14	2.596	1.417	2.293	0.1147	0.002	0.9988

Benchmark ID	Case No.	Enrichment (wt% U-235)	Fuel Pin Diameter (cm)	Fuel Pin Pitch (cm)	EALF (eV)	Meas. Uncertainty (delta k)	k_{eff}
	15	2.596	1.417	2.293	0.1174	0.002	0.9983
	16	2.596	1.417	2.293	0.1200	0.002	0.9991
	17	2.596	1.417	2.293	0.1228	0.002	0.9987
	18	2.596	1.417	2.293	0.1254	0.002	0.9985
LCT-7	1	4.738	0.940	1.260	0.2411	0.0014	0.9959
	2	4.738	0.940	1.600	0.1090	0.0008	0.9980
	3	4.738	0.940	2.100	0.0708	0.0007	0.9976
	4	4.738	0.940	2.520	0.0605	0.0008	0.9983
LCT-8	1	2.459	1.206	1.636	0.2792	0.0012	0.9969
	2	2.459	1.206	1.636	0.2467	0.0012	0.9971
	3	2.459	1.206	1.636	0.2465	0.0012	0.9978
	4	2.459	1.206	1.636	0.2465	0.0012	0.9970
	5	2.459	1.206	1.636	0.2468	0.0012	0.9967
	6	2.459	1.206	1.636	0.2461	0.0012	0.9977
	7	2.459	1.206	1.636	0.2459	0.0012	0.9964
	8	2.459	1.206	1.636	0.2440	0.0012	0.9963
	9	2.459	1.206	1.636	0.2437	0.0012	0.9962
	10	2.459	1.206	1.636	0.2498	0.0012	0.9969
	11	2.459	1.206	1.636	0.2549	0.0012	0.9980
	12	2.459	1.206	1.636	0.2489	0.0012	0.9970
	13	2.459	1.206	1.636	0.2489	0.0012	0.9975
	14	2.459	1.206	1.636	0.2510	0.0012	0.9970
	15	2.459	1.206	1.636	0.2509	0.0012	0.9967
	16	2.459	1.206	1.636	0.2278	0.0012	0.9972
	17	2.459	1.206	1.636	0.1991	0.0012	0.9971
LCT-9	1	4.310	1.415	2.540	0.1127	0.0021	0.9980
	2	4.310	1.415	2.540	0.1122	0.0021	0.9986
	3	4.310	1.415	2.540	0.1125	0.0021	0.9979
	4	4.310	1.415	2.540	0.1121	0.0021	0.9981
	5	4.310	1.415	2.540	0.1136	0.0021	0.9993
	6	4.310	1.415	2.540	0.1127	0.0021	0.9985
	7	4.310	1.415	2.540	0.1137	0.0021	0.9994
	8	4.310	1.415	2.540	0.1130	0.0021	0.9981
	9	4.310	1.415	2.540	0.1135	0.0021	0.9986
	16	4.310	1.415	2.540	0.1135	0.0021	0.9987
	17	4.310	1.415	2.540	0.1127	0.0021	0.9991
	18	4.310	1.415	2.540	0.1138	0.0021	0.9977
	19	4.310	1.415	2.540	0.1129	0.0021	0.9986
	20	4.310	1.415	2.540	0.1137	0.0021	0.9982
	21	4.310	1.415	2.540	0.1129	0.0021	0.9988
	22	4.310	1.415	2.540	0.1138	0.0021	0.9984
	23	4.310	1.415	2.540	0.1130	0.0021	0.9994
	24	4.310	1.415	2.540	0.1122	0.0021	0.9979
	25	4.310	1.415	2.540	0.1120	0.0021	0.9983
	26	4.310	1.415	2.540	0.1121	0.0021	0.9987
	27	4.310	1.415	2.540	0.1119	0.0021	0.9985
LCT-10	5	4.310	1.415	2.540	0.3547	0.0021	1.0000
	6	4.310	1.415	2.540	0.2615	0.0021	1.0003
	7	4.310	1.415	2.540	0.2092	0.0021	1.0006

Benchmark ID	Case No.	Enrichment (wt% U-235)	Fuel Pin Diameter (cm)	Fuel Pin Pitch (cm)	EALF (eV)	Meas. Uncertainty (delta k)	k_{eff}
	8	4.310	1.415	2.540	0.1844	0.0021	0.9979
	9	4.310	1.415	2.540	0.1221	0.0021	1.0007
	10	4.310	1.415	2.540	0.1183	0.0021	1.0013
	11	4.310	1.415	2.540	0.1154	0.0021	1.0006
	12	4.310	1.415	2.540	0.1122	0.0021	1.0000
	13	4.310	1.415	2.540	0.1105	0.0021	0.9968
	14	4.310	1.415	1.892	0.3071	0.0028	1.0014
	15	4.310	1.415	1.892	0.2950	0.0028	1.0018
	16	4.310	1.415	1.892	0.2853	0.0028	1.0021
	17	4.310	1.415	1.892	0.2787	0.0028	1.0021
	18	4.310	1.415	1.892	0.2749	0.0028	1.0010
	19	4.310	1.415	1.892	0.2677	0.0028	1.0008
	24	4.310	1.415	1.892	0.5990	0.0028	0.9994
	25	4.310	1.415	1.892	0.5536	0.0028	1.0010
	26	4.310	1.415	1.892	0.5122	0.0028	1.0010
	27	4.310	1.415	1.892	0.4780	0.0028	1.0017
	28	4.310	1.415	1.892	0.4485	0.0028	1.0017
	29	4.310	1.415	1.892	0.4232	0.0028	1.0016
	30	4.310	1.415	1.892	0.3679	0.0028	0.9996
LCT-11	1	2.459	1.206	1.636	0.1685	0.0018	0.9968
	2	2.459	1.206	1.636	0.2450	0.0032	0.9967
	3	2.459	1.206	1.636	0.1920	0.0032	0.9971
	4	2.459	1.206	1.636	0.1927	0.0032	0.9972
	5	2.459	1.206	1.636	0.1935	0.0032	0.9970
	6	2.459	1.206	1.636	0.1951	0.0032	0.9970
	7	2.459	1.206	1.636	0.1959	0.0032	0.9967
	8	2.459	1.206	1.636	0.1972	0.0032	0.9974
	9	2.459	1.206	1.636	0.1984	0.0032	0.9975
	10	2.459	1.206	1.636	0.1866	0.0017	0.9945
	11	2.459	1.206	1.636	0.1628	0.0017	0.9940
	12	2.459	1.206	1.636	0.1670	0.0017	0.9950
	13	2.459	1.206	1.636	0.1475	0.0017	0.9943
	14	2.459	1.206	1.636	0.1508	0.0017	0.9946
	15	2.459	1.206	1.636	0.1387	0.0018	0.9959
LCT-13	1	4.310	1.415	1.892	0.2862	0.0018	1.0005
	2	4.310	1.415	1.892	0.2939	0.0018	1.0004
	3	4.310	1.415	1.892	0.2974	0.0018	1.0003
	4	4.310	1.415	1.892	0.2969	0.0018	1.0007
	5	4.310	1.415	1.892	0.2961	0.0032	1.0003
LCT-16	1	2.350	1.270	2.032	0.0957	0.0031	0.9973
	2	2.350	1.270	2.032	0.0954	0.0031	0.9962
	3	2.350	1.270	2.032	0.0954	0.0031	0.9967
	4	2.350	1.270	2.032	0.0956	0.0031	0.9960
	5	2.350	1.270	2.032	0.0952	0.0031	0.9970
	6	2.350	1.270	2.032	0.0961	0.0031	0.9971
	7	2.350	1.270	2.032	0.0959	0.0031	0.9973
	8	2.350	1.270	2.032	0.0969	0.0031	0.9972
	9	2.350	1.270	2.032	0.0961	0.0031	0.9977
	10	2.350	1.270	2.032	0.0970	0.0031	0.9971

Benchmark ID	Case No.	Enrichment (wt% U-235)	Fuel Pin Diameter (cm)	Fuel Pin Pitch (cm)	EALF (eV)	Meas. Uncertainty (delta k)	k_{eff}
	11	2.350	1.270	2.032	0.0962	0.0031	0.9978
	12	2.350	1.270	2.032	0.0974	0.0031	0.9972
	13	2.350	1.270	2.032	0.0965	0.0031	0.9979
	14	2.350	1.270	2.032	0.0975	0.0031	0.9974
	21	2.350	1.270	2.032	0.0971	0.0031	0.9977
	22	2.350	1.270	2.032	0.0968	0.0031	0.9974
	23	2.350	1.270	2.032	0.0963	0.0031	0.9977
	24	2.350	1.270	2.032	0.0967	0.0031	0.9970
	25	2.350	1.270	2.032	0.0963	0.0031	0.9972
	26	2.350	1.270	2.032	0.0969	0.0031	0.9976
	27	2.350	1.270	2.032	0.0963	0.0031	0.9979
	28	2.350	1.270	2.032	0.0951	0.0031	0.9972
	29	2.350	1.270	2.032	0.0950	0.0031	0.9969
	30	2.350	1.270	2.032	0.0949	0.0031	0.9965
	31	2.350	1.270	2.032	0.0950	0.0031	0.9979
	32	2.350	1.270	2.032	0.0949	0.0031	0.9972
LCT-17	4	2.350	1.270	2.032	0.2017	0.0031	0.9983
	5	2.350	1.270	2.032	0.1779	0.0031	0.9994
	6	2.350	1.270	2.032	0.1685	0.0031	0.9989
	7	2.350	1.270	2.032	0.1597	0.0031	0.9994
	8	2.350	1.270	2.032	0.1333	0.0031	0.9972
	9	2.350	1.270	2.032	0.1092	0.0031	0.9973
	10	2.350	1.270	2.032	0.0998	0.0031	0.9973
	11	2.350	1.270	2.032	0.0979	0.0031	0.9979
	12	2.350	1.270	2.032	0.0968	0.0031	0.9977
	13	2.350	1.270	2.032	0.0953	0.0031	0.9976
	14	2.350	1.270	2.032	0.0946	0.0031	0.9985
	15	2.350	1.270	1.684	0.1777	0.0028	0.9961
	16	2.350	1.270	1.684	0.1711	0.0028	0.9983
	17	2.350	1.270	1.684	0.1665	0.0028	0.9987
	18	2.350	1.270	1.684	0.1648	0.0028	0.9974
	19	2.350	1.270	1.684	0.1622	0.0028	0.9978
	20	2.350	1.270	1.684	0.1607	0.0028	0.9971
	21	2.350	1.270	1.684	0.1592	0.0028	0.9966
	22	2.350	1.270	1.684	0.1584	0.0028	0.9959
	26	2.350	1.270	1.684	0.3741	0.0028	0.9958
	27	2.350	1.270	1.684	0.3203	0.0028	0.9972
	28	2.350	1.270	1.684	0.2806	0.0028	0.9974
	29	2.350	1.270	1.684	0.2505	0.0028	0.9984
LCT-34	4	4.738	0.940	1.600	0.1367	0.0039	1.0003
	5	4.738	0.940	1.600	0.1330	0.0039	0.9999
	6	4.738	0.940	1.600	0.1298	0.0039	1.0017
	7	4.738	0.940	1.600	0.1279	0.0039	1.0002
	8	4.738	0.940	1.600	0.1258	0.0039	0.9992
	15	4.738	0.940	1.600	0.1348	0.0043	0.9947
LCT-35	1	2.596	1.417	1.956	0.2086	0.0018	0.9983
	2	2.596	1.417	1.956	0.2126	0.0019	0.9976
LCT-39	1	4.738	0.940	1.260	0.2218	0.0014	0.9953
	2	4.738	0.940	1.260	0.2119	0.0014	0.9969

Benchmark ID	Case No.	Enrichment (wt% U-235)	Fuel Pin Diameter (cm)	Fuel Pin Pitch (cm)	EALF (eV)	Meas. Uncertainty (delta k)	k_{eff}
	3	4.738	0.940	1.260	0.1923	0.0014	0.9965
	4	4.738	0.940	1.260	0.1836	0.0014	0.9961
	5	4.738	0.940	1.260	0.1393	0.0009	0.9978
	6	4.738	0.940	1.260	0.1452	0.0009	0.9977
	7	4.738	0.940	1.260	0.2132	0.0012	0.9962
	8	4.738	0.940	1.260	0.2031	0.0012	0.9963
	9	4.738	0.940	1.260	0.1976	0.0012	0.9969
	10	4.738	0.940	1.260	0.1732	0.0012	0.9970
	11	4.738	0.940	1.260	0.2218	0.0013	0.9953
	12	4.738	0.940	1.260	0.2166	0.0013	0.9951
	13	4.738	0.940	1.260	0.2146	0.0013	0.9951
	14	4.738	0.940	1.260	0.2124	0.0013	0.9954
	15	4.738	0.940	1.260	0.2112	0.0013	0.9959
	16	4.738	0.940	1.260	0.2104	0.0013	0.9967
	17	4.738	0.940	1.260	0.2099	0.0013	0.9960
LCT-40	1	4.738	0.940	1.600	0.1427	0.0039	0.9966
	5	4.738	0.940	1.600	0.1377	0.0042	0.9951
	9	4.738	0.940	1.600	0.1470	0.0046	0.9993
	10	4.738	0.940	1.600	0.1419	0.0046	0.9931
LCT-42	1	2.350	1.270	1.684	0.1690	0.0016	0.9971
	2	2.350	1.270	1.684	0.1753	0.0016	0.9968
	3	2.350	1.270	1.684	0.1819	0.0016	0.9981
	4	2.350	1.270	1.684	0.1804	0.0017	0.9980
	5	2.350	1.270	1.684	0.1775	0.0033	0.9981
LCT-43	2	4.349	0.980	1.500	0.1553	0.0010	1.0007
LCT-44	1	4.349	0.980	1.500	0.1474	0.0010	0.9993
LCT-48	1	3.005	1.094	1.320	0.6771	0.0025	0.9990
	2	3.005	1.094	1.320	0.6508	0.0025	0.9983
	3	3.005	1.094	1.320	0.6824	0.0025	0.9984
	4	3.005	1.094	1.320	0.6838	0.0025	0.9988
	5	3.005	1.094	1.320	0.6736	0.0025	0.9983
LCT-50	1	4.738	0.940	1.300	0.1998	0.0010	0.9983
	2	4.738	0.940	1.300	0.1907	0.0010	0.9978
	3	4.738	0.940	1.300	0.2075	0.0010	0.9978
	4	4.738	0.940	1.300	0.1977	0.0010	0.9972
	5	4.738	0.940	1.300	0.2230	0.0010	0.9983
	6	4.738	0.940	1.300	0.2141	0.0010	0.9991
	7	4.738	0.940	1.300	0.2095	0.0010	0.9992
LCT-51	1 C10	2.459	1.206	1.636	0.1472	0.0020	0.9965
	2 c11a	2.459	1.206	1.636	0.1968	0.0024	0.9972
	3 c11b	2.459	1.206	1.636	0.1964	0.0024	0.9972
	4 c11c	2.459	1.206	1.636	0.1979	0.0024	0.9975
	5 c11d	2.459	1.206	1.636	0.1989	0.0024	0.9970
	6 c11e	2.459	1.206	1.636	0.1998	0.0024	0.9972
	7 c11f	2.459	1.206	1.636	0.2000	0.0024	0.9973
	8 c11g	2.459	1.206	1.636	0.2011	0.0024	0.9971
	9 c12	2.459	1.206	1.636	0.1669	0.0019	0.9969
LCT-54	1	4.349	0.980	1.500	0.1508	0.0005	0.9996
LCT-71	1	4.738	0.949	1.100	0.7592	0.00076	0.9955

Benchmark ID	Case No.	Enrichment (wt% U-235)	Fuel Pin Diameter (cm)	Fuel Pin Pitch (cm)	EALF (eV)	Meas. Uncertainty (delta k)	k_{eff}
	2	4.738	0.949	1.100	0.6972	0.00076	0.9954
	3	4.738	0.949	1.100	0.6610	0.00076	0.9948
	4	4.738	0.949	1.075	0.8485	0.0008	0.9951
LCT-72	1	4.738	0.949	1.600	0.1117	0.0012	0.9990
	2	4.738	0.949	1.600	0.1077	0.0012	0.9985
	3	4.738	0.949	1.600	0.1099	0.0012	0.9988
LCT-77	3	4.349	0.980	1.500	0.1621	0.0010	1.0006
LCT-82	3	4.349	0.980	1.500	0.1497	0.0010	1.0005
LCT-83	1	4.349	0.980	1.500	0.1516	0.0010	1.0001
LCT-84	1	4.349	0.980	1.500	0.1541	0.0010	1.0008
LCT-89	1	4.349	0.980	1.500	0.1530	0.0010	1.0000
LCT-90	1	4.349	0.980	1.500	0.1459	0.0010	0.9994
LCT-91	4	4.349	0.980	1.500	0.1508	0.0010	0.9999

Since boron is important to criticality analysis of racks, two methods are used to parameterize the boron: the B-10 areal density for plates and the soluble boron ppm. Table A.4.1.3 shows the boron information on boron-containing benchmarks, along with the calculated k.

Table A.4.1.3: Summary of Critical Experiments Containing Boron

Benchmark ID	Case No.	Soluble Boron (ppm)	Separator Plate B-10 Areal Density (gm/cm^2)	No. of Boron Rods	k_{eff}
LCT-8	1	1511			0.9969
	2	1334			0.9971
	3	1337			0.9978
	4	1183		36	0.9970
	5	1181		36	0.9967
	6	1034		72	0.9977
	7	1031		72	0.9964
	8	794		144	0.9963
	9	779		144	0.9962
	10	1245		72	0.9969
	11	1384			0.9980
	12	1348			0.9970
	13	1348			0.9975
	14	1363			0.9970
	15	1362			0.9967
	16	1158			0.9972
	17	921			0.9971
LCT-9	5		0.004549		0.9993
	6		0.004549		0.9985
LCT-9	7		0.006904		0.9994
	8		0.006904		0.9981
	9		0.066946		0.9986
LCT-11	2	1037			0.9967
	3	769			0.9971
	4	764			0.9972
	5	762			0.9970
	6	753			0.9970
	7	739			0.9967
	8	721			0.9974
	9	702			0.9975
	10			84	0.9945
	11			64	0.9940
	12			64	0.9950
	13			34	0.9943
	14			34	0.9946
LCT-13	2		0.004549		1.0004
	3		0.030173		1.0003
	4		0.056950		1.0007
LCT-16	8		0.004549		0.9972
	9		0.004549		0.9977
	10		0.006904		0.9971
	11		0.006904		0.9978
	12		0.066946		0.9972

Benchmark ID	Case No.	Soluble Boron (ppm)	Separator Plate B-10 Areal Density (gm/cm^2)	No. of Boron Rods	k_{eff}
	13		0.066946		0.9979
	14		0.066946		0.9974
LCT-34	4		0.002521		1.0003
	5		0.002521		0.9999
	6		0.002521		1.0017
	7		0.002521		1.0002
	8		0.002521		0.9992
	15		0.046011		0.9947
LCT-35	1	70			0.9983
	2	147.7			0.9976
LCT-40	1		0.002521		0.9966
	5		0.046011		0.9951
	9		0.046011		0.9993
	10		0.046011		0.9931
LCT-42	2		0.004549		0.9968
	3		0.030173		0.9981
	4		0.056950		0.9980
LCT-50	3	822			0.9978
	4	822			0.9972
	5	5030			0.9983
	6	5030			0.9991
	7	5030			0.9992
LCT-51	1 C10	143			0.9965
	2 c11a	510			0.9972
	3 c11b	514			0.9972
	4 c11c	501			0.9975
	5 c11d	493			0.9970
	6 c11e	474			0.9972
	7 c11f	462			0.9973
	8 c11g	432			0.9971
	9 c12	217			0.9969
LCT-77	3			4	1.0006
LCT-82	3			6	1.0005

A.4.1.5 Statistical Analysis of the Fresh UO_2 Critical Benchmark Results

The statistical treatment used follows the guidance provided in NUREG/CR-6698 [2]. The NUREG approach weights the calculated k's by the experimental uncertainty. This approach means the higher quality experiments (i.e.: lower uncertainty – see Table A.4.1.2) affect the results more than the low quality (i.e.: higher uncertainty) experiments. The uncertainty weighting is used for the analysis of the set of experiments as a whole, as well as for the analysis for trends.

Before seeking trends, the 236 critical benchmarks are reviewed as a whole. The unweighted mean k of the 236 samples is 0.9979 with a standard deviation of 0.0016. The weighted mean is 0.9978 and the weighted standard deviation is 0.0024. These results show that the weighting has a negligible effect on the mean, but does increase the standard deviation. This increase in the standard deviation may be dominated by differences in the experimental uncertainty, which ranges from 0.0005 to 0.0046. Further, the average uncertainty of the experiments (interpreted as one sigma) is 0.0022. Since the total one sigma standard deviation is only 0.0024, this suggests that the experimental uncertainty dominates the uncertainty and there is little to be gained with improved methods. Unless stated otherwise, all the results presented will come from the weighted analysis. The bias of the set as a whole is **0.0022**. The uncertainty is the standard deviation multiplied by the single-sided lower tolerance factor (taken as 2.065 from Table 2.1 of Reference 2), so it is **0.0049**.

As recommended by NUREG/CR-6698, the results of the validation are checked for normality. The National Institute of Standards and Technology (NIST) has made publicly available a statistical package, DATAPLOT [4]. The 236 critical experiments were tested with the Wilk-Shapiro normality test and were found to adhere to a normal distribution at only the 99% level. The test results are shown in Table A.4.1.4. Since the Wilk-Shapiro test shows normality only at 99%, a histogram plot of the data was made. This plot suggests that a normal distribution assumption is valid. This plot is Figure A.4.1.1. Notice that the calculated k's are a little closer to the mean than expected in a normal distribution. This means assuming a normal distribution is conservative for this data.

Table A.4.1.4: Wilk-Shapiro Test Results Output From DATAPLOT [4]

WILK-SHAPIRO TEST k

WILK-SHAPIRO TEST FOR NORMALITY

1. STATISTICS:
   NUMBER OF OBSERVATIONS = 236
   LOCATION PARAMETER = 0.9979254
   SCALE PARAMETER = 0.1639522E-02

   WILK-SHAPIRO TEST STATISTIC VALUE = 0.9844111

2. CRITICAL VALUES:
   P-VALUE = 0.1090365E-01

3. CONCLUSIONS:
   AT THE 90% LEVEL, WE REJECT THE NORMALITY ASSUMPTION.
   AT THE 95% LEVEL, WE REJECT THE NORMALITY ASSUMPTION.
   AT THE 97.5% LEVEL, WE REJECT THE NORMALITY ASSUMPTION.
   AT THE 99% LEVEL, WE ACCEPT THE NORMALITY ASSUMPTION.

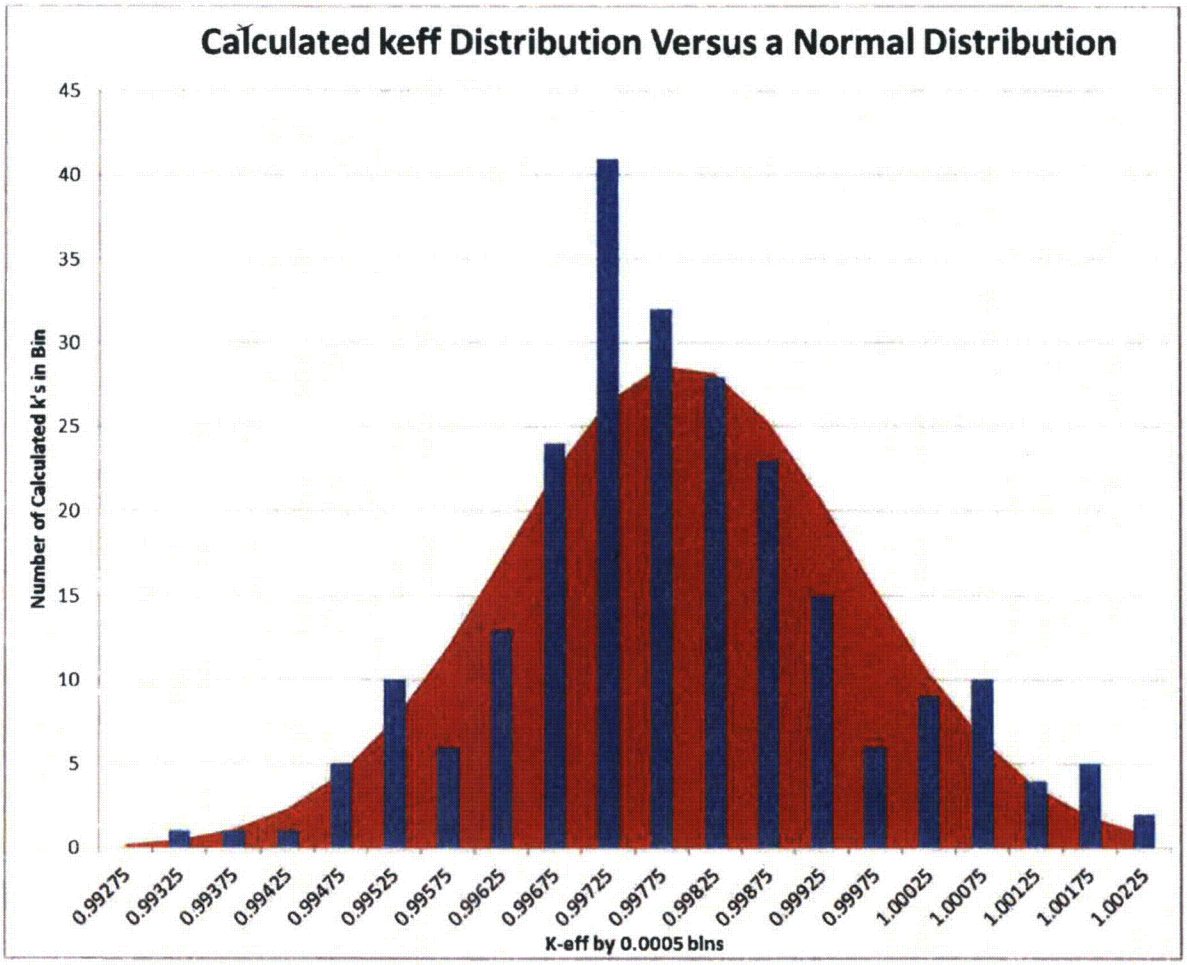

Figure A.4.1.1: Distribution of the Calculated k's Around the Mean

One possible source of the limited normality could be due to a difference in results with some subsets, but this is not the case. There are 76 experiments that have boron in them. The average k of the boron containing cases is 0.9975, which is very close to the average of all cases (0.9979) (Note: the Monte Carlo uncertainty is 0.0002). Similarly, there are 15 cases that used Cadmium absorbers. The mean of these cases is 0.9981. Since the standard deviation of the set as a whole is 0.0016 (unweighted), it is clear these features are not causing the limited normality.

Numerous sources [5, 6, 7] suggest that for the large sample size used here (236 experiments), normality testing is not important. For example, the guide to the PROPHET statistical program [6] states:

"With large sample sizes, most normal-theory-based tests like the t test are robust to non-normality, and if the non-normality is not apparent in the normal probability plot for a large data sample, it probably won't have a serious effect on the results of a normal-theory-based test."

In the textbook, Statistics for Social Science by R. Mark Sirkin [7], it states:

"Law of large numbers. A law that states that if the size of the sample, n, is sufficiently large (no less than 30; preferably no less than 50), then the central limit theory will apply even if the population is not normally distributed along variable x ...

If:	*Then:*
n>= 100	*It is always safe to relax the normality assumption*
50<=n<100	*It is almost always safe*
30<=n<50	*It is probably safe."*

The analysis in this validation assumes that the techniques used here are sufficiently robust for the limited normality data. However, a non-parametric check has been performed. The 236 cases were ranked by increasing k. 95% of the cases are above the 11th case. The k of the 11th case is 0.9951. Since the average of the experiments is 0.9979, a standard deviation of (.9979-.9951)/1.96 = 0.0014 can be inferred. This inferred standard deviation is less than the standard deviation of 0.0024 (or the unweighted value of 0.0016) predicted assuming a normal distribution. Again, this is expected from a visual inspection of Figure A.4.1.1, since the predicted distribution shows a significantly larger number of data points in the center compared to a normal distribution. In conclusion, although the data does not meet the normality tests, it will be treated as normally distributed, yielding a conservative bias uncertainty.

The next step in the analysis is to look for trends in the data. Section 3.2.2 of the DOE/RW technical report in support of validation for burnup credit [8] describes an appropriate trend test. In this test, the null hypothesis is that the slope of the trend is zero (no trend) and it tests to determine if there is confidence that the calculated slope is a more accurate representation than a zero slope. The equations for this test are presented here.

Let the regression fit be of the form:

$$k = a + b\,x$$

Let x-bar be the average value of x for the n cases and define:

$$S_{xx} = \sum_{i=1,n} (x_i - \bar{x})^2$$

and define:

$$SS_R = \sum_{i=1,n} (k_i - a - b * x_i)^2$$

then the test statistic is:

$$T = |b| * \sqrt{\frac{(n-2) * S_{xx}}{SS_R}}$$

This test statistic is then compared to the Student's t-distribution at the desired confidence level and n-2 degrees of freedom. In the past it was assumed that unless there is a high confidence level (95%) that the slope was non-zero, the analysis would assume a zero slope (no trend) on the given parameter. Since the analysis will include consideration of the data as non-trended, it is more conservative to assume there is also a trend. Inverting the statistical test to requiring a high confidence that the slope is zero will result in all cases having a trend. At this time, although a test on the confidence of the trend is performed, the analysis assumes all calculated trends are real.

For this work the weighted k's are used to determine the fit to a straight line. Refer to NUREG/CR-6698 [2] equations 10 through 13.

NUREG/CR-6698 [2] describes the appropriate tolerance band for criticality validation. This work simply applies the equations (equations 23 to 30) given in the NUREG. Note that the tolerance band is found using the weighted experimental data. The width of the tolerance band is the uncertainty. The width of the tolerance band is a small function of the trending parameter. For this analysis, the width of the tolerance band is calculated at the maximum and minimum value of the trending parameter and the maximum of these two widths is taken as the uncertainty. The change in the width as a function of trending parameter is so small that any change in reported uncertainty does not depend on which tolerance band width is used.

In the final analysis, the calculated k of the system must be less than the minimum of k(x) minus the uncertainty minus the administrative safety margin. The uncertainty in k from other independent uncertainties, such as the manufacturing tolerances, burnup, and depletion uncertainties can be statistically combined with the uncertainty in the criticality validation. The rest of this section will evaluate the trends in k as a function of trending parameters using the methods described above. Historically, an Upper Subcriticality Limit (USL) was assigned from the criticality validation analysis. This is not done here, since the other uncertainties (e.g., manufacturing tolerances of the rack, depletion uncertainty, etc.) are not known at this time.

Neutron spectrum

Trends in the calculated k of the benchmarks were sought as a function of the neutron spectrum. Since a large number of things can affect the spectrum, a single index calculated by SCALE is used. This index is the Energy (eV) of the Average Lethargy causing Fission (EALF). Figure A.4.1.2 shows the distribution of k's around the mean k, which is shown as the red line. Visual inspection of the graph and the statistical analysis of the results of the statistical analysis suggest that there is a statistically significant trend on neutron spectrum. Using NUREG/CR-6698 [2] equations 10 through 13 and the data from Table A.4.1.2, the predicted mean k as a function of EALF is:

k(EALF) = 0.99865 - 0.00386 * EALF

The units for EALF are eV. The uncertainty about the trend is calculated using the second term of NUREG/CR-6698 [2] equation 23 and is 0.00431 in k.

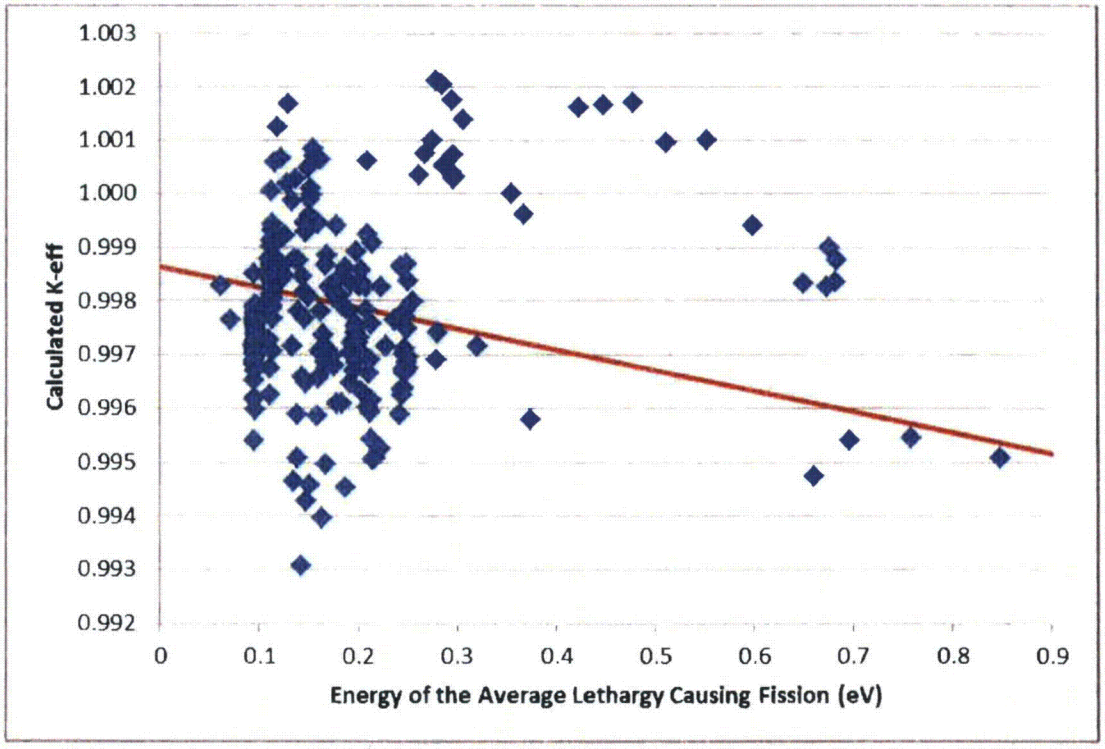

Figure A.4.1.2: k_{eff} as a Function of the Energy of the Average Lethargy Causing Fission

Geometry tests

Two trend tests were performed to determine if lattice/geometric parameters are adequately treated by SCALE 6.1.2. The first parameter is the fuel pin diameter. A small, statistically significant trend was found when the critical experiment analysis results were correlated to the fuel pin diameter. The second lattice parameter tested is the lattice pitch. A statistically significant trend on lattice pitch was found. The trend on pitch or pin diameter could be caused by the spectral trend found in the previous subsection.

Using NUREG/CR-6698 [2] equations 10 through 13 and the data from Table A.4.1.2, the predicted mean k as a function of pin diameter is:

$$\mathbf{k(Pin\ Diameter) = 0.99592 + (1.662E\text{-}03)*Pin\ Diameter}$$

where the pin diameter is in cm. The predicted mean k as a function of pitch is:

$$\mathbf{k(Pitch) = 0.99547 + (1.389E\text{-}03)*Pitch}$$

where lattice pitch is in cm.

The tolerance band widths, using the second term of NUREG/CR-6698 [2] equation 23, are 4.343E-03 and 4.270E-03 for the pin diameter and pitch, respectively. Figures A.4.1.3 and A.4.1.4 graphically present k_{eff} as a function of the pin diameter and the lattice pitch.

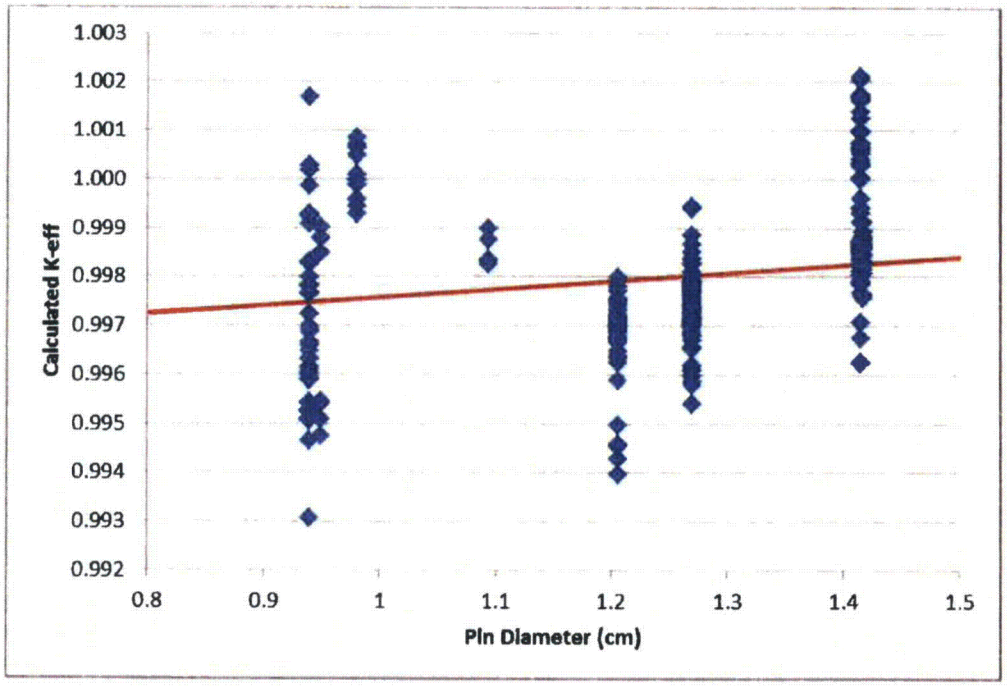

Figure A.4.1.3: k_{eff} as a Function of the Pin Diameter

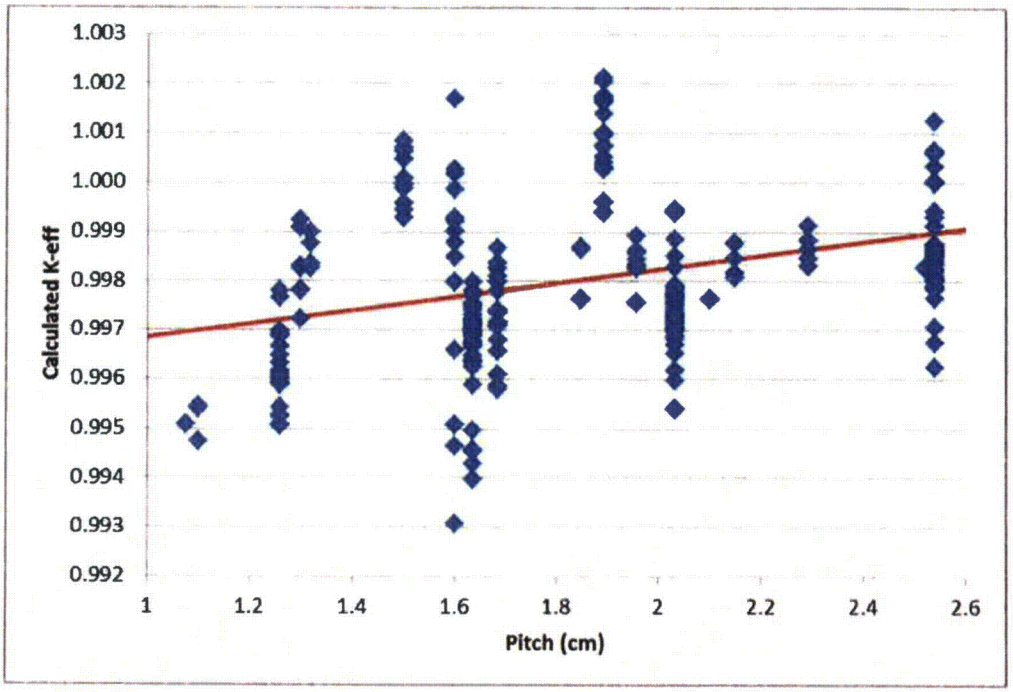

Figure A.4.1.4: k_{eff} as a Function of the Lattice Pitch

Enrichment

The fuel to be stored in the racks ranges in enrichment from 1.6 wt% ^{235}U to 5 wt% ^{235}U. It was determined that there exists a statistically significant trend on enrichment. Using NUREG/CR-6698 [2] equations 10 through 13 and the data from Table A.4.1.2, the trend in the mean k is:

$$\mathbf{k(Enrichment) = 0.99686 + (2.42E\text{-}04)*Enrichment}$$

where Enrichment is wt% ^{235}U.

The tolerance band width is 4.35E-03. Figure A.4.1.5 graphically presents the results.

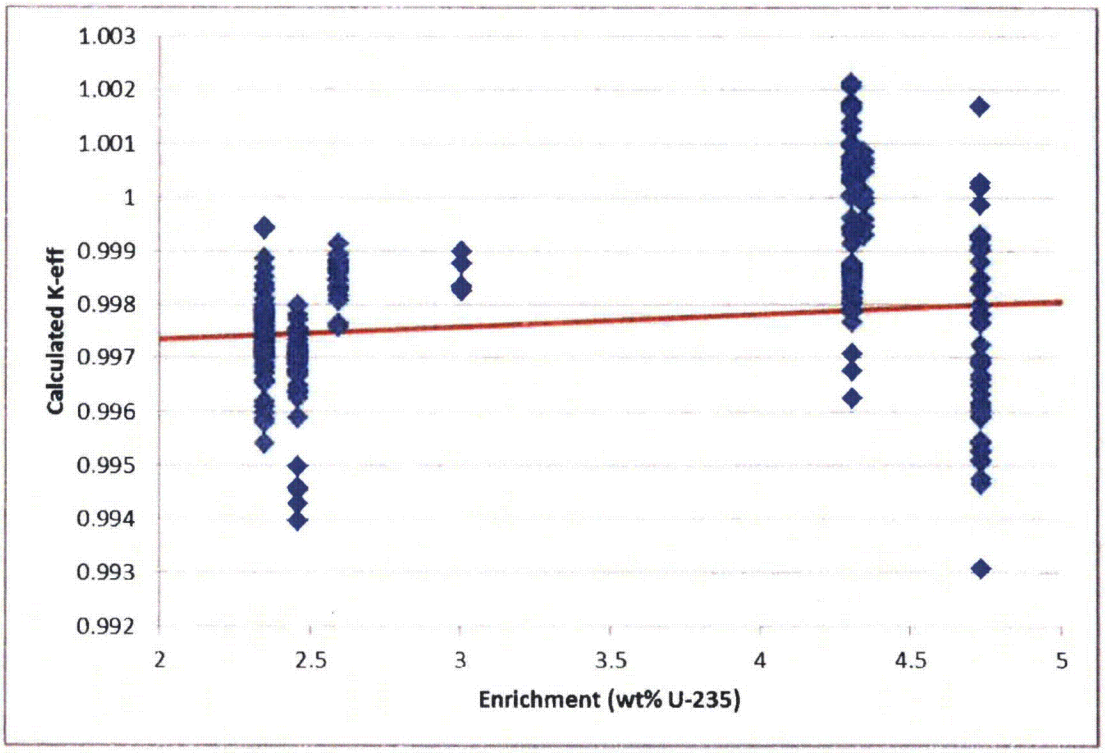

Figure A.4.1.5: k_{eff} as a Function of the Fuel Enrichment

Boron Content

A fit of the calculated k's as a function of the B-10 areal density in the absorber plates or the soluble boron ppm was performed using NUREG/CR-6698 [2] equations 10 through 13 and the data from Table A.4.1.2. Both fits failed the statistically significance test compared to a zero slope. However, to be conservative, both the zero slope and the calculated fit are used for determining the limiting k as a function of boron content.

The following equations are the best fit of the data for k versus soluble boron and areal density. Figures A.4.1.6 and A.4.1.7 show the results of the analyses. The uncertainty around the mean values given in the following equations is 0.00440 and 0.00497.

$$\mathbf{k(ppm\ soluble\ boron) = 0.99777 + (5.24E\text{-}08)*ppm}$$

$$\mathbf{k(B\text{-}10\ Areal\ Density) = 0.99777 + (5.24E\text{-}08)*(B\text{-}10\ Areal\ Density)}$$

where the B-10 areal density is in gm B-10/cm^2.

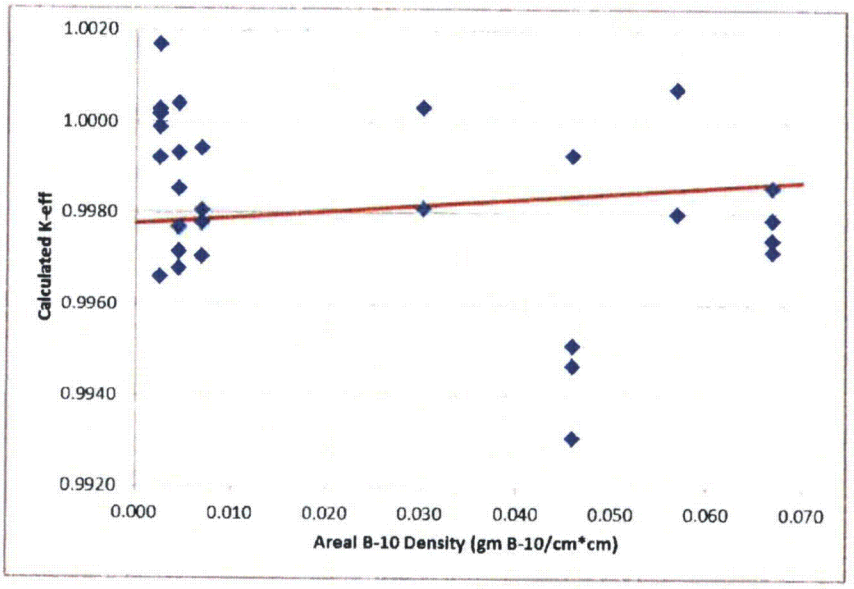

Figure A.4.1.6: k_{eff} as a Function of the B-10 Areal Density in the Separator Plates

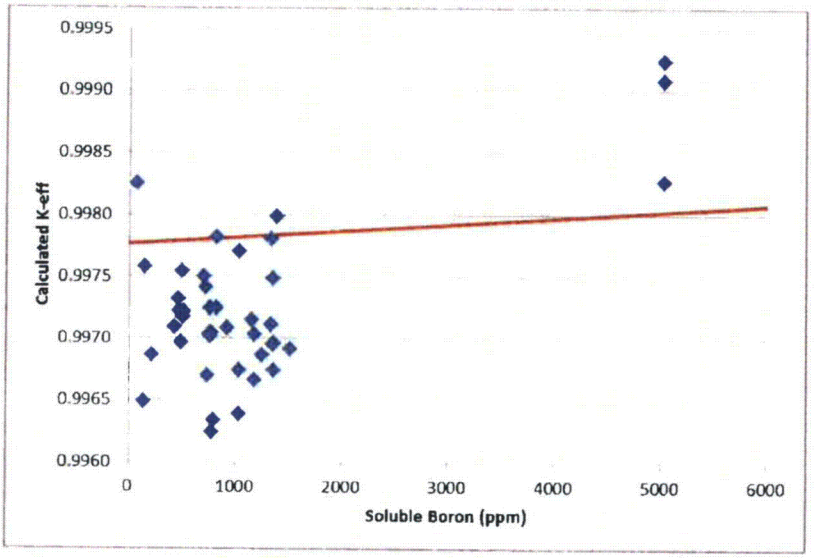

Figure A.4.1.7: k_{eff} as a Function of the Soluble Boron Content

A.4.1.6 Establishing the Bias and the Uncertainty

To make the incorporation of the bias and bias uncertainty in the criticality analysis conservative, the most limiting bias and bias uncertainty from the trends in the range of interest is used. The lattice pitch for Westinghouse fuel is tabulated on Table A.4.1.5 along with the bias, as predicted with the trend on lattice pitch.

Table A.4.1.5: Bias as Predicted Using the Trend in the Bias as a Function of Pitch

Fuel Type	Pitch (cm)	Bias
14x14	1.412	0.0026
15x15	1.430	0.0025
16x16	1.232	0.0028
17x17	1.260	0.0028

The bias as a function of pin diameter decreases with increasing pin diameter and for the smallest pin diameter (Westinghouse 17X17 OFA fuel, 0.360 inches) is 0.0026. The bias for the 15x15 pin diameter (0.422 inches) is 0.0023. Thus the bias as a function of pitch is always more limiting.

The bias as a function of enrichment is given in Table A.4.1.6. As can be seen by comparing Table A.4.1.5 and A.4.1.6, the lattice pitch bias is more limiting at enrichments consistent with reloads. However, for low enriched fuel, the limiting bias is a result of the enrichment trend.

Table A.4.1.6: Bias as Predicted Using the Trend in the Bias as a Function of Enrichment

Enrichment (wt% U-235)	Bias
5	0.0019
4	0.0022
3	0.0024
2	0.0027
1.6	0.0028

The biases as a function of soluble boron or areal density decrease with increasing boron and are not the most limiting biases at zero boron.

The spectrum, as measured by the EALF in the pool with no soluble boron, is generally between 0.2 and 0.4 eV. The bias increases as the spectrum hardens and the bias at 0.4 eV is 0.0029. This is the most limiting bias. For heavily borated cases, the EALF can get almost as high as 0.6 eV. At 0.6 eV the bias is 0.0037. **For this criticality analysis, a bias of 0.0029 will be used for all EALF less than 0.4 (limiting cases for no boron credit) and 0.0037 for EALF values between 0.4 and 0.6 eV (heavily borated cases).** The maximum uncertainty for any trend is 0.0050, which comes from the areal density analysis. This uncertainty is the largest, since it is the smallest sample (only 28 cases), but in order to make the analysis conservative, **0.0050 is selected for the uncertainty in the bias.**

The uncertainty of the set as a whole is 0.0049. The uncertainty for the trended analysis is generally less, (not so for the areal density, due to the small sample size) since taking advantage of the trend reduces the difference between the experimental value and the predicted value.

A.4.1.7 Subcritical Margin

In the USA, the NRC has established subcritical margins for rack analysis. The subcritical margin for borated spent fuel pools, casks, and fully flooded dry storage racks is 0 when the analysis is performed with unborated water. This is actually saying the subcritical margin is contained in the uncredited soluble boron. To make sure there is sufficient soluble boron, analysis is also performed with soluble boron and a subcritical margin of 5% in k is required. For dry storage racks analyzed with optimum moderation, the subcritical margin is 2% and 5% with full moderation. In the analysis of 236 critical experiments, which generously cover the range of expected conditions, the lowest calculated k was 0.9931. This supports the position that the subcritical margin is more than sufficient.

A.4.1.8 Area of Applicability (Benchmark Applicability)

The critical benchmarks selected cover all commercial light water reactor fuel storage racks or casks. To summarize the range of the benchmark applicability (or area of applicability), Table A.4.1.7 is provided below.

Table A.4.1.7: Area of Applicability (Benchmark Applicability)

Parameter	Range	Comments
Fissionable Material/Physical Form	UO_2	The fuel material is the same as in the benchmark experiments
Enrichment (wt% U-235)	2.35 to 4.74	The first core enrichments require extrapolation of the bias to lower enrichments. The predicted difference in bias from the lowest measured data to the lowest enrichment manufactured is only 0.01% in k. An error in the slope used for extrapolation would only produce errors in the hundredths of a percent. The extrapolated bias is less than the limiting bias. Therefore extrapolation of the bias to lower enrichments is justified. An extrapolation from 4.74 to 5 wt% will also be needed but in this direction the bias is decreasing so the data is adequate for this extrapolation.
Spectrum - EALF (eV)	0.0605 to 0.8485	Expected range in applications: 0.1 to 0.6 eV The experiments cover the entire expected range of limiting conditions. For intended applications, dry conditions are never limiting.

Parameter	Range	Comments
Lattice Characteristics Type Pin Pitch (cm)	 Square 1.075 to 2.54	 Hex lattices have been excluded. Expected range of 1.2 to 1.6 cm. The expected range of all fuel types, including both PWR and BWR fuel is covered.
Assembly Spacing in Racks Distance between Assemblies (cm)	0 to 15.4	This covers all spacing. Neutron transport through larger than 15.4 cm has a small effect on k. Note that the spacing is assumed to be filled with full density water. If the water density is less, this separation effectively increases. Therefore, optimum moderation cases of wide spaced racks are covered.
Absorbers Boron Areal Density (B-10 g/cm^2)	0 to 0.067	Spent fuel storage designs are within this range.
Absorbers Soluble Boron Concentration	0 to 5030 ppm	All designs are within this range.
Absorbers Cd (for Ag-In-Cd rods)	Cd Absorber panels	Cd bearing experiments showed no dependence on the number of rods. Credit for these rods is acceptable.
Reflector Experiments included water and steel	Reflectors adequately covered	Most rack analysis will assume optimum reflection or in the case of casks, steel walls. Both of these assumptions are adequately covered.
Temperature	Room Temperature	The criticality calculations are performed with the fuel at low temperatures. No significant Doppler feedback.
Moderating material	Water	The moderator in all benchmark experiments is water, therefore water as a moderating material is covered

A.4.1.9 Summary of Fresh UO_2 Laboratory Critical Experiment Analysis

This validation follows the guidance of NUREG/CR-6698. Key aspects of the guidance are the selection of experiments, analysis of the experiments, statistical treatment, determination of the bias and the bias uncertainty, and finally identification of the area of applicability.

236 UO_2 critical experiments have been selected that cover the range of conditions for rack analysis. The experiments have been analyzed using SCALE 6.1.2 and the ENDF/B-VII 238 group cross-sections and the resulting bias in k is small. The results of the criticality analysis were tested for trends against 6 different parameters important to reactivity. It was conservatively assumed that any trend found was significant. Using the trends, the most limiting bias and bias uncertainty is determined to be **0.0029 for the bias for EALF up to 0.4 eV and 0.0037 for EALF's in the range of 0.4 and 0.6 eV and the uncertainty is 0.0050 for all analyses.**

While this validation is intended to cover all LWR fuel racks, the specific area of applicability is found in Table A.4.1.7.

A.4.1.10 HTC and MOX Critical Experiments

Burned fuel contains a low concentration of plutonium (about 1 wt%), as well as the uranium and thus is actually Mixed Oxide (MOX) fuel. Most classical MOX experiments have plutonium concentrations at least twice as high as that contained in burned fuel. A series of experiments were performed in France and purchased by the US for domestic use, which model the uranium and plutonium concentration, which matches 4.5 wt % U-235 fuel burned to 37.5 GWd/T [12]. This fuel has 1.1 wt% plutonium and 1.57 wt% U-235. Both the HTC critical experiments and a large series of classical MOX experiments were analyzed.

A.4.1.10.1 HTC Critical Experiments

All the HTC critical experiments used the same fuel pins. The criticality of these experiments was controlled by adjusting the critical water height. The fuel pins were used in 156 critical arrangements. 117 of these were relevant to spent fuel pool analysis. The experiments were performed in four phases.

Phase 1 [13] consists of 17 cases where the pin pitch was varied from 1.3 cm to 2.3 cm and different quantities of pins were used to change the critical height. An 18th case was done where the array was moved to the edge of the tank, so the boundary was the steel tank followed by void. This condition is not typical of a spent fuel pool, so this case was not analyzed. The average k of the Phase 1 cases was 0.99910.

Phase 2 [14] consisted of 20 cases where gadolinium of various concentrations was dissolved in the water (Phase 2a) and 21 cases where boron was dissolved in the water (Phase 2b). These experiments also varied the pitch (1.3 to 1.9 cm) and the number of pins. The average k of the gadolinium cases was 0.99815 and the average for the boron cases was 0.99897.

Phase 3 [15] consists of 26 experiments where the pins were arranged as 4 "assemblies." Each assembly used a 1.6 cm pin pitch. The assembly separation was varied, as well as the number of pins in each assembly. Finally, eleven cases boxed the assemblies with an absorber (borated steel, boral, or cadmium). The average k of these 26 cases was 0.99890.

Finally, Phase 4 [16] consisted of redoing the same type of experiments as Phase 3, except with reflector screens. The 38 experiments which used the lead reflector screen were not included in this analysis, since lead reflectors are not common in spent fuel pools. The 33 steel reflector experiments were included. The average k of these cases was 0.99858.

References 13 through 16 provided all the details for the analysis. The modeling was straight forward. The references gave a simple model and a detailed model. The model created for this work followed the detailed model, except that the top grid outside of the array and the basket supports were not modeled. Both of these assumptions were part of the simplified model and have a negligible impact on k. The model used actually exceeded the detailed model, since the spring above the fuel was modeled by homogenizing it with the void.

Tables A.4.1.8 through A.4.1.12 present the results of the analysis. A statistical analysis of the set as a whole was performed consistent with the method provided in NUREG/CR-6698, where the experimental uncertainties were taken from References 13 through 16. The mean uncertainty weighted k is 0.99878 and the uncertainty is 0.00590. This makes the bias 0.00122. Since all the pins are the same, trend analysis on the pin diameter and enrichment are not possible. The pin pitch changes are made to adjust the spectrum, so the only trend analysis performed is on the spectrum (EALF). The trend analysis (performed consistent with NUREG/CR-6698) on EALF yielded the following function:

$$\mathbf{k(EALF) = 0.999538 - 0.00548 * EALF}$$

The units for EALF are eV. The uncertainty about the trending k is 0.0057 in k. Figure A.4.1.8 shows the results of the HTC analysis.

Table A.4.1.8: HTC Phase 1 Results

Case No.	k_{eff}	Monte Carlo Sigma	EALF (eV)	Pitch (cm)
1	0.99913	0.00015	0.069486	2.3
2	0.99893	0.00016	0.066544	2.3
3	0.99892	0.00016	0.066412	2.3
4	0.99974	0.00017	0.084957	1.9
5	0.99983	0.00017	0.082795	1.9
6	0.99946	0.00020	0.082123	1.9
7	0.99977	0.00019	0.102248	1.7
8	0.99962	0.00018	0.100654	1.7
9	0.99903	0.00019	0.099687	1.7
10	0.99991	0.00019	0.140669	1.5
11	0.99898	0.00020	0.135753	1.5
12	0.99906	0.00019	0.133996	1.5
13	0.99813	0.00021	0.256212	1.3
14	0.99776	0.00019	0.234183	1.3
15	0.99812	0.00022	0.230564	1.3
16	0.99952	0.00020	0.101408	1.7
17	0.99882	0.00019	0.099384	1.7

Table A.4.1.9: HTC Phase 2a, Gadolinium Solutions, Results

Case No.	k_{eff}	Monte Carlo Sigma	EALF (eV)	Pitch (cm)	Gadolinium Concentration (g/l)
1	0.99784	0.00020	0.25279	1.3	0.0520
2	0.99792	0.00021	0.24946	1.3	0.0520
3	0.99777	0.00019	0.27074	1.3	0.1005
4	0.99771	0.00018	0.26756	1.3	0.1005
5	0.99784	0.00018	0.26333	1.3	0.1005
6	0.99683	0.00018	0.28513	1.3	0.1505
7	0.99684	0.00019	0.27847	1.3	0.1505
8	0.99623	0.00016	0.29552	1.3	0.1997
9	0.99608	0.00018	0.29253	1.3	0.1997
10	0.99689	0.00017	0.16982	1.5	0.1997
11	0.99766	0.00019	0.16252	1.5	0.1495
12	0.99771	0.00018	0.16101	1.5	0.1495
13	0.99868	0.00017	0.15392	1.5	0.1000
14	0.99861	0.00018	0.15223	1.5	0.1000
15	0.99983	0.00020	0.14727	1.5	0.0492
16	0.99976	0.00019	0.14432	1.5	0.0492
17	1.00053	0.00018	0.10631	1.7	0.0492
18	1.00070	0.00017	0.08783	1.9	0.0492
19	0.99707	0.00016	0.11369	1.7	0.1010
20	1.00050	0.00019	0.10648	1.7	0.0492

Table A.4.1.10: HTC Phase 2b, Boron Solutions, Results

Case No.	k_{eff}	Monte Carlo Sigma	EALF (eV)	Pitch (cm)	Boron Concentration (g/l)
1	0.99835	0.00020	0.24780	1.3	0.100
2	0.99760	0.00020	0.24450	1.3	0.106
3	0.99816	0.00020	0.25528	1.3	0.205
4	0.99904	0.00020	0.26400	1.3	0.299
5	0.99886	0.00019	0.27475	1.3	0.400
6	0.99852	0.00019	0.27125	1.3	0.399
7	0.99933	0.00018	0.27977	1.3	0.486
8	0.99894	0.00019	0.28781	1.3	0.587
9	0.99952	0.00016	0.16627	1.5	0.595
10	0.99811	0.00019	0.16087	1.5	0.499
11	0.99990	0.00017	0.15663	1.5	0.393
12	0.99987	0.00018	0.15007	1.5	0.295
13	0.99887	0.00018	0.14559	1.5	0.200
14	1.00192	0.00018	0.14024	1.5	0.089
15	1.00338	0.00018	0.10325	1.7	0.090
16	1.00202	0.00017	0.10717	1.7	0.194
17	1.00313	0.00017	0.11049	1.7	0.286
18	0.99367	0.00017	0.11577	1.7	0.415
19	1.00021	0.00021	0.10473	1.7	0.100
20	0.99251	0.00017	0.08965	1.9	0.220
21	0.99642	0.00017	0.08611	1.9	0.110

Table A.4.1.11: HTC Phase 3 Results – Water Reflected Assemblies
(1.6 cm pin pitch)

Case No.	k_{eff}	Monte Carlo Sigma	EALF (eV)	Absorber Box Material	Assembly Separation (cm)
1	0.99774	0.00022	0.12377	Borated SS	3.5
2	0.99986	0.00019	0.14095	Borated SS	0
3	0.99710	0.00019	0.12939	Borated SS	2
4	0.99715	0.00018	0.12391	Borated SS	3
5	0.99699	0.00018	0.13503	Borated SS	1
6	0.99987	0.00019	0.12974	Boral	0
7	0.99614	0.00019	0.12866	Cd	2
8	1.00381	0.00018	0.13904	Cd	0
9	0.99646	0.00017	0.13345	Cd	1
10	0.99672	0.00018	0.12952	Cd	1.5
11	0.99571	0.00019	0.13726	Cd	0.5
12	0.99901	0.00017	0.11277	none	18
13	0.99915	0.00018	0.11167	none	14.5
14	0.99934	0.00018	0.11183	none	11
15	0.99910	0.00019	0.11093	none	10
16	0.99961	0.00019	0.11030	none	9
17	0.99930	0.00018	0.10842	none	8
18	0.99980	0.00017	0.10656	none	6
19	1.00016	0.00018	0.10421	none	4
20	1.00044	0.00018	0.10206	none	4
21	0.99976	0.00018	0.10470	none	2
22	1.00047	0.00019	0.10714	none	1
23	0.99893	0.00018	0.11506	none	0
24	0.99949	0.00020	0.15073	none	0
25	0.99996	0.00018	0.12672	none	4
26	0.99937	0.00020	0.11550	none	10

Table A.4.1.12: HTC Phase 4 Results – Steel Reflected Assemblies
(1.6 cm pin pitch)

Case No.	k_{eff}	Monte Carlo Sigma	EALF (eV)	Absorber Box Material	Assembly Separation (cm)	Separation From Reflector (cm)
1	1.00157	0.00019	0.15363	Borated SS	0	0.0
2	0.99845	0.00018	0.15069	Borated SS	0.5	0.0
3	0.99797	0.00018	0.14674	Borated SS	1	0.0
4	0.99826	0.00018	0.14227	Borated SS	1.5	0.0
5	0.99839	0.00019	0.13923	Borated SS	2	0.0
6	0.99712	0.00018	0.13820	Borated SS	2	0.5
7	0.99634	0.00018	0.13705	Borated SS	2	1.0
8	0.99650	0.00018	0.13598	Borated SS	2	1.5
9	0.99658	0.00018	0.13518	Borated SS	2	2.0
10	0.99834	0.00018	0.13430	Borated SS	3	0.0
11	0.99821	0.00018	0.13234	Borated SS	3.5	0.0
12	1.00095	0.00018	0.13558	Boral	0	0.0
13	0.99653	0.00018	0.13386	Boral	0.5	0.0
14	1.00431	0.00017	0.14979	Cd	0	0.0
15	0.99818	0.00020	0.14323	Cd	1	0.0
16	0.99769	0.00017	0.13683	Cd	2	0.0
17	0.99615	0.00018	0.13568	Cd	2	0.5
18	0.99536	0.00019	0.13423	Cd	2	1.0
19	0.99513	0.00018	0.13315	Cd	2	1.5
20	0.99465	0.00018	0.13235	Cd	2	2.0
21	0.99869	0.00018	0.13390	Cd	2.5	0.0
22	1.00060	0.00018	0.17427	none	0	0.0
23	1.00057	0.00018	0.16641	none	1	0.0
24	0.99973	0.00018	0.15852	none	2	0.0
25	0.99935	0.00018	0.15709	none	2	0.5
26	0.99946	0.00018	0.15559	none	2	1.0
27	0.99939	0.00018	0.15431	none	2	1.5
28	0.99937	0.00019	0.15351	none	2	2.0
29	0.99941	0.00019	0.14426	none	4	0.0
30	0.99964	0.00018	0.13456	none	6	0.0
31	0.99953	0.00018	0.12886	none	8	0.0
32	0.99947	0.00017	0.12537	none	10	0.0
33	0.99940	0.00018	0.12333	none	12	0.0

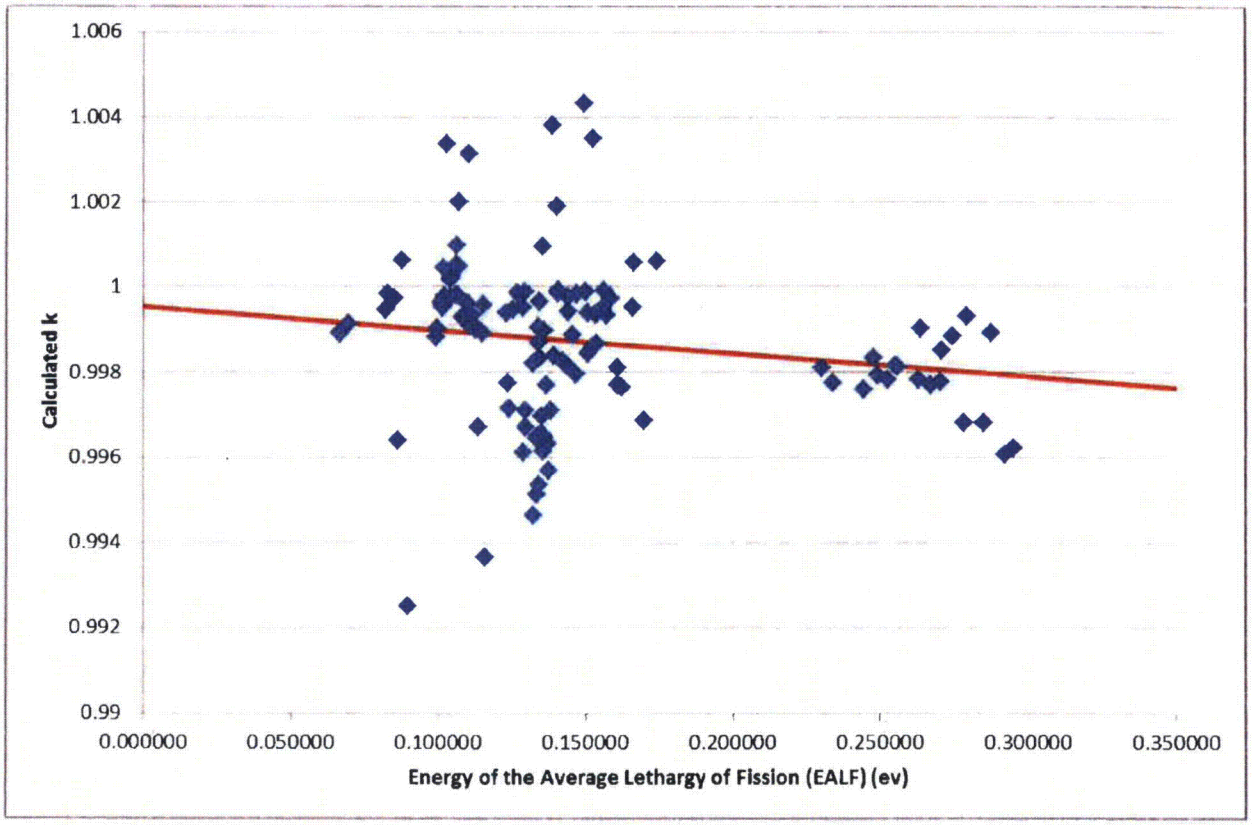

Figure A.4.1.8: k_{eff} as a Function of the Energy of the Average Lethargy Causing Fission for the HTC Experiments

A.4.1.10.2 MOX Critical Experiments

The selection of the MOX critical experiments was limited to the low enriched MOX lattice critical experiments. All 63 of the low enriched MOX pin critical experiments documented in the OECD handbook [17] were utilized. The actual input decks were initiated from available decks found in NUREG/CR-6102 [18] and OECD [17]. The decks were modified to update to the new cross-section library and changes in the SCALE input format.

Table A.4.1.13 presents the results of the 63 selected MOX critical experiments. The Reference column has the evaluation number from the OECD benchmark handbook [17]. For example, OECD-7 refers to the OECD case MIX-COMP-THERM-07.

Trends were investigated as a function of EALF, plutonium content, and the Am-241/U-238 ratio. As the spectrum hardens (higher EALF), there is a small trend to higher k. With more plutonium content, k increases. This is seen in Figure A.4.1.9. This means that the more limiting bias comes from the zero plutonium cases (fresh UO_2). This is confirmed by the average calculated k of the HTC critical experiments being higher than the average calculated k for the fresh UO_2 cases. The average uncertainty

weighted k of the fresh UO_2 criticals is 0.9978. The average uncertainty weighted k for the HTC criticals is 0.9988. The average uncertainty weighted k of the MOX experiments is 0.9984.

The change in k with cooling time is dominated by the reactivity of the decay of Pu-241 to Am-241. By plotting k versus the Am-241/U-238 ratio, it is possible to determine if the bias should be changed for cooling. Figure A.4.1.10 shows that with increasing Am-241 content, the calculated k of the critical experiments increases. This observation shows that the zero cooling time bias conservatively covers the cooling time.

Table A.4.1.13: Results of MOX Critical Benchmarks (SCALE 6.1.2, ENDF/B-VII)

Case ID	Reference	k_{eff}	sigma	EALF (eV)	Pu wt%	Pu 240%	Am241/U238
093array	OECD-7	1.0009	0.00025	0.1903	2.00	16	6.82E-05
105al.in	OECD-7	0.9942	0.00027	0.1369	2.00	16	7.55E-05
105array	OECD-7	0.9960	0.00025	0.1377	2.00	16	7.55E-05
105b1	OECD-7	0.9914	0.00026	0.1379	2.00	16	7.55E-05
105b2	OECD-7	0.9921	0.00024	0.1377	2.00	16	7.55E-05
105b3	OECD-7	0.9933	0.00025	0.1373	2.00	16	7.55E-05
105b4	OECD-7	0.9940	0.00026	0.1371	2.00	16	7.55E-05
1143arra	OECD-7	0.9980	0.00026	0.1166	2.00	16	8.13E-05
132array	OECD-7	0.9971	0.00022	0.0953	2.00	16	8.13E-05
1386arra	OECD-7	0.9942	0.00023	0.0906	2.00	16	6.97E-05
epri70b	OECD-2	0.9992	0.00025	0.7209	2.00	7.8	7.29E-05
epri70un	OECD-2	0.9974	0.00027	0.5409	2.00	7.8	7.29E-05
epri87b	OECD-2	1.0019	0.00022	0.2710	2.00	7.8	7.29E-05
epri87un	OECD-2	0.9981	0.00032	0.1852	2.00	7.8	7.29E-05
epri99b	OECD-2	1.0012	0.00024	0.1772	2.00	7.8	7.29E-05
epri99un	OECD-2	1.0007	0.00027	0.1333	2.00	7.8	7.29E-05
k1mct009	OECD-9	0.9994	0.00024	0.5169	1.50	8	1.06E-05
k2mct009f	OECD-9	0.9941	0.00027	0.2943	1.50	8	9.77E-06
k3mct009	OECD-9	0.9934	0.00024	0.1528	1.50	8	8.96E-06
K4mct009	OECD-9	0.9921	0.00024	0.1155	1.50	8	8.96E-06
K5mct009	OECD-9	0.9925	0.00021	0.0947	1.50	8	8.96E-06
K6mct009	OECD-9	0.9937	0.00024	0.0905	1.50	8	9.77E-06
omct61	OECD-6	0.9954	0.00026	0.3570	2.00	8	2.24E-05
omct62	OECD-6	0.9990	0.00029	0.1885	2.00	8	2.24E-05
omct63	OECD-6	0.9943	0.00027	0.1374	2.00	8	2.24E-05
omct64	OECD-6	0.9982	0.00025	0.1167	2.00	8	2.24E-05
omct65	OECD-6	0.9994	0.00025	0.0956	2.00	8	2.24E-05
omct66	OECD-6	0.9956	0.00024	0.0907	2.00	8	2.24E-05
mct8c1	OECD-8	0.9978	0.00029	0.3776	2.00	24	7.93E-05
mct8c2	OECD-8	0.9977	0.00028	0.1922	2.00	24	7.27E-05
mct8c3	OECD-8	0.9967	0.00024	0.1383	2.00	24	8.59E-05
mct8c4	OECD-8	1.0006	0.00027	0.1170	2.00	24	9.88E-05
mct8c5	OECD-8	1.0000	0.00026	0.0955	2.00	24	9.56E-05
mct8c6	OECD-8	0.9992	0.00023	0.0905	2.00	24	7.27E-05

Case ID	Reference	k_{eff}	sigma	EALF (eV)	Pu wt%	Pu 240%	Am241/U238
mct8ca1	OECD-8	0.9967	0.00025	0.1375	2.00	24	8.59E-05
mct8cb1	OECD-8	0.9931	0.00024	0.1387	2.00	24	8.59E-05
mct8cb3	OECD-8	0.9941	0.00025	0.1381	2.00	24	8.59E-05
mctcb2	OECD-8	0.9937	0.00024	0.1385	2.00	24	8.59E-05
mctcb4	OECD-8	0.9942	0.00026	0.1378	2.00	24	8.59E-05
mixo251k	OECD-5	1.0011	0.00032	0.3732	4.00	18	1.59E-04
mixo252k	OECD-5	0.9985	0.00027	0.2476	4.00	18	1.59E-04
mixo253k	OECD-5	1.0044	0.00027	0.1712	4.00	18	1.59E-04
mixo254k	OECD-5	1.0004	0.00029	0.1425	4.00	18	1.59E-04
mixo255k	OECD-5	1.0034	0.00028	0.1058	4.00	18	1.59E-04
mixo256k	OECD-5	1.0023	0.00024	0.0917	4.00	18	1.59E-04
mixo257k	OECD-5	1.0036	0.00024	0.0875	4.00	18	1.59E-04
saxtn104	OECD-3	1.00044	0.00027	0.0987	6.60	8.6	8.43E-05
saxtn56b	OECD-3	0.99962	0.00028	0.6133	6.60	8.6	8.43E-05
saxtn735	OECD-3	0.99999	0.00031	0.1820	6.60	8.6	8.43E-05
saxtn792	OECD-3	0.99951	0.00031	0.1505	6.60	8.6	8.43E-05
Saxton52	OECD-3	0.99977	0.00028	0.8517	6.60	8.6	8.43E-05
Saxton56	OECD-3	1.00018	0.0003	0.5177	6.60	8.6	8.43E-05
tca1	OECD-4	0.99572	0.00027	0.1418	3.01	22	1.04E-04
tca10	OECD-4	0.9988	0.00024	0.0792	3.01	22	9.31E-05
tca11	OECD-4	0.99886	0.00023	0.0788	3.01	22	2.06E-04
tca2	OECD-4	0.9964	0.0003	0.1409	3.01	22	1.99E-04
tca3	OECD-4	0.99665	0.00028	0.1403	3.01	22	2.96E-04
tca4	OECD-4	0.99644	0.00026	0.1172	3.01	22	9.88E-05
tca5	OECD-4	0.9974	0.00027	0.1167	3.01	22	2.02E-04
tca6	OECD-4	0.99848	0.00025	0.1156	3.01	22	3.90E-04
tca7	OECD-4	0.99753	0.00025	0.0917	3.01	22	8.88E-05
tca8	OECD-4	0.99801	0.00025	0.0913	3.01	22	2.03E-04
tca9	OECD-4	0.99864	0.00025	0.0909	3.01	22	3.02E-04

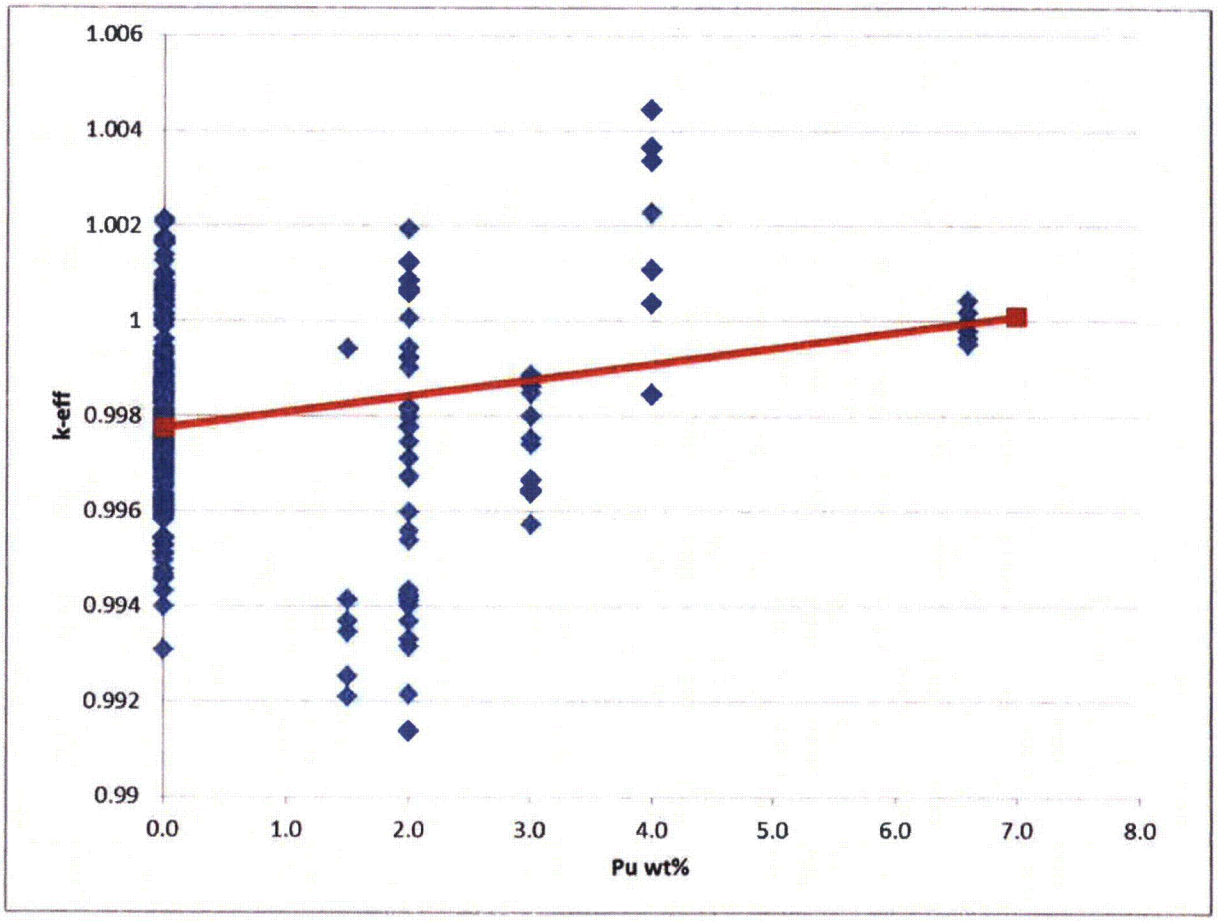

Figure A.4.1.9 Predicted k_{eff} as a Function of the Plutonium Content

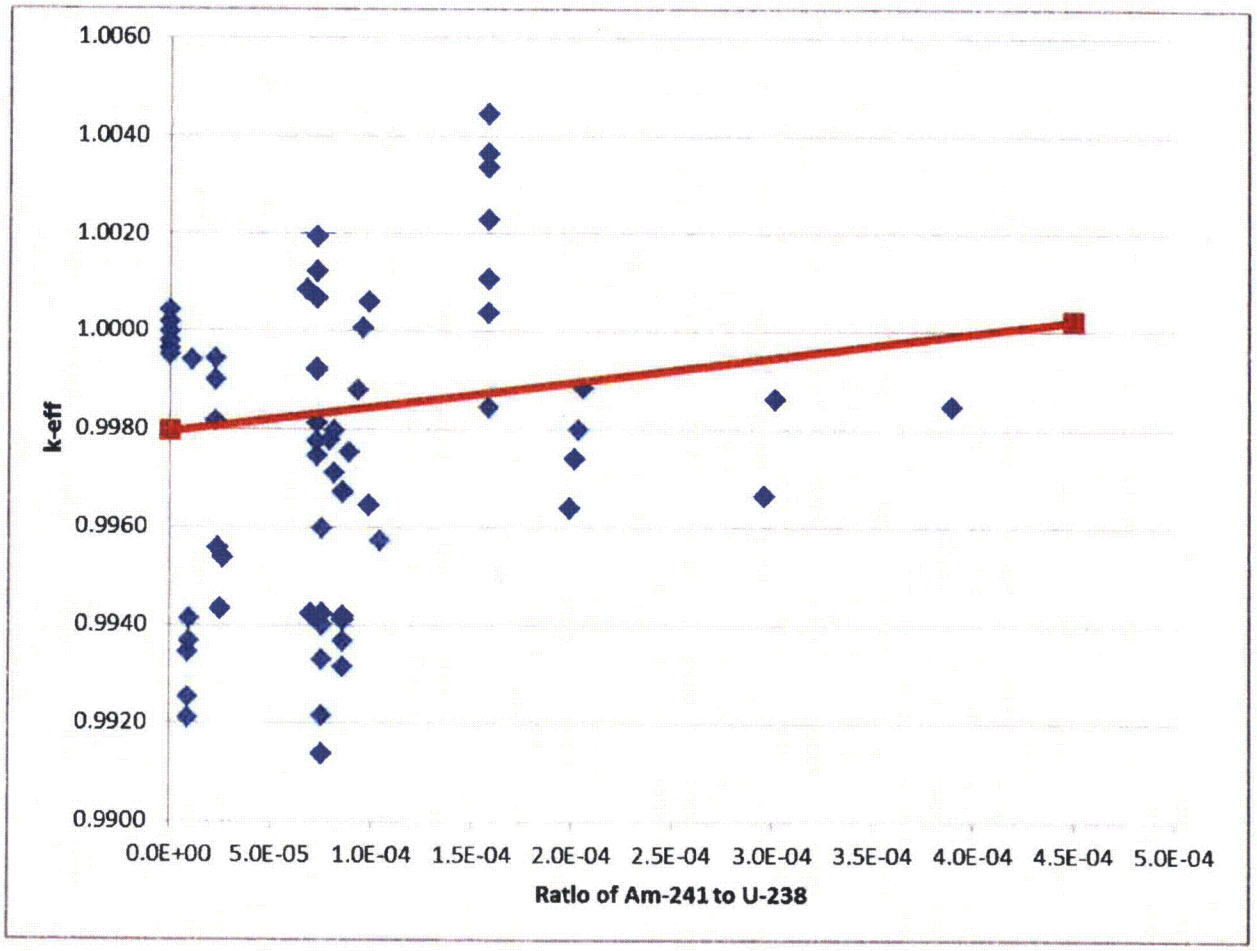

Figure A.4.1.10 Predicted k_{eff} as a Function of the Am-241 Content

A.4.2 Depletion Reactivity Bias and Uncertainty (EPRI Benchmark Analysis)

Measured data from power plants can be used to validate the delta-k of depletion,. EPRI has used power distribution measurements to infer the change in reactivity due to burnup using 680 flux maps taken over 44 cycles from 4 different PWRs [10]. The reactivity change is then captured as a series of benchmarks that can be analyzed using the methods selected for the criticality analysis. The analysis for the benchmarks for utilization in criticality analysis is demonstrated for SCALE 6.1 and the 238-group ENDF/B-VII library in Reference 11, but this work uses a slight modification which requires reanalysis of the benchmarks.

Due to the axial burnup profiles, this effort requires the generation of atom density sets at a large number of different burnups. Reference 11, which demonstrated how to use the EPRI benchmarks, required only 6 burnups (10, 20, 30, 40, 50, and 60 GWd/T). In Reference 11, each burnup atom density set was generated by a separate burn from the initial fresh fuel conditions. This is consistent with the design of TRITON. Reference 11 restarted TRITON to produce the two cooling times needed after the initial 100 hour cooling time. The depletion performed for this work matched that used in Reference 11, however, the isotopes used in the final criticality analysis were reduced from 388 to 185 isotopes and the decay was performed outside of SCALE. The reduction in isotopes is needed for this analysis because the axial burnup profiles multiply the number of isotopes needed for processing by 9. With this multiplier, the processing time becomes large, making the reduction in isotopes significant to the total effort.

For this work, the same steps were followed as in Reference 11, so the reader is referred to Reference 11 for more details regarding this process. Tables A.4.2.1, A.4.2.2, and A.4.2.3 show the results of the benchmark analysis using the methods selected for this analysis.

Table A.4.2.1: EPRI Benchmark Results for 100-hour Cooling

		Bias (Calculated Reactivity Decrement - Measured Reactivity Decrement) For 100-Hour Cooling					
		Burnup (GWd/T)					
Case	Lattice Description	10	20	30	40	50	60
1	3.25% enrichment depletion	-0.0008	-0.0017	-0.0024	-0.0037	-0.0040	-0.0044
2	5.00% enrichment depletion	-0.0001	-0.0003	-0.0005	-0.0012	-0.0014	-0.0018
3	4.25% enrichment depletion	0.0002	-0.0004	-0.0010	-0.0018	-0.0026	-0.0029
4	off-nominal pin depletion	-0.0008	-0.0016	-0.0023	-0.0029	-0.0037	-0.0046
5	20 WABA depletion	0.0000	0.0003	-0.0005	-0.0014	-0.0018	-0.0025
6	104 IFBA depletion	0.0010	0.0007	-0.0004	-0.0020	-0.0027	-0.0042
7	104 IFBA, 20 WABA depletion	0.0007	0.0011	0.0000	-0.0013	-0.0018	-0.0032
8	high boron depletion = 1500 ppm	-0.0003	-0.0006	-0.0011	-0.0017	-0.0018	-0.0024
9	branch to hot rack = 338.7K	-0.0004	-0.0007	-0.0008	-0.0017	-0.0019	-0.0025
10	branch to rack boron = 1500 ppm	-0.0009	-0.0019	-0.0027	-0.0036	-0.0044	-0.0049
11	high power density depletion	-0.0002	-0.0012	-0.0016	-0.0022	-0.0026	-0.0032

Table A.4.2.2: EPRI Benchmark Results for 5-year Cooling

		Bias (Calculated Reactivity Decrement - Measured Reactivity Decrement) For 5 years Cooling					
		Burnup (GWd/T)					
Case	Lattice Description	10	20	30	40	50	60
1	3.25% enrichment depletion	-0.0002	-0.0010	-0.0017	-0.0026	-0.0026	-0.0028
2	5.00% enrichment depletion	0.0006	0.0006	0.0000	-0.0005	-0.0008	-0.0011
3	4.25% enrichment depletion	0.0008	0.0000	-0.0005	-0.0012	-0.0016	-0.0021
4	off-nominal pin depletion	-0.0003	-0.0008	-0.0018	-0.0023	-0.0028	-0.0033
5	20 WABA depletion	0.0006	0.0006	0.0001	-0.0005	-0.0010	-0.0014
6	104 IFBA depletion	0.0019	0.0009	0.0001	-0.0011	-0.0017	-0.0029
7	104 IFBA, 20 WABA depletion	0.0018	0.0019	0.0007	-0.0001	-0.0012	-0.0020
8	high boron depletion = 1500 ppm	0.0005	0.0003	-0.0001	-0.0010	-0.0011	-0.0014
9	branch to hot rack = 338.7K	0.0002	0.0001	-0.0005	-0.0009	-0.0009	-0.0014
10	branch to rack boron = 1500 ppm	0.0000	-0.0012	-0.0018	-0.0029	-0.0033	-0.0038
11	high power density depletion	0.0004	-0.0001	-0.0005	-0.0009	-0.0016	-0.0016

Table A.4.2.3: EPRI Benchmark Results for 15-year Cooling

Case	Lattice Description	Bias (Calculated Reactivity Decrement - Measured Reactivity Decrement) For 15 years Cooling Burnup (GWd/T)					
		10	20	30	40	50	60
1	3.25% enrichment depletion	0.0005	-0.0009	-0.0022	-0.0028	-0.0033	-0.0033
2	5.00% enrichment depletion	0.0009	0.0009	-0.0001	-0.0005	-0.0010	-0.0012
3	4.25% enrichment depletion	0.0012	0.0005	-0.0006	-0.0013	-0.0018	-0.0021
4	off-nominal pin depletion	0.0004	-0.0009	-0.0014	-0.0026	-0.0031	-0.0034
5	20 WABA depletion	0.0012	0.0013	0.0002	-0.0008	-0.0012	-0.0019
6	104 IFBA depletion	0.0023	0.0014	0.0001	-0.0009	-0.0019	-0.0028
7	104 IFBA, 20 WABA depletion	0.0025	0.0024	0.0009	-0.0002	-0.0009	-0.0020
8	high boron depletion = 1500 ppm	0.0009	0.0004	-0.0002	-0.0012	-0.0012	-0.0018
9	branch to hot rack = 338.7K	0.0003	-0.0001	-0.0007	-0.0010	-0.0012	-0.0016
10	branch to rack boron = 1500 ppm	0.0002	-0.0012	-0.0021	-0.0028	-0.0037	-0.0038
11	high power density depletion	0.0009	0.0003	-0.0007	-0.0013	-0.0014	-0.0019

The maximum bias from all the cooling times is 0.0025. This bias is from Case 7 at 10 GWd/T burnup. However, a number of the 11 lattice conditions given on Tables A.4.2.1 to A.4.2.3 can occur simultaneously. To find the highest bias, one starts with the bias from Case 3 and adds the delta biases between Case 3 and the condition of interest. The most limiting condition is 5 years cooling and 30 GWd/T. The values for this case will be used to show how a rack up of biases is performed. The Case 3 bias at 30 GWd/T and 5 years cooling is -0.0005 (see Table A.4.2.2). Since the fuel can be a higher or lower enrichment, the difference between the bias for Case 2 and Case 3 (+0.0005) is added. That is the base -0.0005 plus +0.0005 resulting in a corrected bias of zero. Now we correct for the pin diameter. Case 4 uses a smaller pin diameter than Case 3. The 15x15 fuel pin diameter is larger than the 17X17 fuel by about the same amount as Case 4 is smaller than standard 17X17 fuel. The difference in the bias between Case 4 and Case 3 is added to further correct the bias. That is -0.0005 – (-0.0018) or a +0.0013 correction, making the new corrected bias +0.0013. Note that it is assumed here that the effect is due to the pin diameter rather than the spectrum. 15X15 and 17X17 fuel have about the same spectrum, so this correction may not be necessary if it is actually due to the spectral difference rather than the pin diameter. Case 7 covers both IFBAs and WABAs. The bias is more positive by 0.0007 – (-0.0005) = 0.0012. Adding this effect, the corrected bias is now 0.0025. Finally, the depletion at a higher ppm shows a more positive bias (-0.0001- (-0.0005)). Adding the effect of a higher ppm depletion raises the total corrected bias to 0.0029. (Note that the depletions are performed at less than 1500 ppm, so this effect is over estimated.) The higher power and the higher rack temperature did not change the bias from the reference, Case 3 and adding absorbers to the pool made the bias less positive. **The final selected bias is rounded up to 0.003.**

A similar rackup of biases at 20 GWd/t produces a higher bias, but that is due to the depletion of the burnable absorbers. The depletion reactivity, as defined by the EPRI benchmarks, includes the change in reactivity from the burnable absorbers. From reviewing Tables A.4.2.1 through A.4.2.3, it is clear that

there is an over-prediction of the depletion rate of the burnable absorbers. Although burnable absorbers are included in the depletion analysis in order to harden the spectrum, the final application does not credit any absorption from burnable absorbers. Table 6-1 of Reference 11 shows that at 20 GWd/T the residual boron worth is greater than 0.008, which means the assumption to ignore the residual boron is much larger than the small positive biases from Cases 5, 6, and 7. Ignoring the positive biases for Cases 5, 6, and 7 at 20 GWd/T and below makes the 30 GWd/T, 15 years cooled case most limiting.

The depletion uncertainty is the uncertainty in the EPRI benchmarks which are reported in Table C-1 of Reference 10. The benchmark uncertainty is a function of the specific power. With radial peaking, the specific power of this analysis is between the Case 10 and 11 values. **The depletion uncertainty of 0.0064 from the highest power, EPRI Case 11, is used for this analysis.**

A.4.3 Extended ISG-8 Validation

The validation of the analysis only needs validation of the initial condition (Fresh UO_2 critical experiments) and validation of the depletion reactivity (EPRI benchmarks). However, an alternate approach (the Extended ISG-8 approach) can be taken, where the isotopic content is validated (validation of the depletion calculations), followed by validation of the reactivity worth of the isotopes (MOX and HTC critical benchmarks used for the most important isotopes and conservative use of TSUNAMI analysis for the rest of the isotopes). This validation uses the most limiting of the two approaches.

The validation of the isotopic content has three major steps. The first step is to determine what chemical assays are appropriate. The second step is the analysis of the chemical assays using the depletion methods that will be used for the final criticality analysis of the application. The third step is to convert the results of the prediction of the isotopic content of the chemical assays to a delta-k bias and uncertainty for the final application. This third step is often called the "direct difference" approach. [19]

A.4.3.1 Selection of Assays

ORNL reviewed the chemical assays available and made selections in ORNL/TM-2010/44 [20] and then in NUREG/CR-7108 [19]. This validation generally follows the ORNL selections. ORNL eliminated several sets of chemical assays. Yankee Rowe assays were eliminated due to lack of information on the control rod locations. Many in the industry consider Yankee Rowe assays high quality assays [21] but this validation follows the ORNL recommendation. Mihama samples were eliminated with the statement, "Future use of this set of data was not recommended because of the unexplained variation in the results, which may indicate problems related to the radiochemical analysis of samples or the incomplete documentation of operating data." Soluble boron data is not available for the Mihama samples but previous studies [22] only eliminated one sample. This analysis follows the ORNL recommendation to not use Mihama data. The OECD/NEA has a web site, http://www.oecd-nea.org/sfcompo/, which summarizes chemical assay data. At the time of the writing of this validation (11/1/2013), the only PWR data on the sfcompo website not covered by ORNL are two chemical assays from the Genkai-1 reactor in Japan. These two assays do not include fission products and there is no information provided as to which fuel rod in the assembly was assayed. The Genkai-1 assay data is not used in this validation.

ORNL/TM-2010/44 analyzed 118 assays but NUREG/CR-7108 did not use 18 of these. They were:

1. 3 Gösgen fuel samples that are proprietary.
2. 12 Obrigheim assays taken from rods on the periphery. Obrigheim had used some MOX assemblies and the location of the MOX assemblies was not known, so the peripheral pin could have been next to MOX fuel.
3. 3 Takahama assays were excluded due to their close proximity to the edge of the active core. The flux gradient is strong in this region and this effect is not relevant to the criticality analysis this effort supports.

Like NUREG/CR-7108, this validation does not use these 18 assays.

In addition to the assays selected for NUREG/CR-7108, this validation will use 5 chemical assays performed on fuel from the Spanish reactor, Vandellós II. These samples have been analyzed by ORNL. The ORNL report is NUREG/CR-7013 [23]. The reason these assays were not included in NUREG/CR-7108 was because the data was not available in time to be included in the analysis. These samples include fission products and are at a higher burnup and enrichment compared to the rest of the assays used in this validation. Note that there are actually six chemical assays in the Vandellós II set. However, the sample from rod WZtR160 does not include accurate uranium data [23]. When using the direct difference approach, it is inappropriate to use samples missing high worth isotopes that vary with irradiation, such as U-235 in this case.

This validation does not use the 11 TMI chemical assays performed on Assembly NJ05YU. These assays were done by ANL on a single pin. The 8 other chemical assays from TMI were performed by GE on three rods from Assembly NJ070G. These assays do not have the problems found with the NJ05YU assembly. Figures A.4.3.1, A.4.3.2, and A.4.3.3 show the change in data as the assays go up the same pin axially. Except for the grids, which are shown as red lines, there is nothing in the assembly that should produce non-smooth results, but the figures show strikingly irregular behavior. **The data from TMI Assembly NJ05YU will not be used due to flaws in the measured data.**

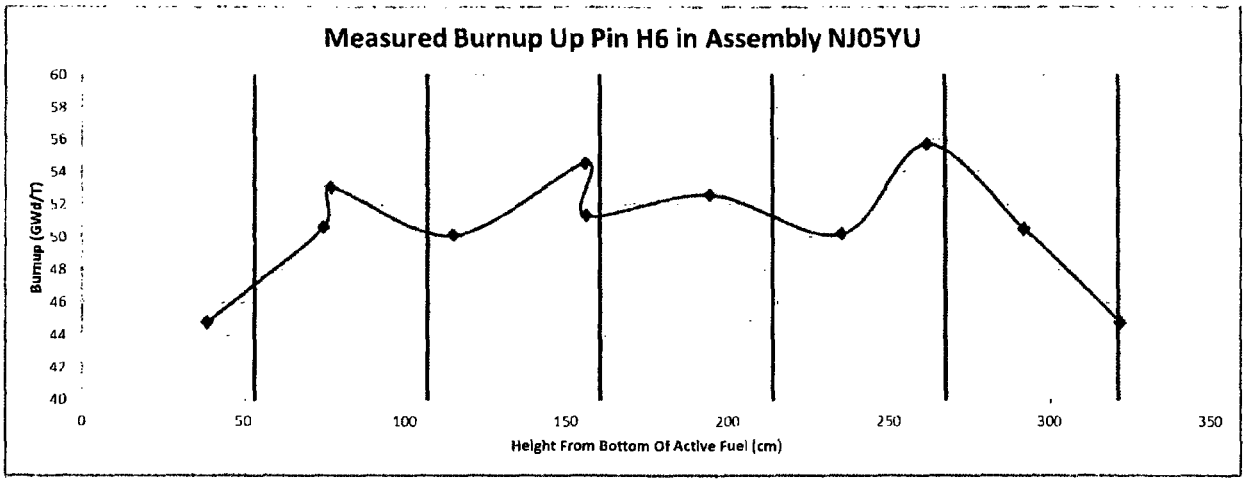

Figure A.4.3.1: Measured Burnup for Pin H6 in Assembly NJ05YU

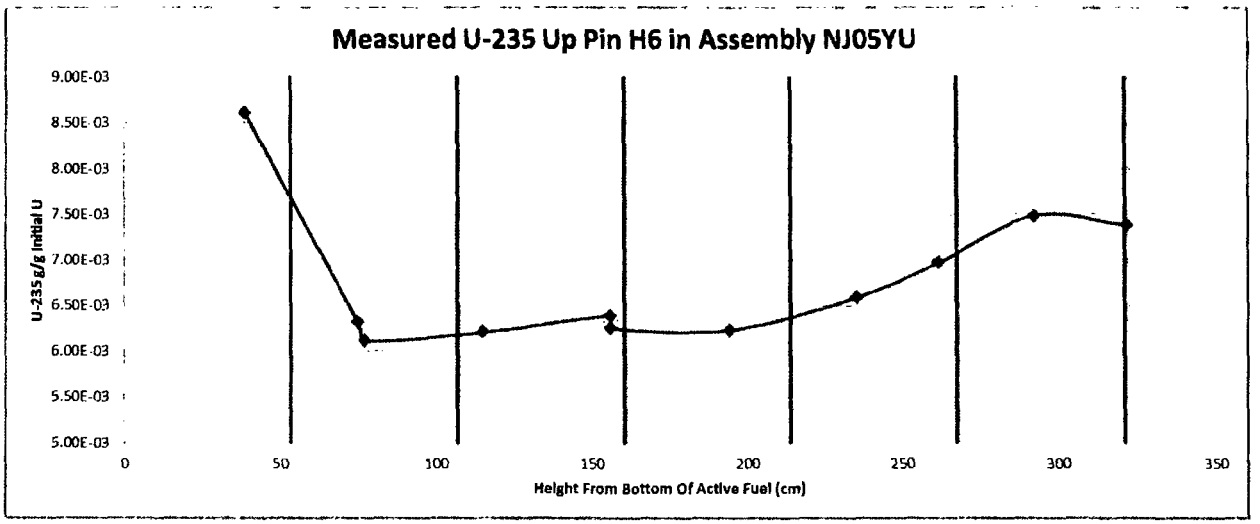

Figure A.4.3.2: Measured U-235 Content for Pin H6 in Assembly NJ05YU

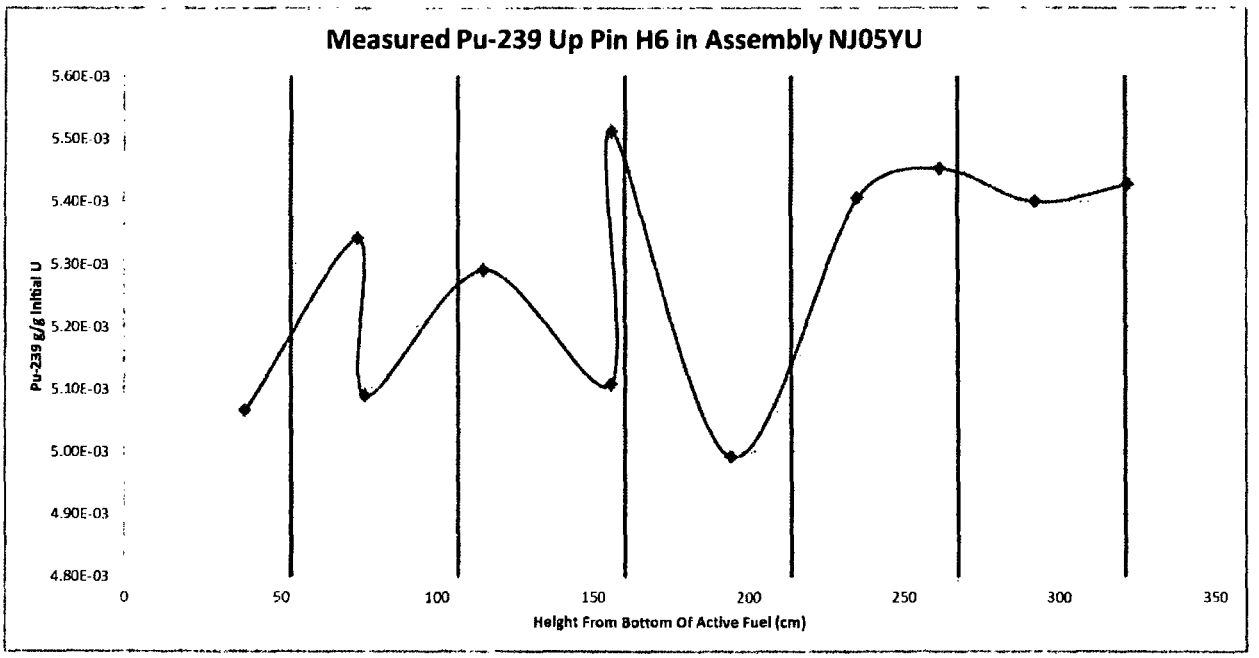

Figure A.4.3.3: Measured Pu-239 Content for Pin H6 in Assembly NJ05YU

The 8 chemical assays performed on the TMI assembly NJ070G were also reviewed for obvious errors in the experimental data. Figures A.4.3.4 through A.4.3.12 show the change in burnup, the change in U-235 content and the change in Pu-239 content going up assembly NJ070G for Pins O1, O12, and O13. An

inspection of the figures shows that the trend in burnup and U-235 content is basically the same for the three pins. However, the Pu-239 content of pin O1 does not follow the trend observed in the other two pins. The burnup at 197 cm from the bottom is significantly higher than at 39 cm (about 15% more), but the Pu-239 content of pin O1 only increases 2.6%. This is not expected and does not follow the increase observed in the other pins (about 9%). It is concluded from review of the data that there is a significant error in the Pu-239 content and this assay will not be used. (**TMI Assembly NJ070G pin O1 height 197.1 sample will not be used.**)

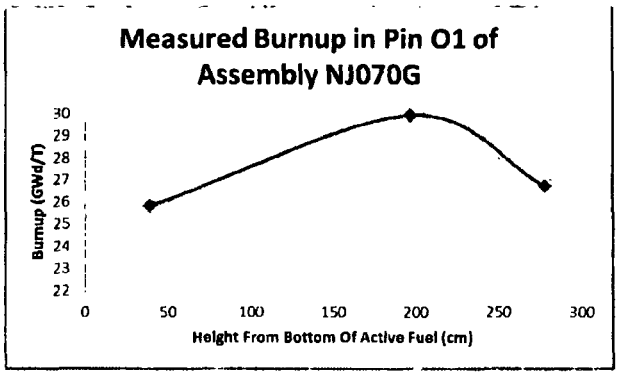

Figure A.4.3.4: Measured Burnup for Pin O1 in Assembly NJ070G

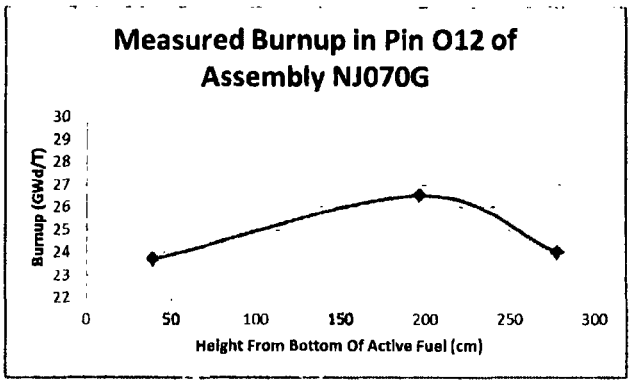

Figure A.4.3.5: Measured Burnup for Pin O12 in Assembly NJ070G

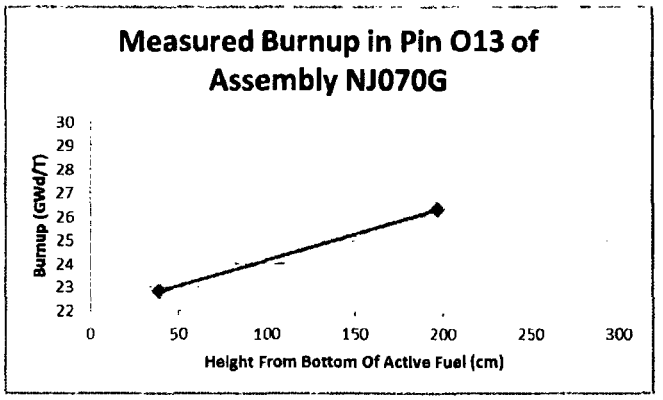

Figure A.4.3.6: Measured Burnup for Pin O13 in Assembly NJ070G

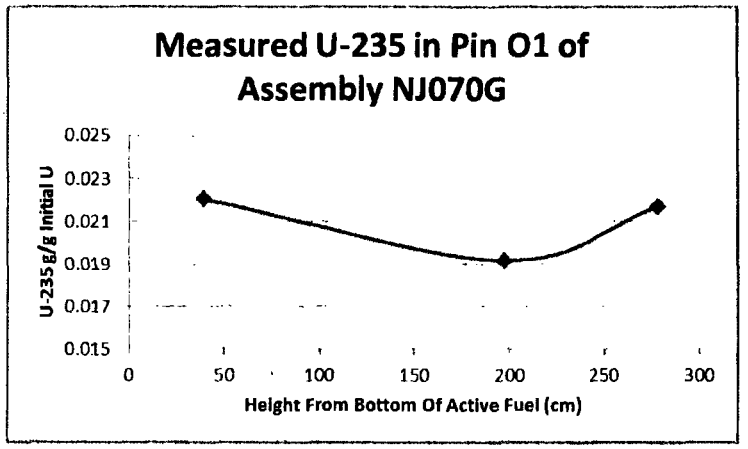

Figure A.4.3.7: Measured U-235 Content for Pin O1 in Assembly NJ070G

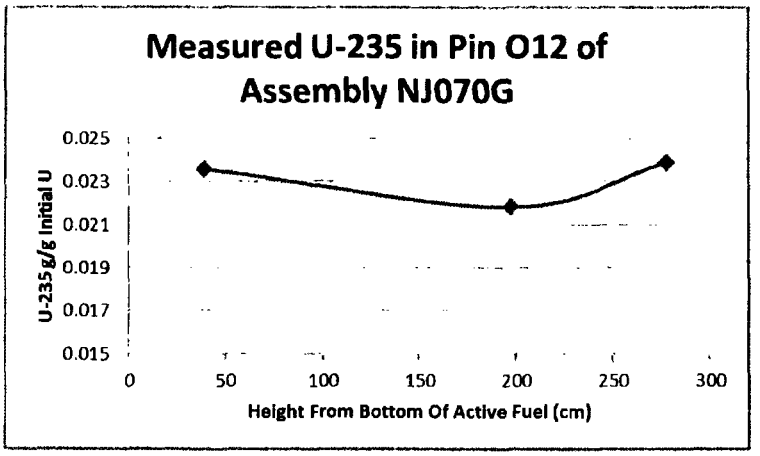

Figure A.4.3.8: Measured U-235 Content for Pin O12 in Assembly NJ070G

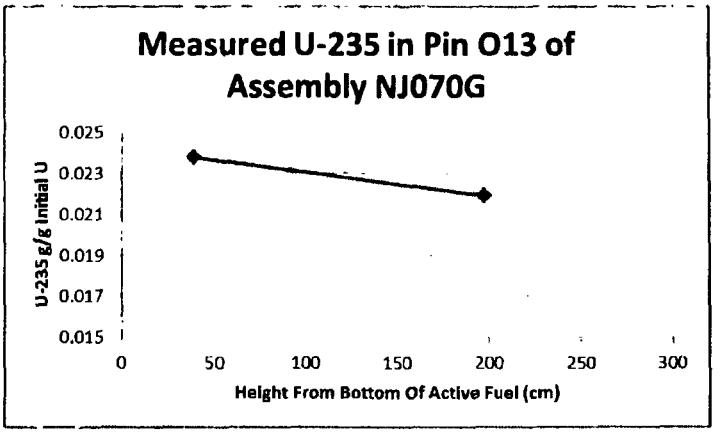

Figure A.4.3.9: Measured U-235 Content for Pin O13 in Assembly NJ070G

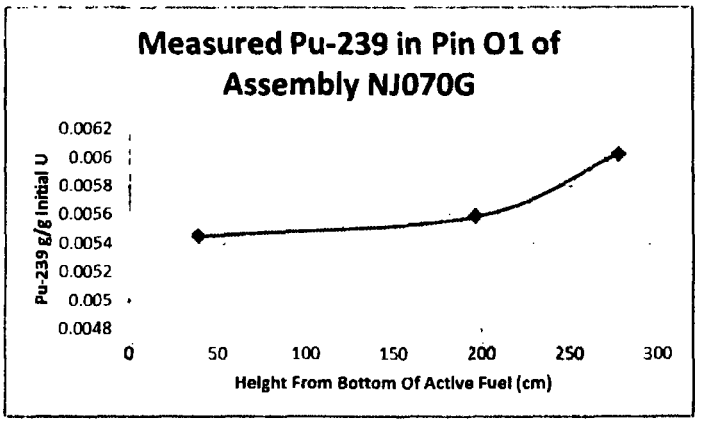

Figure A.4.3.10: Measured Pu-239 Content for Pin O1 in Assembly NJ070G

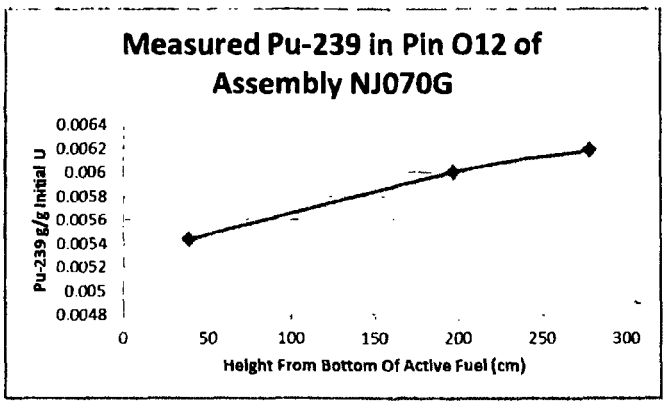

Figure A.4.3.11: Measured Pu-239 Content for Pin O12 in Assembly NJ070G

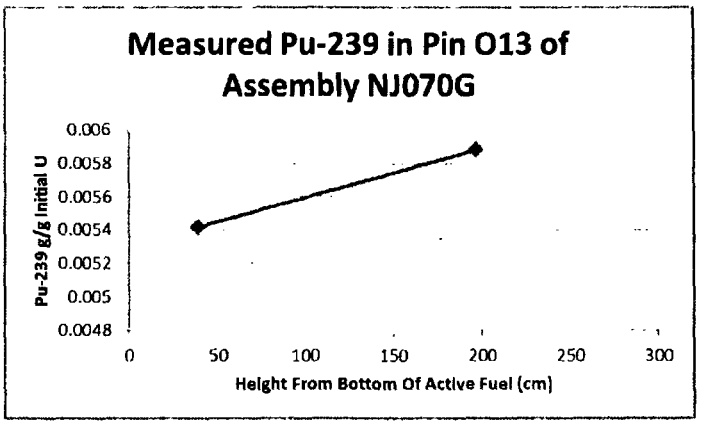

Figure A.4.3.12: Measured Pu-239 Content for Pin O13 in Assembly NJ070G

Sample N-9C-J for H. B. Robinson is eliminated since it is taken from under an Inconel grid. The strong thermal absorption of Inconel makes the 2D methods used to produce the correct assembly average reactivity inadequate for this sample.

The total set used for this analysis consists of 92 chemical assays from 10 different plants. Of these 92 samples, about 25 have significant fission products.

A.4.3.2 Analysis of the Chemical Assays

In general, the information for chemical assay analysis is taken from ORNL/TM-2010/44 [20] and NUREG/CR-7013 [23]. The computer decks for Reference 20 reports are on line at http://scale.ornl.gov/spent_fuel_isotopic_char_input.shtml. The computer decks for Reference 23 are in the report. The moderator temperatures, soluble boron concentrations, power densities, and fuel temperatures as a function of time used for this validation were obtained from the ORNL references [20,23].

For this analysis, KENO-V.a is used for the collapsing of the cross-sections to create the one-group cross-sections for depletion. The ORNL effort used NEWT. In general, the input needed for these two modeling approaches is similar; however, each input deck used in this analysis is different than that produced by ORNL due to the KENO/NEWT change. One other change from the ORNL decks is related to the burnup step sizes. Historically, the industry uses a small step (0.15 GWd/T) for getting equilibrium Xe in the model. The 0.15 GWd/T step is used for this analysis and production runs. Steps used are: 0.15, 0.35, .5, .5, .5, 1, 1, 1, 1, 1, 1, 1, 1, 1, and 2 GWd/T for all burnups thereafter. This step size will be used for all chemical assays to match the production runs. Some variations in these steps for the chemical assays have been taken to match the down times.

The following sections discuss each chemical assay set.

A.4.3.2.1 TRINO VERCELLESE

The original references for Trino have been reviewed to check the ORNL modeling. Reference 24 gives the assembly drawing reproduced in ORNL reports. References 25 and 26 provide details on the one cycle and two cycle irradiation experiments, respectively. Unfortunately, information is missing relating to the assembly design and pitch.

First, the reports state that there is an empty location in the assembly center for the instrumentation tube. No information is given about the instrumentation tube and the drawings suggest it is removed during operation. This is a Westinghouse designed plant and US Westinghouse plants have a tube in the center of the assembly for the instrumentation to traverse. ORNL modeled the hole as empty (no tube) and that modeling is followed in this analysis.

Second, the assembly drawing provides little detail on the can around the assemblies. The ORNL model includes a 0.6 mm stainless steel can inside the standard fuel pin pitch. There is insufficient information to support the positioning of the can, so for the modeling in this analysis, the can is placed outside the standard pin pitch. The ORNL model sets up the separate pitch for the cruciform fuel followers. For this analysis, the cruciform fuel pins are accurately modeled, but the pin pitch is maintained to be the same as the pin pitch for the non-cruciform pins. This creates a full empty pin cell at the ends of the cruciform pins rather than the partial empty cell created by the more accurate ORNL model. Both models have the same fuel, clad and water volumes. Since the sampled pins are *not* next to the cruciform fuel followers, this model simplification is appropriate. There is no information on a can surrounding the cruciform fuel followers. ORNL's model contains a can and models the can around the fuel assembly to follow the irregular boundary. In the model used for this analysis, the can is a simple square around the entire model. The can modeling is not accurate for either ORNL or this effort. The can is perforated. The amount of perforation is not given. Figure 3 of Reference 25 shows a picture of the assembly. From this picture it is assumed that 50% of the steel is removed. ORNL assumed the can was not perforated. This analysis assumes 50% steel and 50% water. The water has soluble boron of varying concentrations, and rather than create a can mixture with 50% water, the thickness of the steel is reduced from 0.6 mm to 0.3 mm.

Third, the assembly separation is not given. Tables in the references give the assembly "side of square cross-section" as 20 cm. This was assumed by ORNL as the assembly pitch. The assembly drawing may suggest an assembly pitch of 20.1 cm. This analysis uses the same 20 cm selected by ORNL.

The ORNL model includes an empty cell with water at the corner opposite from the main cruciform fuel followers. This is incorrect. That corner should have a fuel follower pin. That error is corrected for this analysis.

ORNL did not use all the chemical assay data available from Trino. The pins from the corner were not included. The references report these pins as "perturbed spectrum." However, these corner pins are at the corner away from the cruciform followers and may actually not have much of a "perturbed spectrum." Since the data on assembly separation is weak, these pins are also ignored for this work.

There are 31 chemical assays that are used from the Trino data. They come from three assemblies that were in the Trino core for one cycle and one assembly that was in the core two cycles.

ORNL used reflective boundary conditions. The assemblies are only symmetric on the diagonal, so neither reflective nor periodic boundary conditions match the actual assembly. This work uses periodic boundary conditions, since the cruciform fuel rod assemblies are one row thick. A reflective boundary

condition makes them effectively 2 rows thick. The periodic boundary condition is not precise, since the cruciform rods are on different halves of the assembly, but this error is less significant than doubling up the thickness.

One assembly, 509-104, was on the edge of the core. ORNL modeled this assembly with the reflector. ORNL points out in Reference 20 that since the sampled pin is 11 rows from the periphery, "the core periphery has negligible effects on the measured rod." For this analysis the reflector is not modeled. Further, the cut out section of this assembly actually has a stainless steel filler. No details for this filler were found in the references but ORNL has assumed it is rods. For this work, the filler is assumed to be the standard cruciform fuel rods, since the sampled rod is closer to a standard cruciform fuel insert. In fact, the pin location has been adjusted in this model to preserve the distance from the cruciform fuel inserts.

The ORNL fuel densities were confirmed using the original references. The footnotes in Reference 20, Table 49 are confusing, but the final values for the densities are the same as independently confirmed. The fuel density in the cruciform rods seems low, because no pellet diameter was known, so it was assumed that the pellet extended to the clad ID (no gap). The clad ID was an assumed value based on the control rod clad thickness (see Reference 20).

Note that the ORNL deck for assembly 509-032, pin E11, Plane 7, has an error in the fuel temperatures. The impact of that error is expected to be small, but was corrected for this analysis.

Table A.4.3.1 shows the percent deviation between the predicted and measured content of the measured isotopes for all the Trino samples.

Table A.4.3.1: Trino Predicted Minus Measured % Deviations (Part 1 of 4)

Sample ID	104-M11P7	032-E11P1	032-E11P4	032-E11P7	032-E11P9	032-H9P4	032-H9P7	032-H9P9
Enrichment	**3.897**	**3.13**	**3.13**	**3.13**	**3.13**	**3.13**	**3.13**	**3.13**
Burnup	**12.04**	**7.24**	**15.38**	**15.9**	**11.53**	**16.56**	**17.45**	**12.37**
U-234		15.20	-6.64	34.67			28.95	27.29
U-235	1.15	2.73	3.20	4.80	1.28	0.98	-0.44	3.84
U-236								
U-238	0.07	0.03	0.02	0.00	-0.02	0.03	0.02	1.26
Pu-238								
Pu-239	-1.94	-3.27	1.44	2.45	0.41	1.74	0.71	-1.30
Pu-240	-6.00	-7.60	-1.14	0.85	-1.42	-1.06	-0.23	-2.45
Pu-241	-10.33	-17.91	-3.46	-0.65	-7.97	-6.27	-2.39	-8.93
Pu-242	-17.07	-36.69	-5.98	-9.70	-8.67	-9.24	0.79	

Table A.4.3.1: Trino Predicted Minus Measured % Deviations (Part 2 of 4)

Sample ID	049-J8P1	049-J8P4	049-J8P7	049-J8P9	049-L5P1	049-L5P4	049-L5P9	069-E11P1
Enrichment	**2.719**	**2.719**	**2.719**	**2.719**	**2.719**	**2.719**	**2.719**	**3.13**
Burnup	**8.71**	**14.77**	**15.49**	**11.13**	**14.16**	**14.49**	**10.18**	**12.86**
U-234	33.76	29.39			38.05	23.15	23.40	
U-235	1.76	5.42	3.34	2.03	-0.29	0.83	1.87	0.57
U-236								-5.52

U-238	0.00	0.00	0.07	0.01	0.02	0.01	0.03	-0.11
Pu-238								-6.75
Pu-239	3.84	4.38	1.23	1.96	0.71	2.52	0.87	6.03
Pu-240	5.45	-0.85	-2.98	-1.74	0.70	0.16	-1.98	7.03
Pu-241	2.17	-5.46	-6.34	-5.90	-3.36	-3.63	-9.11	4.90
Pu-242	3.33	-13.54	-12.06	-10.26	-5.22	-3.81	-10.72	2.72

Table A.4.3.1: Trino Predicted Minus Measured % Deviations (Part 3 of 4)

Sample ID	069-E11P2	069-E11P4	069-E11P5	069-E11P7	069-E11P8	069-E11P9	069-E5P4	069-E5P7
Enrichment	**3.13**	**3.13**	**3.13**	**3.13**	**3.13**	**3.13**	**3.13**	**3.13**
Burnup	**20.6**	**23.72**	**24.52**	**24.3**	**23.41**	**19.25**	**23.87**	**24.68**
U-234								
U-235	2.84	5.00	3.40	2.87	3.80	2.21	1.12	2.91
U-236	-5.46	-6.32	-4.61	-5.73	-6.35	-7.26	-3.54	-2.31
U-238	-0.09	-0.12	-0.10	-0.13	-0.09	-0.12	-0.10	-0.05
Pu-238	-11.01	-11.16	-12.51	-16.12	-29.21	-18.37	-18.46	-12.34
Pu-239	6.20	9.14	7.11	4.94	5.96	2.11	8.20	6.64
Pu-240	3.77	3.66	2.73	1.01	3.34	1.50	4.19	4.15
Pu-241	-0.94	2.01	6.57	0.51	-3.07	-2.88	0.91	1.72
Pu-242	-4.87	-6.51	2.89	-8.20	-7.37	-10.18	-4.16	-3.99

Table A.4.3.1: Trino Predicted Minus Measured % Deviations (Part 4 of 4)

Sample ID	069-E5P9	069-J9P4	069-J9P7	069-L11P4	069-L11P7	069-L5P4	069-L5P7
Enrichment	**3.13**	**3.13**	**3.13**	**3.13**	**3.13**	**3.13**	**3.13**
Burnup	**19.21**	**24.85**	**25.26**	**23.93**	**24.36**	**24.33**	**24.31**
U-234							
U-235	1.32	3.09	2.59	1.56	3.37	-1.05	3.11
U-236	-8.57	-4.51	-4.81	-10.22	-0.39	-1.08	-3.63
U-238	-0.05	-0.01	-0.10	-0.03	-0.02	-0.10	0.09
Pu-238	-9.46	-14.17	-27.13	-6.07	-15.41	-6.07	-13.50
Pu-239	8.15	7.26	6.57	6.05	6.24	6.63	6.57
Pu-240	4.15	4.63	1.89	1.97	1.16	5.38	1.47
Pu-241	6.79	0.94	2.29	1.45	2.37	2.39	1.11
Pu-242	1.26	-6.08	-6.86	-5.67	-7.91	-0.45	-3.78

The Trino analysis shows an over-prediction of the Pu-239 and U-235 content. This implies that predicted k's after depletion are conservative. This is the same direction as seen by the EPRI benchmarks, but larger in magnitude. The direct difference section (A.4.3.3) that follows will show the impact on k (see Table A.4.3.12).

A.4.3.2.2 OBRIGHEIM

For the analysis of the Obrigheim chemical assays, the ORNL decks were checked and then used with the following modifications:

1. The geometric model was changed from NEWT to KENO V.a modeling. (This is a change only in input format. There was no change in input parameters, such as materials or dimensions.)
2. The time steps were changed to match the smaller time steps used in the first cycle and the number of libraries in the following cycles was changed to be less than 2 GWd/T between libraries. (Burnup in GWd/T divided by 2, truncated, then plus 1).

Table A.4.3.2 shows the percent deviation between the predicted and measured content of the measured isotopes for all the Obrigheim samples.

Table A.4.3.2: Obrigheim Predicted Minus Measured % Deviations (Part 1 of 2)

Sample ID	BE124-E3P1	BE124-E3P2	BE124-E3P3	BE124-E3P4	BE124-E3P5	BE124-G7P1	BE124-G7P2	BE124-G7P3
Enrichment	**3**	**3**	**3**	**3**	**3**	**3**	**3**	**3**
Burnup	**20.18**	**29.35**	**36.26**	**30.92**	**22.86**	**17.13**	**25.83**	**31.32**
U-235	-1.12	-5.16	-5.70	1.29	-3.93	-2.83	-7.77	3.98
U-236	7.87	-1.31	-2.78	-2.18	-10.39	-5.96	-10.23	-4.27
U-238	-0.11	0.71	-0.09	-0.04	0.00	-0.01	-0.01	-0.07
Pu-239	-9.55	-16.57	-13.63	-6.14	-14.02	-10.42	-8.80	-22.89
Pu-240	4.50	6.18	8.73	5.19	3.73	4.97	8.73	8.98
Pu-241	3.07	4.29	3.50	-0.55	3.07	3.27	4.22	0.68
Pu-242	9.98	6.21	8.25	2.54	2.30	2.49	5.42	4.70
Am-241	9.79	4.53	2.49	-3.47	5.09	0.75	4.29	-6.29
Cm-244	-22.44		-5.48	-41.00	-30.68	-16.61	-21.17	-34.55

Table A.4.3.2: Obrigheim Predicted Minus Measured % Deviations (Part 2 of 2)

Sample ID	BE124-G7P4	BE124-G7P5	BE168	BE170	BE171	BE172	BE176
Enrichment	**3**	**3**	**3.13**	**3.13**	**3.13**	**3.13**	**3.13**
Burnup	**27.71**	**25.81**	**29.35**	**27.01**	**28.74**	**27.89**	**28.78**
U-235	-6.64	2.24	-1.81	-1.74	-1.74	-0.23	-0.73
U-236	-12.42	-3.35	0.91	0.48	1.03	1.44	0.89
U-238	0.00	0.00	-0.03	-0.03	-0.04	-0.08	-0.05
Pu-239	-16.17	-1.68	-18.23	-7.15	-7.57	-3.59	-10.48
Pu-240	6.73	5.48	3.06	4.30	4.28	5.01	4.14
Pu-241	1.69	-0.44	1.84	2.46	3.89	4.07	3.05
Pu-242	2.34	0.40	-1.61	-1.36	0.02	1.45	-1.28
Am-241	-3.76	-7.73	-14.75	-12.30	-9.80	-12.13	-13.35
Cm-244	-35.48		-34.67	-43.81	-33.44	-43.49	-31.23

A.4.3.2.3 TURKEY POINT UNIT 3

Although full details of the operating history of the two assemblies is available through Turkey Point, rather than use potentially proprietary data, only the data documented by ORNL in Reference 20 is used. The ORNL input decks are used to initiate the analysis and only the same two changes noted for Obrigheim are made.

Table A.4.3.3 shows the percent deviation between the predicted and measured content of the measured isotopes for all the Turkey Point samples.

Table A.4.3.3: Turkey Point Predicted Minus Measured % Deviations

Sample ID	D01-G10	D01-G9	D01-H9	D04-G10	D04-G9
Enrichment	**2.556**	**2.556**	**2.556**	**2.556**	**2.556**
Burnup	**30.51**	**30.72**	**31.56**	**31.31**	**31.26**
U-234	4.86	4.32	9.71	3.40	17.24
U-235	2.56	-1.87	-2.79	-1.61	1.47
U-236	2.84	3.09	6.25	3.82	6.51
U-238	-0.17	-0.16	-0.14	-0.17	-0.18
Pu-238	-5.79	-4.31	-5.34	-1.58	-2.61
Pu-239	4.24	4.90	2.16	5.74	2.51
Pu-240	2.48	3.71	4.38	5.70	3.26
Pu-241	1.30	2.28	0.44	2.93	-1.45
Pu-242	-2.24	3.15	1.66	3.03	-0.37

A.4.3.2.4 H. B. ROBINSON UNIT 2

The data from Reference 20 is used for the modeling. The ORNL decks were used to initiate the analysis. The geometric modeling was converted from NEWT to KENO-V.a format and the time steps were changed to the same step sizes used for all the analyses.

Notes:

1. Reference 20, Table 63 has the fuel temperatures for N-9C-D under the column for N-9C-J and vice versa. The input decks are correct.
2. Sample N-9C-J was taken from under the Inconel grid [27]. Inconel is a strong absorber resulting in a significant reduction of the thermal flux. This clearly challenges the 2D methods. This sample is eliminated.

Table A.4.3.4 shows the percent deviation between the predicted and measured content of the measured isotopes for all the H. B. Robinson samples.

Table A.4.3.4: H. B. Robinson Predicted Minus Measured % Deviations

Sample ID	B05-N9BN	B05-N9BS	B05-N9CD
Enrichment	**2.561**	**2.561**	**2.561**
Burnup	**23.81**	**16.02**	**31.66**
U-234	1.71	1.35	11.31
U-235	0.84	0.92	3.40
U-236	-2.78	-2.85	-0.66
U-238	-0.59	0.18	-0.72
Np-237	-13.05	-11.77	-0.95
Pu-238	-19.19	-17.65	-15.36
Pu-239	2.71	2.76	5.31
Pu-240	1.75	2.71	3.18
Pu-241	-2.67	-2.88	1.46
Pu-242	-4.87	-2.76	-3.01
Tc-99	10.93	13.80	13.24
Nd-143	6.77	4.87	10.03
Nd-145	3.49	3.16	6.42

A.4.3.2.5 CALVERT CLIFFS UNIT 1

The modeling of the Calvert Cliff chemical assays starts with the ORNL input decks and Reference 20. Once again, the NEWT model was converted to a KENO V.a model. The large guide tubes, which are not adjacent to the sample, were homogenized with the water in the cell. This allowed for each unit to be the same area (the pin pitch squared). The homogenization preserved the mass of the water and the tube. Thus, for assemblies D101 and D047, the guide tubes in the model are homogenized and for assembly BT03, the central guide tube is modeled with the actual geometry and the other guide tubes are modeled as homogenized.

The soluble boron letdown data was copied from the ORNL decks as was the fuel temperature change with cycles.

Notes:

1. Table 71 in Reference 20 does not come from the referenced source but was instead found to correspond to Table 3.3 in Reference 34.
2. Reference 20, Table 74 values for cumulative burnup (except final burnup) have an unknown source. Attempting to reproduce these values using Table 71 results in the sample burnups as given in References 22 and 28. The specific powers in the ORNL input decks do not match Table 74. For MKP109, the total burnup in the ORNL input decks is too low by from about 0.5% to 1%. The specific powers from Reference 22 with a small adjustment for historical round-off are used in this analysis for MKP109.
3. Reference 20 and the ORNL input decks remove the BPs at the end of cycle 1. CE BPs are not removable. BT03 is a test assembly, so it is possible to remove the BPs but this was not done. The ORNL decks for BT03 used two separate runs due to the BP mistake. This effort uses a single input deck. The soluble boron and temperature adjustment table from the second ORNL decks were used, but the cycle 1 time of 811 was added to each entry. Reference 20 states that the specific power should be calculated by taking the values in Reference 20, Table 74 and divide

them by the duration days. This was not followed by the ORNL input decks and the ORNL decks have some burnup errors. For this analysis, the specific power was calculated by the Table 74 burnups divided by the duration days. The cumulative burnups on Table 74 match the cumulative burnups in References 22 and 28.

Table A.4.3.5 shows the percent deviation between the predicted and measured content of the measured isotopes for all the Calvert Cliffs samples.

Table A.4.3.5: Calvert Cliffs Predicted Minus Measured % Deviations (Part 1 of 2)

Sample ID	D101-MLA098-BB	D101-MLA098-JJ	D101-MLA098-P
Enrichment	**2.72**	**2.72**	**2.72**
Burnup	**26.62**	**18.68**	**33.17**
U-234	13.32	11.31	4.86
U-235	0.98	1.01	6.13
U-236	-2.61	-3.16	-2.84
U-238	-1.77	-1.22	-1.04
Np-237	-9.50	-0.80	4.20
Pu-238	-14.31	-27.88	-8.63
Pu-239	3.92	2.16	9.28
Pu-240	2.90	0.58	4.02
Pu-241	-3.10	-5.72	3.07
Pu-242	-6.99	-8.29	-8.15
Am-241	-1.31	-3.73	1.91
Tc-99	6.13	2.16	6.37

Table A.4.3.5: Calvert Cliffs Predicted Minus Measured % Deviations (Part 2 of 2)

Sample ID	BT03-NBD107-GG	BT03-NBD107-MM	BT03-NBD107-Q	D047-MKP109-CC	D047-MKP109-LL	D047-MKP109-P
Enrichment	**2.453**	**2.453**	**2.453**	**3.038**	**3.038**	**3.038**
Burnup	**37.27**	**31.4**	**46.46**	**37.12**	**27.35**	**44.34**
U-234	-17.60	-29.80	21.35	-2.75	-1.40	1.39
U-235	-7.62	-3.31	-0.26	-0.87	-1.16	2.31
U-236	-0.84	1.11	0.10	2.42	2.05	2.08
U-238	-1.28	-0.77	-0.26	-0.38	-0.67	-0.19
Np-237	8.89	12.34	14.18	11.73	5.45	4.07
Pu-238	-13.18	-13.10	-14.31	-8.50	-8.71	-7.80
Pu-239	-0.70	-0.71	3.36	5.01	3.62	7.82
Pu-240	1.25	0.31	1.88	3.66	2.47	4.52
Pu-241	-5.76	-6.70	-1.21	0.36	0.85	2.52
Pu-242	-7.32	-7.53	-8.71	-2.61	-1.53	-5.00
Am-241	-13.38	-5.82	-59.56	-4.01	-0.20	-1.63
Tc-99	32.08	32.59	30.62	8.07	6.03	12.83
Rh-103	-29.50					
Cs-133				1.42	0.96	2.27
Nd-143	-0.84			1.47	1.19	2.88
Nd-145	-2.71			-1.63	-0.73	-1.94
Sm-147	3.18			4.71	6.63	-3.73
Sm-149	-31.28					
Sm-150	2.55			7.38	7.19	3.57
Sm-151	-8.24			-1.01	12.33	-3.64
Sm-152	2.51			7.67	7.76	-1.43
Eu-153	-6.67			3.23	7.91	0.43
Eu-155	-11.29			5.53	5.13	3.29
Gd-155	20.62			7.68	-30.59	2.93

A.4.3.2.6 TAKAHAMA UNIT 3

There were 16 chemical assays taken from three pins (two from assembly NT3G23 and one from NT3G24). For each pin, a sample was taken so close to the top of the fuel that 2D analysis does not correctly pick up the spectrum. ORNL eliminated these samples in Reference 19 and they are also eliminated for this effort. ORNL in Reference 19 referred to the eliminated samples as "near the extreme ends of the fuel rods (< 20 cm)." This is misleading (but correct). The 20 cm includes the top plenum. A more useful description is that they are < 6 cm from the top of the active fuel (actually, 5.4, 2.9 and 1.6 cm from the top of the active fuel). One of the sampled pins is one of the corner pins of the assembly. This pin is not typical of the average of the pins in the assembly. For example, the average pin pitch used for resonance treatment is not correct. Further, that pin is adjacent to pins with a different burnup and may have a different enrichment. There is no information available on the adjacent assemblies. Normally, this pin would be rejected, but since there are only a limited number of chemical assays that include fission products, this pin is used in this analysis.

For the corner pin, the assembly pitch is very important. Reference 20 gives the assembly pitch as 21.4 cm. Takahama 3 is a MHI 3 loop plant. MHI was a Westinghouse licensee and it is expected that MHI did not change the core design. The Westinghouse 3 and 4 loop plant assembly pitch is 21.5036 cm (see Turkey Point and HB Robinson). This slightly larger pitch is used in the analysis. The ORNL decks used 21.42 cm for the assembly pitch. No reference for this value was found. The pin pitch is given in Reference 20 as 1.259 cm but 1.26 cm is used in the ORNL input decks. This analysis uses 1.26 cm for the pin pitch, which is consistent with the ORNL input decks.

The pin pitch used for the resonance self-shielding for the corner pin and side pins is adjusted to include the assembly gap. The effective pin pitch is defined as the pin pitch derived by averaging the pitch to the four closest pins.

The fuel temperature data is not provided in the references. The ORNL decks use an approximate value of 900° K for all samples. Clearly, there should be a burnup dependent value, but none was used by ORNL and this analysis also uses 900° K for all samples.

The depletion analysis for the ORNL decks used the power option for all depleting material. It is not clear whether the flux option should be used for the Gd pins, but since the fission power dominates over the absorption power, the inputs for this analysis uses the power option as ORNL did.

The specific powers in the ORNL decks did not agree with Reference 20, Table 77, but the differences, though small, can be as much as 1%. This analysis uses the specific powers from Reference 20, Table 77 for all but the last cycle. For the last cycle, the specific power is forced to match the sample burnup. The adjustments needed for matching the burnup were small (less than 0.1%).

Tables A.4.3.6 and A.4.3.7 show the percent deviation between the predicted and measured content of the measured isotopes for all the Takahama samples.

Table A.4.3.6: Takahama SF95 and SF96 Predicted Minus Measured % Deviations

Sample ID	NT3G23-SF95-2	NT3G23-SF95-3	NT3G23-SF95-4	NT3G23-SF95-5	NT3G23-SF96-2	NT3G23-SF96-3	NT3G23-SF96-4	NT3G23-.SF96-5
Enrichment	**4.11**	**4.11**	**4.11**	**4.11**	**2.63**	**2.63**	**2.63**	**2.63**
Burnup	**24.46**	**35.68**	**37.01**	**30.45**	**17.43**	**29.69**	**30.41**	**25.42**
U-234	-0.19	22.08	21.11	-7.33	-2.88	-3.15	-3.37	-3.01
U-235	2.52	2.63	3.29	1.70	5.06	7.21	8.12	5.68
U-236	-2.45	-0.46	-0.56	-1.54	-7.01	-3.96	-4.25	-4.33
U-238	-0.10	-0.10	-0.14	-0.07	0.02	0.06	0.07	0.04
Np-237					25.00	35.07	32.25	29.45
Pu-238	-11.83	-2.97	-2.86	-5.69	-20.48	-18.63	-23.36	-16.08
Pu-239	7.10	8.28	7.44	7.88	4.53	4.73	3.82	4.57
Pu-240	3.12	7.23	6.32	6.42	0.03	1.09	0.44	2.74
Pu-241	-0.55	-1.48	1.22	0.84	-4.51	-1.87	-3.01	-1.38
Pu-242	-5.52	-5.64	-4.43	-1.57	-12.50	-10.78	-12.21	-7.51
Am-241	20.41	21.08	43.10	17.78	29.44	23.99	14.44	32.25
Am-243	8.33	9.53	12.03	10.16	-3.11	0.54	-3.79	2.02
Cm-242	-41.01	-55.63	-77.36	-18.98	-35.76	-30.33	-32.83	-26.56
Cm-244	-8.77	-0.02	-0.38	3.02	-25.73	-18.50	-24.14	-14.32
Nd-143	-1.32	-1.47	-0.62	-0.79	-6.47	-4.64	-3.86	-5.70
Nd-145	-0.79	-1.28	-0.74	-0.39	-5.73	-4.65	-4.05	-4.96

Table A.4.3.7: Takaham SF97 Predicted Minus Measured % Deviations

Sample ID	NT3G24-SF97-2	NT3G24-SF97-3	NT3G24-SF97-4	NT3G24-SF97-5	NT3G24-SF97-6
Enrichment	**4.11**	**4.11**	**4.11**	**4.11**	**4.11**
Burnup	**30.48**	**42.1**	**47.07**	**47.26**	**40.85**
U-234	9.34	6.86	6.42	6.68	8.02
U-235	0.77	1.64	2.12	0.71	2.12
U-236	-0.57	-0.16	-0.31	-0.19	-0.82
U-238	-0.09	-0.06	-0.03	0.03	-0.08
Np-237	0.23	1.32	-0.58	-3.66	-2.45
Pu-238	-9.27	-12.07	-14.70	-17.30	-10.93
Pu-239	5.03	5.48	5.05	2.89	6.44
Pu-240	7.06	9.07	8.05	6.95	7.72
Pu-241	-1.58	-1.38	-1.50	-3.53	0.27
Pu-242	-2.59	-5.22	-5.92	-5.89	-3.82
Am-241	3.30	2.75	1.00	-1.27	4.64
Am-243	7.45	5.35	3.01	0.88	6.95
Cm-242	1.83	7.96	12.22	16.17	8.96
Cm-244	-4.44	-6.79	-9.95	-14.50	-3.27
Nd-143	1.83	1.83	2.37	1.56	1.98
Nd-145	0.64	-0.05	0.08	-0.01	-0.11
Sm-147	4.16	3.61	2.80	3.07	3.71
Sm-149	-11.85	-8.09	0.13	0.13	-7.83
Sm-150	2.79	1.75	1.22	0.48	2.88
Sm-151	-2.52	-3.01	-4.73	-8.09	-0.86
Sm-152	4.34	3.21	2.67	2.73	3.00

A.4.3.2.7 TMI UNIT 1

As described in Section A.4.3.1, all the samples analyzed by ANL are not included due to some problem in the chemical assay process that produced noticeable errors. For assembly NJ070G, data was used for 7 of the 8 samples. The sample O1S2 showed errors noted in Section A.4.3.1.

This analysis utilized the input decks from ORNL, while making the model changes noted previously for the other chemical assays from the other reactors. The following errors were found in the ORNL decks and were corrected for this analysis:

1. The BPs should be depleted with a constant flux. The ORNL decks used power rather than the constant flux option. That is corrected for this validation.
2. For the pin O1 samples, an adjacent assembly was burned for one cycle. In the ORNL burnup analysis for the adjacent assembly, the BPs were not depleted at all. This was changed to a constant flux depletion.
3. For the O1 samples, the 4.75 wt% adjacent assembly had Gd pins. These pins were modeled by ORNL as having 4.75 wt% U-235. The actual wt% was 4.19 wt% [29]. This was corrected.

4. Although not an error, the Gd pins were modeled by ORNL as a single cylinder. Due to the onion ring depletion nature of Gd, for this analysis the Gd pins are modeled as three concentric rings each of one third the area of the fuel pin.

Table A.4.3.8 shows the percent deviation between the predicted and measured content of the measured isotopes for all the TMI samples.

Table A.4.3.8: TMI Predicted Minus Measured % Deviations

Sample ID	NJ070G-O12S4	NJ070G-O12S5	NJ070G-O12S6	NJ070G-O13S7	NJ070G-O13S8
Enrichment	**4.657**	**4.657**	**4.657**	**4.657**	**4.657**
Burnup	**23.54**	**26.26**	**24.09**	**23.21**	**26.1**
U-234	0.19	2.38	1.12	-1.33	0.86
U-235	3.23	3.58	2.09	4.97	3.72
U-236	-4.20	-3.32	-4.99	-4.86	-2.94
U-238	-0.06	-0.06	0.05	-0.03	-0.06
Np-237	-9.23	-4.56	-11.22	-7.96	-6.24
Pu-238	-20.17	-22.21	-34.36	-27.98	-24.13
Pu-239	4.39	2.88	-2.22	3.08	4.32
Pu-240	0.78	-1.45	-4.39	-2.83	-0.11
Pu-241	-3.22	-5.76	-10.63	-7.72	-5.88
Pu-242	-13.17	-14.50	-18.50	-21.85	-15.04
Am-241	-6.67	-2.94	11.85	-5.36	-2.22
Am-243	-1.50	-6.66	12.69	-12.06	-3.23
Cm-242	-30.63	-38.81	-18.09	-36.01	-47.11
Cm-244	-15.68	-23.28	-6.97	-30.97	-19.38
Nd-143	2.45	3.06	1.68	0.72	3.04
Nd-145	1.31	2.00	1.27	-0.67	1.76
Sm-147	-2.16	1.49	-0.65	-0.23	2.06
Sm-149	6.30	6.26	-0.91	6.76	6.34
Sm-150	-0.20	-0.52	-1.18	-2.29	-0.15
Sm-151	0.31	-2.31	-8.55	0.64	-2.92
Sm-152	3.08	3.60	5.22	1.38	3.92
Eu-151	-6.32	0.66	-14.44	3.73	0.73
Eu-153	-2.18	-1.37	-3.28	-4.10	-1.92
Gd-155	-18.63	-14.28	-31.95	-15.90	-16.30

A.4.3.2.8 GÖSGEN: ARIANE PROGRAM

The ORNL input decks from Reference 20 were correct. The only modifications needed were related to changing from NEWT to KENO V.a. The ORNL analysis used separate input decks and collected data via files to put together the final analysis. For this work, the input decks were stacked as a single run.

Sample G4 is only 7.42 cm from the bottom of the active fuel. This sample is the closest to the end of the active fuel of any samples used. The Takahama sample that was 5.4 cm from the end was not used due to 3D effects. It is not clear how much the end of the fuel affects this sample. Even though this sample is near the end of the fuel, the 2D analysis of this sample is included in the validation.

The measured values for all the chemical assays were taken from NUREG/CR-7108 [19]. An error in Table C.1 of NUREG/CR-7108 was found for the U3 sample. The error is in the cooling time used for some of the isotopes in the sample. Table C.1 was to adjust the isotopic content to the cooling time, but several of the isotopes had zero cooling time for Sample U3 in Table C.1. Reference 20, Table 42 identified isotopes which were at zero cooling time by using italics. These isotopes were not adjusted when put into NUREG/CR-7108, Table C.1. Confirmation of this was not straightforward, since Reference 30 did not have the decay time correct. The primary reference is Reference 31 and by using that reference, it was possible to confirm the cooling time error.

Table A.4.3.9 shows the percent deviation between the predicted and measured content of the measured isotopes for all the Gösgen samples.

Table A.4.3.9: Gösgen and GKN Predicted Minus Measured % Deviations

Sample ID	Gösgen 1240-GU1	Gösgen 1701-GU3	Gösgen 1701-GU4	GKN 419-M11
Enrichment	**3.5**	**4.1**	**4.1**	**3.8**
Burnup	**60.7**	**53.2**	**31.1**	**54**
U-234	14.72	29.63	31.17	17.21
U-235	7.94	1.88	3.18	6.43
U-236	1.22	3.46	1.74	-0.40
U-238	-0.36	2.39	1.64	-0.34
Np-237		-9.56	-37.11	18.38
Pu-238	-6.40	-4.07	-4.10	-12.32
Pu-239	7.15	6.02	7.62	9.72
Pu-240	3.81	8.06	5.20	6.09
Pu-241	3.93	3.29	2.74	2.50
Pu-242	-6.46	1.57	0.36	-6.77
Am-241	10.99	17.01	1.72	24.37
Am-243	9.94	18.18	17.03	21.71
Cm-242	-1.82			-20.81
Cm-244	-1.10	0.04	-12.84	-9.31
Mo-95	1.61	1.80	0.97	10.01
Tc-99	5.73	11.17	24.93	-1.97
Ru-101	7.33	4.62	0.30	22.38
Rh-103	16.37	24.23	2.03	18.74
Ag-109	54.32	11.31		24.55
Cs-133	5.75	6.97	4.52	6.06
Nd-143	6.99	6.28	0.10	3.96
Nd-145	0.73	3.72	0.58	-0.73
Sm-147	0.94	11.09	11.26	1.84
Sm-149	-6.21	15.44	3.51	0.90
Sm-150	4.56	9.89	9.67	1.05
Sm-151	0.40	4.37	6.09	0.61
Sm-152	-4.32	10.34	11.58	-0.73
Eu-153	2.14	5.24	8.60	1.03
Eu-155	-2.37	-4.49	2.09	-22.29
Gd-155	3.96	13.01	-39.88	-3.39

A.4.3.2.9 GKN II

The only modifications needed to the ORNL input deck [20] were for the model changes to KENO V.a. Table A.4.3.9 above shows the percent deviation between the predicted and measured content of the measured isotopes for the GKN II sample.

A.4.3.2.10 VANDELLOS II

The starting point for this analysis is Reference 23. A sample set of input decks is provided in the appendix of Reference 23 for one of the chemical assays.

As noted in Section A.4.3.1, the data for sample 160-800 is not used since there was a problem with the uranium measurements [23]. It is inappropriate to do direct difference analysis missing the U-235 isotope that has such a high reactivity worth. Furthermore, fuel rod 160-800 was next to the core baffle for one cycle and data on the core baffle was not provided. Finally, the soft spectrum due to being next to the core baffle for a cycle makes the pin atypical and therefore not appropriate for this analysis.

With sample 160-800 not being used, the 5 remaining samples come from two pins that were initially loaded in Assembly EC45, burned for four cycles and then transferred to Assembly EF05 for the final cycle.

Table A.4.3.10 shows the percent deviation between the predicted and measured content of the measured isotopes for the Vandellos samples.

Table A.4.3.10: Vandellos Predicted Minus Measured % Deviations

Sample ID	Van-58-88	Van-58-148	Van-58-260	Van-58-700	Van-165
Enrichment	4.4982	4.4982	4.4982	4.4982	4.4982
Burnup	42.5	54.8	64.6	77	78.3
U-234	5.02	-4.50	18.02	14.23	17.18
U-235	-1.04	-11.33	5.95	6.37	10.20
U-236	7.45	-1.21	3.42	6.62	5.01
Np-237	-6.20	-18.40	-10.27	-2.56	-19.52
Pu-238	-2.49	12.58	-8.86	-7.01	-14.80
Pu-239	3.75	7.30	6.36	7.53	-1.58
Pu-240	5.37	8.27	5.49	5.11	0.04
Pu-241	3.64	10.53	4.31	7.86	-2.18
Pu-242	58.96	10.34	88.33	92.24	92.65
Am-241	24.97	24.97	20.23	24.60	15.05
Am-243	29.08	13.37	15.46	14.16	-12.94
Cm-244	49.50	47.68	39.70	45.68	33.07
Tc-99	5.55				
Cs-133	1.07	3.33	-6.92	6.38	10.47
Nd-143	-1.45	1.25	0.40	1.63	7.71
Nd-145	-0.83	0.04	-2.75	-3.99	1.41
Sm-147	1.96	2.38	9.70	6.32	-2.87
Sm-149	-4.86	2.49	8.29	16.98	17.75
Sm-150	4.99	3.50	5.85	5.96	8.94
Sm-151	-3.55	6.15	5.82	0.70	4.95

Sm-152	2.31	0.60	-0.14	-1.05	-6.82
Eu-153	-7.77	-8.81	-13.04	-10.76	-13.69
Eu-155	5.78	-0.14	0.25	9.82	10.63
Gd-155	20.58	12.34	18.50	12.47	27.97

A.4.3.3 Determination of the Isotopic Depletion Bias By Direct Difference

The reactivity worth of the error in the isotopic content is determined by finding the difference in the predicted k of the application (the spent fuel pool) between using the measured isotopic content and using the predicted isotopic content. The depletion analysis of the chemical assays was described in the previous section. The isotopic content was output by using the SCALE OPUS module.

Before going into the details of the direct difference calculation of the bias and uncertainty in k due to depletion analysis, the integrated results of the chemical assays should be reviewed. Table A.4.3.11 shows the results of the chemical assay analysis for all the isotopes. The two isotopes that have the biggest effect on k are U-235 and Pu-239 (highlighted in yellow in Table A.4.3.11). The isotopic content of both of these isotopes is over predicted. This implies that the depletion analysis is conservative. The over prediction of some of the absorbing isotopes compensates for the over prediction of U-235 and Pu-239, but the net effect, as will be seen shortly, is that the depletion analysis is conservative and no bias will be needed. However, the standard deviation for the chemical assays is large. This implies that the uncertainty will be significant in the computation of $k_{95/95}$.

Table A.4.3.11: Performance of All the Chemical Assay Analyses

Isotope	Number of Assays	Average % Deviation	Maximum % Deviation	Standard Deviation	Average M/C
U-234	56	9.12	38.05	11.4	0.9088
U-235	92	1.48	10.20	3.3	0.9852
U-236	77	-1.72	7.87	3.8	1.0172
U-238	87	-0.07	2.39	0.4	1.0007
Np-237	36	0.23	35.07	13.0	0.9977
Pu-238	77	-12.64	12.58	8.0	1.1264
Pu-239	92	4.51	9.72	2.8	0.9549
Pu-240	92	2.39	9.07	3.1	0.9761
Pu-241	92	-0.64	10.53	4.8	1.0064
Pu-242	91	-2.14	92.65	19.0	1.0214
Am-241	50	2.27	43.10	29.1	0.9773
Am-243	39	0.74	29.13	13.6	0.9926
Cm-242	51	-28.20	16.17	17.7	1.2820
Cm-244	58	-1.81	49.50	17.3	1.0181
Mo-95	4	3.60	10.01	4.3	0.9640
Tc-99	17	12.96	32.59	10.7	0.8704
Ru-101	4	8.66	22.38	9.6	0.9134
Rh-103	5	6.37	24.23	8.5	0.9363
Ag-109	3	30.06	54.32	22.0	0.6994
Cs-133	12	3.52	10.47	4.3	0.9648
Nd-143	36	1.51	10.03	3.5	0.9849
Nd-145	36	-0.25	6.42	2.5	1.0025

Sm-147	25	2.74	11.26	4.1	0.9726
Sm-149	22	1.37	17.75	8.5	0.9863
Sm-150	25	3.14	9.89	3.7	0.9686
Sm-151	25	-0.40	12.33	5.0	1.0040
Sm-152	25	2.66	11.58	4.1	0.9734
Eu-151	7	-3.82	3.73	6.3	1.0382
Eu-153	20	-2.34	8.60	6.3	1.0234
Eu-155	13	0.15	10.63	9.3	0.9985
Gd-155	20	-4.31	27.97	21.4	1.0431

For the calculation of the direct differences in reactivity, a model of the application is needed. The model selected is that of the Indian Point Region 2 with an absorber plate in every cell. The predicted g/gU were converted to atom densities for KENO calculations by multiplying by the gU in 97% TD pellets times 0.6022 barn atoms per mole and dividing by the atomic weight of the isotope. For isotopes that were assayed, the measured g/gU were similarly converted to atom densities. If an isotope was not assayed, then the "measured" atom density was determined as the predicted atom density multiplied by the average ratio of the measured divided by calculated (M/C) g/gU (given in Table A.4.3.11). Since the cooling times were not the same for all the chemical assays, they were all adjusted to zero and 15 years cooling time.

For the determination of the direct difference bias and uncertainty, 368 input decks (92 for each: predicted zero cooling, measured zero cooling, predicted 15 years cooling and measured 15 years cooling) for the Indian Point Region 2 were generated. Table A.4.3.12 shows the direct differences for each assay. The results for this analysis are plotted on Figure A.4.3.13. Also on Figure A.4.3.13 is a bounding line. There is one sample out of the 92 samples that exceeds the bounding curve, so this curve meets the 95/95 criteria. The bounding line is

Isotopic Uncertainty in k = 0.0002 * Burnup in GWd/T

Notice that the bias is negative, meaning the predictions over-predict k. This **negative bias is ignored and only the uncertainty is used**.

Table A.4.3.12: Direct Difference Results for Each Assay

Sample ID	Enrichment (wt% U-235)	Burnup (GWd/T)	Measured Minus Predicted k ORNL	Measured Minus Predicted k No Cooling	Measured Minus Predicted k 15 yr Cooling
BE124-E3P1	3.00	20.18	-0.0004	-0.0028	-0.0011
BE124-E3P2	3.00	29.35	0.0027	-0.0011	0.0006
BE124-E3P3	3.00	36.26	-0.0065	-0.0102	-0.0085
BE124-E3P4	3.00	30.92	-0.0058	-0.0090	-0.0094
BE124-E3P5	3.00	22.86	0.0067	0.0030	0.0035
BE124-G7P1	3.00	17.13	0.0045	0.0019	0.0020
BE124-G7P2	3.00	25.83	0.0058	-0.0001	0.0016
BE124-G7P3	3.00	31.32	-0.0148	-0.0193	-0.0196
BE124-G7P4	3.00	27.71	0.0058	0.0005	0.0005
BE124-G7P5	3.00	25.81	-0.0047	-0.0093	-0.0102
BE168--	3.13	29.35	0.0092	0.0011	-0.0002
BE170--	3.13	27.01	0.0070	-0.0002	-0.0016

Sample ID	Enrichment (wt% U-235)	Burnup (GWd/T)	Measured Minus Predicted k ORNL	Measured Minus Predicted k No Cooling	Measured Minus Predicted k 15 yr Cooling
BE171--	3.13	28.74	0.0077	-0.0011	-0.0012
BE172--	3.13	27.89	0.0013	-0.0040	-0.0043
BE176--	3.13	28.78	0.0064	-0.0017	-0.0028
104-M11P7	3.90	12.04	0.0000	-0.0007	-0.0015
032-E11P1	3.13	7.24	-0.0036	-0.0039	-0.0046
032-E11P4	3.13	15.38	-0.0035	-0.0054	-0.0064
032-E11P7	3.13	15.90	-0.0068	-0.0085	-0.0101
032-E11P9	3.13	11.53	-0.0004	-0.0011	-0.0021
032-H9P4	3.13	16.56	0.0010	-0.0016	-0.0025
032-H9P7	3.13	17.45	0.0027	0.0016	0.0014
032-H9P9	3.13	12.37	-0.0022	-0.0029	-0.0043
049-J8P1	2.72	8.71	-0.0042	-0.0046	-0.0044
049-J8P4	2.72	14.77	-0.0111	-0.0120	-0.0139
049-J8P7	2.72	15.49	-0.0032	-0.0052	-0.0070
049-J8P9	2.72	11.13	-0.0038	-0.0040	-0.0053
049-L5P1	2.72	14.16	0.0027	0.0016	0.0010
049-L5P4	2.72	14.49	-0.0001	-0.0023	-0.0029
049-L5P9	2.72	10.18	-0.0029	-0.0029	-0.0042
069-E11P1	3.13	12.86	-0.0031	-0.0040	-0.0036
069-E11P2	3.13	20.60	-0.0080	-0.0082	-0.0094
069-E11P4	3.13	23.72	-0.0149	-0.0162	-0.0181
069-E11P5	3.13	24.52	-0.0110	-0.0161	-0.0154
069-E11P7	3.13	24.30	-0.0067	-0.0108	-0.0121
069-E11P8	3.13	23.41	-0.0083	-0.0098	-0.0122
069-E11P9	3.13	19.25	-0.0027	-0.0041	-0.0054
069-E5P4	3.13	23.87	-0.0070	-0.0095	-0.0104
069-E5P7	3.13	24.68	-0.0083	-0.0106	-0.0111
069-E5P9	3.13	19.21	-0.0076	-0.0096	-0.0094
069-J9P4	3.13	24.85	-0.0103	-0.0105	-0.0114
069-J9P7	3.13	25.26	-0.0079	-0.0110	-0.0117
069-L11P4	3.13	23.93	-0.0058	-0.0083	-0.0090
069-L11P7	3.13	24.36	-0.0082	-0.0112	-0.0115
069-L5P4	3.13	24.33	-0.0014	-0.0046	-0.0048
069-L5P7	3.13	24.31	0.0000	-0.0130	-0.0141
D01-G10	2.56	30.51	-0.0026	-0.0073	-0.0084
D01-G9	2.56	30.72	0.0027	-0.0039	-0.0043
D01-H9	2.56	31.56	0.0088	0.0025	0.0024
D04-G10	2.56	31.31	0.0007	-0.0052	-0.0057
D04-G9	2.56	31.26	0.0050	-0.0013	-0.0030
D101-MLA098-BB	2.72	26.62	-0.0019	-0.0055	-0.0073
D101-MLA098-JJ	2.72	18.68	-0.0008	-0.0028	-0.0046
D101-MLA098-P	2.72	33.17	-0.0194	-0.0219	-0.0232
BT03-NBD107-GG	2.45	37.27	0.0151	0.0045	0.0015
BT03-NBD107-MM	2.45	31.40	0.0166	0.0094	0.0068
BT03-NBD107-Q	2.45	46.46	0.0055	-0.0093	-0.0105
D047-MKP109-CC	3.04	37.12	-0.0033	-0.0041	-0.0045
D047-MKP109-LL	3.04	27.35	-0.0010	-0.0042	-0.0037
D047-MKP109-P	3.04	44.34	-0.0135	-0.0142	-0.0150

Sample ID	Enrichment (wt% U-235)	Burnup (GWd/T)	Measured Minus Predicted k ORNL	Measured Minus Predicted k No Cooling	Measured Minus Predicted k 15 yr Cooling
B05-N9BN	2.56	23.81	0.0006	-0.0020	-0.0039
B05-N9BS	2.56	16.02	0.0005	-0.0015	-0.0021
B05-N9CD	2.56	31.66	-0.0059	-0.0094	-0.0105
NT3G23-SF95-2	4.11	24.46	-0.0109	-0.0085	-0.0095
NT3G23-SF95-3	4.11	35.68	-0.0134	-0.0085	-0.0115
NT3G23-SF95-4	4.11	37.01	-0.0142	-0.0095	-0.0108
NT3G23-SF95-5	4.11	30.45	-0.0110	-0.0074	-0.0088
NT3G23-SF96-2	2.63	17.43	-0.0054	-0.0078	-0.0100
NT3G23-SF96-3	2.63	29.69	0.0090	-0.0093	-0.0125
NT3G23-SF96-4	2.63	30.41	0.0092	-0.0087	-0.0123
NT3G23-SF96-5	2.63	25.42	0.0037	-0.0077	-0.0101
NT3G24-SF97-2	4.11	30.48	-0.0056	-0.0025	-0.0038
NT3G24-SF97-3	4.11	42.10	-0.0068	-0.0041	-0.0062
NT3G24-SF97-4	4.11	47.07	-0.0072	-0.0036	-0.0068
NT3G24-SF97-5	4.11	47.26	-0.0014	0.0015	-0.0024
NT3G24-SF97-6	4.11	40.85	-0.0110	-0.0066	-0.0088
NJ070G-O12S4	4.66	23.54	-0.0069	-0.0070	-0.0082
NJ070G-O12S5	4.66	26.26	-0.0072	-0.0058	-0.0082
NJ070G-O12S6	4.66	24.09	-0.0001	-0.0011	-0.0036
NJ070G-O13S7	4.66	23.21	-0.0068	-0.0093	-0.0118
NJ070G-O13S8	4.66	26.10	-0.0089	-0.0069	-0.0099
NJ070G-O1S3	4.66	26.84	-0.0073	-0.0065	-0.0087
NJ070G-O1S1	4.66	25.53	-0.0088	-0.0069	-0.0087
1240-GU1	3.50	60.70	-0.0171	-0.0143	-0.0160
1701-GU3	4.10	53.20	0.0148	0.0023	-0.0004
1701-GU4	4.10	31.10	-0.0081	-0.0094	-0.0096
419-M11	3.80	54.00	-0.0168	-0.0123	-0.0193
Van-58-88	4.50	42.50	Not Done	0.0026	0.0040
Van-58-148	4.50	54.80	Not Done	0.0016	0.0058
Van-58-260	4.50	64.60	Not Done	-0.0062	-0.0079
Van-58-700	4.50	77.00	Not Done	-0.0074	-0.0051
Van-165	4.50	78.30	Not Done	0.0124	0.0118

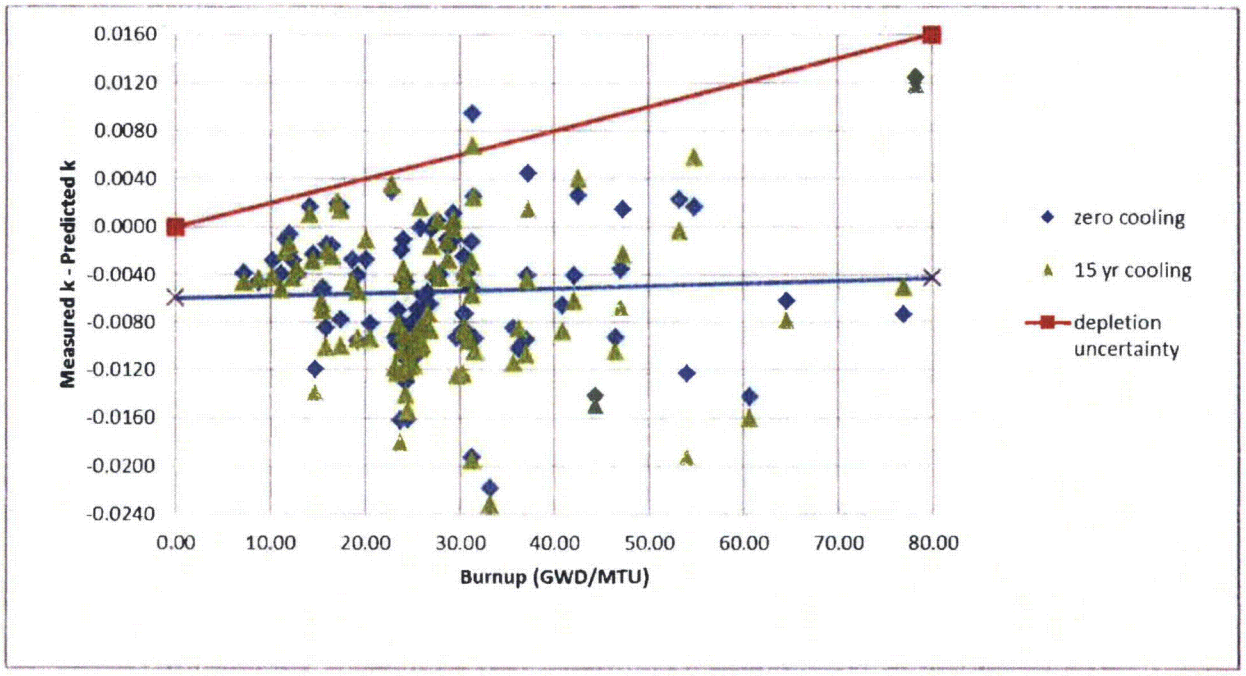

Figure A.4.3.13: Direct Difference for the 92 Chemical Assays and the Bounding Uncertainty

In addition to the traditional graphical approach to determining a limiting uncertainty, a statistical uncertainty was calculated using the equations from NUREG/CR- 6698 [2]. The laboratory uncertainty for the chemical assays is isotope dependent, so an estimate of the reactivity uncertainty for each point would be difficult, so a constant uncertainty was used. Figure A.4.3.14 shows the direct differences with the selected uncertainty and the statistical analysis uncertainty. Note that the equations used for both the bias and the uncertainty do not take into account that the bias and uncertainty is known to be zero at zero burnup. This is a small effect on the bias but would have a large effect on the uncertainty. The non-statistical uncertainty uses this information to establish the intercept. Proper statistical analysis would result in an uncertainty curve that would be more similar to the non-statistical approach taken.

The statistical analysis determines an uncertainty from the mean bias. However, since credit for a negative bias is conservatively ignored, the uncertainty is the difference between zero and the statistical limiting curve found on Figure A.4.3.14. The EPRI benchmark based uncertainty is 0.0064. For all uncertainties greater than 0.0064, the engineering based uncertainty is larger than the statistically based uncertainty. Since this validation uses the most limiting of the EPRI or the Extended ISG-8 approaches, the engineering based limiting curve is always more conservative than the statistically based curve at the burnups where it is used.

The results of this analysis differ from that reported by ORNL in NUREG/CR-7108 [19]. However, ORNL provided their direct difference results in Table 6.3. Figure A.4.3.15 shows the ORNL results for the same assays (note that there are no ORNL results for the 5 Vandellos assays). The rack design for the ORNL work did not have absorber panels and the rack design for this work has absorber panels. Some of

the difference could be due to this but the points that differ the most above the limiting curve all come from cases where significant model improvements have been made in this analysis. There are three points that stand out. Two of these points come from Calvert Cliffs assembly BT03, where ORNL had incorrectly removed the burnable absorber rods. The third point is from Gösgen sample U3 where ORNL used an improper cooling time.

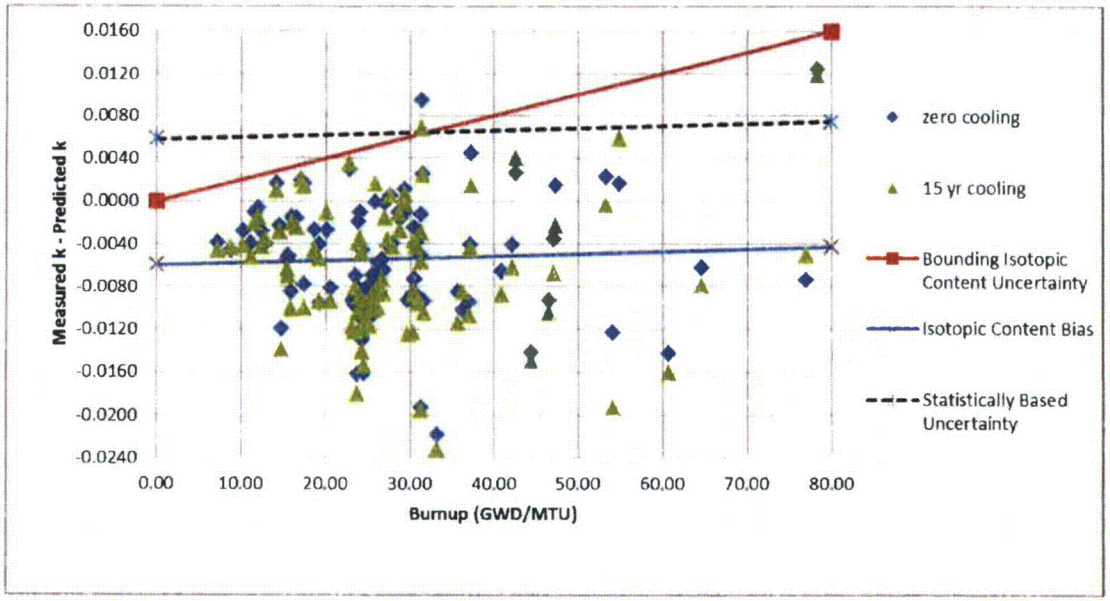

Figure A.4.3.14 Direct Difference for the 92 Chemical Assays and the Bounding Uncertainty As a Statistical Based Uncertainty

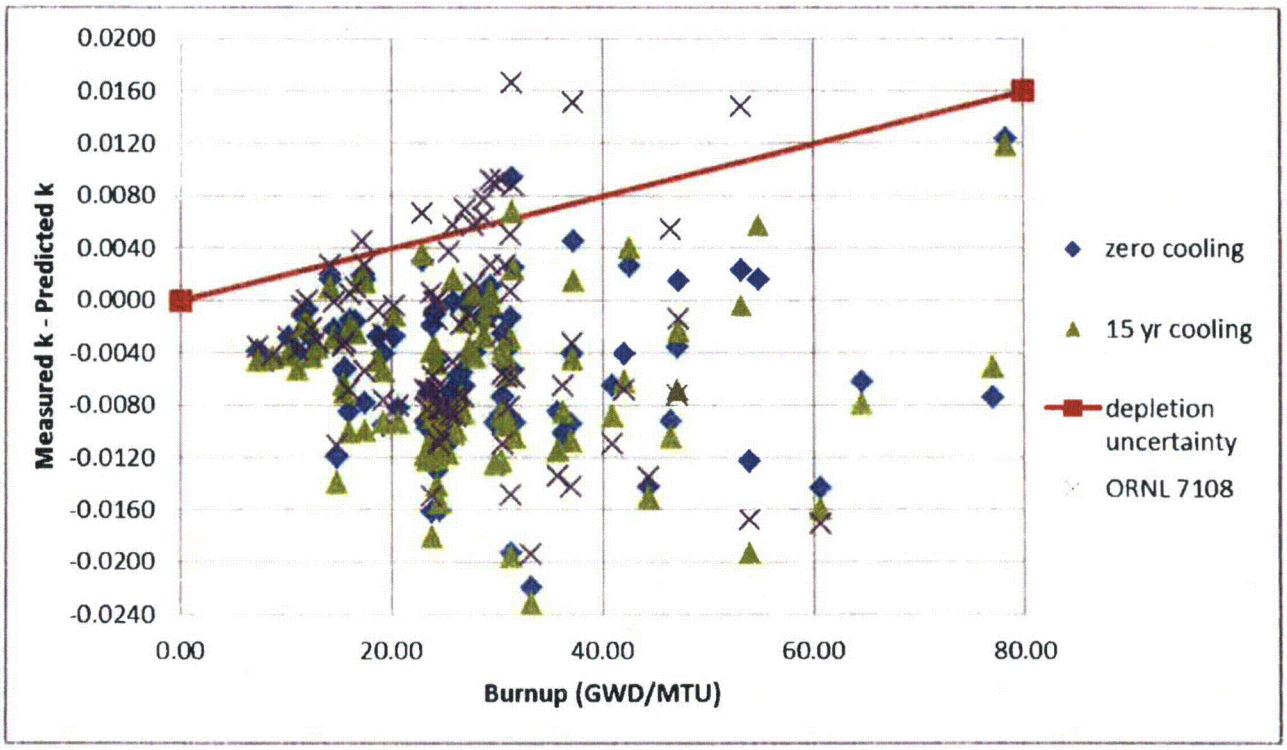

Figure A.4.3.15 Direct Difference for the 92 Chemical Assays and the Bounding Uncertainty Including the Corresponding ORNL Results

One final note on the chemical assay bias and uncertainty. Removing the bad TMI data would not affect the engineering approach to the uncertainty (and may not affect the statistical results). Figure A.4.3.16 is provided, which shows the eliminated data. Note that all the TMI points are well below the limiting curve. The HB Robinson sample that came from under the Inconel grid is the only point not utilized that is above the depletion uncertainty curve, but this sample unquestionably should be excluded, unless 3D analysis were to be used. Figure A.4.3.16 also shows the uncertainty selected for ISG 8, Rev. 3 [9].

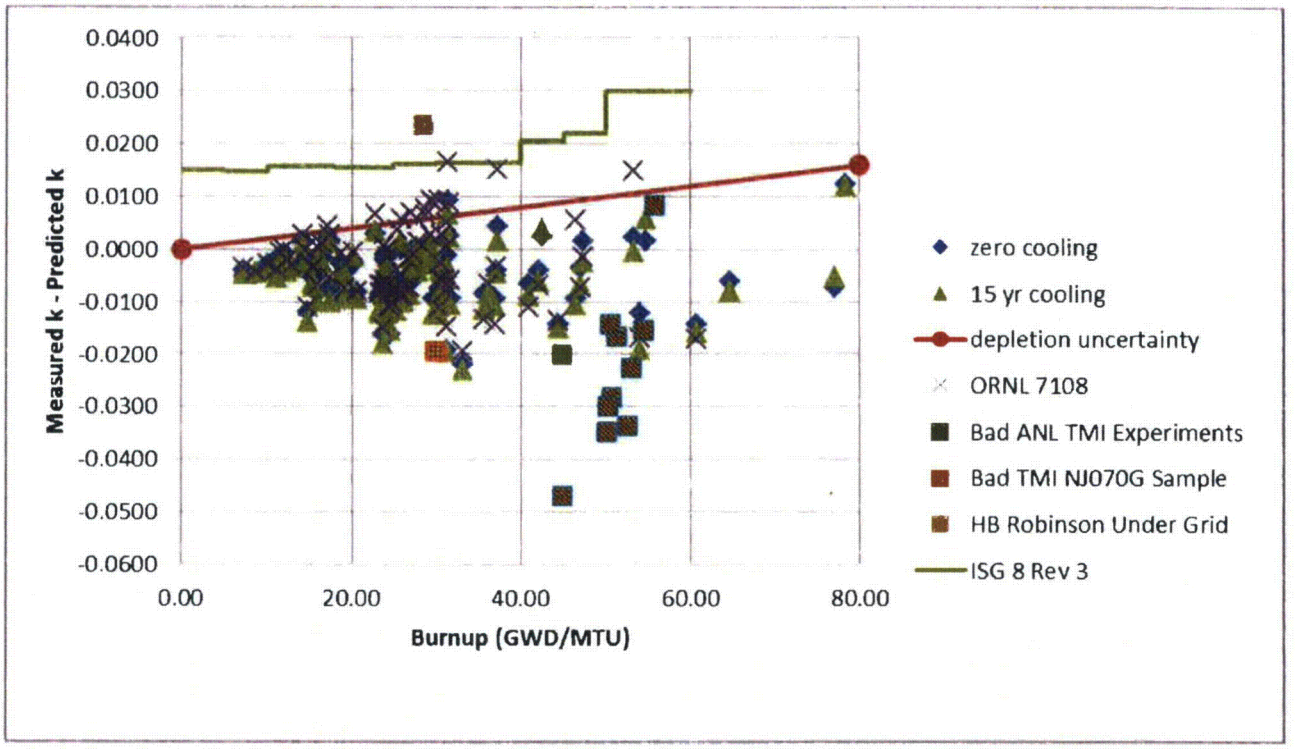

Figure A.4.3.16 Direct Difference for the 92 Chemical Assays and the Bounding Uncertainty Including All ORNL Results and ISG-8 Rev. 3

A.4.3.4 Validation of Isotopic Worth (Extended ISG-8)

Unlike the EPRI depletion reactivity benchmarks where the validation of the isotopic content and worth are done simultaneously, the Extended ISG-8 approach has separate biases and uncertainties for the isotopic content and the isotopic worth. The NRC commissioned ORNL to determine an appropriate method for validation of the isotopic worth of the isotopes not covered by the Laboratory critical experiments. NUREG/CR-7109 [32] found that it is conservative to add a bias of 1.5% of the worth of the minor actinides and fission products to cover the bias and uncertainty in the isotopic worth. This validation follows that recommendation.

A.5. Summary of Results

SCALE 6.1.2, using the 238 group ENDF/B-VII cross-sections, has been validated for analysis of fresh and burned fuel. More specifically, the CSAS5 module for calculation of k's and the t5-depl module with parm=(addnux=4) for calculating depleted isotopic concentrations has been validated. For fresh fuel, **the bias is 0.0029 for EALF up to 0.4 eV and 0.0037 for EALF's in the range from 0.4 to 0.6 eV and the uncertainty is 0.0050 for all analyses.**

For burned fuel, the bias and uncertainty is taken from the more limiting of the EPRI method or the Extended ISG-8 method. The EPRI method **depletion bias is 0.003**. The **depletion uncertainty is 0.0064** at all burnups. For the EPRI method, both bias and uncertainty are not burnup dependent. For the Extended ISG-8 method, there is a **bias for the worth of minor actinides and fission products of 1.5% of this worth**. There is no uncertainty on this term, since the bias is actually an estimate of the uncertainty [9, 32]. There is no bias for the chemical assay portion, since it is negative. The uncertainty from the chemical assays is **0.0002 * Burnup in GWd/T.** For both the EPRI method and the Extended ISG-8 method, the fresh fuel bias and uncertainty in the previous paragraph is used. (The Extended ISG-8 method requires the most limiting of bias and uncertainty for the major actinides at all burnups, which happens to be the fresh fuel condition. The EPRI method requires the use of the fresh fuel bias and uncertainty.)

The worth of minor actinides and fission products at 40 GWd/T is about 11% in k. This means the bias for the minor actinides and fission products is about 0.0016 at 40 GWd/T. Thus, at 40 GWd/T, the EPRI method bias of 0.003 is larger than the Extended ISG-8 method bias. At 40 GWd/T, the EPRI method uncertainty is 0.0064 and the Extended ISG-8 method uncertainty is 0.0080. The uncertainties can be statistically combined (not so for biases), so although the uncertainty at 40 GWd/T is larger for the Extended ISG-8 method, the EPRI method is more limiting. **After the statistical combination of uncertainties, it was found that the EPRI bias and uncertainty is more limiting through 43 GWd/T.**

A.6. Appendix References

[1] *Scale: A Comprehensive Modeling and Simulation Suite for Nuclear Safety Analysis and Design*, ORNL/TM-2005/39, Version 6.1, June 2011. Available from Radiation Safety Information Computational Center at Oak Ridge National Laboratory as CCC-785.

[2] J.C. Dean and R.W. Tayloe, Jr., *Guide for Validation of Nuclear Criticality Safety Calculational Methodology*, NUREG/CR-6698, Nuclear Regulatory Commission, Washington, DC January 2001.

[3] *International Handbook of Evaluated Criticality Safety Benchmark Experiments*, NEA/NSC/DOC(95)3, Volume IV, Nuclear Energy Agency, OECD, Paris, September, 2010.

[4] DATAPLOT is statistical software supported by the National Institute of Standards and Technology. It can be down loaded at: http://www.itl.nist.gov/div898/software/dataplot/

[5] Kleinbaum, Kupper, and Muller, Applied Regression Analysis and Other Multivariable Methods, Second Edition, page 48, PWS-KENT Publishing Company, Boston, MA 1988.

[6] "PROPHET StatGuide: Examining normality test results," http://www.basic.northwestern.edu/statguidefiles/n-dist_exam_res.html, located on 6/8/09.

[7] R. Mark Sirkin, Statistics for the Social Sciences, Third Edition, 2005, page 245, Sage Publications, Thousand Oaks, CA.

[8] M. Rahimi, E. Fuentes, and D. Lancaster, *Isotopic and Criticality Validation for PWR Actinide-Only Burnup Credit*, DOE/RW-0497, U. S. Department of Energy, Office of Civilian Radioactive Waste Management, Washington, DC, May,1997.

[9] U.S. Nuclear Regulatory Commission, *Spent Fuel Project Office Interim Staff Guidance – 8, Rev. 3 – Burnup Credit in the Criticality Safety Analyses of PWR Spent Fuel in Transport and Storage Casks*, U.S. Nuclear Regulatory Commission, April, 2012.

[10] K. S. Smith, et al., *Benchmarks for Quantifying Fuel Reactivity Depletion Uncertainty*, EPRI, Palo Alto, CA, Technical Report Number 1022909 (2011)

[11] D. B. Lancaster, *Utilization of the EPRI Depletion Benchmarks for Burnup Credit Validation*, EPRI, Palo Alto, CA, 1025203 (2012).

[12] D. E. Mueller, K. R. Elam, and P. B. Fox, *Evaluation of the French Haut Taux de Combustion (HTC) Critical Experiment Data*, NUREG/CR-6979 (ORNL/TM-2007/083), prepared for the US Nuclear Regulatory Commission by Oak Ridge National Laboratory, Oak Ridge, Tenn., September 2008.

[13] F. Fernex, "Programme HTC – Phase 1 : Réseaux de crayons dans l'eau pure (Water-moderated and reflected simple arrays) Réévaluation des expériences," DSU/SEC/T/2005-33/D.R., Institut de Radioprotection et de Sûreté Nucléaire, 2008.

[14] F. Fernex, *ProgrammeHTC – Phase 2 : Réseaux simples en eau empoisonnée (bore et gadolinium) (Reflected simple arrays moderated by poisoned water with gadolinium or boron) Réévaluation des expériences*, DSU/SEC/T/2005-38/D.R., Institut de Radioprotection et de Sûreté Nucléaire, 2008.

[15] F. Fernex, *Programme HTC – Phase 3 : Configurations "stockage en piscine" (Pool storage) Réévaluation des expériences*, DSU/SEC/T/2005-37/D.R., Institut de Radioprotection et de Sûreté Nucléaire, 2008.

[16] F. Fernex, *Programme HTC – Phase 4 : Configurations "châteaux de transport" (Shipping cask) - Réévaluation des expériences*, DSU/SEC/T/2005-36/D.R., Institut de Radioprotection et de Sûreté Nucléaire, 2008.

[17] *International Handbook of Evaluated Criticality Safety Benchmark Experiments*, NEA/NSC/DOC(95)3, Volume VI, Nuclear Energy Agency, OECD, Paris, September, 2010.

[18] M. D. DeHart and S. M. Bowman, *Validation of the SCALE Broad Structure 44-Group ENDF/B-V Cross-Section Library for Use in Criticality Safety Analyses*, NUREG/CR-6102 (ORNL/TM-12460), Oak Ridge National Laboratory, Oak Ridge, TN, September 1994.

[19] G. Radulescu, I. C. Gauld, G. Ilas, and J. C. Wagner, *An Approach for Validating Actinide and Fission Product Burnup Credit Criticality Safety Analyses – Isotopic Composition Predictions*, NUREG/CR-7108, Office of Nuclear Regulatory Research, U.S. Nuclear Regulatory Commission, Washington, DC, USA, April 2012.

[20] G. Radulescu, I. C. Gauld, and G. Ilas, *SCALE 5.1 Predictions of PWR Spent Nuclear Fuel Isotopic Compositions*, ORNL/TM-2010/44, Oak Ridge National Laboratory, Oak Ridge, Tennessee, USA, March 2010.

[21] Alan H. Wells, *Burnup Credit – Contribution to the Analysis of Yankee Rowe Radiochemical Assays*, EPRI Technical Report Number 1022910, Electric Power Research Institute, Palo Alto, CA, USA, October 2011.

[22] Meraj Rahimi, Emilio Fuentes, and Dale Lancaster, *Isotopic and Criticality Validation for PWR Actinide-Only Burnup Credit*, DOE/RW-0497, Office of Civilian Radioactive Waste Management, U. S. Department of Energy, Washington, DC, USA, May 1997.

[23] G. Ilas, and I. C. Gauld, *Analysis of Experimental Data for High-Burnup PWR Spent Fuel Isotopic Validation— Vandellós II Reactor*, NUREG/CR-7013, Office of Nuclear Regulatory Research, U.S. Nuclear Regulatory Commission, Washington, DC, USA, January 2011.

[24] S. Guardini and G. Guzzi, *BENCHMARK, Reference Data on Post Irradiation Analysis of Light Water Reactor Fuel Samples – A review of 12 years experience, results obtained and their characterization*, EUR 7879 EN, Commission of the European Communities, Joint Research Centre ISPRA Establishment, ECSC-EAEC, Brussels-Luxembourg, 1982.

[25] A. M. Bresesti, et al., *Post-Irradiation Analysis of Trino Vercellese Reactor Fuel Elements*, EUR 4909 e, Commission of the European Communities, Joint Research Centre ISPRA Establishment, 1972.

[26] P. Barbero, et al., *Post irradiation examination of the fuel discharged from the Trino Vercellese reactor after the 2nd irradiation cycle*, EUR 5605 e, Commission of the European Communities, Joint Research Centre ISPRA Establishment, ECSC, EEC, EAEC, Luxembourg, 1977.

[27] J. O. Barner, *Characterization of LWR Spent Fuel MCC-Approved Testing Material - ATM-101*, PNL-5109, Rev. 1, Pacific Northwest Laboratory, 1985.

[28] O. W. Hermann, S. M. Bowman, M. C. Brady, and C. V. Parks, *Validation of the Scale System for PWR Spent Fuel Isotopic Composition Analyses*, ORNL/TM-12667, Oak Ridge National Laboratory, Oak Ridge, Tennessee, USA, March 1995.

[29] *TMI-1 Cycle 10 Fuel Rod Failures, Volume 1: Root Cause Failure Evaluations*, EPRI, Palo Alto, CA; GPU Nuclear, Parsippany, NJ; and Duke Power Company, Charlotte, NC: 1998. EPRI Report TR-108784-V1.

[30] G. Ilas, I. C. Gauld, and B. D. Murphy, *Analysis of Experimental Data for High Burnup PWR Spent Fuel Isotopic Validation—ARIANE and REBUS Programs (UO_2 Fuel)*, NUREG/CR-6969 (ORNL/TM-2008/072), prepared for the U.S. Nuclear Regulatory Commission by Oak Ridge National Laboratory, Oak Ridge, Tennessee (2010).

[31] *ARIANE International Programme—Final Report*, ORNL/SUB/97-XSV750-1, Oak Ridge National Laboratory, Oak Ridge, Tenn., May 2003.

[32] J. M. Scaglione, D. E. Mueller, J.C. Wagner and W. J. Marshall, *An Approach for Validating. Actinide and Fission Product Burnup Credit Criticality Safety Analyses—Criticality (keff) Predictions*, US Nuclear Regulatory Commission, NUREG/CR-7109, Oak Ridge National Laboratory, Oak Ridge, Tenn. (2012).

ATTACHMENT 3 TO NL-14-083

Affidavits in Support of Request to Withhold Information

Entergy Nuclear Operations, Inc.
Indian Point Unit 2
Docket No. 50-247

Westinghouse

Westinghouse Electric Company
Engineering, Equipment and Major Projects
1000 Westinghouse Drive, Building 3
Cranberry Township, Pennsylvania 16066
USA

U.S. Nuclear Regulatory Commission
Document Control Desk
11555 Rockville Pike
Rockville, MD 20852

Direct tel: (412) 374-4643
Direct fax: (724) 940-8560
e-mail: greshaja@westinghouse.com
Proj letter: NF-IP-14-37, Rev. 1

CAW-14-4059

November 6, 2014

APPLICATION FOR WITHHOLDING PROPRIETARY
INFORMATION FROM PUBLIC DISCLOSURE

Subject: NET-300067-01, Rev. 0, "Criticality Safety Analysis of the Indian Point Unit 2 Spent Fuel Pool with Credit for Inserted Neutron Absorber Panels" (Proprietary)

The proprietary information on pages 10, 24-26, 34, 46, 88, 89 & 91 for which withholding is being requested in the above-referenced report is further identified in Affidavit CAW-14-4059 signed by the owner of the proprietary information, Westinghouse Electric Company LLC. The Affidavit, which accompanies this letter, sets forth the basis on which the information may be withheld from public disclosure by the Commission and addresses with specificity the considerations listed in paragraph (b)(4) of 10 CFR Section 2.390 of the Commission's regulations.

Accordingly, this letter authorizes the utilization of the accompanying Affidavit by Entergy Nuclear Operations, Inc.

Correspondence with respect to the proprietary aspects of the application for withholding or the Westinghouse Affidavit should reference CAW-14-4059, and should be addressed to James A. Gresham, Manager, Regulatory Compliance, Westinghouse Electric Company, 1000 Westinghouse Drive, Building 3 Suite 310, Cranberry Township, Pennsylvania 16066.

Very truly yours,

James A. Gresham, Manager
Regulatory Compliance

Enclosures

AFFIDAVIT

COMMONWEALTH OF PENNSYLVANIA:

ss

COUNTY OF BUTLER:

I, James A. Gresham, am authorized to execute this Affidavit on behalf of Westinghouse Electric Company LLC (Westinghouse), and that the averments of fact set forth in this Affidavit are true and correct to the best of my knowledge, information, and belief.

James A. Gresham, Manager
Regulatory Compliance

(1) I am Manager, Regulatory Compliance, Westinghouse Electric Company LLC (Westinghouse), and as such, I have been specifically delegated the function of reviewing the proprietary information sought to be withheld from public disclosure in connection with nuclear power plant licensing and rule making proceedings, and am authorized to apply for its withholding on behalf of Westinghouse.

(2) I am making this Affidavit in conformance with the provisions of 10 CFR Section 2.390 of the Commission's regulations and in conjunction with the Westinghouse Application for Withholding Proprietary Information from Public Disclosure accompanying this Affidavit.

(3) I have personal knowledge of the criteria and procedures utilized by Westinghouse in designating information as a trade secret, privileged or as confidential commercial or financial information.

(4) Pursuant to the provisions of paragraph (b)(4) of Section 2.390 of the Commission's regulations, the following is furnished for consideration by the Commission in determining whether the information sought to be withheld from public disclosure should be withheld.

(i) The information sought to be withheld from public disclosure is owned and has been held in confidence by Westinghouse.

(ii) The information is of a type customarily held in confidence by Westinghouse and not customarily disclosed to the public. Westinghouse has a rational basis for determining the types of information customarily held in confidence by it and, in that connection, utilizes a system to determine when and whether to hold certain types of information in confidence. The application of that system and the substance of that system constitute Westinghouse policy and provide the rational basis required.

Under that system, information is held in confidence if it falls in one or more of several types, the release of which might result in the loss of an existing or potential competitive advantage, as follows:

(a) The information reveals the distinguishing aspects of a process (or component, structure, tool, method, etc.) where prevention of its use by any of

Westinghouse's competitors without license from Westinghouse constitutes a competitive economic advantage over other companies.

(b) It consists of supporting data, including test data, relative to a process (or component, structure, tool, method, etc.), the application of which data secures a competitive economic advantage, e.g., by optimization or improved marketability.

(c) Its use by a competitor would reduce his expenditure of resources or improve his competitive position in the design, manufacture, shipment, installation, assurance of quality, or licensing a similar product.

(d) It reveals cost or price information, production capacities, budget levels, or commercial strategies of Westinghouse, its customers or suppliers.

(e) It reveals aspects of past, present, or future Westinghouse or customer funded development plans and programs of potential commercial value to Westinghouse.

(f) It contains patentable ideas, for which patent protection may be desirable.

(iii) There are sound policy reasons behind the Westinghouse system which include the following:

(a) The use of such information by Westinghouse gives Westinghouse a competitive advantage over its competitors. It is, therefore, withheld from disclosure to protect the Westinghouse competitive position.

(b) It is information that is marketable in many ways. The extent to which such information is available to competitors diminishes the Westinghouse ability to sell products and services involving the use of the information.

(c) Use by our competitor would put Westinghouse at a competitive disadvantage by reducing his expenditure of resources at our expense.

(d) Each component of proprietary information pertinent to a particular competitive advantage is potentially as valuable as the total competitive advantage. If competitors acquire components of proprietary information, any one component may be the key to the entire puzzle, thereby depriving Westinghouse of a competitive advantage.

(e) Unrestricted disclosure would jeopardize the position of prominence of Westinghouse in the world market, and thereby give a market advantage to the competition of those countries.

(f) The Westinghouse capacity to invest corporate assets in research and development depends upon the success in obtaining and maintaining a competitive advantage.

(iv) The information is being transmitted to the Commission in confidence and, under the provisions of 10 CFR Section 2.390, it is to be received in confidence by the Commission.

(v) The information sought to be protected is not available in public sources or available information has not been previously employed in the same original manner or method to the best of our knowledge and belief.

(vi) The proprietary information sought to be withheld in this submittal is that which is appropriately marked in pages 10, 24-26, 34, 46, 88, 89 & 91 of NET-300067-01, Rev. 0, "Criticality Safety Analysis of the Indian Point Unit 2 Spent Fuel Pool with Credit for Inserted Neutron Absorber Panels" (Proprietary), for submittal to the Commission, being transmitted by Entergy Nuclear Operations, Inc. letter and Application for Withholding Proprietary Information from Public Disclosure, to the Document Control Desk. The proprietary information as submitted by Westinghouse is that associated with the Indian Point Unit 2 spent fuel pool criticality analysis, and may be used only for that purpose.

(a) This information is part of that which will enable Westinghouse to:

(i) Assist customers in obtaining licensing changes.

(ii) Assist customers in analyzing the spent fuel pool and absorber panels to ensure criticality does not occur.

(b) Further this information has substantial commercial value as follows:

(i) Westinghouse plans to sell the use of the information to its customers for the purpose of assisting in obtaining license changes.

(ii) Westinghouse can sell support and defense of spent fuel pool criticality analyses.

(iii) The information requested to be withheld reveals the distinguishing aspects of a methodology which was developed by Westinghouse.

Public disclosure of this proprietary information is likely to cause substantial harm to the competitive position of Westinghouse because it would enhance the ability of competitors to provide similar criticality analyses and licensing defense services for commercial power reactors without commensurate expenses. Also, public disclosure of the information would enable others to use the information to meet NRC requirements for licensing documentation without purchasing the right to use the information.

The development of the technology described in part by the information is the result of applying the results of many years of experience in an intensive Westinghouse effort and the expenditure of a considerable sum of money.

In order for competitors of Westinghouse to duplicate this information, similar technical programs would have to be performed and a significant manpower effort, having the requisite talent and experience, would have to be expended.

Further the deponent sayeth not.

PROPRIETARY INFORMATION NOTICE

Transmitted herewith is the proprietary version of a document furnished to the NRC associated with the Indian Point Unit 2 spent fuel pool criticality analysis, and may be used only for that purpose

In order to conform to the requirements of 10 CFR 2.390 of the Commission's regulations concerning the protection of proprietary information so submitted to the NRC, the information which is proprietary in the proprietary versions is contained within brackets, and where the proprietary information has been deleted in the non-proprietary versions, only the brackets remain (the information that was contained within the brackets in the proprietary versions having been deleted). The justification for claiming the information so designated as proprietary is indicated in both versions by means of lower case letters (a) through (f) located as a superscript immediately following the brackets enclosing each item of information being identified as proprietary or in the margin opposite such information. These lower case letters refer to the types of information Westinghouse customarily holds in confidence identified in Sections (4)(ii)(a) through (4)(ii)(f) of the Affidavit accompanying this transmittal pursuant to 10 CFR 2.390(b)(1).

COPYRIGHT NOTICE

HOLTEC INTERNATIONAL

Holtec Center, One Holtec Drive, Marlton, NJ 08053
Telephone (856) 797-0900
Fax (856) 797-0909

SENT BY ELECTRONIC MAIL ONLY
Document ID: 2441-003

Nov. 7, 2014

Mr. Roger Waters
Regulatory Assurance
Indian Point Energy Center
450 Broadway
GSB Second Floor
Buchanan, NY 10511-0249

Subject: **Affidavit Related to "Criticality Safety Analysis of the Indian Point Unit 2 Spent Fuel Pool with Credit for Inserted Neutron Absorber Panels"**

Dear Mr. Waters:

Holtec is pleased to approve the release, from a proprietary perspective, the following information to the United States Nuclear Regulatory Commission (USNRC):

Attachment 1- NET-300067-01 Rev. 0, "Criticality Safety Analysis of the Indian Point Unit 2 Spent Fuel Pool with Credit for Inserted Neutron Absorber Panels" (Proprietary)
Attachment 2 - AFFIDAVIT PURSUANT TO 10 CFR 2.390

We require that you include this letter along with the affidavit (Attachment 2) pursuant to 10CFR2.390 when submitting Attachment 1 to the USNRC.

Holtec is looking forward to working with Indian Point to complete this project. If you have any questions or concerns please do not hesitate to reach out to Haizhen Pan (h.pan@holtec.com) or Jordan Landis (j.landis@holtec.com).

Sincerely,

Haizhen Pan
Program Manager
Holtec International

CC: Mr. Jordan Landis (j.landis@holtec.com)
Mr. Rick Trotta (r.trotta@holtec.com)

Document ID: 2441-003

U.S. Nuclear Regulatory Commission
Document ID 2441-003
Non-Proprietary Attachment 2

AFFIDAVIT PURSUANT TO 10 CFR 2.390

I, Haizhen Pan, being duly sworn, depose and state as follows:

(1) I have reviewed the information described in paragraph (2) which is sought to be withheld, and am authorized to apply for its withholding.

(2) The information sought to be withheld is information provided in Attachment 1 to Holtec letter 2441-003. This Attachment contains Holtec Proprietary information denoted by the shaded areas.

(3) In making this application for withholding of proprietary information of which it is the owner, Holtec International relies upon the exemption from disclosure set forth in the Freedom of Information Act ("FOIA"), 5 USC Sec. 552(b)(4) and the Trade Secrets Act, 18 USC Sec. 1905, and NRC regulations 10CFR Part 9.17(a)(4), 2.390(a)(4), and 2.390(b)(1) for "trade secrets and commercial or financial information obtained from a person and privileged or confidential" (Exemption 4). The material for which exemption from disclosure is here sought is all "confidential commercial information", and some portions also qualify under the narrower definition of "trade secret", within the meanings assigned to those terms for purposes of FOIA Exemption 4 in, respectively, Critical Mass Energy Project v. Nuclear Regulatory Commission, 975F2d871 (DC Cir. 1992), and Public Citizen Health Research Group v. FDA, 704F2d1280 (DC Cir. 1983).

AFFIDAVIT PURSUANT TO 10 CFR 2.390

(4) Some examples of categories of information which fit into the definition of proprietary information are:

a. Information that discloses a process, method, or apparatus, including supporting data and analyses, where prevention of its use by Holtec's competitors without license from Holtec International constitutes a competitive economic advantage over other companies;

b. Information which, if used by a competitor, would reduce his expenditure of resources or improve his competitive position in the design, manufacture, shipment, installation, assurance of quality, or licensing of a similar product.

c. Information which reveals cost or price information, production, capacities, budget levels, or commercial strategies of Holtec International, its customers, or its suppliers;

d. Information which reveals aspects of past, present, or future Holtec International customer-funded development plans and programs of potential commercial value to Holtec International;

e. Information which discloses patentable subject matter for which it may be desirable to obtain patent protection.

The information sought to be withheld is considered to be proprietary for the reasons set forth in paragraphs 4.a, 4.b and 4.e above.

(5) The information sought to be withheld is being submitted to the NRC in confidence. The information (including that compiled from many sources) is of a sort customarily held in confidence by Holtec International, and is in fact so held. The information sought to be withheld has, to the best of my knowledge and belief, consistently been held in confidence by Holtec International. No public disclosure has been made, and it is not available in public sources. All disclosures to third parties, including any required transmittals to the NRC, have been made, or must be made, pursuant to regulatory provisions or proprietary agreements which provide for maintenance of the information in confidence. Its initial designation as

proprietary information, and the subsequent steps taken to prevent its unauthorized disclosure, are as set forth in paragraphs (6) and (7) following.

(6) Initial approval of proprietary treatment of a document is made by the manager of the originating component, the person most likely to be acquainted with the value and sensitivity of the information in relation to industry knowledge. Access to such documents within Holtec International is limited on a "need to know" basis.

(7) The procedure for approval of external release of such a document typically requires review by the staff manager, project manager, principal scientist or other equivalent authority, by the manager of the cognizant marketing function (or his designee), and by the Legal Operation, for technical content, competitive effect, and determination of the accuracy of the proprietary designation. Disclosures outside Holtec International are limited to regulatory bodies, customers, and potential customers, and their agents, suppliers, and licensees, and others with a legitimate need for the information, and then only in accordance with appropriate regulatory provisions or proprietary agreements.

(8) The information classified as proprietary was developed and compiled by Holtec International at a significant cost to Holtec International. This information is classified as proprietary because it contains detailed descriptions of analytical approaches and methodologies not available elsewhere. This information would provide other parties, including competitors, with information from Holtec International's technical database and the results of evaluations performed by Holtec International. A substantial effort has been expended by Holtec International to develop this information. Release of this information would improve a competitor's position because it would enable Holtec's competitor to copy our technology and offer it for sale in competition with our company, causing us financial injury.

(9) Public disclosure of the information sought to be withheld is likely to cause substantial harm to Holtec International's competitive position and foreclose or reduce the availability of profit-making opportunities. The information is part of Holtec International's comprehensive spent fuel storage technology base, and its commercial value extends beyond the original development cost. The value of the technology base goes beyond the extensive physical database and analytical methodology, and includes development of the expertise to determine and apply the appropriate evaluation process.

The research, development, engineering, and analytical costs comprise a substantial investment of time and money by Holtec International.

The precise value of the expertise to devise an evaluation process and apply the correct analytical methodology is difficult to quantify, but it clearly is substantial.

Holtec International's competitive advantage will be lost if its competitors are able to use the results of the Holtec International experience to normalize or verify their own process or if they are able to claim an equivalent understanding by demonstrating that they can arrive at the same or similar conclusions.

The value of this information to Holtec International would be lost if the information were disclosed to the public. Making such information available to competitors without their having been required to undertake a similar expenditure of resources would unfairly provide competitors with a windfall, and deprive Holtec International of the opportunity to exercise its competitive advantage to seek an adequate return on its large investment in developing these very valuable analytical tools.

U.S. Nuclear Regulatory Commission
Document ID 2441-003
Non-Proprietary Attachment 2

AFFIDAVIT PURSUANT TO 10 CFR 2.390

STATE OF NEW JERSEY)
) ss:
COUNTY OF BURLINGTON)

Haizhen Pan, being duly sworn, deposes and says:

That she has read the foregoing affidavit and the matters stated therein are true and correct to the best of her knowledge, information, and belief.

Executed at Marlton, New Jersey, this 7th day of November, 2014.

Haizhen Pan
Program Manager
Holtec International

Subscribed and sworn before me this 7 th day of November, 2014.

11/7/14

ABBEY D. HEBLER
NOTARY PUBLIC
STATE OF NEW JERSEY
ID # 2444647
MY COMMISSION EXPIRES APRIL 14, 2019